UNIVERSITY OF TEXAS ARLINGTON

TxDOT Report 0-7201-R1 Appendix B

HYDROLOGIC APPROACHES TO PLAYA LAKES, AREAS OF SIGNIFICANT KARST GEOLOGY, AND ARID REGIONS: Appendix B

Habib Ahmari
Saman Baharvand
Mohammad Moradi

Report Publication Date:	Published: April 2026
Project:	0-7201
Project Title:	Synthesis of Hydrologic Approaches to Playa Lakes, Areas of Significant Karst Geology, and Arid Regions

Appendix B

LITERATURE REVIEW (TASK 2)

EXECUTIVE SUMMARY

Playa lakes, arid regions, and karst terrains constitute important geographic and hydrological features across Texas, each presenting unique challenges due to their complex and varied hydrology. Currently, there are no uniform guidelines or standards for the hydrological and hydraulic design of transportation infrastructures in these landscapes, leading designers to heavily rely on project-specific judgment to determine suitable hydrological parameters. The primary objective of this review is to provide a comprehensive overview of the current state of knowledge and practices regarding hydrological approaches to playa lakes, arid regions, and karst terrains.

The methodology employed to achieve the project's objective involves a systematic review of design guidance, standards, and recommendations relevant to hydrology and hydraulic design of transportation infrastructure such as drainage and stormwater systems. This involved reviewing various sources, including state departments of transportation drainage design manuals, publications from the Federal Highway Administration (FHWA), and stormwater design manuals from various states, cities, and communities, as well as international drainage design guidance and manuals. Additionally, a review of research studies and technical reports was conducted. This review aimed to identify new approaches to hydrology and hydraulic studies tailored to regions characterized by playa lakes, karst terrains, and arid conditions.

In our review of design guidance and standards, we focused on two key aspects: identifying acceptable methods for hydrological analysis by the DOTs and other relevant agencies; and determining if their manuals offer approaches to hydrology of playa lakes, karst terrains, and arid areas. The Rational Method, NRCS (SCS) Method, and Regional Regression Equations (or similar methods developed outside of the U.S.) are widely adopted by national and international transportation agencies, states, cities, and communities. These methods are recommended for estimating peak flow and developing flow hydrographs. Moreover, certain manuals have incorporated specific approaches and methods to address the hydrologic characteristics unique to these environments. These approaches are listed here:

For Playa Lakes:

- Excluding non-contributing areas such as playas and dry lakebeds from the watershed area.
- Assigning different runoff coefficient (*C*) values in Rational Method for isolated and non-isolated playas.

For Arid Areas:

- Employing Rational Method runoff coefficient (*C*) values recommended for desert regions.
- Utilizing NRCS curve numbers (*CN*) recommended for arid and semi-arid areas.

- Applying regional regression equations and methods for flood frequency developed specifically for arid regions.
- Employing SCS Type II cumulative type curve for hydraulic modeling.

For Karst Terrains:

- Excluding non-contributing areas (due to karst topography features) such sinkholes and depressions from the watershed area.
- Applying empirical reduction factors to peak runoff.
- Adjusting the Rational Method runoff coefficient (C).
- Using an NRCS Type I rainfall distribution (low-intensity, longer-duration rainfall) within a Type II area (characterized by intense, shorter-duration rainfall events).
- Modifying curve number values or peak rate factors using the TR-20 method.
- Employing regression equations tailored for karst terrain.

We also reviewed over 300 research studies and technical reports. This review aimed to uncover new approaches to the hydrology of playa lakes, karst terrains, and arid areas. The regions covered in these studies include not only the United States but also other parts of the world facing similar hydrology challenges. A summary of the review for each region is as follows:

Playa Lakes

While playa lakes can contribute significantly to flooding and flood mitigation, the primary focus of research studies on these features centers around various aspects such as their distribution, inundation characteristics, estimation of depth, storage volume, duration, and infiltration rates. Nonetheless, some research efforts have targeted flood forecasting and management in these vital components of arid and semi-arid regions. These efforts encompass developing models to simulate playa lake behavior under different rainfall scenarios, analyzing hydrologic connectivity within watersheds, and examining the correlation between rainfall and playa lake response. Despite these efforts, there is still much to learn about playa lake hydrology, as no study has exclusively addressed the effect of these features on rainfall-runoff relationships, time of concentration, and peak flow estimates.

Arid Areas

The hydrology of arid and semi-arid regions is characterized by low and highly variable precipitation, high evapotranspiration, and limited surface water resources. Research in this area, therefore, has focused on developing hydrologic models to simulate watershed responses to rainfall events, analyzing precipitation variability, and studying the impacts of land use and climate change on flood risk. Challenges arise in accurately estimating parameters such as initial abstraction and time of concentration (T_c) due to limited data availability.

Since conventional methodologies for estimating peak flow rate and flood hydrographs are tailored for non-arid regions, several studies have attempted to modify these methods for arid areas. These modifications include adjusting the curve number in the NRCS method and proposing equations

to calculate *CN* for dry and wet conditions based on antecedent moisture condition (AMC) and antecedent runoff condition (ARC). While these methods have shown promising results in various arid regions, their applicability in other areas requires further investigation.

The time of concentration (T_c) in arid regions can be estimated using various methods, but studies evaluating these methods show wide variability in their performance. Despite challenges, recent research has shown promise in refining empirical equations through graphical analyses, leading to more accurate estimations of T_c in arid environments.

Karts Terrains

The literature review revealed that past and current research in karst regions primarily focuses on geotechnical and structural issues related to karstic features, groundwater movement and quality, water availability, and interactions between groundwater flow, erosion, and subsurface processes. Few studies concentrate on hydrologic challenges for flood forecasting in karst landscapes, at both national and international levels.

Unlike modeling drainage areas with soil pores, which have limited infiltration rates, karstic fissures and shafts allow for rapid and substantial flow discharge, contributing to shorter response times and higher peak flooding magnitudes. Additionally, water retention in voids and aquifers within karst formations can delay movement and reduce peak flood levels. Therefore, research on karst hydrology has focused on developing methods for estimating infiltration or loss through sinkholes and fissures within karst zones. One approach is modifying the NRCS curve number (*CN*) for karstic regions based on factors such as permeability, land use, and watershed drainage capacity. The modified NRCS-CN method has been extensively applied in Mediterranean karst regions for estimating surface runoff, peak discharge, and flash flooding, showing promising performance in assessing flood risks.

Researchers have also proposed modifications to soil moisture calculation to better account for the unique characteristics of karstic watersheds. In conventional methods, peak runoff estimation heavily relies on soil moisture conditions, determining infiltration rates and surface runoff generation. However, in karstic environments, where water rapidly infiltrates into subsurface conduits, soil moisture loss rates can differ significantly from non-karstic areas. To address these challenges, it is suggested to adopt soil moisture calculation methods to reflect the rapid drainage and subsurface flow processes characteristic of karstic watersheds. This may involve incorporating additional parameters or refining existing models to account for the complexities of flow pathways in these environments.

APPENDIX B TABLE OF CONTENTS

Appendix B List of Figures

Appendix B List of Tables

CHAPTER B1 : INTRODUCTION

This chapter presents the findings from Task 2 of Project 0-7201 titled "*Hydrologic Approaches to Playa Lakes, Areas of Significant Karst Geology, and Arid Regions*". The research team conducted an extensive literature review utilizing various widely used databases and the Google search engine. The review covered design guidance, standards, recommendations, and research studies on hydrologic and hydraulic methodologies applicable to playa lakes, karst terrains, and arid regions.

B.1.1 Project Background

Playa lakes, arid regions, and karst terrains are significant features of the Texas landscape, dispersed throughout different areas of the state. The hydrology of these regions is complex and subject to variation, influenced by factors such as climate, soil composition, and land use. Consequently, designing infrastructure for these areas presents numerous challenges. Key challenges related to hydrological studies and the design, operation, and maintenance of transportation infrastructure in these regions are as follows.

B.1.1.1 Hydrology of Playa Lakes and Challenges Regarding Transportation Infrastructures

Playa Lakes can pose challenges for transportation infrastructure in several ways. For example, during significant rainfall occurrences, playa regions are prone to flash flooding, which can damage roads and other infrastructure. Some other challenges associated with transportation infrastructures in Playas include:

- *Road closures*: Playa lakes are often located near roads and highways, and flooding during storms may lead to road closures and detours. This can disrupt transportation networks and cause traffic.
- *Damage to infrastructure*: The water flowing through playa lakes can cause erosion and damage to roadways and other transportation infrastructure. This can be particularly challenging in areas where the soil is susceptible to erosion or if the roadways are built on unstable soil.
- *Safety risk*: Flooding in playa lakes can also pose a safety risk for drivers, especially if the water is deep enough to submerge vehicles or cause them to lose traction.
- *Aviation safety risk*: In semi-arid and arid regions, playas, known for their flat topography and typically dry conditions, have been historically utilized for airport sites. Beyond aviation, these areas offer recreational activities like dry land sailing. However, their intermittent inundation lasting from days to months poses operational challenges for aviation, particularly when runways and taxiways are submerged. Also, playa lakes, often situated along migratory bird flyways, attract birds when flooded, creating a collision risk with aircraft.

Hydrological studies in playa lakes pose several challenges related to the design of transportation infrastructure including:

- *Rainfall-Runoff*: Estimating rainfall-runoff in playa lake regions encounters difficulties due to their variable hydrological behavior, the scarcity of comprehensive hydrological data for model calibration, and the intricate topography and drainage networks complicating runoff estimation from storm events.
- *Peak Flows*: Estimating peak flows in playa lake regions is hindered by the rapid response times of water levels and flows during rainfall events, as well as the potential alteration of flow patterns by sediment mobilization, leading to increased uncertainties in peak flow calculations.
- *Time of Concentration*: Calculating time of concentration in playa lake regions presents challenges stemming from complex drainage patterns, the impact of depression storage on runoff timing, challenges in quantifying infiltration rates and other losses in heterogeneous soil and land cover conditions, and limited availability of hydrological data, which may introduce uncertainties in input parameters required for calculation.
- *Depression Storage*: Characterizing depression storage in playa lake regions faces challenges due to variability in depression characteristics, such as size, shape, and depth, necessitating accurate quantification accounting for these differences. Temporal changes in storage capacity due to factors such as sedimentation, vegetation growth, and human activities also pose challenges for long-term hydrological studies. Moreover, limited surface water storage capacity, as playa lakes often lack outlets, can result in flooding during heavy rainfall events and drought conditions during dry periods.
- *Infiltration Rate*: Estimating infiltration rates in playa lake regions is complicated by the heterogeneous soil properties, influencing infiltration rates and patterns, requiring precise characterization for accurate estimation. Additionally, the impact of vegetation cover on infiltration rates alters soil moisture content and hydraulic conductivity, further complicating infiltration modeling efforts.
- *Losses*: Estimating losses in playa lake regions presents challenges, including accurately estimating evapotranspiration losses, which vary due to climatic conditions, vegetation cover, and soil moisture availability. Furthermore, understanding groundwater-surface water interactions and quantifying losses to groundwater requires detailed hydrogeological investigations.
- *Hydrological Models*: Modeling hydrological processes in playa lake regions presents challenges due to the complex interactions between surface water, groundwater, and sediment transport processes, increasing the complexity of model development. Furthermore, careful parameterization of hydrological models in data-scarce regions is essential to accurately capture the unique hydrological characteristics.

B.1.1.2 Hydrology of Arid Regions and Challenges Regarding Transportation Infrastructures

Arid areas can pose challenges for transportation infrastructure, particularly where flash floods and other extreme weather events are common. These floods can quickly erode and undermine roadways, bridges, and other infrastructures making them unsafe or impassable. Furthermore, the high rates of evaporation and low precipitation in arid regions may lead to the accumulation of salts and other minerals on the surface of roadways, which can degrade the pavement and reduce its lifecycle. Wind-blown sediment eroded from surrounding dry soils can also accumulate on roadways, reducing visibility and creating hazardous driving conditions. Some other challenges associated with transportation infrastructures in arid regions include:

- *Extreme Temperatures*: Arid regions often experience high temperatures, which can lead to deterioration of roads, bridges, and other transportation infrastructure over time.
- *Sand and Dust*: Arid regions are prone to sand and dust storms, which can reduce visibility and cause damage to roads, railways, and airports.
- *Limited Water Resources*: Arid regions typically have limited water resources, which can impact the availability of water for construction and maintenance of transportation infrastructure.
- *Soil Erosion*: Arid environments are susceptible to soil erosion, particularly during heavy rainfall events, which can undermine the stability of roads and other transportation structures.
- *Remote Locations*: Many arid regions are located in remote areas with limited access to transportation networks, making it challenging to build and maintain infrastructure.
- *Desertification*: Desertification, the process of land degradation in arid and semi-arid regions, can affect transportation infrastructure by altering soil properties and increasing the risk of landslides and erosion.

Some of the challenges associated with hydrology of arid areas include:

- *Rainfall-runoff:* Hydrological methods expressing the relationship between rainfall and runoff are typically developed for specific climate conditions, with parameters primarily tailored to humid climates where rainfall is more evenly distributed. Factors such as time of concentration, rainfall intensity, soil type, and land cover play crucial roles in predicting flow intensity and direction, but these parameters may vary significantly from one region to another.
- *Peak Rate Factors*: Hydrological studies in arid areas face challenges due to sparse data availability, making it difficult to assess peak rate factors accurately, particularly in predicting flash floods.
- *Climate Variability:* Extreme weather events, including droughts and intense rainfall, are common in arid areas, and climate change is expected to exacerbate these challenges by altering precipitation patterns and intensifying weather extremes. Climate variability greatly impacts the performance of hydrological models, with rainfall events in arid regions often being more intense and shorter in duration compared to humid regions. Several hydrological

models are specifically designed to analyze continuous precipitation events, which contrasts with the patterns observed in arid lands.

- *Vegetation Cover*: Vegetation cover differs significantly between humid and arid regions, influencing water retention strategies and overall hydrological processes. Arid areas experience high evapotranspiration due to intense solar radiation, high temperatures, and sparse vegetation cover, which depletes soil moisture and surface water resources.
- *Flash Flooding*: Arid areas are prone to flash flooding, which can result from intense rainfall events over short durations. These sudden floods can overwhelm drainage systems and cause rapid increases in streamflow, making it difficult to predict peak flows and time of concentration.
- *Limited Channel Storage*: Many arid regions have ephemeral or intermittent streams with limited channel storage capacity. This can result in rapid runoff response to rainfall events, influencing the timing and magnitude of peak flows.
- *Hydrological Models*: The main difficulty in simulating rainfall-runoff in arid and semi-arid regions arises from the climatic conditions. Models used in these areas frequently lack essential components necessary for precise and dependable results. This inadequacy originates from employing models primarily designed for humid regions, with parameters unsuitable for arid environments.

B.1.1.3 Hydrology of Karst Terrain and Challenges Regarding Transportation Infrastructures

Karst terrains can pose significant challenges for transportation infrastructure due to their unique characteristics. Underground channels and caverns allow water to move quickly and unpredictably through soluble rocks such as limestone leading to sinkholes, subsidence, and other hazards that can threaten transportation infrastructures. Some other challenges associated with transportation infrastructure in karst areas include:

- *Sinkholes*: Sinkholes can be caused by the collapse of underground caverns or the dissolution of soluble rocks by water. They can pose threats to transportation infrastructures causing roadways and bridges to collapse or become unstable.
- *Subsidence*: The movement of water through underground tunnels and caverns can lead to land subsidence or sinking of the ground surface causing damage to transportation infrastructure, especially in areas with heavy traffic or heavy loads.
- *Unpredictable Hydrology*: Predicting the water movement through karst can be difficult because it may vary significantly depending on many factors including precipitation, temperature, and land use changes. This can make it challenging to design transportation infrastructure that can withstand the hydrological variability in these areas.
- *Erosion*: Water movement through underground spaces may erode the surrounding rock and soil, leading to instability and potential damage to transportation infrastructure.

Karst hydrology presents several challenges, including:

- *Rainfall-runoff*: The existence of sinkholes, caves, and underground rivers poses challenges with rainfall-runoff analysis and how to incorporate losses in hydrologic models. Floodwater can appear and disappear quickly, making it difficult to predict and respond to flood events. During heavy rainfalls, water can enter these underground features and move rapidly through the karst aquifer, leading to sudden and sometimes catastrophic flash flooding.
- *Peak Flows*: Karst landscapes are often highly heterogeneous and anisotropic making the prediction of water movement in karst aquifers unpredictable and difficult to model accurately. Karst aquifers can also have a high degree of connectivity, with water moving swiftly through rock fractures, conduits, and other drainage systems which makes it challenging to determine the source of water, flow direction, and peak flow.
- *Losses*: In karst regions, streams abruptly enter and exit grounds resulting in a non-uniform loss in the downstream direction. It would be misleading to compute the loss of flow per unit stream length between the gauge stations and apply this loss rate to various sites along the stream where it is not gauged.
- *Data Collection and Modeling:* The highly complex and heterogeneous karst regions make data collection on groundwater resources and hydrological processes very challenging. This can make it difficult to develop accurate models for flood water availability prediction and developing mitigation measures.

B.1.2 Objective and Methodology

The primary objective of this review is to provide a comprehensive overview of current state of knowledge and practices regarding hydrological approaches to playa lakes, arid regions, and karst terrains. The methodology used to accomplish this objective can be outlined as follows:

- *Review of Design Guidance, Standards, and Recommendations*: A total of 55 documents were reviewed, extracting information pertinent to practical approaches for hydrology and hydraulic studies and design of transportation infrastructure, particularly focusing on drainage and stormwater systems in playa lakes, karst terrains, and arid regions. The following sources were consulted for this purpose:
    - State Departments of Transportation hydraulic/drainage design manuals,
    - Federal Highway Administration (FHWA) publications,
    - Stormwater design/management manuals from states, cities, and communities,
    - International hydraulic/drainage design guidance and manuals.
- *Review of Research Studies and Technical Reports*: A comprehensive review of more than 300 research studies and technical reports, presented at national and international conferences and published in scientific journals, was conducted. This review aimed to identify new approaches to hydrology and hydraulic studies in areas characterized by playa lakes, karst terrains, and arid conditions. The regions covered in these studies include not only the United States but also other parts of the world facing similar hydrology challenges.

B.1.3 Report Structure

This memorandum is structured as follows: **Chapter B1** provides an overview of the project background, and the methods used in conducting the literature search. **Chapter B2** summarizes the findings from the review of various state and federal design guidance and recommendations on hydrologic approaches to playa lakes, karst areas, and arid regions. **Chapters B3**, **B4**, and **B5** review research studies conducted in playa lakes, karst areas, and arid regions, respectively, and summarize approaches to addressing challenges regarding hydrology and hydraulic studies in these areas. Finally, **Chapter B6** provides a summary and conclusions of this literature review.

CHAPTER B2 : REVIEW STATE AND FEDERAL DESIGN GUIDANCE AND RECOMMENDATIONS ON HYDROLOGIC APPROACHES TO PLAYA LAKES, KARST AREAS, AND ARID REGIONS

A comprehensive review was undertaken to examine relevant design guidance and standards of practice developed by/for entities and regions facing hydrological challenges in areas such as playa lakes, karst terrains, and arid regions. This review included various sources, including state departments of transportation's hydraulic/drainage design manuals, the TxDOT Hydraulic Design Manual, the Federal Highway Administration (FHWA) publications, as well as states, cities, and communities stormwater design guidelines, and international design guidelines, among others. The findings of this review are presented in the subsequent sections.

B.2.1 States Departments of Transportation Hydraulic/Drainage Design Manuals

In order to conduct this review effectively, it was imperative to identify states situated in regions characterized by playa lakes, karst terrains, and arid conditions. Subsequently, a selection of Department of Transportation (DOT) manuals pertaining to hydraulic/drainage design from these identified states was made for review. The list of DOTs chosen for the examination of their manuals is provided in **Table B.1**.

Table B.1 List of DOTs selected for reviewing hydraulic/drainage manuals

Department of Transportation	Playa Lakes	Karst Areas	Arid Regions
Alabama (ALDOT)		x	
Arizona (ADOT)			x
California (Caltrans)			x
Colorado (CDOT)	x		
Florida (FDOT)		x	
Indiana (INDOT)		x	
Kansas (KDOT)	x		
Kentucky (KYTC)		x	
Minnesota (MDOT)		x	
Missouri (MoDOT)		x	
Nevada (NDOT)			x
New Mexico (NMDOT)	x	x	x
Oklahoma (ODOT)	x		
Pennsylvania (PennDOT)		x	
Tennessee (TDOT)		x	
Texas (TxDOT)	x	x	x
Utah (UDOT)		x	x
Virginia (VDOT)		x	
West Virginia (VWDOT)		x	

In this review, two types of information were sought: 1) the acceptable methods for hydrological analysis by the DOT, and 2) whether approaches to hydrological studies of playa lakes, karst terrains, and arid areas are provided in the manual. A summary of this review is presented in the following sections and summarized in **Tables B.2** to **B.5** for the playa lakes, karst regions, and arid areas, respectively.

B.2.1.1 Approaches to Hydrology of Playa Lakes by DOTs

Among the manuals examined concerning playa lakes, only the Oklahoma Department of Transportation Roadway Drainage Manual (ODOT, 2014) provides limited information on playas hydrology. Chapter 7 of this manual addresses the consideration of non-contributing areas within a drainage basin when utilizing the Oklahoma Rural Regression Equations (developed by the USGS), as detailed in **Table B.2**.

B.2.1.2 Approaches to Hydrology of Karst Regions by DOTs

The Florida, Kentucky, Pennsylvania, Virginia, and West Virginia Departments of Transportation offer some guidance on the hydrology of the karst region, each at different levels (**Tables B.3**).

The Florida Department of Transportation Drainage Design Guide (FDOT, 2019) mandates the exclusion of any areas containing sinkholes or depressions (non-contributing areas) from the total drainage area when determining drainage from 7.5-minute topographic maps.

The Kentucky Transportation Cabinet's Drainage Manual (KYTC, 2010) advises against deducting non-contributing areas (due to the presence of karst topography) in runoff calculations because of uncertainty and inaccuracy in determining the existing and future hydraulic capabilities of karst features.

The Pennsylvania Department of Transportation Drainage Manual (PennDOT, 2010) suggests that when determining runoff from basins containing karst topography, it may be appropriate to exclude all karst areas, as they may not contribute to flood runoff. Another approach to reducing runoff in karst topography is to apply a reduction factor. A reduction factor ranging between 0.84 and 0.86 may be applied for $Q_{2.33}$ to Q_{500}.

The Virginia Department of Transportation Drainage Manual (VDOT, 2023) offers guidance on constructing stormwater management facilities (SWMFs) if they are necessary along the periphery of a sinkhole. The design of these facilities must adhere to the guidelines outlined in **Chapter B5** of the VDOT Drainage Manual (VDOT, 2023), Virginia Department of Environmental Quality (DEQ) Technical Bulletin No. 2 "*Hydrologic Modeling and Design in Karst*" (VA DCR, 1999), and relevant sections of the Virginia Storm Water Management Handbook (VDEQ 1999).

The West Virginia Department of Transportation Drainage Manual (VWDOT, 2007) offers the most comprehensive approach to the hydrology of karst regions compared to other DOT manuals reviewed. It suggests a procedure for estimating infiltration loss in karst areas as part of runoff estimate. Additionally, it recommends methods that can be utilized to account for karst loss. These

methods are listed in **Table B.3**. Some of these methods are adopted by the Federal Highway Administration (FHWA, 2023) and discussed in **Section B.2.3.2.1**.

B.2.1.3 Approaches to Hydrology of Arid Areas by DOTs

The design manuals of the Arizona, California, and New Mexico Departments of Transportation include provisions for hydrological studies of arid areas, which are summarized in **Table B.4**.

The Arizona Department of Transportation Highway Drainage Design Manual (ADOT, 2014) offers recommendations on selecting the Rational Method's runoff coefficients (C), as well as specific values for surface retention loss and initial soil moisture, within the Green-Ampt method in HEC-HMS, for desert areas. Additionally, it provides an equation for calculating the time of concentration (T_c) for watersheds in desert areas. Moreover, the manual acknowledges that transmission loss may result in significant reductions in runoff volume, especially in ephemeral watercourses in Arizona that are initially dry. However, it recommends not incorporating such losses into a watershed rainfall-runoff model.

The California Department of Transportation Highway Design Manual (Caltrans, 2020) elaborates on the characteristics of storms in desert areas. It advises the use of the Rational Method for California's desert regions with areas smaller than 160 acres (0.25 mi^2), employing runoff coefficients (C) for Desert Areas provided in the manual. Additionally, the manual offers specific guidance on rainfall-runoff simulation and how hydrological factors such as rainfall, rainfall losses, transformation of effective rainfall, and channel routing should be addressed for desert areas. It suggests the utilization of new Regional Regression Equations developed for California's Desert regions. While these regression equations for the Northern Basin and Range region yield more accurate results than previous USGS-developed equations, there remains some uncertainty associated with them. Therefore, the manual suggests that developing a rainfall-runoff model may be preferable for ungauged watersheds in this region.

The New Mexico Department of Transportation Drainage Design Manual (NMDOT, 2018) suggests employing the Rational Method for desert regions with areas smaller than 160 acres (0.25 mi^2), utilizing provided runoff coefficients (C) specific to Desert Areas. In cases where the NRCS method is utilized, it recommends using curve numbers (CNs) for Arid and Semiarid Rangelands provided in the manual.

B.2.2 Texas Department of Transportation (TxDOT) Hydraulic Design Manual

The TxDOT Hydraulic Design Manual (TxDOT, 2019) offers very limited guidance on the hydrology of playa lakes, karst terrains, and arid areas. It does not provide provisions for rainfall-runoff studies in playa lakes; however, playas are mentioned in the context of mapping floodplains and special hazard areas (**Table B.2**). The manual also does not address challenges with hydrology studies in karst areas of Texas (**Table B.3**). In terms of hydrological studies in Texas arid zones, it mandates the use of runoff curve numbers (CNs) for Arid and Semiarid Rangelands if the NRCS Method is employed (**Table B.4**).

Table B.2 Summary of acceptable methods for estimating design discharge and pertinent hydrological information of playa lakes as detailed in the DOT's hydraulic/drainage manuals

Department of Transportation	Acceptable Methods for Estimating Design Discharge	Notes from the Manual on Hydrology of Playa Lake
Colorado (CDOT, 2019)	• Rational Method • UDFCD Modified Rational Method • NRCS (TR-55) • Colorado Urban Hydrograph Procedure • NRCS Unit Hydrograph Method • USGS Regional Regression • Statistical Method (gauge data) - Log-Pearson Type III	• No provision for playa lakes
Kansas (KDOT, 2023)	• Rational Method • Three Variable Regression Equations • USGS Regression Method • NRCS (TR-55) • Flood Hydrograph Simulation Method (HEC-1 and HEC-HMS)	• No provision for playa lakes
New Mexico (NMDOT, 2018)	• Rational Method • NRCS Simplified Peak Discharge Method • NRCS (SCS) Unit Hydrograph Method within HEC-HMS • USGS Regional Regression Equations • Statistical Method (gauge data)	• No provision for playa lakes
Oklahoma (ODOT, 2014)	• Rational Method • Modified Rational Method • NRCS (TR-55) • USGS Regional Regression Equations - Oklahoma Rural Regression Equations - Oklahoma Urban Regression Equations • USGS StreamStats Program • Statistical Method (gauge data) - Log-Pearson Type III	• If Rational Method is used, the recommended upper limit is 640 acres. • If Oklahoma Rural Regression Equations are utilized: - "Non-contributing Areas" such as playas, dry lakebeds, depression lakes, etc. should be identified. Such areas may be large enough to be designated as hydrologic units at any level of the hierarchy if they are within the size range for a given level. - Semi-confined basins contributing surface water to another area in wet years, but acting as a sink in dry years, may be considered as a hydrologic unit or non-contributing area. These types of special situations should be reviewed, coordinated and agreed upon at the State level. Assistance or consultation with climatologists or NOAA on prevailing water/precipitation regimes that may have a long-term influence on non-contributing areas should be explored.

		- If non-contributing areas are small and dispersed relative to the hierarchical level being delineated or if they are scattered throughout a drainage area, they should be considered as part of the encompassing delineated hydrologic unit. Note the size of the non-contributing area in the attribute file for the hydrologic unit containing the noncontributing area. Isolated non-contributing areas larger than 3000 acres should be delineated. - In addition, the user should consider the storage covered by lakes, ponds, wetlands, etc., in the watershed. If the percent of storage within the total contributing drainage area is significant (greater than 10%), the user should consider using a hydrograph.
Texas (TxDOT, 2019)	• Statistical Analysis of Stream Gauge Data - Log-Pearson Type III - Bulletin #17B • Omega EM Regression Equations • Rational Method • Hydrograph Method - Unit Hydrograph (UH) Model o Snyder's Unit Hydrograph o NRCS Dimensionless Unit Hydrograph - Kinematic Wave Overland Flow Model	• No provision for playa lakes is included in the manual; however, plays are mentioned in the manual in the following context: - Most of the mapped floodplains or special flood hazard areas (SFHAs) are riverine designated Zone A, AE, or A1-30; other types are playas (AH), flatlands with standing waters (AO), and coastal floodplains (V, VE, or V1-30). - ZONE AH: SFHAs inundated by 1% AEP (100-year) flood depths of 1 to 3 feet, usually areas of ponding. Best Flood Elevations (BFEs) are determined. In Texas, Zone AH usually applies to playas, low areas with no outflow. The only escapes are infiltration and evaporation. - Zone AH - Places of no outflow, such as playas, in which the BFE has been determined are labeled Zone AH. Structures in playas are equalizers and as such, the bridges and culverts typically need no hydraulic modeling. However, the designer is required to calculate how much the BFE will be raised because the roadway and structure will reduce storage in the playa if any roadway work is in Zone AH and below the BFE.

Table B.3 Summary of acceptable methods for estimating design discharge and pertinent hydrological information of karst regions as detailed in the DOT's hydraulic/drainage manuals

Department of Transportation	Acceptable Methods for Estimating Design Discharge	Notes from the Manual on Hydrology of Karst Regions
Alabama (ALDOT, 2022)	• Rational Method • NRCS TR-55 • USGS Regression Equations • Small Storm Hydrology	• No provision for karst regions
Florida (FDOT, 2019)	• Rational Method • Modified Rational Method • USGS Regression Equations • Developed Tampa Equations • Developed Leon Equations • NRCS Unit Hydrographs	• In areas of karst topography for the Tampa Area and Leon County regression equations, some basins may contain closed depressions and sinkholes, which do not contribute to direct runoff. When determining the drainage area from 7.5-minute topographic maps, subtract any area containing sinkholes or depressions (non-contributing areas) from the total drainage area.
Indiana (INDOT, 2014)	• Rational Method • NRCS (SCS) Unit Hydrograph Method TR-20/HEC-HMS • IDNR Coordinated Discharge Curves • StreamStats Program • Frequency Analysis of Stream-Gauging Records (Bulletin #17B) • Purdue Regression Equations (Rural Areas) • FEMA	• No provision for karst regions
Kentucky (KYTC, 2010)	• Rational Method • USGS Regression Equations • NRCS Unit Hydrograph	• It is acknowledged that runoff reaching a highway structure in a karst area might decrease as water gets intercepted by karst features. However, due to the uncertainty and inaccuracy in determining existing and future hydraulic capabilities of karst features, drainage areas are generally not reduced in the runoff calculations due to the presence of karst topography. • If Rational Method is used, the recommended upper limit is 200 acres. • Drainage in karst topography often requires the use of sinkholes as drainage outlets. However, this practice outlets require special consideration due to several factors, the best option is to avoid karst elements altogether. Early alignment development should consider the location of individual karst elements such as sinkholes and strive to avoid impacting them.
Minnesota (MnDOT, 2000)	• Rational Method • USGS Regression Equation • NRCS Unit Hydrograph	• No provision for karst regions

	• Statistical Method (gauge data) - Log-Pearson Type III and Bulletin #17B	
Missouri (MoDOT, 2019)	• Rational Method • USGS Regression Equation • NRCS Unit Hydrograph	• No provision for karst regions
New Mexico (NMDOT, 2018)	• Rational Method • NRCS Simplified Peak Discharge Method • NRCS (SCS) Unit Hydrograph Method within HEC-HMS • USGS Regional Regression Equations • Statistical Method (gauge data)	• No provision for karst regions
Pennsylvania (PennDOT, 2010)	• Rational Method • NRCS Unit Hydrograph • USGS Regional Regression Equations • Pennsylvania Regional Regression Method IV (PSU-IV) • HEC-1 & HEC-HMS • NRCS (WINTR-55 and TR55) • NRCS EFH-2 • Statistical Method (gauge data) - Log-Pearson Type III and Bulletin #17B	• It is acknowledged that regions underlain by soluble rock formations, especially limestone, often have characteristics of "karst" topography, which produce little surface runoff. In these areas, the runoff usually enters the ground through sinkholes and pursues its course to an outlet through a system of underground passages. In determining the runoff from basins containing karst topography, it may be appropriate to exclude all karst areas, for they may not contribute toward flood runoff. Another approach to reduce the runoff in karst topography would be to apply a reduction factor such as the procedure outlined in Pennsylvania Regional Regression Method IV (PSU-IV). A reduction factor between 0.84 to 0.86 may be applied for $Q_{2.33}$ to Q_{500}.
Tennessee (TDOT, 2021)	• Rational Method • HEC-1 & HEC-HMS • NRCS (TR20, TR-55) • USGS Regional Regression Equations • Tennessee Regional Regression Equations	• No provision for karst regions
Texas (TxDOT) (2019)	• Statistical Analysis of Stream Gauge Data - Log-Pearson Type III and Bulletin #17B • Omega EM Regression Equations • Rational Method • Hydrograph Method - Unit hydrograph (UH) Model o Snyder's Unit Hydrograph o NRCS Dimensionless Unit Hydrograph • Kinematic Wave Overland Flow Model	• No provision for karst regions
Utah (UDOT, 2018)	• Rational Method • NRCS Curve Number Method • Statistical Method (Bulletin #17C)	• No provision for karst regions

	• USGS Regression Equations • Other Hydrologic Methods (Based on the complexity of the project)	
Virginia (VDOT, 2023)	• Rational Method • Modified Rational Method • NRCS Unit Hydrograph Method • NRCS Graphical Peak Discharge Method • NRCS EFH-2 • Anderson Method (USGS) for Northern Virginia • USGS Regional Regression • Stream Gauge Data	• Construction of stormwater management facilities (SWMFs) within a sinkhole is prohibited. If SWMFs are required along the periphery of a sinkhole, the design of such facilities shall comply with the guidelines in Chapter 5 of the VDOT Drainage Manual (see below), DEQ's Technical Bulletin No. 2 (Hydrologic Modeling and Design in Karst) and applicable sections of the Virginia SWM Handbook. <u>Excerpts from Chapter 5 of the VDOT Drainage Manual</u> • Karst terrains primarily occur within the Valley and Ridge Physiographic Province of western Virginia. Karst type terrains are also known to occur in very limited areas of the Blue Ridge, Piedmont and Coastal Plain Physiographic Provinces of Virginia. While information contained in these guidelines is directed more to those sinkholes located in the Valley and Ridge Physiographic Province, the same considerations should be applied to sinkholes located in other areas of the state. • In areas of karst topography, roadside ditches with a gradient of less than 5% may need to be lined to inhibit the infiltration of surface waters. • Where the roadway traverses over or through a sinkhole area, the sinkhole should be treated in accordance with one of the typical details shown on Standard Insertable Sheet No. isd/msd 2944 unless otherwise directed by the District Materials Engineer: - Detail No. 1 should be used for sinkholes that receive stormwater runoff from relatively large areas and have a well-defined opening (throat). This treatment involves cleaning out soil and debris to expose the throat, installing a length of pipe to convey surface drainage into the sinkhole and backfilling with riprap and successive layers of smaller aggregate and a geotextile fabric prior to the placement of the regular roadway embankment material. - Detail No. 2 should be used for sinkholes with broad, flat depressions and which have no defined throat. These sinkholes typically receive stormwater runoff from relatively small areas. The width of the roadway embankment is generally less than the width of the depression. This treatment involves the placement of riprap in the bottom of the roadway embankment to allow for the continued infiltration of surface flows. The riprap is capped with successive layers of smaller aggregate and a geotextile fabric before placement of the regular roadway embankment material. - Detail No. 3 should be used for small shallow sinkholes that receive stormwater runoff from relatively small areas and where the roadway embankment will cover most or all of the depression. This treatment involves

		filling the depression with successive layers of smaller aggregate and a geotextile fabric before placement of the regular roadway embankment material. Since this treatment effectively "caps" the sinkhole and precludes the entry of surface water, a drainage ditch or other hydraulic conveyance is typically required along the edge of the roadway embankment to convey stormwater runoff to an adjacent outfall.
West Virginia (VWDOT, 2007)	• Rational Method • NRCS Graphical Peak Discharge Method (TR-55) • NRCS Unit Hydrograph Method • Modified Rational Method • USGS Regional Regression • Stream Gage Data (USGS Bulletin #17B) • Watershed Models (TR-20 and HEC-HMS)	• The influence of karst topography (areas) on hydrologic process is discussed in this manual. Since standard hydrologic methods do not account for the infiltration losses in karst terrain, the following procedure is recommended for estimating karst loss as part of a runoff estimate: 1. Define any areas within the apparent contributing drainage area where surface drainage has no means of escaping offsite other than through the karst strata. These areas can be assumed to contribute no surface runoff and can be subtracted from the contributing drainage area. 2. Areas on the mapping that show no defined streams or streams that disappear may also be subtracted from the contributing drainage area. These areas should be verified in the field. 3. Determine the remainder of the drainage area underlain by karst strata in %. 4. Calculate the peak rate of runoff using the standard hydrologic methods presented in this manual and multiply that value by the karst loss coefficient (Table 4-1 of the manual) based on the percent of area underlain by karst. The coefficient is intended to depict projected flow losses into bedrock. • Other methods that can be utilized to account for karst loss include: - Manipulating the runoff coefficient in the Rational Method. - Use of a Type I rainfall distribution (low-intensity, longer-duration rainfall) within a Type II areas (characterized by intense, shorter-duration rainfall events), or manipulating the curve number values within the TR-55 method. • The USGS method should be avoided in a karst area if excessive runoff flows into a cavity. If the method is applied to a karst area, there should be a field investigation to ensure the previous statement does not hold true. The equations are empirically based, and the gauge data used to derive the east region equations cover areas of karst topography where the data used to derive the south region equations cover less area influenced by karst topography. • Karst Surcharge: A rare event that may require consideration in areas of karst topography is the possibility of sinkhole surcharge. In this case, the opposite condition than what is expected occurs and water flows out of a depressed surface area during rainfall events. This occurs due to the connectivity of the underground conveyance network. These natural runoff detention areas may not be significant in the overall hydrology of an area, but they could exert a significant impact by inundation during an extreme rainfall. The effect of this type of event may be considered similar to the effect of a check storm.

Table B.4 Summary of acceptable methods for estimating design discharge and pertinent hydrological information of arid areas as detailed in the DOT's hydraulic/drainage manuals

Department of Transportation	Acceptable Methods for Estimating Design Discharge	Notes from the Manual on Hydrology of Arid Areas
Arizona (ADOT, 2014)	• Rational Method • Regional Regression Equations • Unit Hydrograph (HEC-HMS) • FLO-2D	• If Rational Method is used, the recommended upper limit is 160 acres. Runoff coefficients (C) for desert areas are provided through a C-P_1 (1 hr precipitation) curve. • If the HEC-HMS model is utilized to develop a flow hydrograph: - Specific values for surface retention loss (in the Green-Ampt method) are recommended for desert areas. - The initial soil moisture is recommended to be set as "dry" for desert areas. • An equation for calculating the time of concentration (T_c) for watersheds in desert areas is provided. • It is recognized that transmission loss may lead to significant reductions in runoff volume, especially in ephemeral watercourses in Arizona that are initially dry. However, incorporating such losses into a watershed rainfall-runoff model requires approval from ADOT, as procedures and reliable data for estimating transmission losses are generally unavailable.
California (Caltrans, 2020)	• Rational Method • USGS Regional Regression Equations (USGS Water-Resources Investigation 77-21, Improved Highway Design Methods for Desert Storms) • NRCS (TR55) • Unit Hydrograph (gauged data) • Synthetic Unit Hydrograph • SCS Unit Hydrograph • S-Graph Unit Hydrograph • Statistical Method (gauge data) - Log-Pearson Type III - Bulletin #17B	• The characteristics of storms in desert areas are explained in the manual. • New Regional Regression Equations are developed for California's Desert regions. While the regression equations for the Northern Basin and Range region provide more accurate results than previous USGS-developed equations, there is some uncertainty associated with them. Therefore, the development of a rainfall-runoff model may be preferable for ungauged watersheds in this region. • If Rational Method is used, the recommended upper limit for California's desert regions is 160 acres (0.25 mi^2). Runoff coefficients (C) for Desert Areas are provided. • For rainfall-runoff simulation, specific information is provided on how hydrological factors such as rainfall, rainfall losses, transformation of effective rainfall, and channel routing should be addressed.
Nevada (NDOT, 2006)	• Rational Method • Regression Equations • Statistical Analysis • Synthetic Modeling - SCS(NRCS) Unit Hydrograph • NRCS (TR55)	• No provision for arid areas

	• Other Methods (Local published hydrologic methods may be used with prior written approval by the Principal Hydraulic Engineer.	
New Mexico (NMDOT, 2018)	• Rational Method • NRCS Simplified Peak Discharge Method • NRCS (SCS) Unit Hydrograph Method within HEC-HMS • USGS Regional Regression Equations • Statistical Method (gauge data)	• If Rational Method is used, the recommended upper limit is 160 acres. Runoff coefficients (*C*) for Desert Areas are provided. • Runoff Curve Numbers for Arid and Semiarid Rangelands should be used if NRCS method is employed. • It is acknowledged that dryland streams typically flow during spring and after major storms, making their response more hydrologically dependent compared to streams in humid environments. Therefore, the lack of significant morphological changes in dryland streams over time should not necessarily be interpreted as indicative of system stability. • It is recognized that designing for water quality protection in the desert southwest is a relatively nascent field. Due to the infrequency and unreliability of precipitation, data on the effectiveness of Best Management Practices (BMPs) is not easily accessible.
Texas (TxDOT, 2019)	• Statistical Analysis of Stream Gauge Data - Log-Pearson Type III - Bulletin #17B • Omega EM Regression Equations • Rational Method • Hydrograph Method - Unit hydrograph (UH) Model o Snyder's Unit Hydrograph o NRCS Dimensionless Unit Hydrograph - Kinematic Wave Overland Flow Model	• If NRCS Method is employed, runoff curve numbers for (*CN*s) Arid and Semiarid Rangelands should be used.
Utah (UDOT, 2018)	• Rational Method • NRCS Curve Number Method • Statistical Method (Bulletin #17C) • USGS Regression Equations • Other Hydrologic Methods (Based on the complexity of the project)	• No provision for arid areas

B.2.3 Federal Highway Administration (FHWA) Publications

Two publications from the Federal Highway Administration (FHWA) were identified, addressing the hydrology of arid areas and karst regions. However, no FHWA document is presently available regarding the hydrology of playa lakes. The following sections present a summary of the discussions contained within these two federal publications.

B.2.3.1 Highway Hydrology – Hydraulic Design Series No. 2

The Federal Highway Administration- Highway Hydrology (FHWA, 2024) covers several special topics in hydrology. Section 11.3 of this document addresses various aspects of hydrology specific to arid regions. It discusses topics such as gauged flow analysis, regression equations customized for the southwestern United States, transmission losses, formation and behavior of alluvial fans, and bulked flow. By examining these subjects, the section offers valuable insights into understanding the distinctive hydrological dynamics and challenges prevalent in arid environments. The following passages are acquired for this document.

B.2.3.1.1 Gauged Flow Analysis in Arid Areas

In arid regions, annual floods typically follow a Log-normal or Extreme Value Distribution (EVD) pattern. Log Pearson Type III curve fitting techniques can be used if annual peak flow series have non-zero values. However, it is common for annual maximum flood records in these regions to include zero values. When zero values are present, logarithmic frequency curves, such as the Log Pearson Type III, need to be adjusted because the logarithm of zero is negative infinity. The USGS Bulletin 17B (USGS,1982) outlines a method known as the conditional probability adjustment, to compute frequency curves for records containing zero-flood years. This method calculates three types of frequency curves: *the initial curve*, *the conditional frequency curve*, and *the synthetic frequency curve.* The choice of curve for estimating flood magnitudes depends on the judgment of the hydrologist. The procedure to follow when analyzing records that include zero-flood years consists of the following six steps:

- Conduct a preliminary analysis,
- Check for outliers,
- Compute unadjusted frequency curve,
- Compute conditional frequency curve,
- Compute synthetic frequency curve,
- Select frequency curve to make estimates.

Each of these steps is discussed in detail in Section 9.3.1 of the "*Highway Hydrology – Hydraulic Design Series No. 2"* publication (FHWA, 2002).

B.2.3.1.2 Regression Equations for Arid Areas of Southwestern U.S.

The document presents a summary of findings from the USGS report that provides regression equations for the southwestern U.S. including Arizona, Nevada, and Utah, and parts of California, Colorado, Idaho, New Mexico, Oregon, Texas, and Wyoming. These equations are developed for estimating 2-, 5-, 10-, 15-, 50-, and 100-year peak discharges at ungauged sites in the southwestern United States. The equations are applicable to ungauged streams that drain basins of less than about 200 mi^2 (500 km^2).

B.2.3.1.3 Transmission Losses in Arid Areas

As the initial part of a runoff hydrograph enters and traverses a dry stream channel, considerable quantities of water have the potential to permeate into the stream's bed and banks. This infiltration is referred to as transmission loss. Rates of transmission loss exhibit substantial variability throughout the duration of a flood hydrograph and across different regions. These losses are significant as they have the capacity to considerably alter the shape of a hydrograph and because the volume of seepage can diminish the flow volume at downstream channel sections.

The magnitude of losses depends on several factors, including the material characteristics of the stream cross-section, the surface area of the bed and banks within the reach, the position of the groundwater table, and the antecedent moisture of the cross-section. Additionally, the presence and type of vegetation in the stream also play a significant role. Although the latter two factors are typically overlooked in design processes, they may require consideration during data analysis.

For situations where observed inflow and outflow data are available, and there is no consistent lateral inflow or out-of-bank flow, the approach that is discussed in Chapter 19 of the National Engineering Handbook (Lane, 1983) can be employed to estimate transmission losses. It is advisable to refer to this chapter for a thorough understanding of the assumptions and limitations inherent in this methodology.

B.2.3.1.4 Alluvial Fans in Arid and Semi-arid Areas

Alluvial fans in arid and semi-arid regions are sedimentary deposits found at topographic breaks, such as mountain fronts or valley sides, taking on a fan-shaped appearance. Their formation requires a source of sediment and debris, with mechanisms to transport this material to the depositional area. In this zone, the stream's sediment-carrying capacity reduces due to increased flow area. Key features of alluvial fans include the topographic apex and the hydrographic apex, defining the highest points on active fans where flow commences and terminates. Flow paths on active fans are unpredictable, often diverging and rejoining, presenting significant design challenges for highway construction.

Assessing the hydrologic and hydraulic characteristics of alluvial fans involves three key phases. Firstly, identifying the presence of alluvial fans within the project area, which can be done through various maps and aerial photographs, supplemented by on-site visits. Secondly, distinguishing between active and inactive regions of the fan, where active areas exhibit newer sediment deposits and less vegetation, potentially leading to channel avulsion. Inactive regions typically support

vegetation and maintain channel capacity. Lastly, defining the design flow at specific points on the fan, considering factors such as precipitation, runoff, and the probability of flooding. Sediment content in flows varies, requiring careful design of channel crossings and structures. Evaluating the conditional probability of flooding aids in determining the T-year flood at particular locations across the active portion of the fan.

FEMA's Guidelines for Determining Flood Hazards on Alluvial Fans (FEMA, 2000) describes the three phases of flood assessment specific to these environments. The U.S. Army Corps of Engineers (USACE, 1993) has devised a methodology and computer program employing risk-based analyses to estimate flood hazards on alluvial fans, detailed in the Guidelines of Risk and Uncertainty Analysis in Water Resources Planning (USACE, 1992). FEMA suggests employing the FAN computer program (FEMA, 1990). Additionally, two-dimensional models can be utilized to simulate various flow characteristics on alluvial fans, including those with significant sediment, unconfined flow, split flow, mud and debris flow, and complex urban flooding. The Flood Insurance Study Guideline and Specifications for Study Contractors by FEMA (1995) offer applicable guidelines and methods for such conditions. Moreover, USACE's Assessment of Structural Flood-Control Measures on Alluvial Fans (USACE, 1993) outlines various flood control measures, their pros and cons, and provides case studies of their implementation.

B.2.3.2 Highway Hydrology: Evolving Methods, Tools, and Data – HEC-19

Chapter 7 of this newly published Federal Highway Administration - Highway Hydrology (FHWA, 2023) provides engineers with an introduction to karst terrain, including methods for its identification and the implications for roadway design. It highlights the distinctive characteristics of karst terrain that significantly influence runoff patterns within watersheds, especially when compared to nonkarst areas. In karst terrain, initial abstraction and rainfall losses tend to be higher due to the increased storage capacity of karst features, resulting in amplified runoff effects during smaller, more frequent storms compared to larger ones. Urban development in karst regions, such as covering surfaces with impermeable materials and filling sinkholes, may reduce rainfall losses but can potentially exacerbate post-development runoff volumes and peak flows. The document outlines various methods for estimating runoff in karst regions, which are briefly discussed in the following section.

B.2.3.2.1 Estimating Runoff in Karst Regions

Drainage designers employ numerous methods to incorporate karst loss into estimates of runoff. These methods include:

- Adjusting the runoff coefficient in a rainfall-runoff method,
- Using an NRCS Type I rainfall distribution (low-intensity, longer-duration rainfall) within a Type II area (characterized by intense, shorter-duration rainfall events),
- Adjusting the curve number values or peak rate factors using the TR-20 method,
- Applying regression equations developed for karst terrain, and
- Applying empirical reduction factors.

The first three methods employ standard hydrological tools that can be applied across various conditions. For instance, Laughland (1996) utilized a curve number adjustment approach within the Pennsylvania State University (PSU-IV) software. While the NRCS rainfall type distributions are gradually being replaced with newer ones, the principles of the second method could still be adapted to accommodate these updates. Designers rely on engineering judgment and site-specific information to make appropriate adjustments for each situation. As an illustration of the fourth method, the U.S. Geological Service (USGS) conducted a study across eight distinct hydrological regions, developing regression models using rainfall data and stream gauge records (Flippo, 1977). One of these models, applicable to drainage basins primarily underlain by limestone or dolomite bedrock in West Virginia and Pennsylvania is:

$$Q = cA^x \quad \text{(B-1)}$$

where Q is runoff (ft^3/s), c and x are constant values depending on AEP (Annual Exceedance Probability), and A is the drainage area (mi^2). **Table B.5** provides c and x values for different AEPs.

Table B.5 Values of c and x in the USGS Regression Equation (Adopted from Flippo, 1977)

Annual Exceedance Probability (AEP)	Return Period (yr)	c	x	Standard Error
0.5	2	23.5	0.880	-
0.1	10	39.8	0.933	26
0.04	25	49.1	0.952	27
0.02	50	56.0	0.970	31
0.01	100	64.4	0.979	33

The drainage area in **Equation B.1** refers to the part of the watershed that ultimately flows to the outlet. However, the total drainage area should exclude regions that drain to streams ending or disappearing in karst features, as well as any surface areas where drainage is not directed to the outlet but instead passes through the underlying karst formations (WVDOT, 2007). The karst system has the capability to redirect surface flow to groundwater or alternate streams, consequently reducing the effective drainage area (**Figure B.1a**). Conversely, karst features can increase the watershed area (**Figure B.1b**).

The methodology presented by **Equation B.1** relies on empirical data specific to each region. Given that empirical coefficients can differ regionally, and hydrologic data are frequently restricted in karst regions, practitioners must take into account evolving technologies and associated limitations when utilizing this method.

The final method for estimating runoff involves utilizing a peak flow method, which is then multiplied by an empirical reduction factor or "*karst loss coefficient"*. Laughland (1996) introduced a karst loss coefficient, determined as a function of the percentage of the watershed area with underlying karst, as outlined in **Table B.6**. This coefficient accommodates the abstraction

conveyed to the bedrock. Designers have the option to validate and fine-tune these coefficients through field observations and measurements, where feasible.

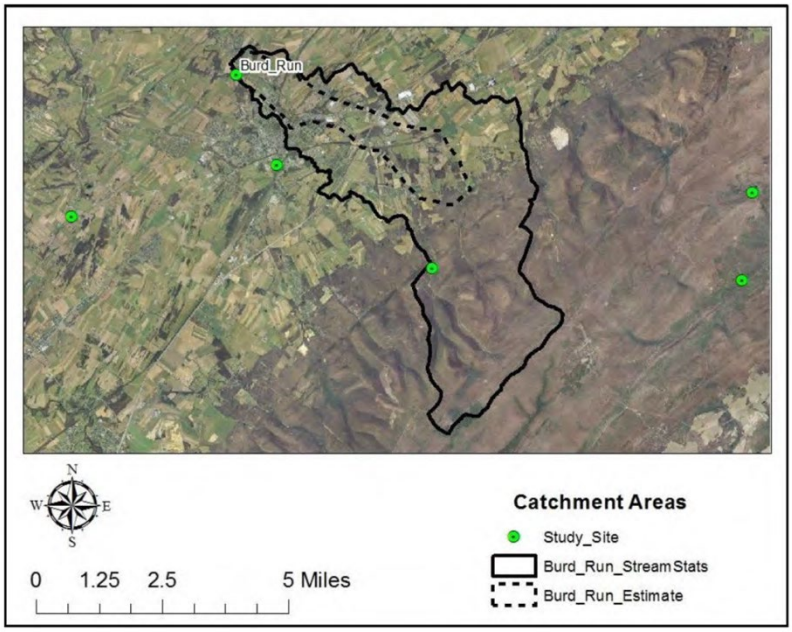

(a)

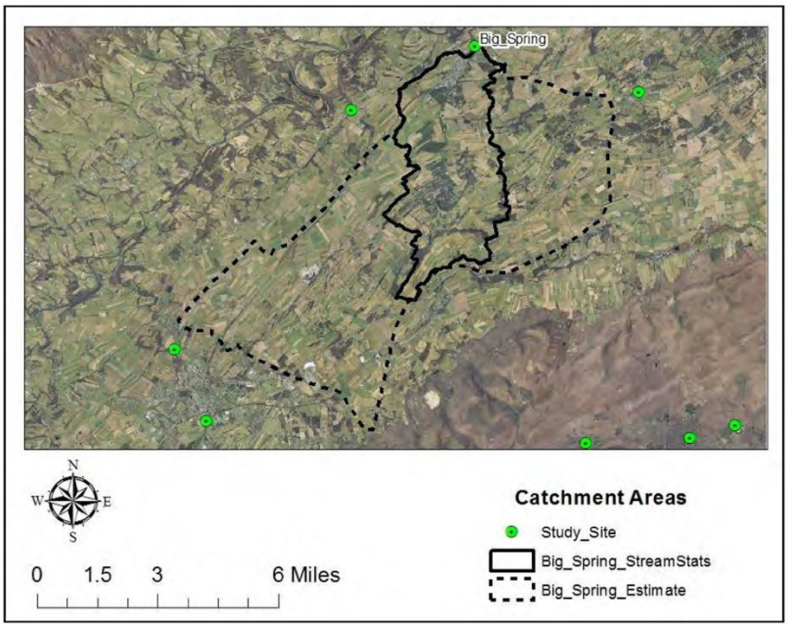

(b)

Figure B.1 Examples of (a) increase in effective drainage area (Burd Run watershed), and (b) decrease in effective drainage area (Big Spring Creek watershed) in south central Pennsylvania (Hawkins and Weichel, 2015)

Table B.6 Karst loss coefficients (Adopted from FHWA, 2023)

Karts Area (%)	Annual Exceedance Probability (Return Period (yr))				
	0.5 (2)	**0.1 (10)**	**0.04 (25)**	**0.02 (50)**	**0.01 (100)**
100	0.33	0.43	0.44	0.46	0.50
90	0.35	0.46	0.48	0.5	0.56
80	0.38	0.51	0.53	0.56	0.62
70	0.47	0.58	0.60	0.62	0.68
60	0.55	0.66	0.67	0.70	0.74
50	0.64	0.73	0.74	0.76	0.80
40	0.73	0.80	0.81	0.82	0.85
30	0.82	0.86	0.87	0.87	0.89
20	0.91	0.92	0.92	0.92	0.93
10	1.00	0.98	0.98	0.98	0.97
0	1.00	1.00	1.00	1.00	1.00

B.2.4 Stormwater Design/Management Manuals

Several stormwater manuals from various states and cities offer guidance on the hydrology of playa lakes, karst regions, and arid areas. The contents of these manuals pertaining to approaches to hydrology of these areas are summarized in the following sections.

Playa Lakes

The City of Lubbock Drainage Criteria Manual (City of Lubbock, 2019) and the City of Amarillo Stormwater Management Criterion Manual (City of Amarillo, 2008) address the challenges associated with designing stormwater systems in playa lake areas. They offer various approaches to hydrology and hydraulic design tailored to these systems. The following sections provide a summary of the pertinent discussions presented in these manuals regarding hydrology and hydraulic studies of playas.

City of Amarillo Stormwater Management Criterion Manual

The manual mandates the following general considerations for stormwater design and management in playas:

- *Playa Effect and Tailwater*: The depth of flow in the receiving drainageway or playa must be taken into consideration for backwater computations for both minor and major storm runoffs.
- *Playa Management*: Predicted levels for the playas for return intervals of 2-year through 100-year shall be determined by the Playa Simulation Model (ASAPP).
- *Detention and Retention*: Stormwater runoff may be stored in detention and retention basins and playas.
- *Operations and Maintenance*: Operation and maintenance of stormwater facilities and playas are required to ensure that they will perform as designed.

Chapter 8 of the manual covers design considerations for detention facilities within playas. Here is a summary of these considerations:

- *Expected Water Surface Elevation*: The City has computed expected water surface elevations (based on ultimate development conditions) for the 2- and 100-year return periods as well as the maximum historical level for many of the playas in the vicinity of the City. These levels were determined using the Amarillo Simulation Analysis of Playa Performance (ASAPP) model.
- *Analysis of Tailwater Control Conditions Caused by Playas:* When designing or evaluating hydraulic systems influenced by tailwater from playas, it is crucial to base the design level on specific flood levels associated with playas. These levels can be acquired from the City Engineer and should align with the return interval of the contributing drainage system. For instance, if a bridge is designed to withstand the peak of a 100-year storm and is situated near a playa where backwater effects control tailwater conditions at the bridge, computations should begin with the playa's 100-year flood level. Although experiencing a 100-year storm and a 100-year tailwater condition simultaneously is unlikely, it is a prudent design approach. Deviations from this method require approval from the City Engineer.
- *Detention Basin Design Criteria:* The Rational Method shall be used for detention basin design for small areas (20 acres or less). For watersheds larger than 20 acres, methods incorporating a runoff hydrograph, such as HEC-1, must be employed. Runoff hydrographs must be developed for evaluating drainage system performance during minor and major storm events. When computing runoff hydrographs without continuous accounting of antecedent moisture conditions, assume antecedent moisture condition II (i.e. average soil moisture conditions).
- *Design Storm*: Detention basins shall be designed to restrict the peak rate of discharge from the basin for both the 2-year and 100-year events to either the pre-development rate or a rate that avoids exacerbating flooding or channel instability downstream when combined with overall watershed development and downstream drainage capacities.
- *Freeboard*: A minimum of one (1) foot of freeboard shall be added to the design water surface elevation. Backwater computations for runoff entering playas should begin with an elevation based on a compatible storm. It is the developer's responsibility to assess if extra freeboard is needed. The City Engineer may mandate additional freeboard if deemed necessary for safety or maintenance reasons. The design storm must flow through the outlet without surpassing the structure's crest.
- *Hydraulic Design Method Analysis:* Various methods for calculating the runoff peak and volume from a watershed situated in playas are outlined in the manual. These methods comprise the Modified Rational Method (for watersheds of 20 acres or less), the hydrograph procedure for storage analysis, and the Modified Pulse Routing Procedure.

City of Lubbock Drainage Criteria Manual

The manual covers various aspects related to playa lakes, including considerations for stormwater management and design in areas affected by playas. Key points from the manual include hydrological considerations, design guidelines, regulatory requirements, and maintenance considerations. Some aspects of hydrology and hydraulic studies specific to playas are discussed in Chapters 3 and 4 of the manual, respectively. However, Chapter 5 is dedicated solely to playas. The chapter provides guidance on the appropriate methodologies and assumptions for analyzing playas and playa systems including hydrological calculations, storage calculations, initial playa conditions, hydrologic playa routing, and playa analysis. Details of these methodologies and assumptions are presented in **Chapter B3** of the present document, along with information gathered from other references.

Karst Regions

In karst landscapes, the presence of porous limestone or other soluble rock formations allows for rapid infiltration of water into underground aquifers and conduits, rather than surface runoff. This rapid infiltration can lead to several hydrological challenges for stormwater management including reduced surface water availability, contaminant transport, increased flooding risk, groundwater recharge, and erosion and sinkhole formation. Several states, cities, and communities situated in karst regions of the United States have devised guidelines and strategies tailored to the distinctive features of karst landscapes. Examples of the manuals reviewed are:

- Minnesota Stormwater Manual (Minnesota Pollution Control Agency, 2008),
- St. Johns River Water Management District, Florida: Application Handbook, Volume II (St. Johns River Water Management District, 2018),
- Stormwater Design Guidelines for Karst Terrain in the Chesapeake Bay Watershed (Chesapeake Stormwater Network, 2009),
- Tennessee Permanent Stormwater Management and Design Guidance Manual - Appendix B (Tennessee Department of Environment and Conservation, 2014),
- Town of Cutler Bay Stormwater Manual, Florida (Town of Cutler Bay, 2018),
- Virginia Stormwater Management Handbook: Appendix 6-B: Stormwater Design Guidelines for Karst Terrain in Virginia (Virginia Department of Environmental Quality, 2013),
- Water Resource Management Manual Carroll County, Maryland (Carroll County, 2011), and
- West Virginia Stormwater Management and Design Guidance Manual (West Virginia Department of Environmental Protection, 2012).

These manuals primarily focus on additional features that should be considered in designing stormwater systems in karst areas. They also provide guidelines and approaches for preliminary and detailed site karst investigations, assessing future groundwater contamination risk, general stormwater design principles in karst, design criteria for specific stormwater treatment practices, and sinkhole remediation in stormwater practices.

Those stormwater design manuals that address the estimation of runoff in karst terrains rely solely on the *karst loss coefficient method* introduced by Laughland (1996). Examples include the Tennessee Permanent Stormwater Management and Design Guidance Manual (Tennessee Department of Environment and Conservation, 2014), the Stormwater Design Guidelines for Karst Terrain in the Chesapeake Bay Watershed, and the Virginia Stormwater Management Handbook. These manuals highlight that many traditional NRCS hydrologic models tend to overestimate pre-development runoff in karst terrains due to high initial abstraction and rapid conversion of storm flows to subsurface flows. Over-predictions are common for smaller storms but less so for larger events like the 100-year storm. Therefore, designers must adjust NRCS computations to reflect lower pre-development peak discharge rates accurately. Further hydrologic monitoring and modeling research are crucial for more reliable predictions.

The Virginia Stormwater Management Handbook (Virginia Department of Environmental Quality, 2013) presents a method for estimating stormwater runoff losses in karst settings, adapted from Laughland (2007). This method offers multiplier factors (presented in **Table B.6**) used to adjust TR-55 and TR-20 pre-development rates, as follows:

1. Delineate the contributing drainage area or watershed to be studied.
2. Define any sinkhole areas within the contributing drainage area where surface drainage has no means of escaping offsite, other than downward through the karst strata (i.e., cracks, sinks, etc.). These areas can be assumed to contribute no surface discharge and can be subtracted from the contributing drainage area from Step 1.
3. Determine the amount of the contributing drainage area (from Step 2) underlain by karst strata (in percent).
4. Calculate the peak rate of runoff from the contributing drainage area using standard hydrologic methods and reduce the calculated value by multiplying by the *Karst Loss Modification Value* (**Table B.6**), based on the percent karst (% Karst) calculated in Step 3.

This method is adopted in HEC-19 – Highway Hydrology: Evolving Methods, Tools, and Data publication (FHWA, 2023) (see **Section B.2.3.2**) and by VWDOT (see **Table B.3**).

Arid Areas

The drainage manuals of various communities situated in arid regions of the United States were reviewed to analyze their approaches to hydrological design for stormwater management. Examples of these manuals include:

- Drainage Policies and Standards for Maricopa County, Arizona (Maricopa County, 2018),
- City of El Paso Stormwater Design Manual (City of El Paso, 2022),
- Drainage Criteria and Design Manual, Gainesville, Texas (City of Gainesville),
- San Bernardino County, California, Hydrology Manual (San Bernadino County,1986 and 2010), and
- Stormwater Design Manual, City of South Salt Lake, Utah (City of South Salt Lake, 2020).

Except for the San Bernardino County Hydrology Manual, the NRCS method and associated curve numbers from the FHWA HEC-22 publication (FHWA, 2001) are adopted by other manuals for estimating stormwater peak discharge in desert areas.

The San Bernardino County Hydrology Manual (San Bernardino, 1986) discusses criteria and parameter selection for desert hydrology, particularly focusing on calculating losses and the unit hydrograph. This manual provides isohyetal maps corresponding to various rainfall durations and frequencies for desert areas of San Bernardino County. It recommends selecting curve numbers based on vegetative cover types, the hydrologic condition of cover types, and the hydrologic soil group for the drainage area. Furthermore, in order to develop synthetic hydrographs for estimating the time distribution of watershed runoff in drainage basins where stream gauge data is inadequate, an S-graph is developed specifically for the desert areas of San Bernardino County.

The manual was amended in 2010 to incorporate changes in rainfall statistics and trends as per the NOAA Atlas 14 (San Bernardino, 2010). The primary topics covered in the Addendum include rainfall quantities for various peak durations, associated return periods, antecedent moisture conditions (AMC) utilized in hydrology studies for design and planning, and soil grouping designations along with related maps.

B.2.5 International Drainage Design Manuals and Guidance

The drainage design manuals and guidelines from different countries located in regions with playa lakes, arid zones, and karst landscapes were examined to explore their hydrological approaches. The following sections will provide a summary of this examination, including key details from selected guidelines and manuals.

B.2.5.1 Playa Regions and Arid Areas

This section offers an overview of drainage design manuals from countries located in arid regions and playa lakes, detailing the hydrological practices and guidelines for transportation infrastructure design in these environments.

B.2.5.1.1 Australasian Road Transport and Traffic Agencies (Austroads)

The *Austroads Guide to Road Design* is a comprehensive resource offering guidance and standards for road design in Australia. Part 5 of this document "*Drainage – General and Hydrology Considerations*" provides information on the elements that need to be considered in the design of a drainage system including the hydrology, safety and environmental aspects, and the maintenance and operations of these systems (Austroads, 2023). In this document, the methodologies for estimating rainfall and runoff, along with other considerations in drainage design, are drawn from the content outlined in the *Australian Rainfall and Runoff -ARR 2019* document (Ball et al. 2019).

In this document, Australia is divided into zones based on broad geographic regions. The boundary between the humid coastal zones and the arid/semi-arid zones was selected as the 500 mm/year (20 in/year) mean annual rainfall isohyet. The following discussion on the hydrology of arid and semi-arid regions of Australia is obtained from this document.

Design Peak Flow Estimation - Regional Flood Method

Peak flow estimation in small to medium rural catchments is required for designing infrastructure such as culverts, bridges, causeways, and soil conservation works. Often, there is limited streamflow data, regional equations may be used to transfer flood frequency characteristics from gauged catchments to ungauged ones. This approach is quick and relies on easily accessible catchment data, even if some streamflow data is available.

As part of the *Australian Rainfall and Runoff (ARR)* revision, a Regional Flood Frequency Estimation (RFFE) method has been developed and is now accessible for flood estimation across Australia. The adopted approach for arid and semi-arid regions follows an index-type. The 10% AEP flood quantile (Q_{10}) was used as the index variable and a dimensionless Growth Factor (GF_x) for X% AEP (GF_x) was used to estimate Q_x (**Equation B.2)**:

$$Q_x = Q_{10} \times GF_x \quad \text{(B-2)}$$

Q_{10} was predicted using an equation developed based on catchment characteristics, and GF_x was derived based on the estimated at-site flood quantile. A Bayesian parameter estimation procedure with Log Pearson Type III distribution was used to estimate flood quantiles for each gauged site for AEPs of 50%, 20%, 10%, 5%, 2%, and 1%.

The prediction equation adopted for the index variable Q_{10} has the form of **Equation B.3**:

$$log_{10}Q_{10} = b_0 + b_1 \ log_{10}(A) + b_2 log_{10} I_{6,50} \quad \text{(B-3)}$$

where b_0, b_1, and b_2 are regression coefficients, estimated using ordinary least squares regression; A represents catchment area (km^2), and $I_{6,50}$ is the design rainfall intensity (mm/hr) at catchment centroid for 6-hour duration and 50% AEP. The values of b_0, b_1,b_2, and GFx are embedded into the RFFE Model 2015.

It should be noted that in arid areas, the reliability of Regional Flood Frequency Estimation (RFFE) is expected to be lower due to its reliance on a small number of gauged catchments across a vast area. Estimating design floods in such zones is challenging due to factors like sparse streamflow data and diverse regional conditions. While RFFE's reliability is compromised, alternative methods face similar limitations (Ball et al. 2019).

Transmission Loss

Many catchments in arid and semiarid areas exhibit a significant initial and transmission losses; however, studies on transmission losses tend to focus on specific reaches and hence the results are site-specific. Also, the majority of research on transmission losses for rural catchments was focused on long term losses relevant to water resource modeling and planning, rather than flood estimation. For very large arid catchments, transmission losses can be substantial; however, for most design flood applications the channel losses will not be significant and can be combined with other processes that are implicitly covered by lumped conceptual models.

Urban catchments may also be subject to transmission losses. While the losses identified for rural catchments are generally less pronounced in urban catchments, transmission losses can occur along the drainage system.

The following are recommended for estimation of very rare to extreme floods in rural areas located in arid and semi-arid regions:

- When estimating initial loss values for use with *design bursts*, the few data available indicate that no initial loss should be deducted from the Probable Maximum Precipitation Flood (PMP).
- When estimating initial loss values for use with *design storms*, the few data available indicate that a slightly higher value of loss rate may be appropriate than for more humid regions in the south-east of the continent. It is unlikely that this value would be greater than 3 mm/hr.

B.2.5.1.2 Abu Dhabi Standards Guideline For Stormwater and Sub-soil Drainage Systems

Arid areas and playas (sabkhas in the local language) in Abu Dhabi present unique challenges for hydrology and drainage design due to their specific environmental conditions. Abu Dhabi's climate is predominantly hot and dry with minimal rainfall, which impacts water resource management and infrastructure planning significantly. The *Storm Water and Sub-soil Drainage Systems Design Manual - Drainage Manual* (Abu Dhabi Department of Municipalities and Transport, 2022) covers the key technical requirements for designing stormwater and sub-soil drainage systems within the jurisdiction of Abu Dhabi Emirate. Two rainfall-runoff methods, i.e., Rational Method and SCS Method are presented in Section 3 of the manual.

Rational Method

The Rational Method is applicable for catchment areas less than 80 hectares (200 acres) and/or a time of concentration (T_c) less than 30 minutes, in scenarios where there is no significant retention or backwater effects. It should be noted that this method is not particularly effective in modeling the impact of external inflows, backwater, or routing through lagoons and soakaways. Using it in such contexts could lead to uneconomical designs.

For calculating runoff coefficients (*C* values) in rural areas, factors such as slope, soil types, vegetation, and surface storage should be considered. These factors are detailed in **Table B.7**. To determine the appropriate *C* values using this table, one should select the coefficient from each of the four specified categories and then aggregate these to arrive at the composite *C* value for use in the Rational Method.

In instances where sabkha areas (playa lakes) are directly connected by surface flow within the drainage catchment (not isolated), a *C* value of 0.85 should be used for those areas. Conversely, if sabkha areas lack a surface outlet, a significantly lower *C* value should be used for the *surface storage* portion of *C*, specifically 0.06, as noted in **Table B.7**.

SCS Method

For catchment areas larger than 80 hectares (200 acres) and/or time of concentration T_c >30 mins, the SCS method is recommended for use in the design of new drainage networks. However, the SCS method can be used in the design and analysis of networks for all sizes of catchments. In selecting the curve number (*CN*) for the catchment, the SCS Type II Cumulative type curve should be selected for hydraulic modeling, unless otherwise specified by the Department.

Table B.7 Typical runoff coefficient in Rational Method for rural areas (Abu Dhabi Department of Municipalities and Transport, 2022)

Type	Extreme	High	Normal	Low
Relief	0.35	0.28	0.20	0.14
	Steep, rugged terrain with average slopes above 30%	Hilly, with average slopes of 10% to 30%.	Rolling, with average slopes of 5% to 10%.	Relatively flat land, with average slopes of 0 to 5%.
Soil infiltration	0.16	0.12	0.08	0.06
	No effective soil cover, either rock or thin soil mantle of negligible infiltration capacity	Clay or shallow loam soils of low infiltration capacity or poorly drained.	Normal; well-drained light or medium textured soils, sandy loams, silt and silt loams	High; deep sand or other soil that takes up water readily, very light, well-drained soils.
Vegetal cover	0.16	0.12	0.08	0.06
	No effective plant cover, bare or very sparse cover.	Poor to fair; natural cover, with less than 20% of drainage area having been irrigated landscape.	Fair to good; about 50% of area in crop or other irrigated landscaping.	Good to excellent; about 90% of drainage area in crop or other irrigated landscaping.
Surface storage	0.12	0.10	0.08	0.06
	Negligible surface depression few and shallow; drainage ways steep and small.	Low; well-defined system of small drainage ways; no isolated low areas.	Normal; considerable surface depression storage.	High; surface storage, high; drainage system not sharply defined, typical for interior areas of Regions 1 and 3. Applies also to isolated sabkha areas that have no surface outlet*.

How to use this table: Select the appropriate coefficient value from each of the four relief categories and cumulate to find the composite 'C' value to use in the rational equation. For example: for a catchment area with rolling terrain with 8 percent slopes (0.20), with well-drained sandy loam soil (0.08), no plant cover (0.16), and normal surface depression storage (0.08), $C = 0.20 + 0.08 + 0.16 + 0.08 = 0.52$.

*Special case '*C*' for sabkha areas: Where sabkha areas have a direct surface flow connection (not isolated) within the drainage catchment area, use $C = 0.85$ for the sabkha area

B.2.5.1.3 Kuwait Highway Drainage Design Manual

Kuwait is characterized by an arid climate with very low annual rainfall, extreme temperatures, and predominantly sandy desert terrain. These conditions present unique challenges for hydrology and drainage design. The *Kuwait Highway Drainage Design Manual* (Kuwait Ministry of Public Works, 2012) sets forth minimum stormwater management requirements to guide drainage efforts across the country. According to the manual, Kuwait's rainfall is scarce and typically occurs as severe, geographically limited thunderstorms. Consequently, an instantaneous peak flow rate, such as that determined by the Rational Method, is recommended for designing highway drainage systems in Kuwait. For more complex drainage systems that incorporate pumping stations and storage facilities and require the use of hydrographs, the Soil Conservation Service (SCS) Synthetic Unit Hydrograph Method is recommended.

Rational Method

The manual restricts the use of the Rational Method to estimating runoff from areas no larger than 80 ha (200 acres). However, it does not include provisions for selecting runoff factors (*C* values) specific to arid areas or playas.

Soil Conservation Service (SCS) Synthetic Unit Hydrograph Method

This method is recommended for drainage areas exceeding 80 ha (200 acres). The *CN* values for agricultural land in semi-arid rangelands and desert shrubs are derived from data provided by the U.S. Natural Resources Conservation Service (NRCS).

The manual does not consider any other provisions for the hydrological study of arid areas.

B.2.5.1.4 Oman Highway Design Standard

Oman, like many parts of the Arabian Peninsula, is characterized by its arid climate, with most of the country receiving minimal rainfall, extreme temperatures, and a predominantly desert terrain. Chapter 4 of the *Oman Highway Design Standard* (Sultan of Oman, 1994) outlines two methods for calculating catchment discharges:

a) Catchment areas greater than 10 km² (2,500 acres): The discharge is determined using Flood Frequency Curves provided in the manual.

b) Catchment areas less than 10 km² (2,500 acres): The discharge is calculated using the Rational Method. This calculated value should be compared with the value obtained using method (a), and the lesser of the two discharges should be used for design purposes.

The manual does not include any additional provisions for the hydrological study of arid areas.

B.2.5.2 Karst Areas

In this section, an overview of the drainage design manuals from the UK and Ireland concerning karst hydrology is provided. Both countries feature karst landscapes, which have posed challenges for transportation agencies.

B.2.5.2.1 Highways England

Karst areas in England, characterized by soluble rock types such as limestone and chalk, are distributed across the country, with significant concentrations in regions like the Yorkshire Dales, the Peak District, and parts of the Southwest. The presence of karst topography presents distinct challenges for infrastructure development, including road schemes. For instance, gypsum karst issues in the Permian and Triassic sequences of England have created problematic conditions for bridge and road construction. In Northern England, specifically, the Ripon Bypass traverses Permian strata that are impacted by active gypsum karst, resulting in severe subsidence issues (Cooper and Saunders, 2002). In response to these challenges, drainage design in karst areas in England often involves detailed geotechnical investigations, adaptive drainage systems, monitoring and maintenance, and pollution control measures. However, no special provisions were found in Highways England publications regarding the hydrology of karst terrains.

For instance, the *Design Manual for Roads and Bridges* (Highways England, 2020) outlines requirements and recommendations for managing surface water runoff from natural catchments that drain toward motorways or all-purpose trunk roads. This guidance aims to reduce the frequency and severity of flooding incidents caused by runoff originating beyond the highway boundary. According to this manual, the estimation of runoff from natural catchments shall be undertaken using one of the following runoff methodologies:

- Institute of Hydrology Report 124 (IH 124): This method should be used exclusively to estimate flood flows for catchments with surface areas smaller than 25 hectares (62 acres). It is a runoff methodology designed to estimate runoff from natural catchments without requiring hydraulic modeling. The design flows calculated using this methodology represent surface runoff flows, incorporating the effects of soil saturation.
- Flood Estimation Handbook (FEH)*:* This method along with the earlier Flood Studies Report (FSR), comprises a suite of methods and associated data designed to establish recognized standard national methods for rainfall and flood estimation, as well as rainfall-runoff modeling. These methods are calibrated against extensive hydro-meteorological datasets from gauged locations across the UK.

The Flood Studies Report (FSR) rainfall-runoff method is one of the principal methods used in the UK for estimating the magnitude of floods of a given frequency. This method employs the unit hydrograph and losses model, which incorporates three parameters. These parameters relate to the catchment's response to rainfall (time-to-peak of the unit hydrograph), the proportion of rainfall that directly contributes to river flow (percentage runoff), and the flow in the river prior to the event (baseflow). Where possible, model parameters are derived from observed rainfall and runoff records. However, if no records are available, the parameters may be estimated using physical and climatic descriptors of the catchment (CEH, 2008).

B.2.5.2.2 Ireland National Roads Authority (NRA)

Karst landscapes pose specific challenges for road design, construction and maintenance due to their unique geological characteristics. In Ireland, where karst features are prominent, especially in the western regions such as in County Clare and parts of County Galway, these challenges are particularly significant. The Transport Infrastructure Ireland (TII) Road Drainage and Water Environment Standard (NRA, 2015) provides guidance for evaluating and addressing the potential impacts of road projects on the water environment. This document does not focus on the hydrology of karst; instead, it offers guidance on managing the discharge of surface runoff into karst features. It also provides strategies for preventing or mitigating adverse effects associated with these discharges, including the potential for karst reactivation, groundwater flooding, and other related issues.

The publication "*Drainage Design for National Road Schemes - Sustainable Drainage Options*" (TII, 2013), another NRA document, presents the following in the context of karst hydrology:

- *Karst Environments*: Road projects crossing karst terrains are of primary concern in Ireland because of the impacts of stormwater runoff on water quality, flooding, and also concerns of sinkhole collapse. In addition, many designated wetland features such as turloughs are associated with these terrains and are protected under the Habitats Directive. This often leads to the requirement for extensive hydrogeological surveys in these areas.
- *Peak Flow Calculations Related to Design of Culverts and Bridges*: The following methods are recommended for gauged and ungauged watersheds.
  - *Gauged Catchments:* Where gauged data is available, flows can be calculated using statistical distributions from the annual maximum series or peaks over threshold series. The Flood Studies Report (FSR) recommends distributions such as Gumbel Extreme Value 1 (EV1) and the Generalized Extreme Value (GEV). The Weibull distribution is also used. If the gauged data covers a period that is less than the required return period, the Flood Estimation Handbook (FEH) recommends a pooling analysis. This involves using data from hydrologically similar catchments based on three catchment descriptors, i.e., area, rainfall, and soil properties.
  - *Ungauged Catchments:* Recommended methods for calculating greenfield runoff rates (pre-construction) for ungauged catchments include:
    - IH 124
    - FSR 6-variable method
    - FSR 3-variable method
    - FEH 1999
    - Unit hydrograph

The Rational Method or Modified Rational Method is recommended for estimating peak flow rates. However, it has been noted that these methods may produce conservative discharge rates, particularly for less permeable soils. Such conservative estimates are beneficial in situations where minimizing flooding is crucial, such as in karst areas. For most other scenarios, the IH 124 method is preferred.

No other provisions were found in these documents or any other NRA publications regarding the hydrology of karst areas.

CHAPTER B3 : REVIEW LITERATURE ON HYDROLOGIC APPROACHES TO PLAYA LAKES

This chapter first introduces fundamental knowledge about playas, covering their global distribution as well as their prevalence in the United States and specifically in Texas, with a focus on playas situated within the Southern High Plains region. Subsequently, it transitions to an exploration of the hydrology of these unique ecosystems through an extensive review of available scientific and technical publications.

B.3.1 Playas

The terms "*playa*" and "*playa lake*" (when the playa is inundated) are sometimes used interchangeably or replaced by regional synonyms like "*dry lake*" in California (Briere, 2000). Globally, these features are known by different names, such as "*pans*" in South Africa, "*Qa's*" in Jordan, "*kahabra*" in Saudi Arabia, and "*sabkha*" in North Africa and parts of the Middle East (French and Miller, 2012). Playa lakes are unique and important features of the hydrological landscape. These shallow, temporary lakes, primarily found in arid and semi-arid regions, play a vital role in the local habitats for wildlife and as significant recharge areas for groundwater resources. These lakes have evolved over time due to various factors, with their water evaporating and leaving behind vast areas rich in sediment and minerals. According to Haukos and Smith (1992; 2003), the formation of playa lakes is heavily influenced by climate and geographical location. These lakes act as local discharge sites, typically receiving water from precipitation and runoff within their watersheds. Additionally, they can also receive groundwater inflows from both their local watershed and regional aquifers. **Figure B.2** shows examples of inundated and dry playas in different regions of the United States.

(a) (b) (c)

Figure B.2 Examples of playa lakes: (a) Inundated Playa in Floyd County Texas (Photo by Doug Wechsler, obtained from www.texashighways.com), (b) Aerial imagery of dry lake (obtained from https://www.depts.ttu.edu/geospatial/center/pwd/about.html), and (c) Black Rock Playa, Nevada (Adams and Sada, 2014)

B.3.2 Distribution of Playa Lakes

B.3.2.1 Distribution of Playa Lakes Around the World

Playa and playa lake systems are widespread and vary in size from small, less than 250 acres (1 km²), to very large, up to 2,400,000 acres (9500 km²), exemplified by Lake Eyre in Australia (Briere, 2000). These systems are highly sensitive to weather changes, experiencing filling during wet periods through river inflow or groundwater discharges and drying during arid phases on seasonal or longer timescales (De Deckker, 1988). Gouramanis et al. (2015) have provided a comprehensive overview of the global distribution of 130 playa lakes or playa-like systems designated as Wetlands of International Importance (see **Figure B.3**). Their study emphasizes the hydrological and ecological significance of these playas, highlighting their importance across different regions worldwide.

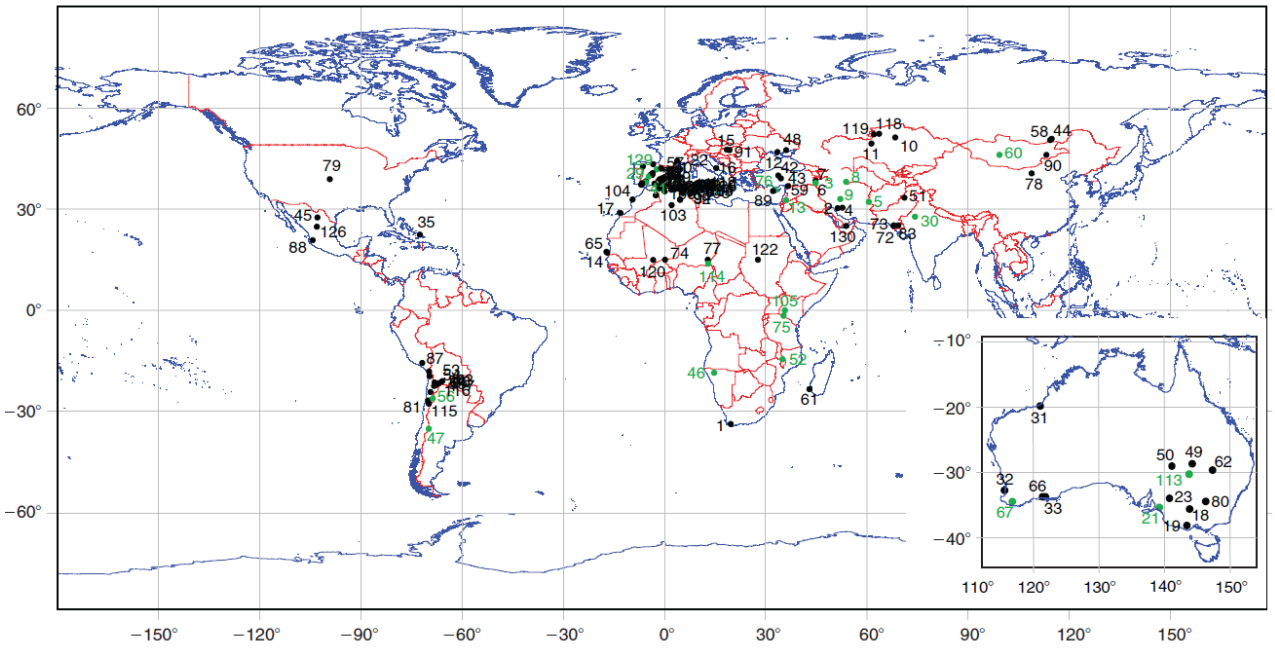

Figure B.3 Global distribution of 130 playa lake or playa-like systems listed under the Wetlands of International Importance (Inset: Location of playa lakes and playa-like systems in Australia (Gouramanis et al., 2015))

B.3.2.2 Distribution of Playa Lakes in the United States

The distribution of playa lakes in the United States varies across different regions, with notable concentrations found in areas such as the Great Plains, the southwestern states, and parts of the western United States. Playa lakes are particularly prevalent in states such as Texas, Kansas, Oklahoma, New Mexico, and Colorado. As per the scope of this study, the hydrology of Southern High Plains (SHPs) Playa Lakes is examined in the following section, given that Texas is located in this region.

B.3.2.2.1 Southern High Plain Regions

The High Plains aquifer, also known as the Ogallala aquifer, spans over 174,000 square miles across eight U.S. states, including Colorado, Kansas, Nebraska, New Mexico, Oklahoma, South Dakota, Texas, and Wyoming (Gurdak and Roe, 2009) as shown in **Figure B.4**. High Plains region features several crucial playa lakes essential for floodwater storage, irrigation, livestock support, and wildlife habitats, potentially aiding aquifer recharge into its northern, central, and southern High Plain (SHP) regions (Steiert and Meinzer, 1994; Luo et al., 1997; Smith, 2003).

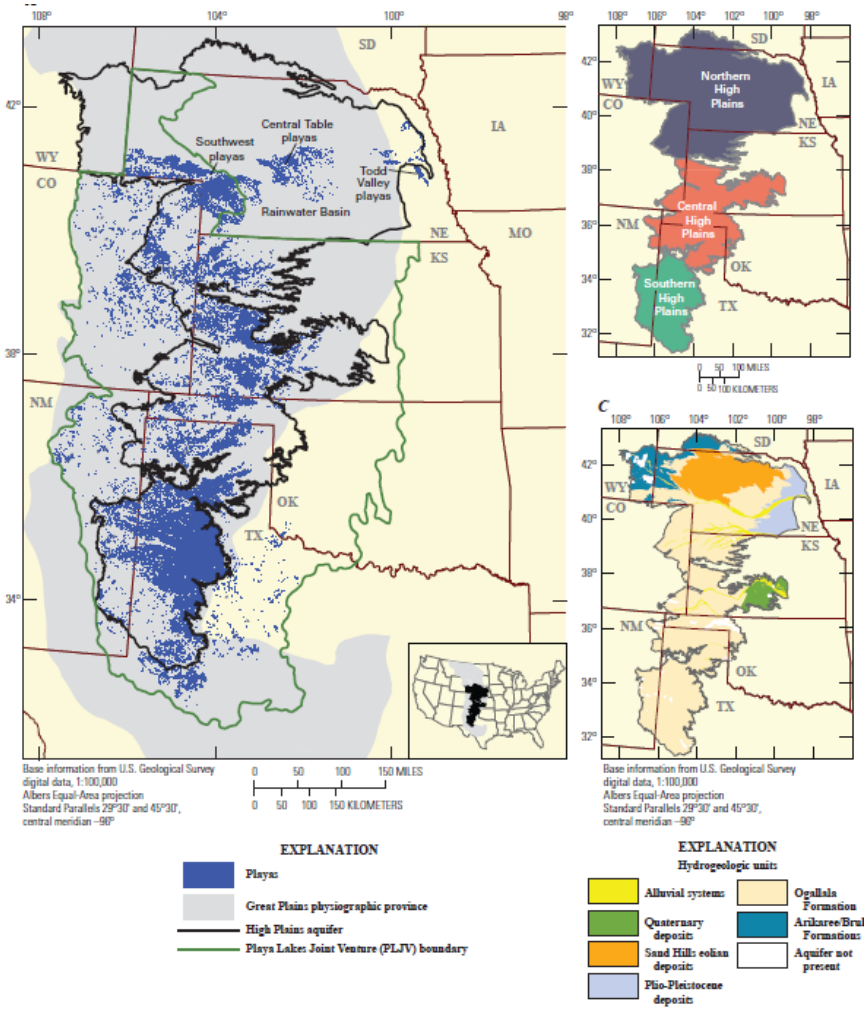

Figure B.4 Distribution of playa lakes in the High Plains Aquifer in the United States (Gurdak and Roe, 2009)

Playa lakes in the SHPs play a crucial role in concentrating runoff and various chemical constituents. The dynamics of water fate, whether through evaporation or ground infiltration, have evolved over time. Early studies, such as Theis (1937), attributed water level changes in playas to evaporation. However, other studies such as Wood and Sanford (1994) and Wood et al. (1997), emphasize groundwater infiltration as a significant process and critical contributor to groundwater recharge in this region.

The subsequent sections present the geomorphology, distribution and orientation, and classification of SHP playa lakes.

Geomorphology of SHP Playas

Playas are characterized by a hydric soil-lined floor, a sloped margin (annulus), and an interplaya region. The interplaya region comprises upland drainage areas and spaces between playas (Hovorka, 1995). **Figure B.5** shows different physical features of playa lakes in the High Plains aquifer in the United States. Interplaya refers to the land surface surrounding playas, including the upland areas that drain into these features. The playa floor and annulus consist of interbedded clay and loam, reflecting temporal changes in the size of the playa lake.

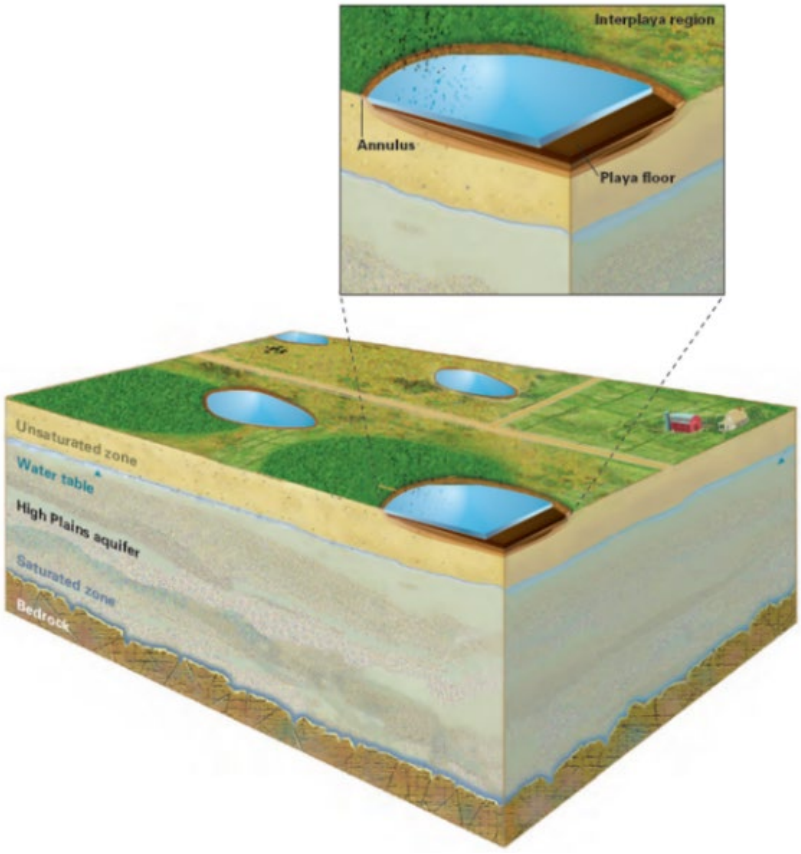

Figure B.5 Physical features of playa lakes in the High Plains Aquifer (Gurdak and Roe, 2009)

Extensive research on the geomorphology of playas have been conducted (e.g., Curtis and Beierman, 1980; Gustavson et al.,1995). Guthery and Bryant (1982) utilized Soil Conservation Service (SCS) maps to analyze the size and distribution of playas in the Southern High Plains (SHPs), revealing an average playa floor size of approximately 15.6 acres (6.3 hectares). Most SHP playas are located within the Blackwater Draw Formation, characterized by silty clay loam sediments. Grubb and Parks (1968) divided SHPs based on soil texture, showing larger playas in fine-textured soil areas. These playas have a higher volume per unit of surface area compared to those in medium-textured soil regions. The floors of SHP playa lakes consist of 3.3-6.6 ft (1-2 m)

of hydric soils and Vertisol clays prone to swelling and cracking (Hovorka, 1997), with clay-rich lacustrine sediments, intermixed with sand layers up to 33 ft (10 m) below the surface (Hovorka, 1995; Claborn et al., 1985). Beneath these playas, numerous paleosols formed under more stable past climates (Bauchert, 1996), while the annulus exhibits layers of clay and loam, indicative of historical fluctuations in playa lake sizes (Hovorka, 1995). Interplaya areas contain silty clay loam soils and thick caliche layers, formed through evaporative processes (Hovorka, 1995). These findings underscore the significant role of soil texture in determining the physical characteristics and distribution of playa lakes in the SHPs, highlighting the complex interplay between geological and hydrological factors (Casula, 1995).

Significant progress in spatial analysis of playa lakes has been achieved through various means, notably, the digitization efforts documented by Fish et al. (1998), who recorded 20,577 playas, and the comprehensive documentation conducted by Gurdak and Roe (2010), who identified 66,000 playas across the Southern High Plains (SHPs). These Geographic Information System (GIS) databases offer intricate insights into physical and morphological characteristics such as surface area, perimeter, soil composition, elevation, depth, and shoreline length. Moreover, the U.S. Fish and Wildlife Service's National Wetland Inventory provides comprehensive digital data specifically for Nebraska's playas, as highlighted by Gurdak and Roe (2010).

Distribution and Orientation of Playas in SHP

The distribution of playas in SHP exhibits non-random patterns, with higher concentrations observed north of the Canadian River, near the Llano Estacado escarpment, and in the Southwestern High Plains (Quillin et al., 2005). In the northern part of this region, larger but fewer playas with finer soil types are prevalent (Lotspeich et al., 1971). The study by Zartman and Fish (1989) in Castro County, Texas, revealed primary east-west and secondary north-south orientations of playa lakes, initially raising concerns about contamination risks due to this alignment. Subsequent research showed variations in size and orientation, with larger lakes more common in the east and deeper ones in the south and west, generally aligning along a 160-degree axis from west-northwest to east-southeast.

Classification of SHP Playa Lakes

Playa lakes have been classified based on various criteria. The City of Lubbock Drainage Manual categorized playas based on their overflow characteristics as "*overflo*w" and "*non-overflow*" (City of Lubbock, 2019). Non-overflow playas may accommodate runoff from a 100-year, 24-hour runoff event, with potential overflow during a 500-year, 24-hour storm. Overflow playas lack sufficient storage to contain runoff and may experience discharge when water levels surpass natural overflow elevations.

Wood and Jones (1990) categorized playa lakes into saline and freshwater types, with larger saline lakes typically in the southern SHP. Reeves (1966; 1990) developed a classification system for playa basins in the SHPs based on evolutionary development, differentiating from classifications focusing on habitat use (Guthery and Bryant, 1982). Reeves (1990) identified three main types of

lake basins in the SHP, each corresponding to different developmental stages: young, mature, and old. Descriptions of these playa types are presented in **Table B.8**. The characteristics of each type are presented in **Table B.9**.

Table B.8 Description of three types of SHP playa lakes (Revees, 1990)

Playa Type	Description
Type I (Young)	Originated from small depressions caused by either deflation or hydro-compaction over 1,000 years in the uppermost Tertiary and Quaternary eolian sands.
Type II (Mature)	Formed through the enlargement and deepening of Type I basins due to infiltration of intermittently ponded water over 10,000 years.
Type III (Old)	Formed as a result of the long-term dissolution of underlying Permian salt beds beneath the Type II basins. This process, which might have spanned around 100,000 years, likely involved the gradual seepage of groundwater through well-established sediments above these salt beds. These basins eventually evolved into larger subsidence basins, often exceeding 1.5 to 5.8 mi^2 (4 to 15 km^2) in size, through this prolonged geological process.

Table B.9 Classification of playas and their characteristics (Revees, 1990)

Characteristic	Type I (Young)	Type II (Mature)	Type III (Old)
Basin			
Diameter	< 0.6 km	0.6 - 1.6 km	> 1.6 km
Shape	Round	Roundish	Irregular
Playa			
Diameter	< 0.3 km	0.3 - 0.7 km	-
Shape	Round	Round to Rectangular	Elongate
Area	< 0.07 km^2	0.07 - 0.4 km^2	-
Topographic Relief			
Adjacent	3 - 5 m	8 - 15 m	10 - 30 m
Dunes	No	Some	Yes
Number of dunes	-	1	2-3
Caliche			
Under basin	Yes	Some	No
Under playa	Locally	Mostly gone	No
Caliche Displaced	No	Some	Yes
Pipes	No	Yes	-
Subsidence Area	No	Yes	Yes
Terraces	No	Yes	Yes
Drainage	No	Yes	Yes
TLS*	1 - 3 m	8 - 20 m	>20 m
Numbers**	12.63	4.10	40

*TLS: Thickness of lacustrine sediment.

**Based on counts derived from measurements of playa areas only on the Texas part of the Southern High Plains.

B.3.2.3 Distribution of Playa Lakes in Texas

Playa lakes are found in the Southern High Plains region of the United States, including Texas. The drainage basin for SHP playas encompasses about 19 million acres (77,700 km²), roughly 90% of the area (Nativ, 1992; Gurdak and Roe, 2010). Playa lakes in SHP are highly dynamic, and their size and number may change from year to year depending on the amount of precipitation, and evaporation. Therefore, it is difficult to determine the exact percentage of the Texas landscape that is covered by playa lakes. It is reported that there are approximately 20,000-24,000 playa lakes throughout the Texas Panhandle and western North Texas covering 3.0-4.5 million acres of land, i.e., 0.4-2.56% of the total land in Texas (TPWD, n.d.; Playa Lakes Joint Venture (PLJV), 2009; Fish et al., 1998).

The distribution of playa lakes in different counties of Texas is shown in **Figure B.6**. This information is exported using the Playa Lake geospatial dataset obtained from the USDA data repository. **Table ABSM.1** (**Supplemental Materials**) shows the total area of playa lakes within each county in SHPs of Texas.

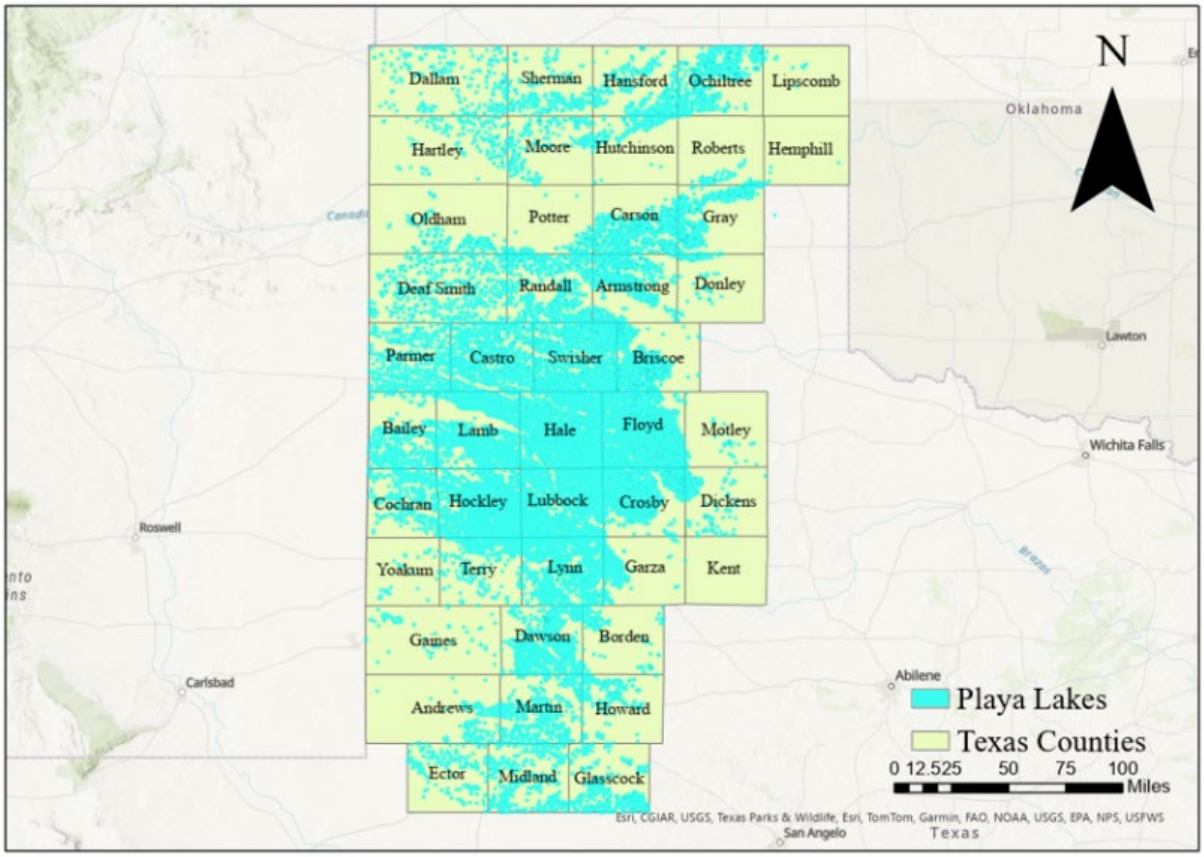

Figure B.6 SHPs playa lakes in the Texas counties

B.3.3 Hydrology of Playa Lakes

Understanding the hydrology of playa lakes is vital for water resource management and ecosystem conservation (Bexfield, 1995; Ganesan et al., 2016; Sallenave and Ganguli, 2021). Playa lakes exhibit complex hydrological dynamics influenced by climate, geology, land use, and anthropogenic activities (Gitz and Brauer, 2016). Factors such as soil type, subsurface geology, and land use practices affect water balance and recharge rates (Ganesan et al., 2016). The fluctuating hydrology of playa lakes, characterized by alternating periods of flooding and drying, is influenced by precipitation patterns and evapotranspiration rates (Smith, 2003; Hovorka, 1997). While runoff from heavy rains contributes to water accumulation in playas, the high evaporation rates in arid and semi-arid regions pose challenges to water retention (Dugan and Zelt, 2000; Gustavson et al., 1995). Moreover, uncertainties persist regarding the extent of aquifer recharge from playa lakes due to variable recharge rates and infiltration processes. The water accumulation in Southern High Plains playas is estimated to vary between 1.8 and 5.7 million acre-ft annually (Nativ, 1992; Zartman and Fish, 1989).

Playa hydrology is also affected by factors such as vegetation cover, soil permeability, and evaporation rates, which influence water volume and aquifer recharge potential (Brown et al., 1976; James, 1998). Despite the significant water accumulation in playa lakes, particularly in the SHPs, estimating recharge remains challenging due to various factors including soil characteristics and precipitation variability (Hauser and Lotspeich, 1968). Evaporation from playa surfaces, influenced by seasonal variations and soil composition, further complicates the hydrological balance, with evaporation rates ranging from 13 to 24 inches against potential evapotranspiration of 65 to 69 inches in SHPs (Brown et al., 1976). Additionally, infiltration dynamics in playas vary, with implications for groundwater recharge and chemical transport (Claborn et al., 1985; Knowles et al., 1984).

The interplay of peak runoff and water loss significantly impacts the inundation process of playa lakes, which is pivotal in flood mitigation and eco-environmental studies. The following sections present key findings from the review of literature on playa lake's hydrology, specifically focusing on methods for determining inundation characteristics (e.g., flow depth and duration), hydrological approaches for runoff calculations, and estimation of infiltration and recharge rates beneath playa lakes.

B.3.3.1 Playas Inundation Characteristics

In playa hydrology, understanding inundation is essential because it greatly influences different hydrological processes. Inundation depth and duration are critical parameters influencing the hydrological calculations and ecosystem dynamics within playas. The depth of inundation directly affects the storage capacity of playas, altering groundwater recharge rates and influencing sediment transport patterns. Similarly, the duration of inundation governs the temporal availability of water resources, affecting vegetation growth cycles and wildlife habitat suitability. Furthermore, inundation dynamics play a vital role in regulating peak flow events, influencing flood risk

assessment and management strategies in surrounding regions. Subsequent sections will discuss commonly used methodologies for calculating inundation depth and duration for playa lakes.

B.3.3.1.1 Estimation of Playas Inundation Depth and Storage Volume

There is a lack of standardized guidance for quantifying flood hazards on playas. In a study addressing this issue, French and Miller (2012) utilized a methodology that was previously used by French et al. (2006) to estimate the depth of Rogers (playa) Lake inundation, particularly for a 100-year event at the Edwards Air Force Base (EAFB). Situated in the Mojave Desert, EAFB experiences hot summers and cool winters, with an average annual temperature of around 62.2 $^{\circ}$F and annual precipitation of 5.2 inches (Miller and French, 2002). They used a 100-year flood scenario, following the delineation of the watershed covering fluvial fans draining toward the playa lake, as the main flood frequency to estimate the inundation characteristics of EAFB playa lake. At the EAFB, 100-year, 24-hour precipitation depth was 3.55 inches (Miller and French, 2002), and the relationship between rainfall and runoff changes with elevation was influenced by soil types, land use, and vegetation. The Natural Resources Conservation Service's curve number (*CN*) method was employed to estimate initial abstraction, infiltration, and runoff at the EAFB playa lake. Once the total volume of water conveyed to the lakebed was estimated based on the specified rainfall event, the depth of the water in the playa lake was determined to identify flood hazard zones within the study area. This comprehensive method facilitates the accurate estimation of inundation depths for flood events of varying return periods, critical for effective water resource management and hazard mitigation at Rogers Lake. The impact of strong, consistent winds in Rogers Lake required the calculation of two types of flood depths: one for no wind conditions and another factoring in wind setup. While wind setup is recognized as a factor in inland lakes, its specific effects on playa lakes have not been thoroughly studied. This was the case at the EAFB, where wind effects were acknowledged in floodplain delineation but did not significantly alter the regulatory depth of water (French and Miller, 2012).

A similar methodology was employed by Weinberg et al. (2015) to estimate the runoff volume in playa lakes in Texas. They studied the temporal changes in inundation area, elevation, and detention volume using combined field survey and remote sensing techniques. As part of field surveys, land use around each playa was determined, and playas were classified based on the predominant land use in their watershed. However, no distinction was made between different types of irrigation methods. Field measurements were conducted at selected playas to validate Landsat-derived estimates. These measurements involved the utilization of ultrasonic sensors and pressure transducers. A regression model was developed using multiple datasets, such as playa's size, watershed area, geographic longitude, and average watershed slope, to estimate the annual inundation volume within playa lakes. The correlation of each parameter with the annual water volume was examined to determine their effectiveness in influencing the hydrology of playa lakes. To estimate the water volumes for all Texas playas, the study's results were extrapolated using the ratio of the total playa area overlying the Ogallala Aquifer in Texas to the sampled playa area. The combined area of all playa lakes over the Ogallala in Texas amounts to 374,587 acres, while the

playas studied by Weinberg et al. (2015) encompassed 2,503 acres. This results in an extrapolation ratio of roughly 150.

The developed regression model by Weinberg et al. (2015) to predict runoff volume in regions with playa lakes in Texas accounts for over 70% of the variance in annual water volume. Key factors identified in the model included playa size, watershed area, and geographic longitude, while the average watershed slope exhibited comparatively less significance. Notably, the model performance remained acceptable across diverse land use patterns, highlighting its robustness in predicting runoff volume in such environments. Additionally, detention volume trends from 1996 to 2013 showed significant fluctuations, with a peak of 512,000 acre-ft in 1999 and notable declines during drought years. The average volume decreased from 88,000 to 21,000 acre-ft over this period, particularly in non-irrigated watershed playas. Moreover, the developed regression model aids in identifying potential sites for detaining water using GIS, supplemented by Landsat imagery and field surveys for detailed assessment.

B.3.3.1.2 Estimation of Playas Inundation Duration

Predicting the duration of inundation on playa lakes is a complex process due to several dynamic and interrelated factors. These factors include the nature of precipitation events, the physical characteristics of the watershed, and the unique hydrological and geological properties of the playa itself. Several studies have utilized a combination of field measurements and remote sensing to estimate the inundation duration in playa lakes (e.g., Bryant and Rainey, 2002; French et al. 2006; Doña et al., 2016; Solvik et al., 2021).

Remote sensing, using satellites or aircraft, is a highly effective method for determining playa inundation, as water significantly absorbs or reflects most electromagnetic energy wavelengths. Visible wavelengths (0.4 to 0.7 μm) can penetrate water, with penetration depth influenced by water turbidity, while Infrared (IR) wavelengths (0.7 to 2.35 μm) are almost entirely absorbed by water. The relationship between water and soil moisture is evident in the analysis of Landsat TM bands, where different bands yield varied representations (French and Miller, 2012).

French et al. (2006) utilized remote sensing to establish a relationship between local precipitation and changes in the water surface area of Rosamond Lake, demonstrating the method's potential in accurately predicting playa lake inundations. Rosamond Lake is positioned roughly 20 miles (32.2 km) to the northeast of Lancaster and 10.3 miles (16.6 km) east of Rosamond City, California (French et al. 2003). The lakebed primarily consists of fine-grained silt and clay, remnants from the Pleistocene era when it was part of Lake Thompson. The runoff volume in the study area was calculated using the SCS-CN method, which was evaluated through temporal remote sensing analysis of playa lake inundation. By analyzing precipitation data in conjunction with the observed changes in the lake's surface area, a clear correlation was observed between precipitation depth and the extent of the inundation footprint captured by remotely sensed images. Techniques such as image subtraction followed by binary thresholding were employed to quantify changes in surface water. The image subtraction shows differences in surface water area over time, and the binary thresholding enhances contrast to delineate these changes. Also, this approach provided the

threshold precipitation depth required to generate flow towards the lake by considering direct precipitation over the lake itself (i.e., the lake was considered as 100% impervious area). **Figures B.7(a)** and **(b)** show Band 1 (visible) and Band 7 (IR) responses to surface water of Rosamond Lake. Also, **Figures B.8(a)** and **(b)** illustrate temporal composite images from the lake inundation footprint that were used to calculate the duration and depth of playa lake inundation.

It is important to note that the methodology proposed by French et al. (2006) overlooked several factors that may carry significant importance in playas hydrology, including:

- *Channel Transmission Losses*: In many watershed systems, water can be lost during its flow toward the lake through processes such as seepage and evaporation. These losses can be substantial and can significantly affect the volume of water that eventually reaches the lake.
- *Evaporation from the Lakebed*: Particularly in spring and summer, evaporation can significantly reduce the water volume on the lakebed. In arid or semi-arid regions like those around EAFB, high temperatures, and wind conditions can enhance evaporation rates.
- *Infiltration*: The study also did not consider the infiltration of water into the lakebed. Depending on the soil composition and structure of the lakebed, a considerable amount of water might seep into the ground rather than remain on the surface which might not be correctly addressed using curve number (*CN*) values in the SCS method.

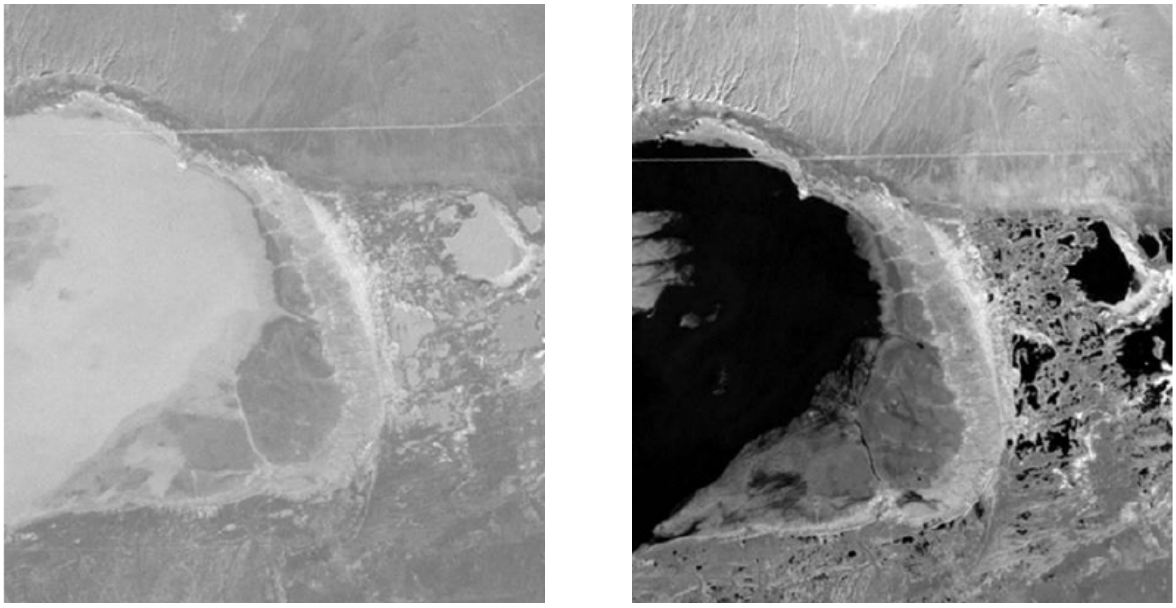

(a) (b)

Figure B.7 Spectral responses to surface water: (a) Band 1 (visible), and (b) Band 7 (IR) (French et al. 2006)

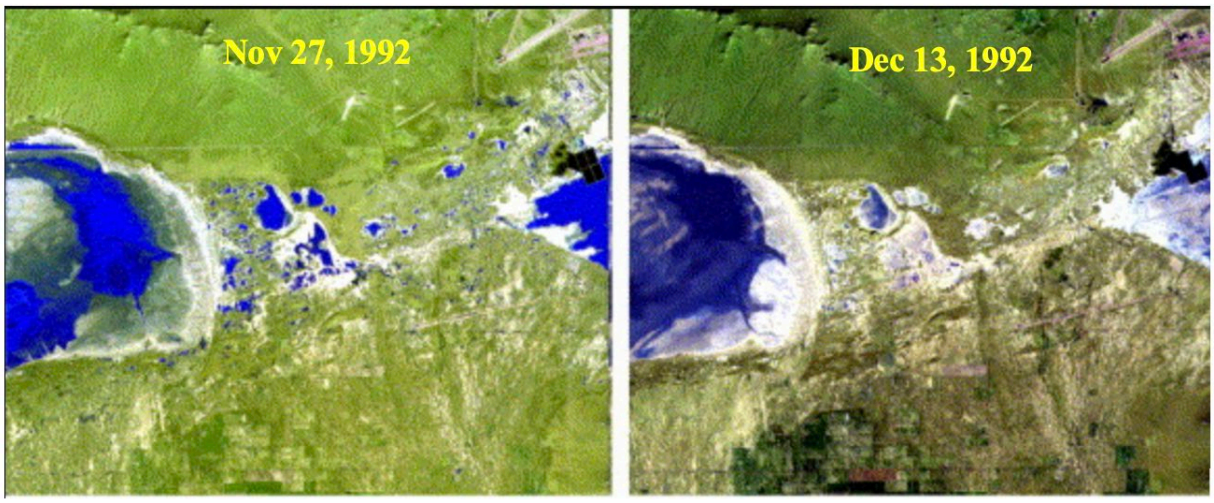

Figure B.8 Color composite image of Rosamond Lake inundation footprint: (a) Nov 27,1992 and (b) Dec 13, 1992. Images were created from composite images using Bands 4, 5, and 7 (French et al. 2006)

The methodology outlined above suggests that by identifying particular precipitation events that result in surface runoff and considering factors such as losses through infiltration and/or evaporation, it becomes feasible to estimate the volume of water flowing into playas. Furthermore, integrating these flow estimates with calculated evaporation rates enables predictions regarding the duration for which water will remain on the lakebed. Consequently, this integrated approach emerges as a vital tool in estimating both the frequency and duration of flooding events in playa lakes (French and Miller, 2012).

B.3.3.2 Rainfall-Runoff Computations in Playa Regions

This section covers two topics: a review of methods for estimating peak flow in playa lake regions, and the required design flood frequency in hydrological studies of infrastructure built within playa basins.

B.3.3.2.1 Computation of Peak Flow in Playa Regions

There are several methods for computing rainfall-runoff relationships that serve as the foundation for designing stormwater drainage and flood control systems. The City of Lubbock Drainage Manual (2019) recommends two primary methods: the Rational Method and the Unit Hydrograph (UH) method. However, in certain studies, such as that conducted by French et al. (2006), the SCS-CN method was utilized for peak flow estimation in regions with playa lakes. A summary of each method is as follows.

Rational Method

The peak flows in playa basins can be determined using the Rational Method (**Equation B.4**):

$$Q = CiA \quad \text{(B-4)}$$

where

Q = peak flow (cfs)

C = runoff coefficient

i = rainfall intensity (in/hr)

A = watershed area (acres)

The runoff coefficient, which signifies the fraction of total rainfall reaching the design point, is influenced by various factors including surface imperviousness, slope, ponding characteristics, and the design storm event. Playa lake beds are commonly recognized as impervious surfaces in several studies (e.g., French et al., 2006; City of Lubbock Drainage Manual, 2019), indicating their limited capacity for water infiltration. Therefore, the runoff coefficient (C) for these regions is typically assigned a value of 1, reflecting their tendency to generate surface runoff from all precipitation events.

The City of Lubbock Drainage Manual (2019) proposed that the rainfall intensity (i) should be determined based on the Texas Department of Transportation Hydraulic Design Manual (TxDOT, 2016). **Equation B.5**, known as the rainfall intensity-duration-frequency (IDF) power-law model, may be utilized for this purpose.

$$i = \frac{b}{(T_c+d)^e} \quad \text{(B-5)}$$

where

i = design rainfall intensity (in/hr)

T_c = time of concentration (min)

b, d, e = coefficients for specific frequencies obtained from the TxDOT Hydraulic Design Manual (TxDOT, 2016). It should be noted that the coefficients for specific frequencies are updated in the latest version of the TxDOT Hydraulic Design Manual (2019) which considers the Atlas-14 NOAA precipitation frequencies.

Time of Concentration and Lag Time

Regardless of the hydrologic method employed to estimate peak discharge, the time of concentration (T_c) for drainage basins in playa regions may be calculated using either the SCS method or the Kerby-Kirpich method (City of Lubbock, 2019). The time of concentration calculated using the Kerby-Kirpich method depends on the slope of the flow paths as runoff moves

through the watershed, the roughness of the surface, attenuation effects caused by storage or ponded areas, and increased conveyance efficiency caused by storm sewers or channels. It is recommended that the calculation of the time of concentration be divided into the time of travel of overland flow and the time of travel in well-defined channels or storm sewers using **Equation B.6**.

$$T_c = T_{ov} + T_{ch} \quad \text{(B-6)}$$

where

T_c = total time of concentration of the watershed (min)

T_{ov} = time of travel in the form of overland or sheet flow (min)

T_{ch} = time of travel in well-defined channels or storm sewers (min)

Irrespective of the method employed, a minimum total time of concentration of 15 min should be considered for any residential area (City of Lubbock, 2019).

Also, the lag time (T_{lag}) is determined from the time of concentration (T_c), utilizing **Equation B.7**.

$$T_{lag} = 0.6 \times T_c \quad \text{(B-7)}$$

Unit Hydrograph Method

The Soil Conservation Service (SCS) Unit Hydrograph method is a hydrological technique used to estimate the runoff response of a watershed to a rainfall event. The utilization of the Unit Hydrograph method may be warranted in various scenarios, even for small drainage areas. Such circumstances include the presence of features like open channels, playa lakes, playa overflows, floodplain reclamation, or the implementation of regional detention/retention facilities.

In the Unit Hydrograph method, the curve number (*CN*) value is used in conjunction with other parameters to develop a hydrograph that represents the runoff response of the watershed to a given rainfall event. The *CN* value helps quantify the initial abstraction, which is the amount of rainfall intercepted by the watershed before runoff begins. The selection of a curve number (*CN*) for a drainage area is influenced by various factors, including the hydrologic soil group, percentage of impervious cover, vegetative cover condition, and the antecedent moisture condition of the area. Playa lakes are typically treated as impermeable surfaces in different studies (e.g., French and Miller, 2012). Therefore, a *CN* value of 98 is often assigned to represent 100% impervious cover for all soil hydrologic groups (i.e., A, B, C, and D) (City of Lubbock, 2019).

When estimating peak flow and developing a runoff hydrograph using the SCS method and dimensionless unit hydrograph, a consistent peaking factor of 484 is recommended for all analyses within the City of Lubbock (City of Lubbock, 2019).

B.3.3.2.2 Required Design Flood Frequency in Playa Regions

The required design frequency depends on the project's scope. However, several studies have considered 100-yr flood as a critical scenario in hydrology of regions with playa lakes (e.g., Busby, 1975, French et al., 2006; French and Miller, 2012). Among the literature reviewed, the City of Lubbock Drainage Manual (2019) provides the most comprehensive recommendations for required flood frequencies for different infrastructures built within playa lake basins. These recommendations are shown in **Table B.10**. Playas are classified into overflow and non-overflow in this manual. For overflow playas, the minimum storm to be considered is a 100-year, 24-hour event, whereas for non-overflow playas, a 500-year, 24-hour storm event should be considered. In certain urban playa scenarios, the City Engineer may mandate using the 500-year, 24-hour storm event for overflow playas. Also, for culvert design across various roadways, it is suggested to use 100-year flood for flood mitigation purposes.

Table B.10 Required design frequencies by design type for areas within playa basins (Adopted partially from the City of Lubbock Drainage Manual (2019)

Design Type	Minimum Design Frequency
Playa Lake (Overflow)	100-year
Playa Lake (Non-Overflow)	500-year
Culverts (where Playa Overflow Route Included)	
Street Classification:	
Type R-1A Residential	100-year
Type R-1 Residential	100-year
Type R-2 Residential	100-year
Type C-1 Collector	100-year
Type I Industrial	100-year**
Type T-1 Thoroughfare	100-year**
Type T-2 Thoroughfare	100-year**
Type E-1 Expressway (Including Frontage Roads)	100-year
Type E-2 Expressway (Including Frontage Roads)	100-year

*Refer to current City of Lubbock Master Thoroughfare Plan (MTP) for definitions of street classifications. The level of protection listed will govern where topographic conditions, inlet and outlet conditions and street profile grades permit the installation of the appropriate culvert dimensions. Where conditions are not conducive to achieving the listed level of protection, Developer shall coordinate with the Engineering Department to determine an acceptable level of protection.

** Outside lane, on upstream side, can be inundated by culvert headwater.

In a study conducted by Busby (1975) on Apple Valley's dry lake in California (a playa lake region), while using 10-year flood for any stream channel in the area was established, there was a need to predict floods larger than a 10-year event, especially to define the boundaries for areas likely to flood during 100-year events. This was essential for identifying flood-prone zones and planning for major flood events. The study proposed a methodology to define the 100-year peak flow and contributing inundation boundary using the 10-year flood scenario for those areas lacking a 100-year flood estimation. This approach included examining the ratios of the 10-year flood to different flood levels at all measurement stations in the desert areas of southern California. Despite some discrepancies in the data points, the average values at various recurrence intervals showed a fairly distinct pattern. These specific ratios were then used to predict the 100-year flood level.

B.3.3.3 Infiltration and Recharge Rate Beneath Playa Lakes

Infiltration and recharge, while related, are distinct processes. Infiltration refers to the process by which water from precipitation, irrigation, or surface water sources penetrates the soil surface and enters the subsurface layer. Recharge refers to the volume or rate of water entering groundwater and interacting with the water table (Gurdak and Roe, 2009). Infiltration can occur within playa lakes as well as fluvial fans located within playa basins.

The subsequent section will discuss the dynamics of infiltration and recharge rate beneath playa lakes, covering various aspects crucial to understanding these processes. Firstly, conceptual models of recharge beneath playas will be reviewed. Additionally, the relationship between infiltration rate and factors such as geographic location and water depth will be explored, explaining how environmental variables influence the infiltration process within playa ecosystems. Moreover, methods for estimating infiltration and recharge rates will be examined, offering insights into quantifying the flux of water into groundwater aquifers. Lastly, the section will address the potential impact of climate change on playa infiltration, investigating how changing climatic conditions may affect infiltration rates and consequently alter groundwater recharge dynamics within playa environments.

B.3.3.3.1 Conceptual Models of Recharge Beneath Playas

Gurdak and Roe (2009) presented three conceptual models based on a comprehensive review of literature on recharge beneath playas in the High Plain aquifers. These models include:

- *Playas as Evaporation Pans:* This model suggests that playas primarily function as evaporation pans, with water accumulating in them mostly evaporating back into the atmosphere, contributing minimally to groundwater recharge.
- *Recharge Restricted to Playa Annulus:* Advocated by Osterkamp and Wood (1987), this perspective argues that while playas are not exclusively evaporation pans, recharge mainly occurs in the annulus or the perimeter area of the playa. This implies that the central clay soils of the playa contribute less to recharge.

- *Recharge Through Playa Floor:* This model suggests that significant recharge occurs through the clay soils of the playa floor. Despite common beliefs about clay soils impeding water movement, this model highlights the role of desiccation cracks in facilitating recharge.

It is well documented that playas can have recharge rates significantly higher than surrounding interplaya areas. This challenges the idea of playas as purely evaporative pans (first model). Evidence for higher recharge rates beneath playas includes high water flux and contents in playa soils, low chloride concentrations, and high tritium levels indicating recent infiltration, low caliche content in sediments, and a positive correlation between infiltration rates and clay content of the playa floor (Gurdak and Roe, 2009). This evidence suggests that water movement beneath clay-lined playas is significant and not confined to the playa annulus, contradicting the second conceptual model. The third model, arguing for significant recharge through the clay soils of the playa floor, is most strongly supported by the findings of the study by Gurdak and Roe (2009). Recharge rates beneath playa floors vary widely but often exceed those through the annulus and in most interplaya settings. Regional recharge estimates, integrating recharge beneath both playas and interplaya settings, could be significantly lower without contributions from playas, possibly by one to two orders of magnitude. Hence, properly functioning playa wetlands with shrink-swell soils that produce desiccation cracks are vital for the overall recharge contribution to the aquifer. **Figure B.9** shows the recharge estimates through different recharge settings in Southern High Plain playa lakes developed based on previous studies dataset provided by Gurdak and Roe (2009).

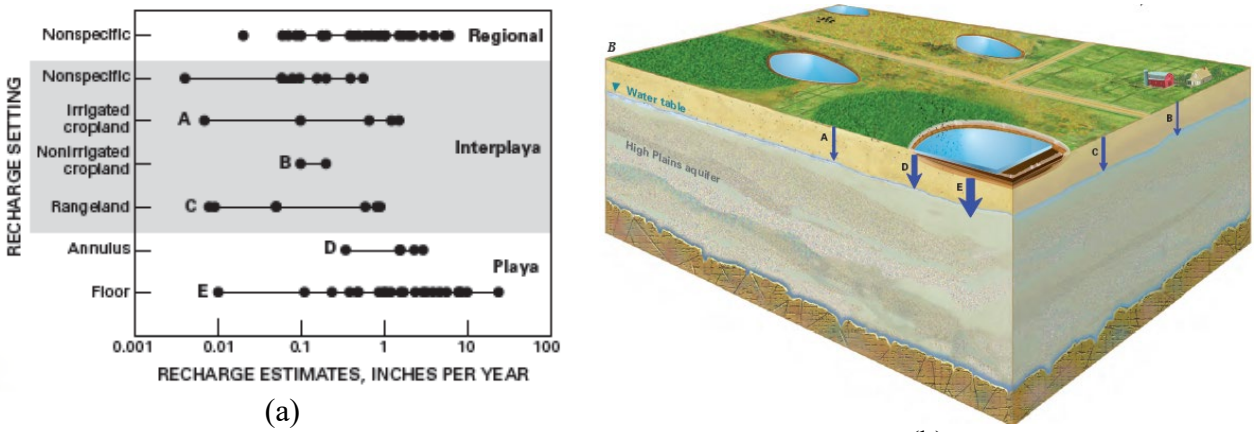

(a) (b)

Figure B.9 (a) Recharge estimates for High Plain playas for recharge setting A–E, and (b) relative magnitude of recharge rates, shown by size of arrows, in each setting (Gurdak and Roe, 2009)

B.3.3.3.2 Factors Influencing Infiltration and Recharge Rate in Playa Lakes

Scanlon and Goldsmith (1997) showed that recharge in playas is strongly influenced by the volume of surface water accumulation and the depth of infiltration. Zartman et al. (1996) stated that recharge beneath playas relies on the infiltration occurring within the playa itself. However, it should be noted that recharge rates typically do not match infiltration rates due to various factors,

such as soil type. Rapid initial infiltration rates decline due to ponding water in playas. This decline triggers clay swelling, leading to the closure of desiccation cracks and preferential flow paths which cause differences between infiltration and recharge rates in playas (Zartman et al., 1994).

Infiltration rates in SHPs' playas can vary from 0 to 116 in/hr, typically being higher near the center due to desiccation cracks in the clay floor (Gurdak and Roe, 2009). These high rates are caused by water moving rapidly through these cracks. Zartman et al. (1994) observed a positive correlation between clay content and infiltration beneath a single playa, challenging the traditional view that high clay content leads to low infiltration. Infiltration rates are generally highest during initial flooding but decrease as the clays swell and seal the desiccation cracks. This trend was observed in other studies as well (e.g., Evans, 1990; James, 1998; Parker et al., 1998).

Scanlon and Goldsmith (1997) also observed a direct relationship between the volume of ponded water on the surface and the geometric characteristics of each playa, the drainage pattern of the surrounding interplaya area, and local climate conditions. Their research demonstrated that preferential flow pathways were more pronounced beneath areas where surface water accumulated on playa floors characterized by initially drier sediments and visible cracks, compared to locations like the playa center that experienced more frequent flooding. These preferential flow pathways, which may include desiccation cracks, interpedal pores, root tubules, and other macropores, play significant roles in the recharge process.

The infiltration rate plays a critical aspect of playa lakes hydrology as it relates the volume of detained water in playas with the loss from the lakebed. Several studies have directly assessed infiltration in playas (e.g., Evans, 1990; Zartman et al., 1996; Huda, 1996; Scanlon and Goldsmith, 1997). However, the water balance method is a widely used method to estimate infiltration rates in playas (Weinberg et al., 2021). This method involves calculating differences between water level changes, evaporation rates, and direct precipitation. In this method, the water level and precipitation are measured directly, while evaporation rates can be calculated using the Penman-Montieth equation. Several studies have been conducted to investigate the temporal variation of infiltration rates of different plays within SHP. **Table ABSM.2** (**Supplemental Martials**) presents a summary of studies and datasets prepared by Gurdak and Roe (2010) on infiltration estimates beneath playas of the SHPs.

The debate surrounding the recharge process beneath playas is ongoing. While some studies propose that the playa annulus serves as a notable recharge zone, where organic material oxidizes to CO_2, forming carbonic acid that enhances subsurface porosity (Gurdak and Roe, 2009), others suggest that recharge predominantly occurs through the playa floors. Scanlon and Goldsmith (1997) observed that sediments in the annulus were only slightly coarser compared to those beneath the playa floor, indicating consistent water drainage beneath the playa floors. Also, the absence of elevated chloride and carbonate concentrations beneath playas could indicate significant water fluxes, possibly attributed to rapid water movement that prevents the accumulation or flushing out of these elements. While evidence of preferential flow beneath certain playa floors has been observed, such flow might face hindrance from layers of sediment with

varying hydrological properties (Scanlon and Goldsmith, 1997). Geologic investigations generally uphold the notion of higher recharge rates beneath playas compared to interplaya areas. Additionally, the presence of low chloride concentrations and calcium carbonate profiles in sediments beneath playas lends further support to this conclusion (Hovorka, 1997; Gustavson et al., 1995).

Several factors affect the estimation of infiltration rate beneath playas. The playa infiltration rate may be correlated with geographic characteristics (such as particular land use, geometry and location of playas, and soil moisture) and hydraulic characteristics (water depth) in the playa basin (Weinberg et al., 2021). In the following sections, the relationships between infiltration beneath SHP playa lakes with geographic and hydraulic characteristics are discussed. Also, estimation methods and studies on infiltration and recharge beneath playas are summarized.

Relationship Between Infiltration Rate and Geographic Location

Weinberg et al. (2021) studied the relationship between infiltration rate and the geographical location of sixteen playa lakes in Texas, spanning an area of 11,000 mi^2. Following the severe drought from 2011 to 2013, small floods were experienced by Texas playas in 2014 due to near-normal rainfall, followed by record floods in 2015. These events were crucial for analyzing the geographic variability of playa infiltration rates and differentiating between macro-pore and matrix infiltration types. The location and average infiltration rates calculated for each playa within SHPs are shown in **Figure B.10**. The period of flooding for these playas ranged from 77 days for the Birkenfeld Playa to 680 days for the Bivins Playa. The 2015 data showed that infiltration generally decreased as water levels dropped. Notably, sudden increases in infiltration correlated with additional flooding. The result of this study showed a clear geographic pattern in infiltration rates for SHP, with higher rates in the southwestern part and lower rates in the northeastern part. This pattern correlates with regional soil type variations, suggesting that local soil composition significantly affects infiltration rates. These findings corroborate earlier research, like that of Ganesan et al. (2016), who similarly observed diverse infiltration rates across various Texas counties. Their study highlighted increased infiltration in the southern and western regions of the examined area.

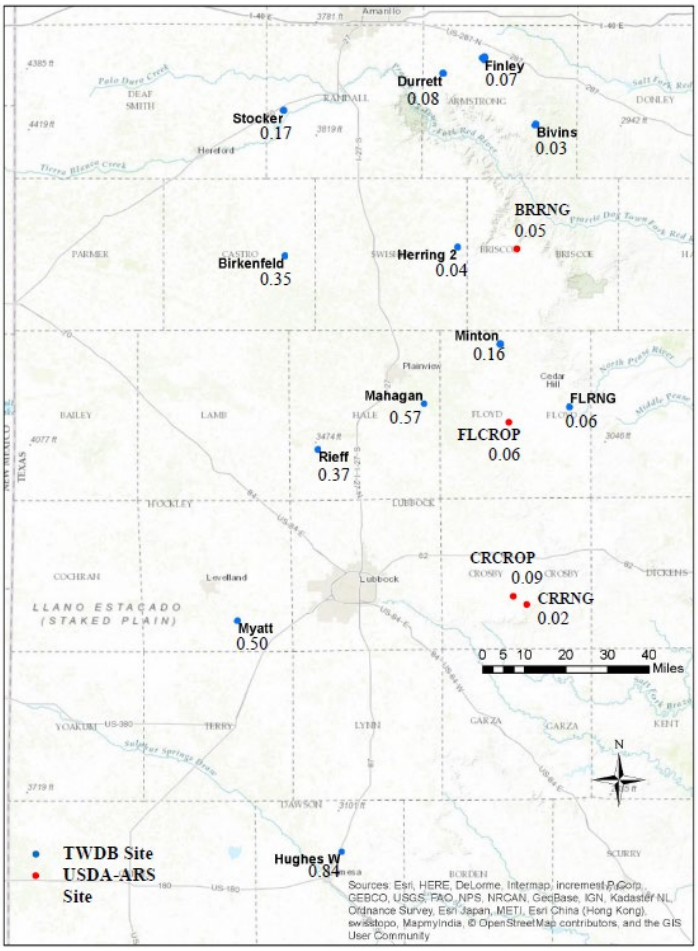

Figure B.10 Distribution of average infiltration rates in SHPs Playas for flood events in 2015 (Weinberg et al., 2021)

Relationship Between Infiltration Rate and Water Depth

Infiltration rates in Texas playas are reported to rise with flood depth, primarily due to increased hydraulic gradients and the presence of more permeable soils near the edges of the playa (Weinberg et al., 2021). This trend is evident through the observed linear correlation between estimated monthly average infiltration rates and pressure head (water depth) for playa lakes within the area studied by Weinberg et al. (2021). They specifically investigated the correlation between infiltration rate and water depth for the FLRNG Playa Lake during the 2014-2015 period. Situated northeast of the City of Lubbock in an area characterized by diverse land use, this playa covers a watershed area of 536 acres, with a focal playa area of 27.9 acres (**Figure B.11**). It typically experienced a flood duration averaging 197 days, with a total flood volume of 1,179 acre-ft (based on data from 1996 to 2017). **Figure B.12** depicts the relationship between average water depth and infiltration rate at the FLRNG Playa, showing a linear correlation. This finding aligns with previous research on flow through porous media in playa lakes and is consistent with historical data from the study conducted by Hauser's (1966) on playas near Lubbock, Texas.

The analysis of data from the FLRNG Playa yielded an effective infiltration rate for the entire sediment thickness in the playa basin, estimated at 1.6×10^{-3} in/day for each inch of pressure head. Specifically, if the top 6.5 ft of soil constitutes the most restrictive layer, it results in an infiltration rate of about 0.12 in/day. While this rate is typical for silty clay, it notably surpasses what soil core samples had suggested.

B.3.3.3.3 Infiltration and Recharge Rate Estimation Methods

The rates of infiltration and recharge can be estimated using indirect or direct methods. Water budget analysis is a commonly used method for indirect estimation of infiltration and recharge under playas. The techniques developed for unsaturated zones may be utilized to directly estimate recharge rates, particularly in semi-arid and arid regions. These techniques encompass physical methods, chemical-tracer techniques, and occasionally numerical models, albeit predominantly applied at a small spatial scale (Gurdak and Roe, 2009). Physical methods commonly involve the use of infiltrometers for measuring infiltration rates, while numerical models face reduced application in playa regions due to the intricate processes within clay-lined playa floors (McMahon et al., 2006; Gurdak and Roe, 2009).

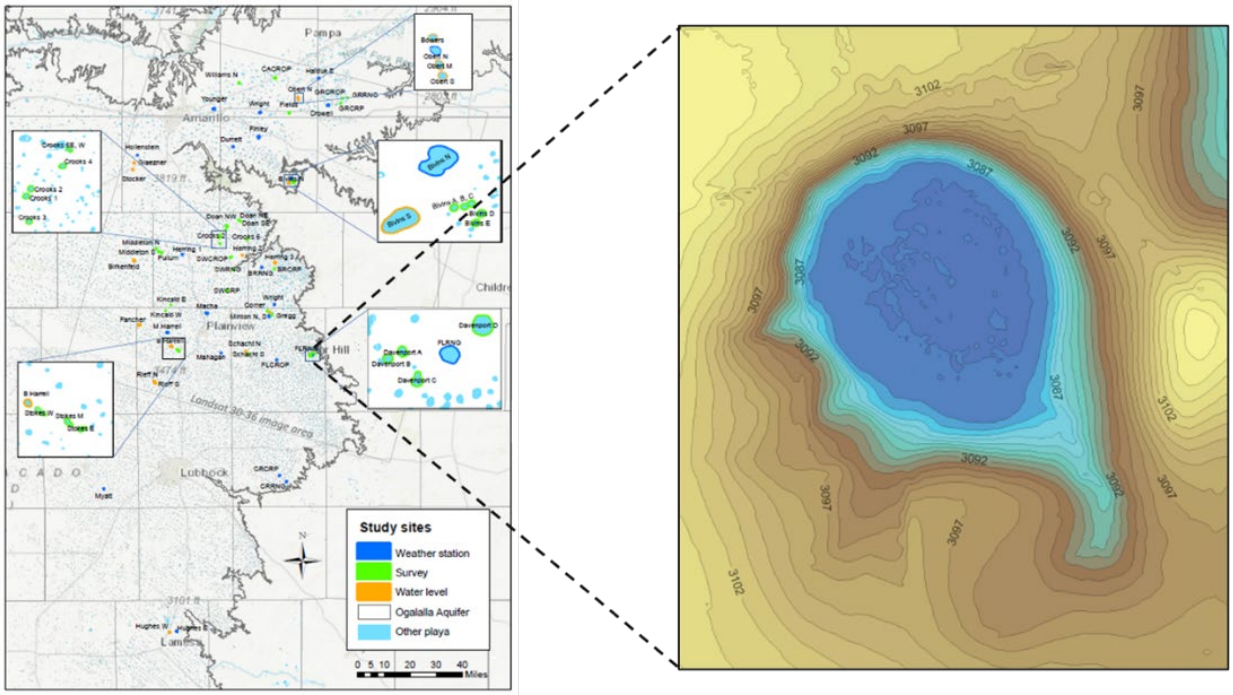

(a) (b)

Figure B.11 (a) Location of playa lakes, and (b) Survey map of FLRNG Playa Lake in the study conducted by Weinberg et al. (2021)

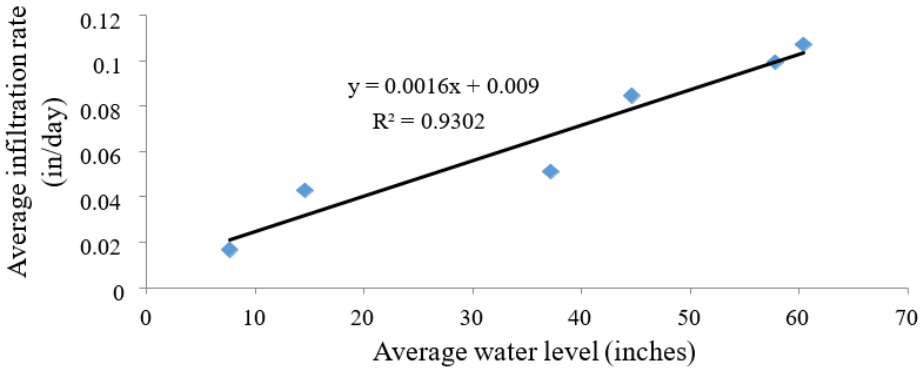

Figure B.12 Relationship between infiltration rate and water depth for FLRNG Playa Lake based on 2014-2015 data (Weinberg et al., 2021)

Estimation of Infiltration Using Water-Budget Analysis

This water-budget method is based on the principle that incoming water into a playa equals its outflow considering evapotranspiration or infiltration (Gurdak and Roe, 2009). By calculating the runoff to a playa and subtracting the water lost to evapotranspiration, the remainder is the volume infiltrating beneath the playa. However, this method rarely uses direct measurements for infiltration or recharge (West, 1998).

The water-budget analysis method was used by Claborn et al. (1985) to study infiltration and recharge processes in 22 playas in the SHPs. Their study revealed that between 30 to 50 percent of the runoff entering playas could potentially infiltrate through the playa annulus, contributing to recharge. However, it should be noted that they relied on indirect techniques to estimate water volume above the clay-lined floor and did not collect data directly to confirm either the precise volume of water in the playa or the actual infiltration into the annulus.

In most unsaturated-zone studies, water fluxes are estimated rather than recharge being directly measured, often under the assumption that these fluxes represent actual recharge rates. Recharge rates reported range from 0.11 to 4.72 in/yr in playa floors and 0.004 to 1.26 in/yr in interplaya settings, with a consensus emerging that recharge rates tend to be higher beneath playas compared to interplaya areas (Scanlon and Goldsmith, 1997).

Measurement errors in water-budget calculations introduce uncertainties in infiltration or recharge estimates. Accurately determining the water surface elevation in playas to estimate volume over time requires precise knowledge of playa geometry. Surveying errors can lead to uncertainties in these estimates. Additionally, these studies often lack data on subsurface water movement, which is crucial to determine whether infiltrated water reaches the water table as recharge. The potential for subsurface water movement in the SPHs aquifer, including lateral or upward directions, has been observed, but water-budget methods alone cannot determine this potential (McMahon et al., 2006; Gurdak et al., 2007; Gurdak and Roe, 2009).

Estimation of Recharge Rate Using Direct Measurements

Estimating recharge rates using direct measurements involves directly measuring the influx of water into the groundwater system. This typically includes techniques such as monitoring groundwater levels, measuring changes in soil moisture content, and employing lysimeters or infiltration meters to directly quantify the amount of water infiltrating into the subsurface.

Direct measurement methods were employed to assess the movement of soil moisture from the unsaturated zone to the Ogallala Aquifer (Weinberg et al., 2021). This data is essential for comprehending aquifer recharge processes. However, at most study sites, the absence of monitoring wells hindered direct observation of aquifer response to playa flooding, which limits the capacity to definitively estimate how quickly infiltration leads to recharge. At the Hollenstein Playa (shown in **Figure B.13**), water level data from an unused irrigation well, situated within 25 ft of the playa, showed signs of recharge approximately a month after the May 2015 flooding. The water level in the measuring well increased 21.7 inches over about 90 days, then stabilized as the flood reduced. Recharge at this location was calculated using **Equation B.8**.

$$R_{tj} = S_y \times \Delta H_{tj} \quad \text{(B-8)}$$

where R_{tj} represents recharge, S_y is specific yield, and ΔH_{tj} is the peak water level rise.

Weinberg et al. (2021) used a specific yield of 0.15 for the Ogallala Aquifer and ΔH_{tj} = 21.7 inches, to estimate recharge as 3.25 inches, translating to six acre-ft from the 22-acre water area. It should be noted that this approach underestimates actual recharge since recharge is not a discrete event and the gradual and slow water table rise allows lateral dispersion of water.

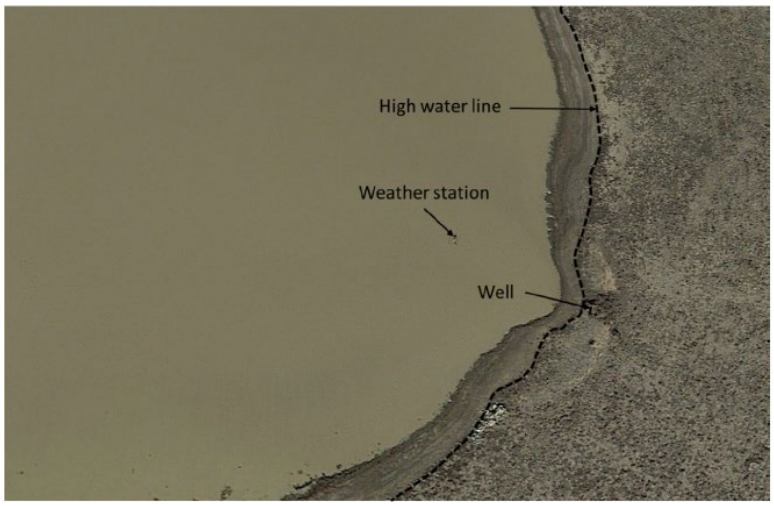

Figure B.13 Location of the irrigation well at the Hollenstein flooded Playa basin (Weinberg et al., 2021)

Groundwater studies focusing on playa recharge often employ tracer-based techniques, such as dating groundwater age using tritium (3H) and environmental tracers such as chloride (Cl^-) (Gurdak and Roe, 2009). These techniques offer recharge estimates on broader spatial scales, making them more appropriate for extensive groundwater resource investigations. Unlike the point-specific estimates from unsaturated-zone studies, groundwater studies provide spatially averaged recharge rates. However, they may lack the spatial resolution to assess the impact of individuals or groups of playas (Scanlon et al., 2002, 2003).

Nativ and Smith (1987) used tritium in groundwater as a tracer, and estimated playa recharge rates between 0.5 and 3.24 in/yr. Compared to diffuse recharge settings, which range from 0.01 to 0.57 in/yr, their finding suggested that the High Plains aquifer primarily receives recharge through focused percolation from playa lakes (Barnes et al., 1949; Stone and McGurk, 1985; Stone, 1990).

Wood and Sanford (1995) provided a regional recharge estimate of 0.43 inches/yr for the northern part of the southern High Plains using a chloride-mass balance approach from groundwater. Fryar et al. (2001) reported data from shallow monitoring wells near playas, revealing a pattern of episodic precipitation, evaporative concentration of solutes, runoff, and infiltration, including return flow from wastewater and irrigation. **Table ABSM.3 (Supplemental Materials)** shows some of the studies with different approaches for assessing recharge from playa lake obtained from a review study presented by Gurdak and Roe (2009).

B.3.3.3.4 Impacts of Climate Change on Playa Infiltration

The impact of climate change and variability on water resources, including playa habitats in the High Plains, is a growing concern. Predictions suggest various changes in precipitation patterns that could affect regional water resources and playa hydrology (Gurdak and Roe, 2009), including:

- *Winter Precipitation Changes*: Reduced snowfall in winter could potentially increase winter recharge beneath playas due to reduced evapotranspiration losses.
- *Decrease in Annual Precipitation*: Particularly in New Mexico and Texas, reduced annual precipitation might lead to decreased recharge beneath playas.
- *Increase in Summer Precipitation:* This increase might initially seem beneficial for playa recharge, but it could lead to higher erosion and sedimentation rates, potentially reducing recharge.
- *Local Variability and Extreme Weather Events*: Continued high variability in precipitation, with potential local droughts and regional flooding, could have complex impacts on playas.

CHAPTER B4 : REVIEW LITERATURE ON HYDROLOGIC APPROACHES TO ARID REGIONS

This chapter presents fundamental insights into arid regions, including their global distribution and importance, notably in the United States, with a specific emphasis on Texas arid areas. It also explores the hydrology of arid and semi-arid areas through an extensive review of available scientific and technical publications.

B.4.1 Arid Regions

Arid regions are characterized by low precipitation and humidity, as well as high temperatures and evaporation rates. These regions cover approximately 30% of the Earth's land surface, where potential evapotranspiration exceeds rainfall (Herczeg and Leaney, 2011).

Various studies have proposed different ranges of rainfall for arid and semi-arid regions (e.g., Barakat, 2009; Soliman, 2010; IFAD, 2021). Soliman (2010) proposed a general classification of rainfall ranges in different climate conditions, including:

- *Deserts*: Areas receiving less than 2.7 inches (70 mm) of rainfall annually, where evaporation surpasses precipitation.
- *Arid Regions*: Areas experiencing annual rainfall ranging between 2.7 and 7.8 inches (70 and 200 mm), characterized by sparse vegetation.
- *Semi-arid Regions*: Delineated areas by total annual rainfall ranging from 7.8 to 17.7 inches (200 to 450 mm).

Water in arid regions is often scarce and primarily located in specific areas, such as streams, lakes, and aquifers. These water sources are crucial for both natural ecosystems and human populations, requiring effective management. This management entails an understanding of how these sources are replenished, and how they interact with each other and the surrounding environment.

Hydrology of arid regions is complex and involves a wide range of topics and hydro-meteorological and ecological characteristics (Goodrich, 2017). The hydrological processes may include surface runoff, infiltration, evaporation, and transpiration. In some arid regions, there may be seasonal floods, which can be beneficial for recharging aquifers and supporting plant growth; however, floods can also cause erosion and damage to infrastructure and communities.

B.4.2 Distribution of Arid Regions

B.4.2.1 Distribution of Arid Regions Around the World

Arid regions are distributed worldwide, encompassing areas such as the Sahara Desert in Africa, the Mojave Desert in North America, the Australian Outback, and the Arabian Desert in the Middle East. A substantial portion of the Earth's land surface, totaling 41%, is inhabited by approximately 2.5 billion people residing in arid and semi-arid regions, as illustrated in **Figure B.14**. It is

estimated that arid regions cover around 10.8 million mi^2 (28 million km^2) while semi-arid regions cover around 17.8 million mi^2 (46 million km^2) (Qader et al., 2021).

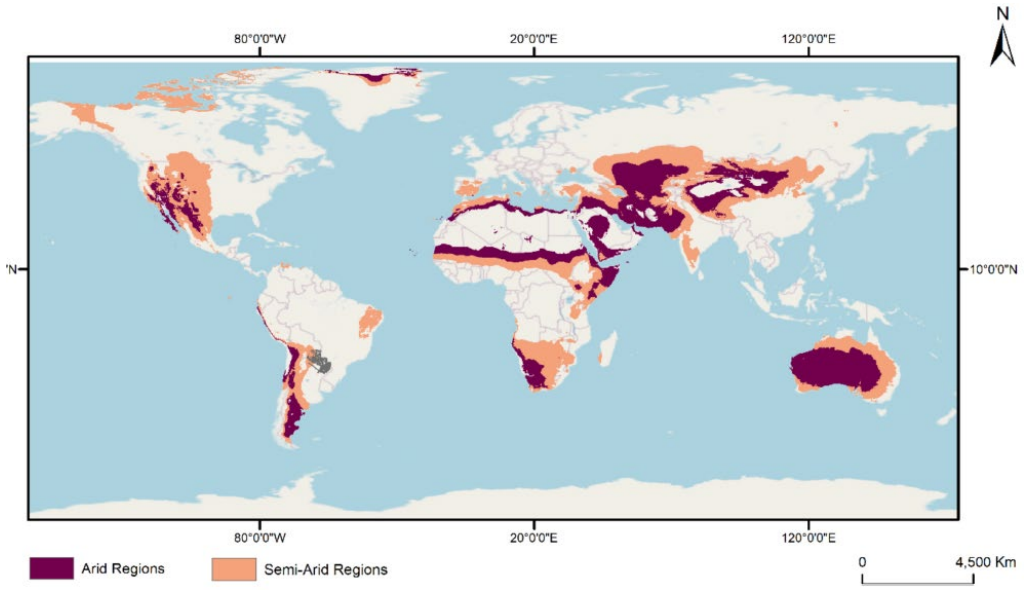

Figure B.14 Global distribution of arid and semi-arid regions (Qader et al., 2021)

B.4.2.2 Distribution of Arid Regions in the United States

The distribution of arid areas in the United States varies across different regions. Some of the notable arid regions in the U.S. include:

- *The Southwest*: This region encompasses states such as Arizona, New Mexico, Nevada, and parts of California, Utah, and Texas. It is characterized by desert landscapes, including the Mojave Desert, Sonoran Desert, and parts of the Great Basin Desert (Seager et al., 2007).
- *The Great Plains*: Portions of the Great Plains, particularly in states such as Kansas, Nebraska, Oklahoma, and parts of Texas, experience semi-arid conditions with low precipitation and high evaporation rates (Rosenberg, 1987).
- *Intermountain West*: This region includes parts of Idaho, Montana, Wyoming, Colorado, and Utah, where arid and semi-arid conditions prevail, especially in valleys and basins surrounded by mountain ranges (Comer & Schulz, 2007).
- *The Pacific Coast*: Some coastal areas of California, Oregon, and Washington experience arid or semi-arid conditions, particularly in rain shadow areas where mountains block moisture-laden air from reaching inland regions (Baldocchi et al., 2004).

The distribution of arid and semi-arid regions of the United States is shown in **Figure B.15**.

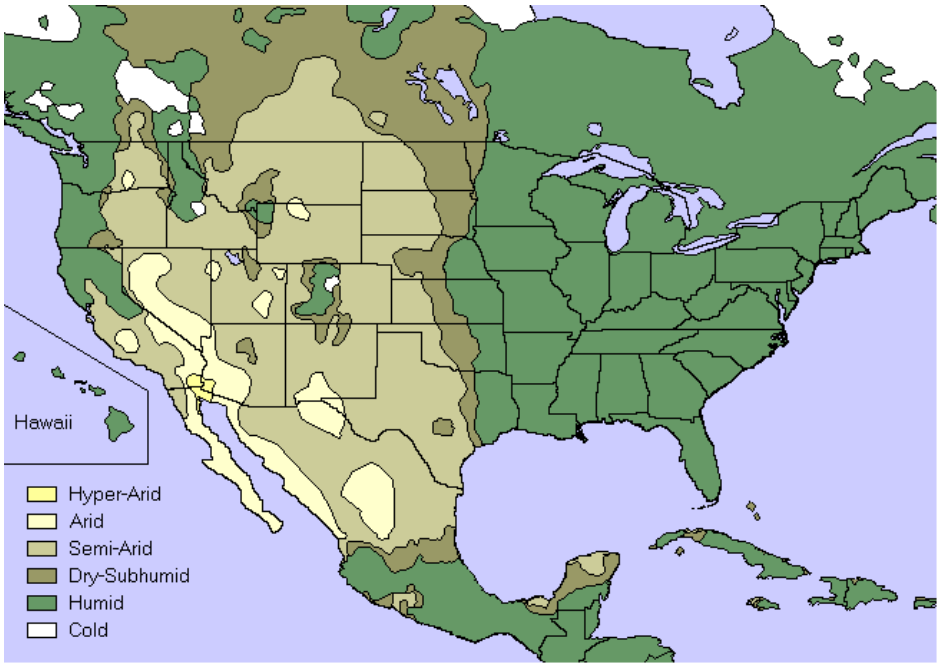

Figure B.15 Arid and semi-arid regions of the United States
(Source: https://cales.arizona.edu/OALS/soils/surveys/states.html)

B.4.2.3 Distribution of Arid Regions in Texas

Texas has a diverse climate and landscape, with some regions being more arid than others. The weather in Texas varies widely, from arid in the western regions to humid in the east; the part of Texas that lies to the east of I-35 is subtropical, while the portion that lies to the west of I-35 is arid. Approximately 39% of Texas is classified as arid or semi-arid based on the Köppen climate classification system (**Figure B.16**).

According to the United States Department of Agriculture (USDA), approximately 61% of Texas falls within the arid and semi-arid regions, which are characterized by hot summers, mild winters, and annual precipitation of less than 20 inches (508 mm). This includes large areas of West Texas, the Big Bend region, and the Panhandle. The eastern and southeastern parts of Texas, on the other hand, receive more rainfall and are characterized by more humid subtropical climates. The USDA estimates that about 39% of Texas falls within these regions. The arid region of Texas is characterized by desert and semi-desert ecosystems, including the Chihuahuan Desert and the Great Plains grasslands.

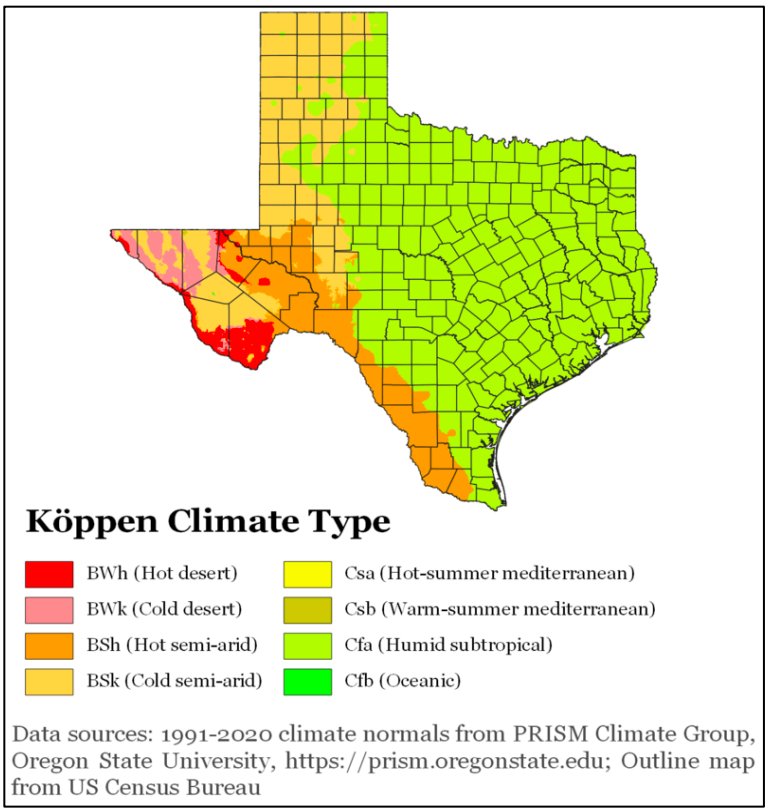

Figure B.16 Distribution of arid and semi-arid regions in Texas and Köppen climate classification (Source: https://en.wikipedia.org/wiki/Climate_of_Texas)

B.4.3 Hydrology of Arid and Semi-arid Regions

Hydrology of arid and semi-arid (ASA) regions is characterized by low and highly variable precipitation, high evapotranspiration, and limited surface water resources. These conditions present significant challenges for water resource management and the design of infrastructures in these regions. Seasonal floods may be experienced in some ASA regions, potentially contributing to the recharging of aquifers and the promotion of plant growth. Flooding can also lead to erosion and inflict damage to infrastructure and communities. Although the hydrological processes in ASA regions may include the same functions as those in humid environments (i.e., surface runoff, infiltration, evaporation, and transpiration), their hydrology cannot be readily predicted by inference and extrapolation from wetter regions (Goodrich, 2017).

Flooding is reported as the most important natural disaster in arid regions, as the most severe floods occur in these areas. However, flood forecasting in these regions has not shown much improvement due to the complex hydrological process in arid regions and the lack of data.

B.4.3.1 Rainfall-Runoff Relationship in Arid Regions

The relationship between rainfall and runoff in arid regions is highly variable and often depends on a range of factors, including soil type, land cover, topography, and rainfall pattern. In general, rainfall in arid regions is often characterized by short, intense precipitation, rather than steady,

continuous rainfall in wet regions. This can limit the amount of runoff that is generated because a major portion of the surface runoff may be absorbed by the soil or lost through evaporation. However, during heavy and prolonged rainfall, runoff can become a significant source of water for rivers, streams, and groundwater recharge. In addition, the topography can play a significant role in the rainfall-runoff relationship in arid areas. The steep-sided canyons and arroyos that are common in West Texas and the Panhandle can funnel water and increase the risk of flash flooding and erosion (Jiang et al., 2015).

Land use and land cover can also have a significant impact on the relationship between rainfall and runoff in arid regions. In arid areas with poor vegetation, such as deserts, or bare rock, runoff can be high as there is little to no vegetation to intercept and absorb runoff. In contrast, areas with dense vegetation may have lower rates of runoff as vegetation can absorb and store water, reducing the amount of surface runoff.

Table B.11 provides a summary outlining the similarities and differences between arid and non-arid regions across various hydrological parameters, including rainfall patterns, runoff dynamics, evaporation and transpiration processes, time of concentration, and the availability of relevant data, as presented by Alsubeai (2021).

Table B.11 Similarities and differences between the hydrology of arid and non-arid regions (Alsubeai, 2021)

Hydrology Factor	Arid Regions	Non-arid Regions
Rainfall	Intensive short events, with low annual rainfall amounts. Rainfall tends to be more variable than other regions. Most of the rainfall occurs in summer.	Low-intense rainfall events occur evenly throughout the year.
Runoff	Extreme rainfall events cause severe stream flows with irregular infiltration capacity.	Surface runoff occurs when rain falls on saturated areas in these regions. Uniform infiltration capacity is considered for these regions.
Evaporation and Transpiration	High evaporation rate from bare soil and low transpiration due to low vegetation cover.	Potential evapotranspiration is less than in arid regions causing rainfall to occur when temperature is low (winter).
Method of Estimating Time of Concentration	In arid and non-arid regions, time of concentration (T_c) may be estimated using the SCS and velocity methods	
Data Availability	Very rare	Widely available

All the considerations highlighted in the hydrology of arid and semi-arid (ASA) regions must be considered when selecting the appropriate methodology to calculate hydrological parameters such as peak flow rate, storage, curve number, rainfall losses, runoff coefficient, etc. The following sections present approaches for estimating these parameters in arid and semi-arid areas.

B.4.3.1.1 Estimation of Peak Flow in Arid Regions

Estimating the peak flow is directly related to the storage capability of the watershed and the amount of rainfall loss in the region, which requires an understanding of the local hydrological processes that govern the movement of water through the landscape. Site-specific data collection and analysis are often necessary to accurately estimate these parameters. Additionally, calculating rainfall loss is a key factor to consider in hydrological studies, accounting for the total loss of precipitation due to evaporation, infiltration, etc. However, calculating these parameters in arid regions can be challenging due to several factors, including limited data availability, high spatial and temporal variability, complex topography, non-uniform soil moisture distribution, limited accessibility, and logistics (Elfeki and Bahrawi, 2017; Kamis et al., 2018; Marko et al., 2019). According to Soliman (2010), when estimating peak flow rates in arid and semi-arid (ASA) regions, the most commonly used methodologies include: the infiltration method, overland flow hydrograph, the rational method, the Soil Conservation Service (SCS) method, and the unit hydrograph method; with a crucial consideration being the calculation of rainfall loss, which accounts for precipitation lost through processes such as evaporation and infiltration.

The SCS method is a widely used technique for estimating peak flow rates in arid and semi-arid regions because it effectively accounts for losses using the curve number methodology (Wang et al., 2012; Al-Ghobari et al., 2020; Niyazi et al., 2022). Moreover, the method is considered applicable in arid areas because it incorporates the initial abstraction, which is a critical factor in the hydrological behavior of ASA regions (Niyazi et al., 2022).

The SCS Curve Number (SCS-CN) and the SCS-Unit Hydrograph (SCS-UH) are two commonly used methods for simulating flood events. Their performance was evaluated in the arid region of the Wadi Al-Lith basin in western Saudi Arabia, which has a watershed area of 1260 mi^2 (3262 km^2) and experiences average annual precipitation ranging from 3.9 to 6.5 inches (100 to 165 mm) (Niyazi et al., 2022). The study's findings suggest that modifications to the SCS methodology may be necessary for hydrological studies conducted in arid and semi-arid regions. The SCS-CN and the SCS-Unit Hydrograph (SCS-UH) methods are discussed in the following sections.

SCS-CN Method

Several studies have employed the SCS method for calculating runoff in arid and semi-arid regions. The advantage of using this method is considering the soil characteristics, land use, and land cover of the study area through curve number values. However, the SCS curve numbers are mainly derived based on normal (humid/semi-humid) conditions and may need some modification to represent the hydro-climatology of the arid and semi-arid regions (Alsubeai, 2021).

The Hydrologic Engineering Center-Hydrological Modeling System (HEC-HMS) developed by the US Army Corps of Engineers is commonly used for analyzing rainfall-runoff processes and designing flood mitigation structures, particularly in the United States. Numerous studies in the literature are based on HEC-HMS, given its accessibility and robust functionality to be used for different climate conditions (Basahi et al., 2016; Bamufleh et al., 2020). Within HEC-HMS, the

SCS-CN model is widely employed for loss estimation, utilizing parameters such as initial abstraction and infiltration losses to predict direct runoff.

Equations B.9 and **B.10** show relationships for estimating direct runoff using the SCS method. A critical parameter in these equations is the initial abstraction which is mainly used for validation purposes in hydrology modeling and refers to all losses prior to runoff and consists mainly of interception, infiltration, evaporation, and surface depression storage (Rammal and Berthier, 2020). The role of this parameter is very important, especially in large events that could increase or decrease the chance of flashiness as a measure of flash flood severity in the region as it directly affects the curve number estimation.

$$R = \begin{cases} 0 & P \leq \lambda S \\ \dfrac{(P-\lambda S)^2}{P+(1-\lambda)S} & P > \lambda S \end{cases} \quad \text{(B-9)}$$

$$S = \frac{1000}{CN} - 10 \quad \text{(B-10)}$$

where R refers to direct runoff depth (inches), P is to precipitation depth (inches), λ is the initial abstraction ratio, S is soil maximum potential retention (inches), and CN refers to curve number.

In ungauged basins, CN is commonly estimated using a series of tables (USDA-SCS, 1985), and then R is estimated assuming $\lambda = 0.2$ as a common value. In the case of gauged basins where P is known, one may estimate CN for a given value of λ by combining **Equations B.9** and **B.10**.

Additional information on the SCS-CN method and the factors influencing curve numbers (CN) is provided in the **Supplemental Materials**.

Alternative Methods for Calculation of CN in Gauged Arid and Semi-arid Areas

Methods, such as the least square method (LSM) and the Asymptotic Fitting Method (AFM), have been developed for calculating CN values for gauged areas in arid and semi-arid (ASA) regions. The LSM determines the curve number and initial abstraction ratio by minimizing direct runoff and estimates runoff using **Equations B.9** and **B.10**. Conversely, the AFM, developed by Hawkins (1993), is a technique aimed at analyzing storm precipitation behavior by investigating the relationship between precipitation and CN, termed the CN-P relationship. This method entails plotting precipitation (P) and CN values and fitting an exponential model to the data to understand storm behavior, which can be classified as complacent, standard, or violent based on the characteristics of the fitted curve (Niyazi et al., 2022)

Farran and Elfeki (2020a,b) employed the LSM to determine the optimized initial abstraction value for several arid areas in Saudi Arabia. They concluded that the best initial abstraction for arid regions in Saudi Arabia is 0.01, in contrast to the typical initial abstraction ratio of 0.2 suggested by the USDA-SCS (1985). Niyazi et al. (2022) utilized the initial abstraction of 0.01 and compared runoff generated using seven hydrology scenarios. In each scenario, different methods were utilized to estimate CN values including SCS-CN tables, Least Square Method (LSM), Asymptotic

Fitting Method (AFM), Antecedent Moisture Content Conditions for Curve Number (AMC-CN), and Antecedent Runoff Condition (ARC). The latter three methods are discussed in the following sections.

Asymptotic Fitting Method (AFM)

AFM estimates *CN* using the *CN-P* relationship expressed by **Equation B.11**.

$$CN(P) = CN_* + (100 - CN_*)\,\mathrm{Exp}\left(-\frac{P}{b}\right) \quad \text{(B-11)}$$

where CN_* and b are estimated by solving a minimization problem to find the best values that fit the dataset. As the precipitation approaches infinity ($P \rightarrow \infty$), the Curve Number (*CN*) converges towards an asymptotic value denoted as CN_*. This behavior signifies a limit to the runoff potential of a particular area, indicating that beyond a certain level of precipitation, the soil's ability to absorb water reaches a saturation point, leading to minimal additional runoff despite further increases in precipitation.

The AFM was found to be inadequate for estimating curve numbers to simulate hydrologic response in arid regions of the Saudi Arabia environment (Niyazi et al., 2022). Despite the potential improvement in simulation results with λ = 0.01, it was concluded that both λ = 0.2 and λ = 0.01 are unsuitable for hydrological simulation. However, these values may apply to the design of mitigation structures, providing a reasonable margin of overestimation for safer design considerations.

Antecedent Moisture Content (AMC)

The AMC considers three conditions of the *CN* values (as in the SCS-CN tables (NRCS, 2004)), i.e., CN_I, CN_{II}, *and* CN_{III} for dry, normal, and wet conditions, respectively. Niyazi et al. (2022) utilized AMC equations proposed by Farran and Elfeki (2020c) for two different initial abstraction conditions for Saudi Arabia arid areas, i.e., drier than normal (AMC-I) or wetter than normal (AMC- III). **Equations B.12** and **B.13** were used to calculate *CN* values for the AMC-I condition, while **Equations B.14** and **B.15** were employed for the AMC-III condition, respectively.

$$CN_I = \frac{CN_{II}}{1.906 - 0.00906\,CN_{II}} \quad \text{for} \quad \lambda = 0.01 \quad \text{(B-12)}$$

$$CN_I = \frac{CN_{II}}{1.572 - 0.00572\,CN_{II}} \quad \text{for} \quad \lambda = 0.2 \quad \text{(B-13)}$$

$$CN_{III} = \frac{CN_{II}}{0.459 + 0.00541\,CN_{II}} \quad \text{for} \quad \lambda = 0.01 \quad \text{(B-14)}$$

$$CN_{III} = \frac{CN_{II}}{0.512 + 0.00488\,CN_{II}} \quad \text{for} \quad \lambda = 0.2 \quad \text{(B-15)}$$

Farran and Elfeki (2021) stated that AMC for dry conditions (AMC-I) is deemed optimal for hydrological simulation in arid regions, given their predominance in the region, while AMC-II

may be more appropriate for flood mitigation structure design. The comparison between simulated and observed peak flow and runoff volume in the events examined by $\lambda = 0.01$ is more suitable for simulating hydrological response in Saudi Arabia arid areas compared to the common value of $\lambda = 0.2$.

Niyazi et al. (2022) revealed significant scatter, a common characteristic observed in arid regions. This scatter was attributed to inherent uncertainties in hydrological processes, exacerbated by the lack of detailed measurements of rainfall-runoff interactions. According to this study, $\lambda = 0.01$ is more suitable for simulating hydrological response in Saudi Arabia arid areas compared to the common value of $\lambda = 0.2$.

Antecedent Runoff Condition (ARC)

The ARC serves as a metric of the actual available storage relative to the average available storage at the onset of a rainfall event and is closely linked to the soil's antecedent moisture content. It is categorized into three groups: ARC-I, ARC-II, and ARC-III. Soliman (2010) provided Antecedent Runoff Condition (ARC) for arid and semi-arid regions to be used in the SCS method's *CN* calculations. The average *CN* typically referenced for a specific land area corresponds to ARC-II conditions. However, these *CN* values can be adjusted for conditions that are drier than normal (ARC-I) or wetter than normal (ARC-III) using **Equations B.16** and **B.17**.

$$CN_I = \frac{CN_{II}}{2.3 - 0.0013 CN_{II}} \quad \text{(B-16)}$$

$$CN_{III} = \frac{CN_{II}}{0.43 + 0.0057 CN_{II}} \quad \text{(B-17)}$$

where CN_{I}, CN_{II}, and CN_{III} are the curve numbers under ARC-I, ARC-II, and ARC-III conditions, respectively.

SCS-Unit Hydrograph Method

The Soil Conservation Service (SCS) introduced a parametric Unit Hydrograph (UH) model, which is based on averages of unit hydrographs derived from monitored rainfall and runoff data collected from numerous small agricultural watersheds across the United States. This methodology has been utilized to model hydrology conditions in several arid and semi-arid zones (e.g., Şen, 2007; Albishi, 2015; Niyazi et al. 2022). In this method, once the mean UH is computed using gauge data, it will be transformed into a dimensionless UH by dividing time by time to peak (t/t_p) and discharge by peak discharge (Q/Q_p).

The lag time (T_{lag}) parameter is essential for the Unit Hydrograph (UH) model because it represents the time it takes for rainfall to generate runoff and reach its peak discharge. Accurately estimating this parameter is crucial for modeling hydrological conditions, especially in arid and semi-arid zones where water availability is limited and the response of watersheds to rainfall events can vary

significantly. By incorporating lag time into the dimensionless UH transformation process, the model can more accurately simulate the timing and magnitude of peak discharge, thereby improving its reliability for predicting runoff behavior in different hydrological scenarios. The lag time may be obtained from measured hydrographs at gauge stations or calculated using **Equation B.18**. This equation may be utilized when computing the unit hydrograph using Snyder's method within the framework of the SCS method.

$$T_{lag} = \frac{(L)^{0.8}\,(\frac{1000}{CN} - 9)^{0.7}}{1900\,Y^{0.5}} \quad \text{(B-18)}$$

where T_{lag} is the lag time in hours, L is the hydraulic length of the watershed in ft, and Y is the watershed slope in percent.

B.4.3.1.2 Time of Concentration

The time of concentration (T_c) is a key factor in developing flood hydrographs in ungauged watersheds, reflecting how quickly water flows in response to rainfall. Bondelid et al. (1982) indicated that a significant portion of the error in predicting peak discharge in arid regions stems from inaccuracies in estimating T_c. Estimating T_c presents a major challenge in arid regions due to insufficient data availability (Bondelid et al., 1982; Zahraei et al., 2021). The estimation of T_c typically depends on how the time of concentration is defined. According to Zahraei et al. (2021), the common definitions of T_c are as follows:

i. time required for water to travel from the furthest point in the watershed to the outlet.
ii. duration from the end of rainfall excess to the inflection point on the falling limb of the total runoff hydrograph.
iii. time from the center of mass of rainfall excess to the center of mass of direct runoff.
iv. time from the maximum rainfall intensity to the time of peak discharge.
v. time from the center of mass of rainfall excess to the time of peak of direct runoff.
vi. time from the center of mass of rainfall excess to the time of peak of total runoff.
vii. time from the start of total runoff to the time of peak discharge of the total runoff.

Definition (i) refers to empirical and semi-empirical methods for calculating T_c (**Figure B.17a**). However, definitions (ii) to (vii) represent different perspectives in graphical approaches to determine T_c (**Figure B.17b**).

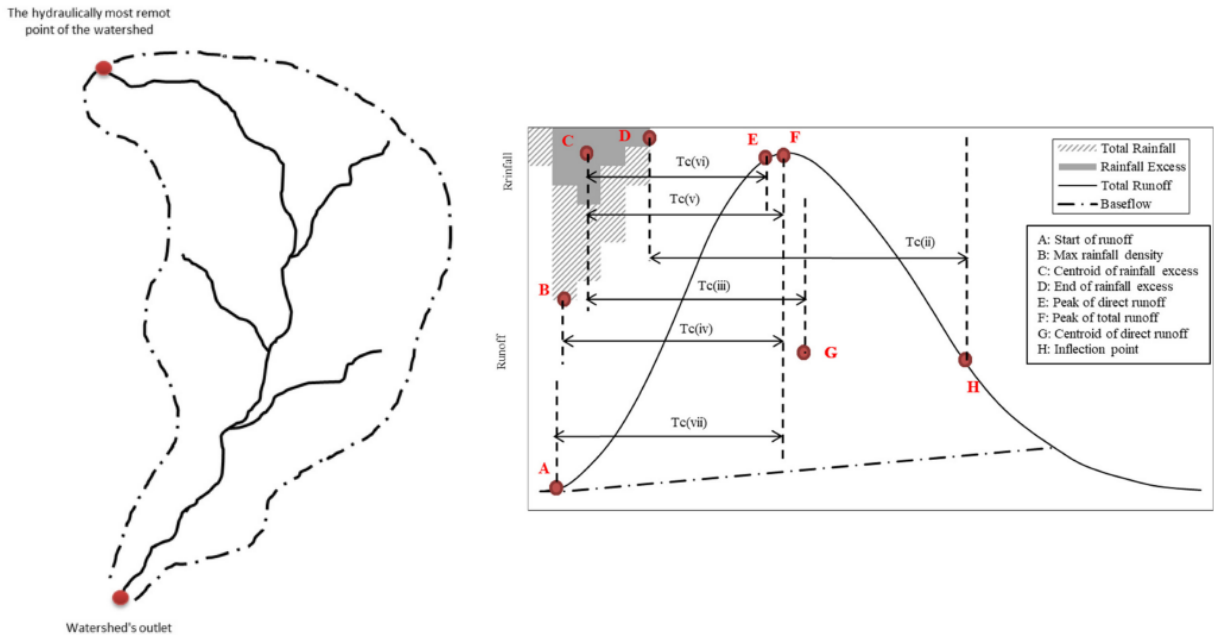

(a) (b)

Figure B.17 (a) Illustration of definition (i) of T_c in a watershed, and (b) rainfall hyetograph and runoff hydrograph to illustrate definitions (ii) to (vii) of T_c (Zahraei et al. 2021)

Numerous empirical and semi-empirical methods stem from definition (i) of T_c are commonly used in ungauged watersheds. These methods rely on watershed characteristics such as area, slope, channel length, and roughness to estimate T_c. Graphical methods, on the other hand, are based on the remaining six definitions, utilizing hyetograph and hydrograph data to define T_c. Among these, definition (ii) is considered the most accurate as it aligns with the saturation of the watershed at the end of rainfall excess (Zahraei et al., 2021).

Two major gaps are identified in the previous studies on the estimation of the time of concentration in ungauged watersheds including arid and semi-arid regions. First, the majority of these studies have concentrated on examining the time of concentration (T_c) in moist, temperate, and tropical zones (Zahraei et al., 2021). However, the behavior of watersheds in arid regions, which exhibit substantial distinctions in rainfall patterns, soil moisture level, and vegetation, has largely been overlooked. Second, while the assessment of hydrographs and hyetographs could offer a more precise determination of T_c as a reference, only a limited number of investigations have utilized actual rainfall-runoff data for this purpose. Nonetheless, these studies have primarily focused on regions outside of arid environments due to the scarcity of available data in such areas. Widely used methods of estimating time of concentration in arid and semi-arid regions are discussed in the following.

Empirical and Semi-Empirical Methods for Estimating T_c

Despite numerous studies on the applicability and modifications of empirical and semi-empirical methods for estimating T_c in temperate and non-arid regions, comprehensive research on utilizing these approaches to calculate T_c in arid regions remains lacking. Several empirical methods are tailored to specific regions with unique characteristics, underscoring the importance of evaluating their accuracy across diverse geographic areas (Wong, 2005). A few recent studies evaluated the accuracy of commonly used empirical and semi-empirical methods for calculating T_c in arid and semi-arid regions. For example, Zahraei et al. (2021) examined fifteen empirical methods from the literature to estimate T_c in an arid region in southern Iran. These methods, originally developed for non-urban watersheds, were selected due to their widespread use. The results of this study showed considerable variability in the value of T_c. The highest T_c values for four sub-watersheds were obtained from the equations proposed by Haktanir and Sezen (1990) and Passini (1914), ranging between 7.5 and 27.9 hours. Conversely, the lowest T_c values were computed using Kirpich (1940) equation, falling between 1 and 2.3 hours. The mean relative differences in T_c obtained by various methods ranged from -82% to 157%. Comparable mean relative differences, spanning from -38% to 207%, were reported by Fang et al. (2008) for central Texas.

The study conducted by Zahraei et al. (2021) also showed notable trends in the T_c values. Specifically, five methods, including Kirppich (1940), California Division of Highways (1960), Giandotti (1940), Williams (1922), and U.S. Corps of Engineers (Linsley et al., 1977), were found to consistently underestimate T_c values, while others tend to overestimate T_c. These results underscore the importance of carefully selecting and evaluating empirical methods, especially in ungauged watersheds. Traditional application of Kirppich (1940) equation without modifications may lead to significant errors, particularly in overestimating peak flood discharge (Zahraei et al. 2021). Furthermore, the estimation of T_c using the Giandotti (1934), Williams (1922), Arizona DOT (1993), and California Division of Highways (1960) methods revealed relatively lower bias (ranging from 8 to 26 hours), suggesting their suitability for accurate predictions of T_c in arid areas.

Discrepancies arise when evaluating these methods based on statistical measures and the coefficient of correlation. Certain methods such as Kirppich (1940), Doog (1973), and Ventura (Mata-Lima et al., 2007) demonstrate high correlation but exhibit notable bias and mean error. This highlights the need for a comprehensive evaluation approach, such as the ranking-based strategy proposed by Sharifi and Hosseini (2011), to select the most suitable methods. Additionally, previous studies in different regions have highlighted the performance of specific methods, suggesting that factors such as watershed characteristics and shape factors play a crucial role in method effectiveness.

In another study conducted by Alamari et al. (2023), various empirical equations were utilized to compute T_c based on the data gathered for each sub-basin of Asir Province in southwest Saudi Arabia, a dryland categorized as an arid region. The empirical equations included Kirpich (1940), USDA-SCS (1972), Federal Aviation Administration (1970), Carter (1961), Kinematic Wave Formula (Kibler and Aron, 1982), Jung (2005), Kraven I (JSCE, 1999), USGS (2000), Chow

(1962), USACE (1954), Albishi et al. (2017), Morgali and Linsley (1965), Izzard and Hicks (1946), McCuen et al. (1984), Johnstone and Cross (1949), Dooge (1973), Giandotti (1934), Haktanir and Sezen (1990), and Sheridan (1994). The estimated values of T_c were subsequently compared to the observed T_c values obtained from direct runoff hydrograph of storm events across all sub-basins. According to this comparison, Dooge (1973) model showed the highest correlation (r = 0.6) with observed T_c, while the Izzard and Hicks (1946) model resulted in the lowest correlation (r = -0.15). The Jung (2005) model performs best in prediction with Nash-Sutcliffe efficiency of 0.33, whereas the USGS (2000) model performs the worst. The Jung (2005) model also has the smallest mean error (-0.10 hr), while the USGS (2000) model showed the largest errors. In general, most models overestimate T_c, especially in arid regions.

Graphical Methods for Estimating T_c

Graphical techniques are commonly favored for the assessment of empirical equations determining the time of concentration. In these methods, T_c may be determined by calculating the time difference between the end of rainfall excess and the inflection point on the hydrograph. These methods of estimating T_c entail visually analyzing hyetographs and hydrographs to estimate the duration it takes for a raindrop to travel from the hydraulically farthest point of a watershed to its outlet.

Zahraei et al. (2021) employed the graphical method as a reference for calculating T_c in an arid region located in the south of Iran. They utilized hyetographs and hydrographs of several storm events in gauged sub-watersheds within the region and used the results to improve the performance of selected empirical equations for calculating T_c. **Figure B.18** shows the hydrograph, hyetograph, and T_c determined using a graphical approach for the March 23, 2017 event in the Salubalm sub-watershed. The results of their study indicated that among these empirical methods, the MacDermott and Pilgrim (1982), Williams (1922), and Arizona DOT (1993) methods emerged as the most suitable for estimating T_c in their study area. Additionally, modifications made to these formulas improved their accuracy. Moreover, the study suggests that utilizing the modified Williams (1922) and Arizona DOT (1993) methods can yield T_c estimations with errors lower than 1%, underscoring their effectiveness in practical applications. The modified empirical methods for estimating T_c, based on the graphical approach, and statistical metrics are presented in **Table B.12**. These equations may be utilized in similar arid regions with comparable climatology and watershed characteristics. However, it is advisable to validate their results before implementing them in different study areas.

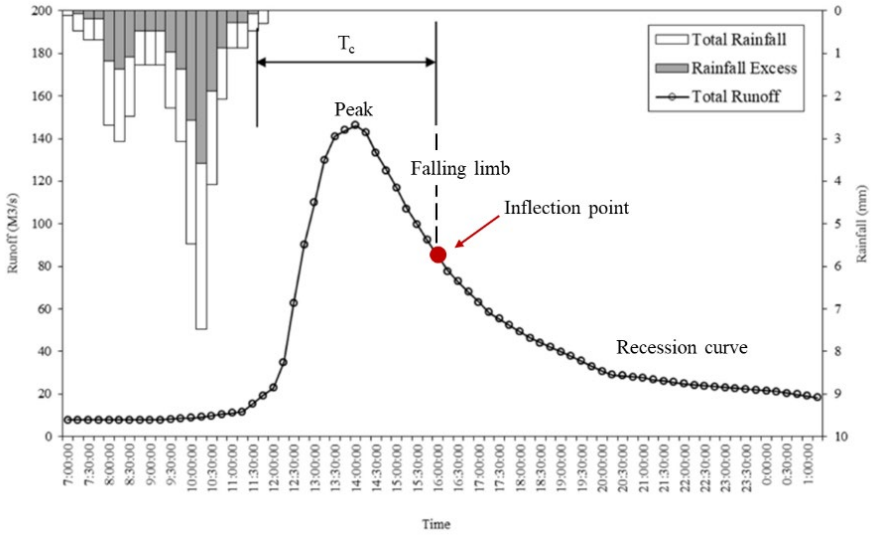

Figure B.18 Hydrograph, hyetograph, and graphically defined T_c for the March 23, 2017 event in the Salubalm sub-watershed (Adopted from Zahraei et al., 2021)

Table B.12 Modified top three empirical methods for estimating T_c in arid areas in Southern Iran (Zahraei et al., 2021)

Empirical Method	Original Equation	Modified Equation	Coeff. of Corr.	Equation No.
Williams (1922)	$T_c = 0.272A^{0.4}\frac{L}{D}S_c^{-0.2}$	$T_c = 1.51A^{0.19}\frac{L}{D}^{-0.16}S_c^{-0.07}$	0.92	(4.1)
MacDermott and Pilgrim (1982)	$T_c = 0.76A^{0.38}$	$T_c = 1.425A^{0.23}$	0.89	(4.2)
Arizona DOT (1993)	$T_c = 0.05508471A^{0.1}(LL_{ca})^{0.25}S_c^{-0.2}$	$T_c = 1.22423A^{0.27}(LL_{ca})^{0.07}S_c^{-0.08}$	0.92	(4.3)

A = area (km^2); S_c = average slope of main channel; S = average slope of watershed; D = equivalent diameter of the catchment (km); L= length of main channel (km); L_{ca} = length measured from the concentration point along L to a point on L that is perpendicular to the watershed centroid (km).

Moreover, Grimaldi et al. (2012) assessed various empirical methods for determining T_c (i.e., Johnstone and Cross, 1949; Department of Public Works, 1995; NRCS, 1997; Giandotti, 1934; Kirpich, 1940; Viparelli, 1961, 1963), as well as the NRCS velocity method, across four small sub-watersheds located in Texas, USA. They used rainfall-runoff analysis through the graphical method in their assessment. **Figure B.19** shows the sub-watersheds examined in their study. Findings from this study revealed substantial variability in T_c estimates from empirical methods, reaching up to 500%. The results of this study underscore the importance of selecting appropriate empirical equations tailored to specific watershed characteristics and climatic conditions. Also, it suggests that refining the NRCS method by appropriately selecting the most hydraulically distant point of the watershed and channel discharge values could improve its accuracy. A critical finding from this study, which must be considered in calculating T_c for arid or non-arid areas, is the

sensitivity of T_c when using the NRCS velocity method with varying DEM resolution. Therefore, it is advisable to investigate the impact of terrain characteristics, especially in 2D flood modeling, especially in arid regions where the risk of flash floods is significant.

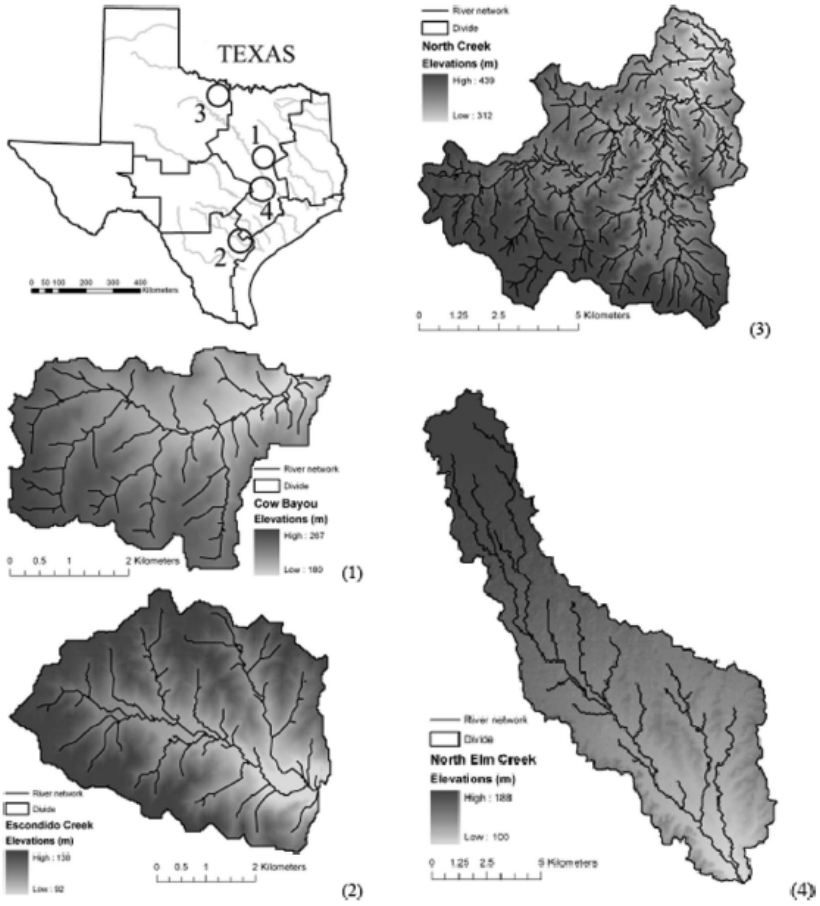

Figure B.19 Location, topography, and drainage networks of the four watersheds examined in the study by Grimaldi et al. (2012)

Velocity Method for Estimating T_c

The Natural Resources Conservation Service (NRCS) commonly employs the velocity method for determining the time of concentration. This method is based on the assumption that the time of concentration equals the combined travel times for segments along the hydraulically most distant flow path, which includes sheet flow, shallow concentrated flow (typically after approximately 100 feet, sheet flow transitions into shallow concentrated flow), and open channel flow (USDA-NRCS, 2010). The travel time for sheet flow can be estimated using **Equation B.19**.

$$T_t = \frac{0.007(nl)^{0.8}}{(P_2)^{0.6}S^{0.4}} \tag{B-19}$$

where T_t is the travel time in hours, n is Manning's roughness coefficient, l is sheet flow length in ft, P_2 is 2-year, 24-hour rainfall in inches, and S is the slope of land surface (ft/ft).

Velocity for different slope ranges in shallow concentrated segment of the longest flow path can be estimated using **Figure B.20**. Also, the flow velocity for open channel flow can be calculated using Manning's equation. Once velocities for shallow concentrated flow and open channel flow are estimated, the time of concentration of each segment can be calculated considering the length associated with each segment of the longest flow path.

The total time of concentration may be calculated using **Equation B.20** considering the length associated with each segment of the longest flow path.

$$T_c = T_{t1} + T_{t2} + T_{t3} + \cdots + T_{tN} \quad \text{(B-20)}$$

where, T_c is the time of concentration, hours, T_{tn} is the travel time of a segment N in hours, and N is the number of segments comprising the total hydraulic length.

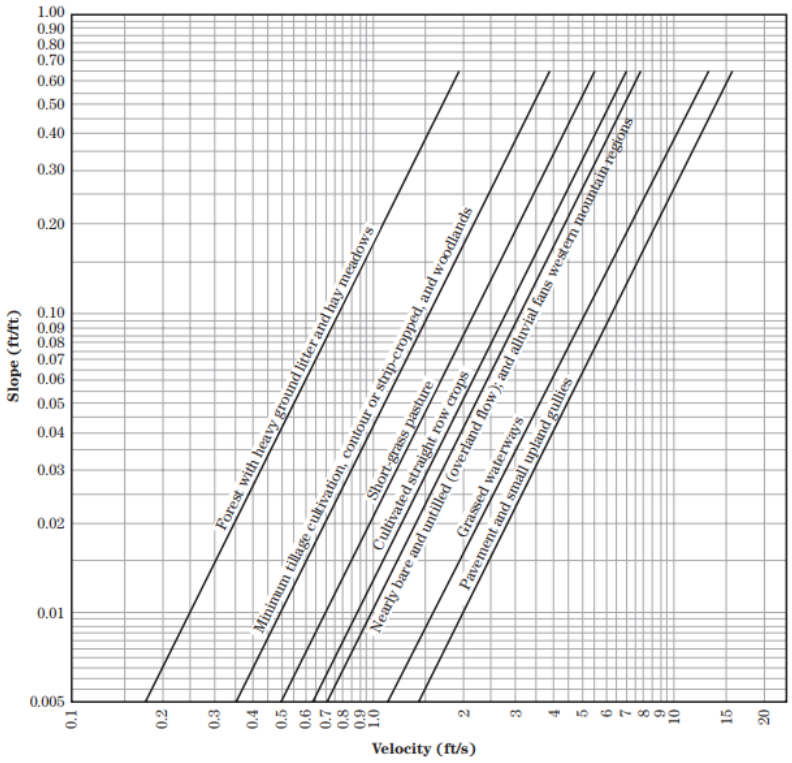

Figure B.20 Velocity versus slope for shallow concentrated flow for different land use and land cover (USDA-NRCS, 2010)

B.4.3.2 Application of Regional Climate-Specific Models in Hydrology of Arid Areas

The primary challenge in simulating rainfall-runoff in arid and semi-arid regions lies in the climatic conditions. Models utilized in these regions often lack components critical for accurate and reliable outcomes. This deficiency stems from using models primarily developed for humid areas with parameters ill-suited for arid environments. Several widely used models for simulating rainfall-runoff in arid regions exemplify this issue. For instance, Mike 11 Nam, originally developed in Denmark with a temperate climate, has been applied in countries like Turkey (Keskin et al., 2007),

Iraq (Kamel, 2008), and Iran (Hafezparast et al., 2013), where climatic conditions vary significantly. Similarly, models such as Sacramento, Pitman, and IHACRES have been employed in Middle Eastern countries with limited modifications to the models' parameters.

Table B.13 provides a summary of four common rainfall-runoff models, their origins, and examples of regions they have been applied. These models, developed in humid regions, have been widely utilized in arid and semi-arid areas, despite potential disparities in parameters that may not be suitable for these regions. Alsubeai (2021) highlighted a longstanding process used to analyze data in arid regions, which often fails to produce accurate results. Factors such as population growth coupled with water scarcity, distinct climate patterns, extreme land use and cover, and variations in rainfall intensity and duration contribute to the complexity of modeling in arid regions. The shortage of substantial data and the absence of suitable simulation software further compound the challenge of modeling in these areas.

Table B.13 Summary of four common rainfall-runoff models utilized in arid and semi-arid areas (Alsubeai, 2021)

Rainfall-Runoff Model	Model Origin and Climate	Regions Model Applied	Climate Classifications
Mike 11 NAM	Mike 11 NAM was originally developed in Denmark where the climate is described as temperate (moderate)	- Turkey (Keskin et al., 2008) - Iraq (Kamel., 2008) - Iran (Hafezparast et al., 2013)	- Mediterranean - Subtropical aridity - Semi-arid
Sacramento	Sacramento model was developed in Sacramento, CA, USA where the Mediterranean climate dominates.	- Jordan (Abdulla et al., 2007) - Thailand (Yang et al., 2020) - Greece (Bournas et al., 2021)	- Hot dry - Tropical - Mediterranean
Pitman	Pitman model was mostly developed and applied in South Africa where the climate is temperate.	- Nigeria (Owolabi et al., 2012) - Angola (Hughes et al., 2006) - Zambia (Mwelwa, 2004)	- Warm tropical - Tropical - Arid or semi-arid
IHACRES	IHACRES model was originally developed by the Australian National University	- Australia (Wheater et al., 2008) - Jordan (Abushandi et al., 2011) - Iran (Ahmadi et al., 2019)	- Tropical - Hot dry - Semi-arid

B.4.3.3 Hydrology of Streams in Arid and Semi-arid Regions of the U.S.

The calculation of streamflow presents complexities and challenges in hydrological studies of arid and semi-arid regions due to the lack of data. Moreover, riparian ecosystems, which surround streams and waterbodies and occupy only small portions of the landscape in arid and semi-arid regions, play a pivotal role in hydrological, geomorphic, and ecological processes (Shaw and Cooper, 2008). Therefore, accurate estimation of the hydrological parameters of streams is essential, requiring appropriate assumptions and modifications to current models to enhance the quality of the hydrology studies of arid and semi-arid regions.

There are two major stream types in arid and semi-arid regions: *ephemeral*, i.e., streams that briefly flow in response to precipitation and remain above the groundwater storage, and *intermittent*, i.e.,

streams flow only at certain times of the year, often receiving water from springs, groundwater sources, or surface runoff (Levick et al., 2008). As mentioned previously, roughly one-third of the Earth's land surfaces are categorized as arid or semi-arid, including vast areas of the Western U.S. (Whitford, 2002). These regions are characterized by low and highly variable annual precipitation, with evapotranspiration exceeding precipitation. The notable contrast between moist riparian areas and adjacent dry upland communities in these dry conditions highlights the significance of streams in arid and semi-arid regions (Levick et al., 2008).

The U.S. Environmental Protection Agency (EPA) has estimated that 59% of streams in the U.S. (excluding Alaska) are ephemeral or intermittent (U.S. EPA, 2005) using the National Hydrography Dataset (NHD) (USGS, 2006). The NHD categorizes streams containing water for only part of the year as ephemeral or intermittent, grouping them in its mapping. Among the six states assessed by Levick et al. (2008), Arizona has the highest percentage of ephemeral and intermittent streams, at 94%, while California has the lowest, at 66%. However, high percentages of non-perennial streams are not limited to the arid southwest; for instance, South Dakota, Kansas, and North Dakota have percentages ranging from 81 to 86%.

The dynamics of desert stream ecosystems extend beyond surface flow, encompassing interactions among surface stream, riparian zone, hyporheic zone (the interface between surface water and groundwater), and parafluvial zone (the stream channel without surface water). These interactions play a crucial role in maintaining the physical, chemical, and biological integrity of streams in arid and semi-arid zones. The parafluvial zone remains less understood compared to hyporheic zone characteristics (Holmes et al., 1994; Boulton et al., 1998; Levick et al., 2008). **Figure B.21** shows four interacting zones of a desert stream ecosystem: the surface stream, hyporheic, parafluvial, and riparian zones.

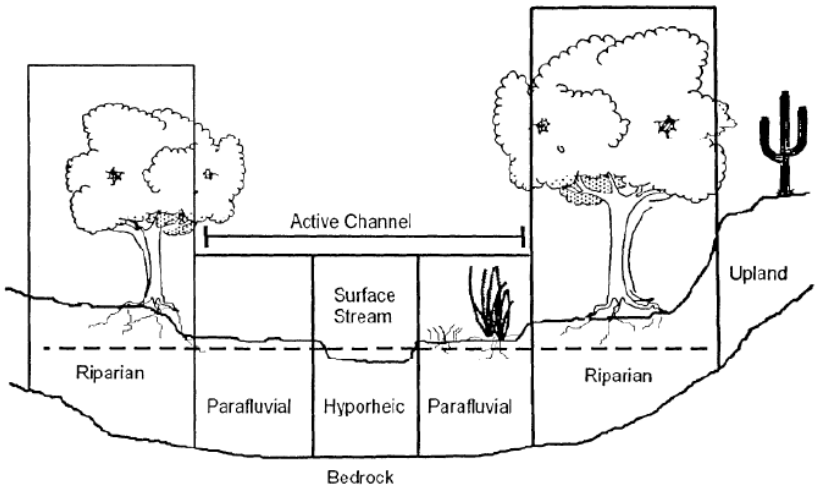

Figure B.21 Interacting zones of arid regions' stream ecosystem: the surface stream, hyporheic, parafluvial, and riparian zones (Holmes et al.,1994)

B.4.3.3.1 Characteristics, Functions, and Ecosystem Significance of Arid Region Streams

Ephemeral and intermittent streams in arid and semi-arid regions exhibit distinct characteristics compared to perennial streams found in wetter, more humid environments. These streams have evolved within a climatic regime marked by wide fluctuations of precipitation, ranging from periods of drought to intense floods.

Human activities, such as urbanization, can further impact these streams, affecting soil quality, vegetation, and overall hydrological and ecological functions within the watershed (Commission for Environmental Cooperation, 1997). Despite their importance, the ecological integrity of terrestrial arid and semi-arid ecosystems is challenged by their limited water availability, hindering rapid recovery from human-induced disturbances, although desert streams tend to rebound more quickly than upland areas (Shaw and Cooper, 2008). While hydrologists typically reject the notion of an "*underground river*", some streams may maintain water below the surface, sustaining diverse plant and animal life, as exemplified by the San Pedro River in Arizona, which borders a groundwater-dependent cottonwood forest (**Figure B.22**).

Figure B.22 Groundwater-dependent cottonwood trees lining an intermittent stream (San Pedro River in Arizona) (Levick et al., 2008)

Ephemeral and intermittent streams can constitute headwater reaches or the main stem within watersheds, typically prevalent in arid and semi-arid regions. The classification of ecoregions provides a valuable framework for understanding the environmental conditions surrounding these streams, facilitating research, assessment, and management efforts.

Ephemeral streams, which lack continuous flow except during rainfall events, and intermittent streams, which flow only under specific conditions, serve crucial hydrological functions similar to perennial streams. In arid and semi-arid regions, ephemeral streams exhibit notably higher

variability in flood magnitudes compared to perennial streams, with extreme events being more frequent. This variability is observed prominently in the southwestern U.S., where the majority of stream reaches are ephemeral or intermittent due to low average annual rainfall (Renard, 1970). Streamflow occurrences in these areas are significantly influenced by rainfall patterns, with contributions from summer monsoons and sporadic winter thunderstorms. However, significant streamflow events in ephemeral channels are rare and typically occur during high-intensity, short-duration rainfall events associated with the summer monsoon season (Gochis et al., 2006).

The influence of rainfall patterns on streamflow varies across the region, with areas like New Mexico receiving a significant portion of annual precipitation during the monsoon season (Hereford et al., 2002; Webb and Betancourt, 1992). Understanding these patterns is essential for managing water resources in arid and semi-arid regions. Effective management strategies must account for the unique hydrological dynamics of these regions, including the transient nature of streamflow in ephemeral and intermittent streams, to ensure sustainable water use and ecosystem health.

B.4.3.3.2 Rainfall Patterns in Arid and Semi-arid Regions and Streamflow Variability

Many characteristics of floods in arid and semi-arid regions are notably distinct due to the low annual precipitation levels, resulting in low annual runoff rates with increased interannual variability as precipitation decreases (McMahon, 1979; Rodier, 1985). The variability in mean annual runoff in North American arid lands is approximately double that of the continental average, highlighting the challenges in predicting runoff in these regions (McMahon, 1979). Moreover, the spatially variable precipitation patterns lead to a wide range of annual runoff totals for watersheds of similar sizes, making watershed areas an unreliable measure of runoff in arid and semi-arid regions (Reid and Frostick, 1997). Ephemeral stream channel transmission losses and partial area storm coverage further complicate watershed rainfall-runoff response, particularly in larger watersheds (Goodrich et al., 1997).

In arid and semi-arid regions, excluding mainly allogenic rivers, most rivers experience long periods without flow, with ephemeral stream channels hydrologically active for only a small fraction of the year (Reid et al., 1998). Consequently, process studies in these regions often focus on flood events due to their infrequent occurrence (Graf, 1988). Floods in these regions are influenced by distinctly different climatic processes, leading to differences in magnitude and frequency relations. For instance, floods caused by precipitation from tropical cyclones typically have greater magnitudes than floods caused by other storm types (USGS, 1997).

The variability of flow in streams in arid and semi-arid regions is a natural continuum influenced by climatic and ecological factors, making the classification of streams challenging and emphasizing the dynamic nature of desert streams (Stanley et al., 1997). Advancements in monitoring and measurement methods may better capture these natural phenomena, potentially altering stream classifications without physical changes to the rivers themselves.

B.4.3.3.3 Types of Floods in Arid and Semi-arid Region

In arid and semi-arid regions, floods exhibit various types, ranging from entirely channeled to largely unchanneled events (Olsen, 1987). Partly channeled floods are observed in the U.S. Southwest during major events when riverbanks are overwhelmed, causing floodwaters to spread across expansive, low-gradient plains (Hedman and Osterkamp, 1982). Conversely, unchanneled floods, described by Graf (1988), occur as sheet floods in piedmont settings.

Channeled floods in arid and semi-arid region rivers manifest in different forms, including flash floods, single-peak events, multiple-peak events, and seasonal floods (Graf, 1988). Flash floods, predominant in ephemeral and intermittent systems, occur suddenly, lasting minutes to weeks depending on climatic conditions and watershed characteristics. These floods, triggered by short-duration, high-intensity precipitation events, can occur throughout the year after sufficient precipitation has generated runoff. **Figure B.23** shows a flash flood in an ephemeral stream in southern Arizona.

Figure B.23 Flash flood in an ephemeral channel, Southern Arizona (Photograph by USDA-ARS/SWRC, obtained from Levick et al., 2008)

Most analyses of floods in arid and semi-arid regions focus on flash flood hydrographs, typically generated by convectional precipitation in small watersheds (Reid, 1994; Dick et al., 1997). These hydrographs are characterized by steep rising and receding limbs, with rapid rise to peak discharge followed by a longer recession period (**Figure B.24**). The recession curve of ephemeral stream hydrographs, characterized by finite duration and exponential decay, is a notable feature (Chow et al., 1988). However, less documented are single and multiple-peak floods generated by tropical storms, frontal systems, or seasonal snowmelt or rainfall, which exhibit a gradual rise in the hydrograph's rising limb and broadening of the flood's time base (Knighton and Nanson, 1997).

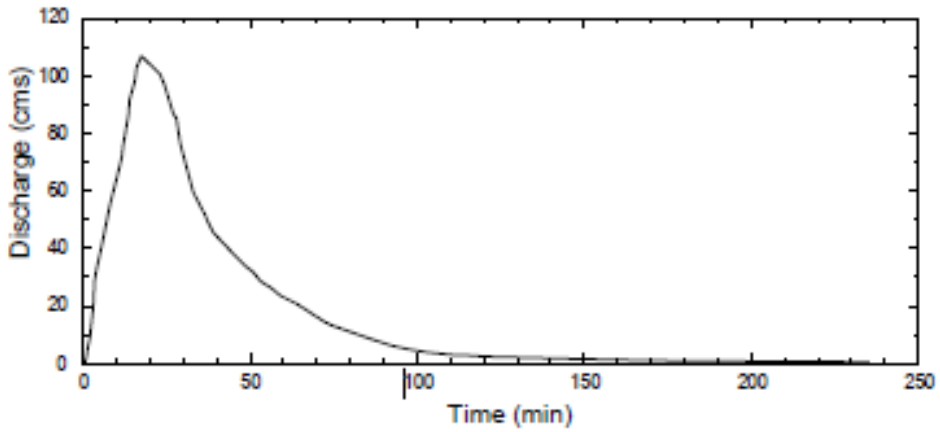

Figure B.24 Example of flash flood hydrograph with rapid rise to peak flow and long recession limb (Levick et al., 2008)

B.4.3.3.4 Transmission Losses

In both spatial and temporal dimensions, streamflow in arid and semi-arid region rivers displays distinctive features. Regardless of the source of water, flows in these rivers typically experience downstream volume decreases, known as influent flows. These reductions in flow volume are primarily attributed to transmission losses, which occur as streamflow infiltrates into the unconsolidated alluvium forming channel boundaries, as well as losses from overbank flooding and evaporation of floodwaters (Babcock and Cushing, 1942; Keppel and Renard, 1962; Sharp and Saxton, 1962; Lane, 1983; Goodrich et al., 1997; Cataldo et al., 2004). Moreover, transmission losses serve as a significant source of water for groundwater recharge.

Downstream flow volume decreases may be insignificant along small, alluvial, or bedrock channels but can be substantial along larger alluvial channels, with many flows failing to traverse the full channel length, resulting in dry lower watershed regions (Keppel and Renard, 1962; Aldridge, 1970). The nature of rainfall events plays a role in these downstream flow reductions. During widespread precipitation, tributary contributions may augment downstream flows despite significant losses. Conversely, spatially localized events, combined with hydrograph attenuation and limited tributary inflows, can lead to notable downstream decreases in total flow volume, flood peak, and flow frequencies (Keppel and Renard, 1962; Lane, 1983; Goodrich et al., 1997; Knighton and Nanson, 1997).

B.4.3.4 Geomorphic Characteristics of Streams in Arid and Semi-arid Regions

The variability in fluvial processes over time and space is a distinctive feature of rivers in arid and semi-arid areas (Tooth, 2000). However, the role of rivers in shaping desert landscapes has often been underestimated, leading to insufficient information on geomorphic processes and forms in these regions. This knowledge gap is critical because fluvial processes are a significant cause of challenges in desert areas (Reid and Frostick, 1989). Additionally, the geomorphology and

hydraulic-geometry relationships of ephemeral and intermittent streams differ significantly from perennial streams in humid areas (Graf, 1988; Thornes, 1994).

Despite the considerable variability in form, several generalizations can characterize ephemeral stream channels in arid and semi-arid regions. These channels are often closely spaced, resulting in high drainage density, and exhibit high width-to-depth ratios, braided patterns, and low sinuosity compared to perennial streams in humid areas. The high drainage density and closely spaced channels are typically due to elevated erosion rates and limited runoff, resulting in high sediment concentrations (Reid and Frostick, 1997).

In most arid and semi-arid rivers, the depth increases with discharge at a faster rate than width, particularly in downstream directions, leading to wider channels in lower reaches. The stabilization of channel width for larger drainage areas may be attributed to transmission losses compensating for additional tributary water (Wolman and Gerson, 1978). However, in channels with no significant tributary inputs, transmission losses can lead to decreasing channel width and capacity downstream, with some evolving into unchanneled floods (Dunkerley, 1992).

Ephemeral stream channels often display an oscillating pattern of narrow, incised reaches and wide, shallow reaches, with alternating erosional and depositional reaches migrating progressively upstream. Perturbations by natural or anthropogenic factors can result in continuous incised channels or arroyos. Furthermore, the lower reaches of ephemeral streams are characterized by particularly flatbed topography, with flat-topped channel bars typically rising only slightly above the thalweg. This flatness of the bed and the width of the channel may be related through flow depth, with wide, shallow flows suppressing the formation of secondary current cells that promote bar development (Reid and Frostick, 1997). Rapidly receding flows can alter or destroy bedforms like ripples, dunes, and antidunes that form at greater flow depths. Overall, understanding the geomorphic characteristics of ephemeral streams in arid and semi-arid regions is crucial for managing water resources and mitigating associated challenges in these environments.

B.4.4 Flooding-related Issues in Arid and Semi-arid Regions

Arid areas can pose challenges for transportation infrastructure, particularly where flash floods and other extreme weather events are common. These floods can quickly erode and undermine roadways, bridges, and other infrastructures making them unsafe or impassable. To address the challenges regarding transportation infrastructures, the unique hydrological conditions of the arid regions should be considered when designing and maintaining roads and bridges. This may include designing drainage systems that can handle high volumes of water during flash floods. Also, effective BMPs for transportation infrastructure in arid areas should be designed based on a holistic approach that considers the complex interactions between hydrology, ecology, and human needs. For example, transportation infrastructure can be integrated with water management systems, such as using roadside swales and infiltration basins to capture and recharge stormwater runoff.

B.4.4.1 Flood Damage to Infrastructures in Arid and Semi-arid Regions

In arid and semi-arid regions, the construction of highways and railroads across streams within catchments entails significant costs, particularly for crossing works like bridges, culverts, or low-water crossings. Occasionally, culverts or bridges are strategically positioned to withstand floods that may exceed their design capacity without sustaining damage, although resulting in temporary interruptions to service during flooding events. **Figure B.25** depicts the flash flood water damage at a stream crossing the roadway in Sinai, Egypt, an arid region experiencing sporadic rainfall primarily during winter (Kotb and El Belasy, 2007).

Flash floods stand as the foremost weather-related hazard claiming lives in the United States, with Texas bearing a significant brunt due to its geography and terrain. Designated as "flash flood alley" by the National Oceanic and Atmospheric Administration (NOAA), Texas has experienced an unsettling surge of more than 500 flash flood incidents in the last ten years, with seven of them officially declared federal disasters (TDI, 2021). While flood hazards span across a significant portion of east Texas and the Gulf Coast region, the Texas Hill Country, positioned at the heart of the state, stands out as the most vulnerable area to flash floods across the continent (TDI, 2021). **Figure B.26** illustrates examples of flash flood damage to the roadways in West Texas. Also, an example of damage to roadways and residential areas due to flash floods in arid regions in Tuscan, Arizona is depicted in **Figure B.27**. In such scenarios, achieving an economic balance between occasional service disruptions and the costs associated with larger drainage structures becomes imperative. This balance between infrastructure resilience and cost-effectiveness underscores the importance of integrating hydrological and hydraulic considerations into the design and implementation of crossing works in arid and semi-arid regions.

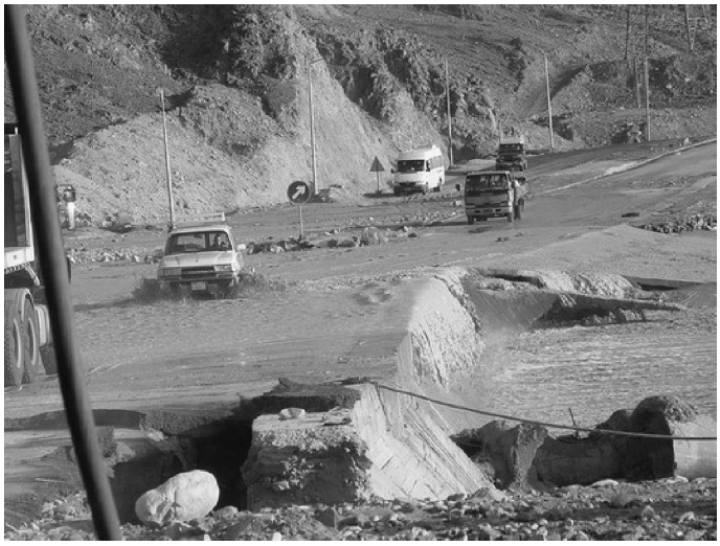

Figure B.25 Flash flood damage to highways crossing a stream in the Wadi Watir Sinai catchment, Egypt (Kotb and El Belasy, 2007)

Figure B.26 Western Texas flash flood damage to a roadway in O'Donnell (ABC News, 2023)

Figure B.27 Examples of a large flood event in an ephemeral stream that damaged roads, bridges, and flooded nearby homes in Tucson, Arizona, July 31, 2006 (Levick et al., 2008)

B.4.4.2 Likelihood of Flash Flood Distribution in the U.S.

Various methodologies have been presented to identify and characterize flash flood-prone zones, including geomorphology-based approaches (Gaume et al., 2009; Marchi et al., 2009), frequency-based analyses (Reed et al., 2007), and flash flood guidance techniques (Georgakakos, 2006).

Saharia et al. (2017) studied flash flood events in the United States and proposed a new geospatial methodology to detect flash flood-prone areas considering hydrology and geomorphology data. The study utilized automated streamflow data collected by the United States Geological Survey (USGS), which collects instantaneous streamflow measurements across a vast network of more than 10,000 gauges. The streamflow database was integrated into the local geomorphological and climatological attributes specific to each basin under investigation. They proposed **Equation B.21**

as a new metric termed "*flashiness*" as a measure of flash flood severity. The flashiness metric is distinct from the annual likelihood of flash flooding, focusing instead on a basin's potential to exhibit a rapid and significant response to heavy rainfall.

$$\emptyset_{ij} = \frac{Q_{ij}^{p} - Q_{ij}^{a}}{A_i T_{ij}} \tag{B-21}$$

where Q^{p} denotes the peak discharge, Q^{a} is the action stage-discharge, A is the basin area, and T is the flooding rise time. Complex relationships between observed flashiness and numerous geomorphological and climatological variables were modeled by employing Generalized Additive Models for Location, Scale, and Shape (GAMLSS). The findings of this study enable predictions of flashiness at various locations in the U.S. **Figure B.28** shows the normalized flashiness distribution map in the United States in which 0 and 1 represent the lowest and highest flashiness factor, respectively. As can be seen in this figure, higher flashiness is distributed within the east and west coasts, and south-central regions, where flash flooding happens due to arid and semi-arid geo-hydrological conditions. Particularly for the State of Texas, while the observation database indicated that flash flood concentration is in central Texas hill country and the Houston area, the study predicted flashiness extended this flash flood-prone area from southwestern Texas through the hill country, further northeastward into adjoining states. **Table B.14** shows a comprehensive overview of the effective parameters considered in analyzing flashiness in the United States by Saharia et al. (2017).

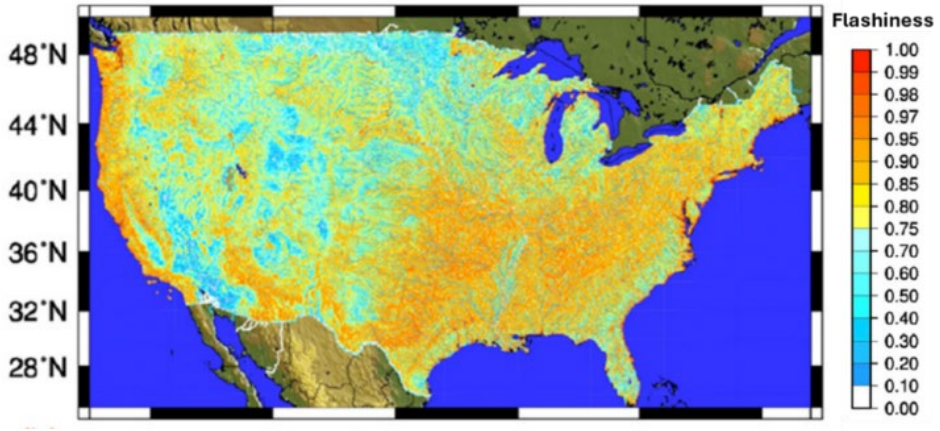

Figure B.28 Flashiness distribution in the United States (modified from Saharia et al., 2017)

Table B.14 Geomorphologic effective parameters for flash flood mapping (Saharia et al., 2017)

Geomorphologic Parameter	Description
Basin area	Total upstream area that contributes to runoff
Shape factor	A dimensionless number that is given by drainage area divided by the square of the main channel length (K = drainage area/channel length^2)
River length	Measured along a line centered from the basin outlet to the intersection of the extended main channel and the basin boundary
Relief ratio	Relief is the difference in elevation between the outlet and the highest point in the basin and relief ratio is relief divided by the basin length (a measure of the basin-wide river slope); the higher the relief ratio, the higher the runoff and the shorter the flooding rise time
Slope index	Slope between two points along the main channel upstream from the mouth of the basin at distances equal to 10% and 85% of the total main channel length
Slope to outlet	Local slope computed at a distance of 1 km over the basin outlet
Basin curve number	Soil Conservation Service Curve Number (SCS-CN) is an empirical parameter that characterizes the runoff properties for a particular soil and ground cover (USDA-SCS1972)
Erodibility factor	Relative index of susceptibility of bare, cultivated soil to particle detachment and transport by rainfall
Rock depth	Depth to bedrock at the outlet
Soil texture (b parameter)	Soil moisture capacity shape parameter, which is a proxy for soil texture, derived from the STATSGO database (Miller and White 1998)

B.4.4.3 Sediment Transport During Flash Floods in Arid Areas Streams

As previously discussed, ephemeral streams, despite their intermittent flow patterns, fulfill essential stream functions such as water, nutrient, and sediment transport. However, unlike perennial streams that continuously transport sediment, non-perennial streams in arid and semi-arid regions typically experience sediment movement as a response to runoff generated by intense, short-duration thunderstorms characteristic of these areas. These thunderstorms often trigger flash floods, characterized by rapidly rising runoff hydrographs carrying heavy sediment loads, including coarse material from uplands and hillslopes.

Stream channels in arid and semi-arid regions typically feature deep sediments predominantly composed of sands and gravels, interspersed with resilient shrubs resistant to strong floodwaters. However, these unconsolidated alluvial sediments are prone to mobilization during flows, unlike the clay-bedded or armored channels in more humid regions. Consequently, the deep sediments contribute to significant transmission losses downstream, resulting in reduced flow volume and velocity along the stream length, and the deposition of bed load materials and coarser suspended sediments downstream.

As discussed, stormwater in ephemeral streams is often absorbed within the channel network before reaching the outlet, leading to transmission losses and decreasing discharge downstream. This promotes a stepwise movement, deposition, and storage of sediment within the stream network, resulting in a pulsing pattern of sediment movement that redistributes within the watershed during subsequent flows. Ephemeral and intermittent channels accommodate a wide range of sediment sizes, with larger material typically remaining stationary but available for transport. These sediment dynamics strongly influence biotic communities, as evidenced by studies in environments like the Namib Desert, where sediment deposition patterns affect moisture availability, plant roots, and the structure of biotic communities (Jacobson et al., 2000). Consequently, disturbances such as the removal of small headwater channels during land development can disrupt flow and sediment dynamics, impacting downstream erosion rates and overall stream productivity as well as increasing threats to infrastructures. **Figure B.29** depicts the sediment-laden floodwater in the ephemeral stream in Walnut Gulch, Arizona, during a large event.

Figure B.29 Photograph showing floodwater in an ephemeral stream (Walnut Gulch, Arizona) (Photograph by USDA-ARS/SWRC, obtained from Levick et al., 2008)

B.4.4.4 Flood Control Strategies in Arid and Semi-arid Regions

Flood control strategies in arid and semi-arid regions demand innovative solutions, given their unique hydrological conditions of sporadic, low rainfall interspersed with high-intensity precipitation. Common strategies include water harvesting through dams and reservoirs for irrigation and drought mitigation, flood diversion structures to keep floodwaters away from urbanized areas, erosion control measures like terracing and reforestation, decentralized stormwater management systems to reduce runoff, vegetation management to stabilize soil and decrease runoff velocity, floodplain zoning to limit development in vulnerable areas, early warning systems for timely alerts, and community engagement for effective preparedness and response.

Soliman (2010) outlined the construction of reservoirs for retaining flash floodwaters alongside channel enhancements to accelerate water movement as a prevalent structural flood control method. Additionally, diversions are employed to redirect floods toward alternative channels (EWRRI, n.d.). These practices vary from local projects like dredging and straightening undertaken by municipalities to extensive basin-wide schemes necessitating significant financial resources. **Figure B.30** shows the construction of a detention dam across streams in an arid region of Wadi Watir, Egypt, to control flash floods.

Figure B.30 Detention dam constructed across streams in an arid region (Wadi Watir, Egypt) to control flash floods (Soliman, 2010)

CHAPTER B5 : REVIEW LITERATURE ON HYDROLOGIC APPROACHES TO KARST AREAS

This chapter starts by presenting essential information about karst terrain, encompassing its global distribution and prevalence in the United States, notably in Texas. It then transitions to explore the hydrology of these unique landscapes, examining the role of groundwater recharge in karst hydrology, as well as the sources of flooding and potential impacts in karst regions, drawing from an extensive review of available scientific and technical publications.

B.5.1 Karst Terrain

Karst regions are characterized by soluble rock formations such as limestone, dolomite, evaporites, halite, etc., which can be dissolved by water (Parise et al., 2018), creating a unique hydrological system. Karstic formations are present on 10-15 % of the continental ice-free surface of the Earth (Ford and Williams, 2007) causing challenges for communities living in these areas. Also, littoral karst drainage zones experience saltwater problems, further complicating freshwater availability (Stevanović and Milanović, 2015).

Hydrological processes in karst regions involve internal drainage, the subterranean diversion of surface streams, storage within shallow epikarst zones, rapid conduit flow, and discharge through sizable springs. The unpredictable connections of water in these areas vary in time due to the numerous and very diverse surface and subsurface karst formations. The hydrology of karst regions is therefore very complex and dynamic due to the interaction between the surface and subsurface features. Apart from hydrological complexities, karst regions are particularly susceptible to an array of geohazards, including sinkholes, slope movements, and floods due to their distinctive characteristics (Stevanović and Milanović, 2015).

Physiographic features in karst landscapes, including sinkholes, disappearing streams, caves, and karst springs are depicted in **Figure B.31**. Sinkholes, as one of the defining features of karst hydrology, are depressions formed by the dissolution of rocks. Other distinctive features of these areas include caves, springs, and disappearing streams. Caves are formed over thousands of years by the slow dissolution of rocks, often containing underground lakes and rivers. Springs are locations where groundwater emerges at the surface, while disappearing streams drain into sinkholes, vanishing underground.

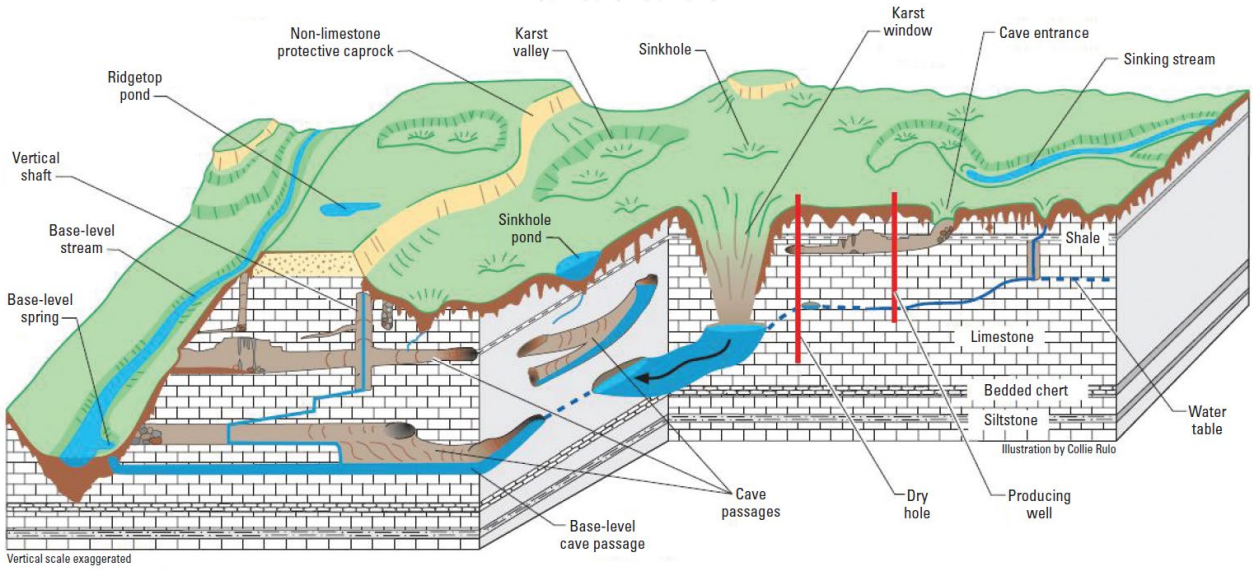

Figure B.31 Physiographic and hydrologic features of well-developed karst terrain (Taylor and Green, 2008)

During storms, the surface runoff drains into sinkholes and caves rather than surface waterbodies (streams, lakes, etc.). Sinkholes are often connected directly to the underlying conduit systems such as underground lakes and rivers (White, 2002) that can transport water quickly and unpredictably, leading to flash floods and droughts. The unpredictable nature of karst environments continues to pose challenges for water management and utilization, with documented successes and failures globally (Milanović, 2000).

While many engineering studies in karst focus on water-related issues, there are also challenges in dry karst or its unsaturated zone, including natural and anthropogenic hazards, as described by Parise and Gunn (2007). Collapse of buildings over sinkholes filled with unconsolidated sediments is a common occurrence in karst environments. Therefore, engineering challenges in karst environments can vary widely, including destructive processes such as massive turbulent flows, rapid erosion of unconsolidated deposits, and propagation of hydraulic pressure over long distances, resulting in significant pressure fluctuations and effects like water-hammer and air-hammer phenomena (Milanović, 2014).

Construction activities in karst regions, including building dams and reservoirs, housing, tunneling, and roads and railways, are inherently delicate endeavors and often result in risks that can have catastrophic consequences, including loss of human lives. The unique characteristics of the karst environment make it highly vulnerable to various geohazards such as sinkholes, slope movements, and floods, compounded by anthropogenic hazards such as pollution events and land use changes (De Waele et al., 2010; Parise, 2015).

The presence of these risks has prompted the development of specialized methodologies for assessing karst hazards and the implementation of specific construction standards in identified problematic zones. Examples include the ASTM D8512-23: *Standard Practice for Preliminary*

Karst Terrain Assessment for Site Development (ASTM, 2023), and specialized construction standards established by the Antikarst and Shore Protection Institute in Dzerzhinsk, Russia, as detailed by Tolmachev (2005).

B.5.2 Distribution of Karst Terrains

B.5.2.1 Distribution of Karst Around the World

The distribution of karst landscapes around the world is extensive and varied, occurring in numerous countries across different continents. Some regions with notable concentrations of karst formations include Southeast Asia, China, Europe, the United States, Mexico, Central America, etc. Karst landscapes occur primarily in areas where soluble rock such as limestone, dolomite, or gypsum is present.

Carbonate rocks, which are found across all climatic zones, experience varying degrees of karst development influenced by climatic conditions (Ford and Williams, 2007). Despite present climatic conditions, karstified carbonate rocks can exist in zones where intense karst development might not be expected, as seen in arid regions like Saudi Arabia, characterized by high rates of water use but limited recharge, leading to groundwater depletion known as *groundwater mining* (Dirks et al., 2018; Schulz et al., 2016).

The relationship between karst and climate is complex and influenced by geological and climatic histories. The Köppen-Geiger climate classification system, which categorizes climates into five main groups based on precipitation and temperature patterns, shows that 34.2% of carbonate rocks are in arid climates, followed by 28.2% in cold climates, and 15.9% in temperate climates. Tropical and polar climates exhibit lower percentages, with 13.1% and 8.6%, respectively. Furthermore, when considering the proportion of karst areas within each climatic zone relative to the total surface area of that zone, temperate climates exhibit the highest percentage (19.1%), followed by cold (16.8%) and arid (14.8%) climates, with lower proportions in tropical and polar zones. These findings highlight the diverse distribution and complex interplay between karst development and climatic conditions globally (Goldscheider et al., 2020). **Figure B.32** shows the distribution of karst zones globally based on the Köppen-Geiger climate classification system.

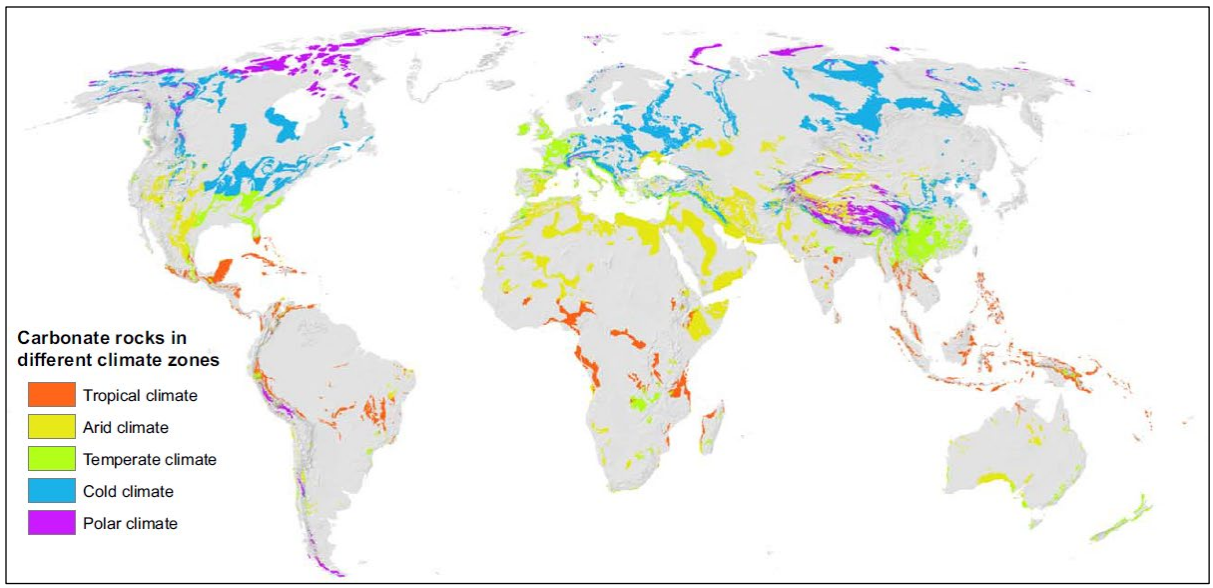

Figure B.32 Carbonate rocks/potential karst aquifers occurrence in different Koppen-Geiger climate zones (Beck et al., 2018)

The World Karst Aquifer Map (WOKAM) is a comprehensive global database detailing the distribution of karstifiable rocks, predominantly carbonates and evaporites, which serve as potential karst aquifers. The database also provides a comprehensive overview of karst aquifers worldwide, showcasing their distribution and significance, highlighting regions where karst landscapes are prevalent and where karst aquifers play a crucial role in water supply and management. According to this database:

- carbonate rocks are prevalent across various landscapes, with 31.1% found in plains, 28.1% in hills, and 40.8% in mountains.
- 15.2% of the ice-free continental surface worldwide is characterized by karstifiable carbonate rock, with Europe representing the highest percentage at 21.8%, and Asia encompassing the largest absolute area at 8.35 million km^2 (18.6% of Asia's land surface)
- 15.7% of marine coastlines are marked by carbonate rocks.
- karst regions accommodate 1.18 billion people globally, constituting 16.5% of the global population.

B.5.2.2 Distribution of Karst in the United States

Karst geology makes up approximately 20% of the land surface in the United States. The distribution of karstic zones in the U.S. varies across different regions, reflecting the geological diversity of the country. Some of the prominent areas with significant karstic features include (Weary and Doctor, 2014):

- *Texas*: Texas is renowned for its extensive karst landscapes, particularly in the central and western parts of the state. The Edwards Plateau region, for example, is characterized by vast limestone formations and numerous caves and sinkholes.

- *Florida*: The entire state of Florida is underlain by limestone bedrock, making it one of the most extensively karstified regions in the United States. Sinkholes, springs, and disappearing streams are common features in Florida's karst terrain.
- *Kentucky*: Kentucky is home to the Mammoth Cave System, the longest known cave system in the world. The state's karst topography is characterized by rolling hills, sinkholes, and underground rivers.
- *Missouri*: The Ozark Plateau in southern Missouri is renowned for its karst landscapes, featuring numerous caves, springs, and sinkholes. Mark Twain National Forest is one area where visitors can explore the unique karst terrain of the region.
- *Pennsylvania*: The Appalachian Mountains in Pennsylvania contain karstic features such as caves, sinkholes, and disappearing streams. The region's limestone bedrock has been extensively sculpted by the erosive forces of water over millions of years.
- *Tennessee*: The karst terrain of Tennessee is highlighted by the Cumberland Plateau region, which is known for its extensive cave systems and underground streams. The state is also home to the Great Smoky Mountains, where karst features can be found amid the rugged mountain landscape.

These are just a few examples of the distribution of karstic zones in the United States. Karst landscapes can be found in various other states, each with its own unique features and geological history. The map of karst areas in soluble rock in the contiguous United States is shown in **Figure B.33**.

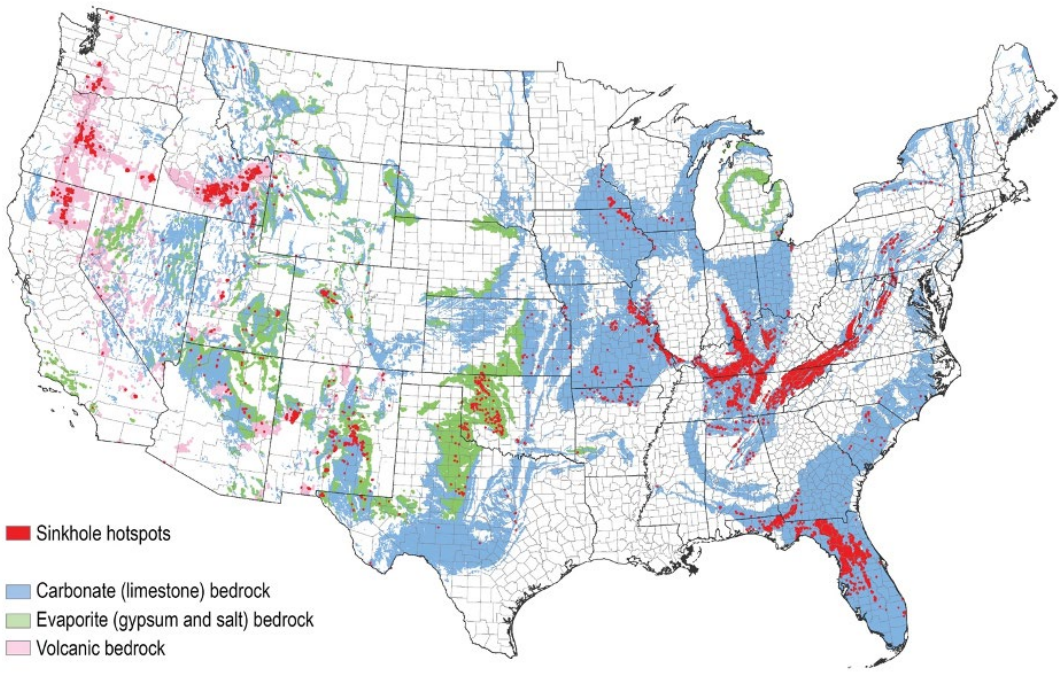

Figure B.33 Karst map of the contiguous United States
(Source: https://www.usgs.gov/media/images/karst-map-conterminous-united-states-2020)

B.5.2.3 Distribution of Karstic Areas in Texas

According to the Texas Water Development Board (TWDB), approximately 20% of Texas' land area is underlain by karst formations. Not all these areas; however, have visible karst features on the surface. The karst regions of Texas are in central, south-central, and southwest Texas and include the Edwards Plateau and the Balcones Escarpment regions. The Edwards Plateau is a large region of rugged hills and canyons that covers much of central Texas, while the Balcones Escarpment is a steep slope that runs from just south of Dallas-Fort Worth (**Figure B.34**). According to the Texas Speleological Survey (TSS), karst regions in Texas can be divided into three main categories based on the type of rock, including:

- *Carbonate regions*: areas where caves are almost entirely formed in limestone or dolomite, although a few are in interbedded gypsum.
- *Gypsum areas*: caves are mostly in gypsum, although some caves are in interbedded dolomite.
- *Pseudokarst regions*: contain caves in rocks that are much less soluble than limestone or that are formed by means other than solution. Although isolated pseudo-karst caves occur throughout Texas, only those areas with several caves of similar origin are presented.

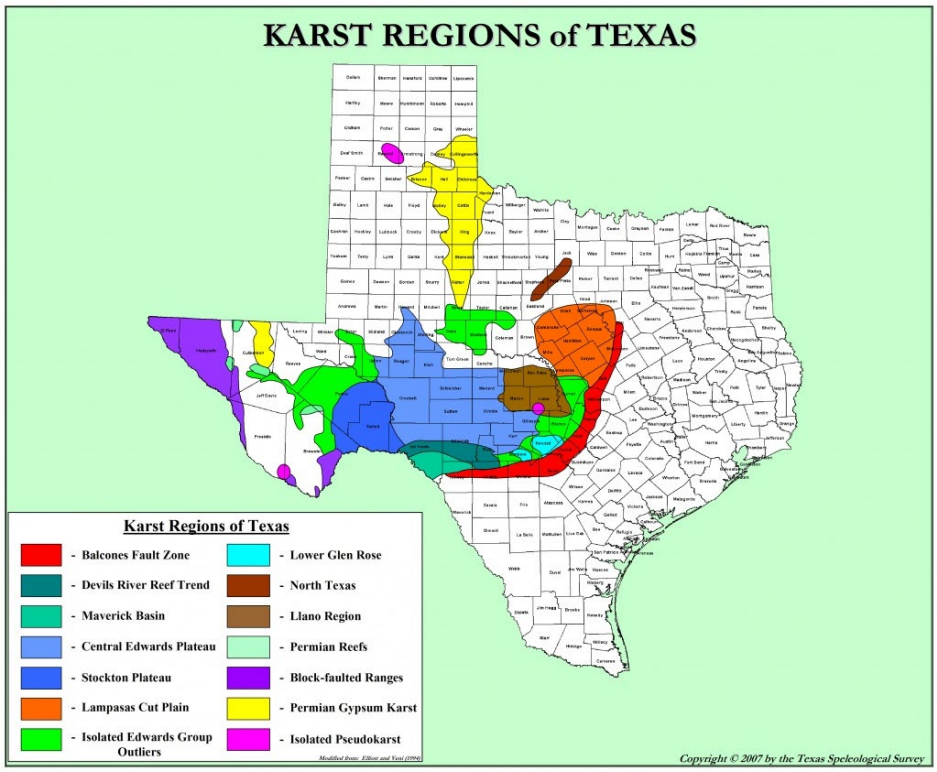

Figure B.34 Distribution of karst zones in Texas (Texas Speleological Survey, 2014)

B.5.3 Hydrology of Karstic Zones

The hydrology of karst zones is characterized by their complexity, driven by the interaction of geological, hydrological, and environmental factors. Understanding these dynamics is essential for effective water resources management and conservation in karst regions, as well as for designing engineering projects such as transportation infrastructures.

Hydrology modeling of drainage basins encompasses two primary approaches: 1) approaches focused solely on estimating peak values, and 2) approaches aimed at stimulating the full hydrograph resulting from a storm event. An example of the first approach is the simple Rational Method (Chow, 1964) where the peak discharge is determined by factors such as catchment area, mean rainfall intensity, and reduction factors accounting for losses such as infiltration and evaporation. Although such methods do not fully capture the dynamics of flow or the underlying physical mechanisms of runoff generation, they offer a rough estimation of maximum discharge based on key parameters. In contrast, the second approach relies on hydrological models incorporating various physical components influencing runoff generation, with different levels of simplification. A critical distinction lies between *event-based* models, such as instantaneous unit hydrograph (IUH), Soil Conservation Service (SCS) Curve Number (*CN*), etc., and *continuous* models, which operate at different temporal scales. Event-based models face limitations regarding the assumption of initial soil moisture conditions, significantly impacting catchment response to precipitation (De Waele et al., 2010).

Unlike modeling drainage areas with soil pores, which have limited infiltration rates, karstic fissures, and shafts allow for a rapid and substantial flow discharge, contributing to shorter response times and higher peak flooding magnitudes. Additionally, water retention in voids and aquifers within karst formations can delay its movement and reduce peak flood levels (Dai et al., 2022). However, the complex nature of karst hydrology, characterized by open basins and hidden drainage networks, presents challenges for accurate flood prediction, even with the application of modeling techniques, due to inherent inaccuracies and uncertainties (Jiang et al., 2020).

In response to the complexity of flood routing and the diverse range of environmental factors involved, computer models have been developed to incorporate numerous influencing factors and perform extensive data processing and analysis. One widely used model in this domain is the Hydrologic Engineering Center - Hydrologic Modeling System (HEC-HMS) (USACE, 2002).

A general drainage hydrology modeling procedure in HEC-HMS initiates with utilizing unit hydrograph methods such as Snyder or SCS (Soil Conservation Service) methods to calculate peak flow and hydrographs and later incorporates the Muskingum method for flood routing (Dai et al., 2022). These models often rely on empirical formulas, making their simulation accuracy environment-dependent and requiring modification and calibration (Zhang et al. 2013). The variability seen in models derived from empirical equations versus actual conditions underscores the necessity for enhanced hydrological modeling, especially in distinctive environments like karst regions. In these areas, the complexities of karstic sinkholes have been examined through

hydrograph modeling, resulting in specialized models, for example, the two-piece model for recession limb analysis (Şen, 2020).

B.5.3.1 Rainfall-Runoff Relationship in Karstic Zones

The transformation of rainfall into runoff within a watershed is heavily influenced by various factors such as the characteristics of rainfall, soil-rock properties, and land use practices. This transformation process differs significantly between watersheds with mineral soils and those in carbonate-karst terrain drainage systems. In karst watersheds, rainfall can either flow over the surface or infiltrate into the porous karst rock. The high porosity and surface cracks of karst landscapes facilitate significant infiltration of rainwater through these features, filling reservoirs and river networks beneath the karst layer.

The distinct geomorphology and hydrogeology of karst areas pose challenges to accurate estimation of surface runoff. The processes of water storage and replenishment in karst watersheds differ significantly from those in non-karst areas, where river flow typically occurs above the surface compared to the subterranean flow of karst rivers. The primary distinction between hydrology in karst and non-karst regions lies in the magnitude of infiltration or loss through sinkholes and fissures within karst zones. Infiltration within these zones can significantly alter the peak flow of drainage basins, affecting various aspects such as the duration of concentration and available storage within the basin by retaining water in karstic aquifers. Additionally, the geological characteristics of karst zones influence the spatiotemporal infiltration and storage capacity (Wahyullah et al., 2023).

B.5.3.1.1 Peak Flow Estimation in Karstic Zones

The estimation of cumulative surface runoff at watershed outlets is commonly conducted using the Soil Conservation Service Curve Number (SCS-CN) method (Parvez and Inayathulla, 2019; Wahyullah et al., 2023). The applicability of this model to karst basins, characterized by excessive *CN* values, has been assessed by different researchers such as Iacobellis et al. (2015), Savvidou et al. (2018), and Mo et al. (2021). Most research has integrated the SCS-CN method into the HEC-HMS model for karst basins, but these studies overlooked geological factors, particularly in carbonate rock formations. Hence, adjustments to the SCS-CN method are imperative to accommodate karstic terrains characterized by high infiltration rates (Wahyullah et al. 2023).

Modified SCS-CN Method for Karst Regions

The SCS-CN method has been utilized in various studies within karstic zones to estimate peak runoff of drainage basins. Among previous studies, Savvidou et al. (2018) modified the SCS-CN method to consider the effect of karstic zone infiltration in peak flow calculation. **Equation B.21** shows the modified *CN* for karst regions, taking into account factors such as permeability, land use, and watershed drainage capacity.

$$CN = 10 + (9 \times i_{perm}) + (6 \times i_{veg}) + (3 \times i_{slope}) \quad \text{(B-22)}$$

where i_{perm} refers to permeability (soil, geology), i_{veg} represents the land cover and land use (vegetation), and i_{slope} is the drainage capacity (slope, building structure).

The modified SCS-CN method has been extensively applied in Mediterranean karst regions for estimating surface runoff, peak discharge, and flash flooding and has demonstrated promising performance in estimating peak discharge and assessing flood risks (e.g., Kastridis and Stathis, 2020).

Tables B.15 to **B.17** present the required parameters for estimating modified *CN* values based on permeability, land cover, and drainage capacity of karstic zones, as proposed by Savvidou et al. (2018). The *CN* values are categorized into five classes considering permeability class characteristics (**Table B.15**), type of land use (**Table B.16**), and drainage capacity (**Table B.17**).

Wahyullah et al. (2023) examined the accuracy of the modified SCS-CN method in predicting peak runoff in the Karst Leang Lonrong sub-watershed in Indonesia, while also evaluating the influence of changes in land use on river discharge. Their findings showed that the modified SCS-CN method exhibited high accuracy in estimating peak flow, contingent upon the observed linearity between rainfall and direct flow with a Nash-Sutcliffe efficiency of 0.8.

The modified SCS-CN approach was also proposed and tested for Mediterranean regions; however, its applicability for different catchments needs to be examined. Furthermore, accurate estimation of direct runoff using this method requires field data to determine *CN* values corresponding to specific land use conditions, particularly in karst regions where closer proximity to field-derived *CN* values is imperative.

Table B.15 Permeability classes (i_{pem}) based on soil and geological characteristics of the basin and the dominant type of construction (Savvidou et al., 2018)

Permeability Class	i_{pem}	Soil Characteristics	Geological or Hydro-lithological Characteristics	Structural Characteristics
Very high	1	Very light and well drained soils	Highly karstic carbonates, extensively developed, fragmented limestones, dolomites, marbles	-
High	2	Sandy and gravelly soils with a low content of sludge and clay	River deposits, non-coherent conglomerates, Triassic breccias	Very small settlements
Medium	3	Sandy thick soils, sludges and silty soils, sandy clay	Granular sediments, schists, cohesive sandstones, slate or fine-grained limestones in alternations with schist formations	Sparsely built areas, significant garden development, urban parks
Low	4	Fine clay soils, clay soils, soils poor in organic materials	Flysch, metamorphic, plutonic and volcanic rocks, alternations of sands, marls, clays, conglomerates, marl limestones, sandstones, molassic deposits	Discontinuous urban fabric with small gardens
Very low	5	Shallow soils that swell when are wet, clays	Impermeable solid rocks (granite)	Shopping centers, areas with dense building construction

Table B.16 Vegetation classes (i_{veg}) based on land cover characteristics (Savvidou et al., 2018)

Vegetation Class	i_{veg}	Land cover characteristics
Very dense	1	Forests (coniferous, broad-leaved, mixed)
Dense	2	Transitional woodland shrubs, orchards, olive groves, riparian vegetation
Sparse	3	Pastures, crops, vineyards, grasslands, shrubs
Very sparse	4	Sparsely vegetated, non-irrigated arable land, dunes, wetlands, discontinuous urban fabric
No vegetation	5	Bare or rocky terrain, artificial surfaces (roads, buildings)

Table B.17 Drainage capacity classes (i_{slope}) based on mean slope and associated soil characteristics (Savvidou et al., 2018)

Drainage Class	i_{slope}	Mean Slope (%)	Other Characteristics
Negligible	1	0	Inadequate drainage system, frequent and extensive floods, unformed hydrographic network
Low	2	1-2	Significant floodplain areas, occasional floods, poorly formed hydrographic network
Medium	3	2-10	Small floodplain areas, rare floods, shallow, low-depth hydrographic network
High	4	10-30	Insignificant floodplain areas, a well-formed hydrographic network, the existence of an artificial drainage network
Very high	5	> 30	Mountainous relief

SCS- Snyder Unit Hydrograph Method

As discussed, karstic watersheds present unique challenges for hydrological modeling due to their distinctive surface and subsurface drainage networks, including sinkholes, caves, and underground rivers, which significantly impact the movement of water within the watershed. Traditional hydrological modeling techniques, such as those used in HEC-HMS, which rely on assumptions about surface runoff and infiltration, may not accurately capture the hydrological processes in karstic environments. One commonly used technique in hydrological modeling is the Soil Conservation Service (SCS) unit hydrograph method or the Snyder unit hydrograph (SUH) method. These methods are based on empirical relationships between rainfall and resulting hydrographs and are widely applied in non-karstic watersheds. However, in karstic areas, the presence of hidden drainage networks can lead to rapid infiltration and subsurface flow, bypassing traditional surface pathways. This renders the assumptions underlying the SCS or SUH methods invalid and makes it challenging to estimate flow hydrographs accurately.

Researchers have proposed modifications to conventional hydrological modeling approaches to better account for the unique characteristics of karstic watersheds. One critical aspect that requires modification is the calculation of soil moisture dynamics. In conventional methods, the estimation of peak runoff is heavily influenced by soil moisture conditions, which determine the rate of infiltration and surface runoff generation. However, in karstic environments, where much of the water may rapidly infiltrate into subsurface conduits, the loss rates of soil moisture can be significantly different from those in non-karstic areas. To address these challenges, it is suggested to adapt soil moisture calculation methods to better reflect the rapid drainage and subsurface flow processes characteristic of karstic watersheds. This may involve incorporating additional parameters or refining existing models to account for the complexities of flow pathways in these environments. By improving the representation of soil moisture dynamics, hydrological models can more accurately simulate the timing and magnitude of peak runoff events in karstic watersheds, thereby enhancing the reliability of flood forecasting and water resource management in these areas. The following section provides a summary of such attempts to modify soil moisture calculation methods.

Soil Moisture Loss Adjustment

While soil moisture calculation has been studied by several researchers, hydrological soil moisture remains a less-explored subject (Vereecken, 2018). Various studies have applied soil moisture to calculate storage and loss to modify hydrological models and formulas. Wang (2018) proposed a function to describe the relationship between soil wetting capacity and precipitation, improving the determination of the SCS-CN method parameters that are used in hydrological models. In the context of flood analysis in karst regions, several studies have shown the significant role of karst in flood formation, highlighting groundwater contribution to the water budget and the unique behavior of floods influenced by karst conditions (Cao et al., 2018; Rad, et al., 2022). Recent efforts by Mo et al. (2021) aimed at improving HEC-HMS flood simulation accuracy in karst regions in the Lijiang watershed, China by adding a reservoir unit to the HEC-HMS model. This

improvement technique resulted in 22% enhancement in model accuracy, yet further refinements of applied models remain an ongoing pursuit.

Dai et al. (2022) enhanced flood prediction using the HEC-HMS model for the karstic watershed of the Lijiang River, Guangxi, South China. Karst evolution progresses through various stages, including juvenile, youthful, mature, complex, extreme, and old stages. In the old stage observed in Guangxi, drainage networks such as cracks, dolines, underground streams, and caves are extensively developed, contributing to relatively stable river flows. Consequently, the incorporation of soil moisture accounting loss was expected to have a consistent impact on the flood formation process, particularly for certain precipitation events characterized by specific intensity, duration, and return periods.

Given the complexities arising from hidden drainage networks in karst hydrology, Dai et al. (2022) proposed incorporating soil moisture accounting loss to represent the available reservoir capacity of karst (ARCK) in flood forecasting. They analyzed soil moisture loss in relation to daily rainfall-runoff data over a period of 1.5 years. **Figure B.35** shows the relationship between soil moisture and precipitation in the Lijiang River watershed, showing fluctuations in soil water content following rainfall events and subsequent declines during dry intervals. Notably, longer intervals between precipitation events corresponded to lower soil water content, while shorter intervals exhibited higher water content levels.

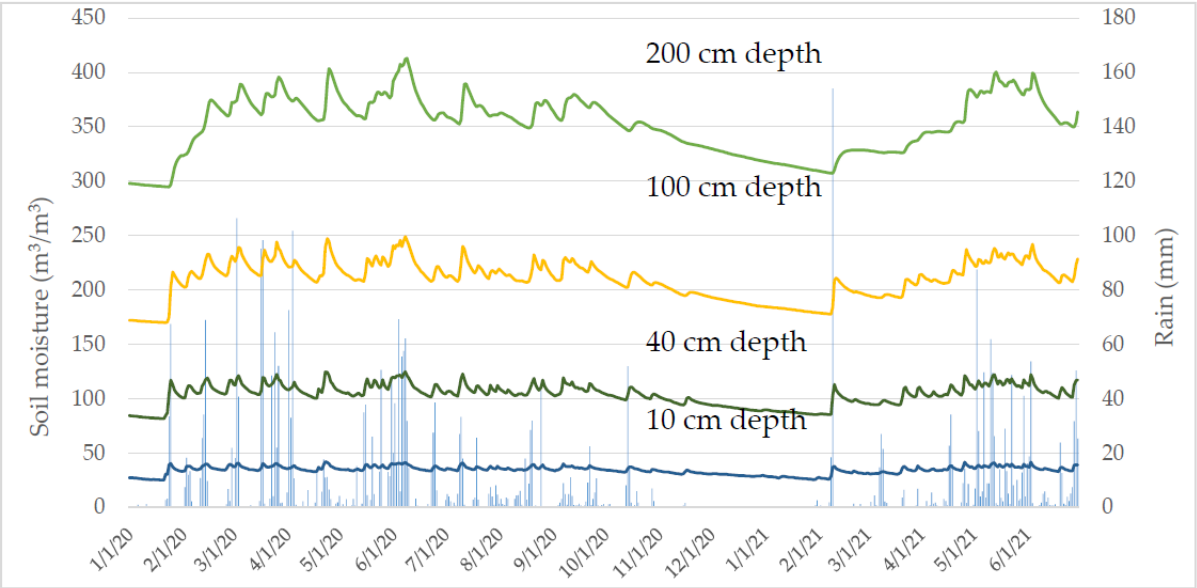

Figure B.35 Average daily soil moisture of ten locations at different soil depths vs. rainfall at Lijiang River, Guangxi, South China (Dai et al., 2022)

Dai et al. (2022) utilized the Muskingum method for flood routing in conjunction with the SUH method in HEC-HMS for modeling karst basin peak flow. This method considers the shape and features of catchment components in prism and wedge storage volumes, representing steady and extra portions of flow, respectively (**Figure B.36**). They introduced X and K as adjustment

coefficients to improve the reliability of peak flood calculations considering recharge and loss through the karst terrain. The resulting form of the estimated hydrograph was influenced by various criteria. The correlation between *K* and *X* may be expressed by **Equation B.23**.

$$Storage\ volume = K \times (wedge + prism) = K\ [(X \times \text{inflow}) + ((1 - X) \times \text{outflow})] \qquad \text{(B-23)}$$

where the flow-specific gravity index *X* shows the weightage criterion for flow segmentation to the wedge and prism, and *K* is an index showing the flow traveling time (propagation time) in hours. If *X* is set to 0.2, this means that 20% of the total flow volume is allocated to the wedge component, while the remaining 80% is assigned to the prism component. Regarding parameter *K*, a higher value signifies a longer duration for the peak flood to propagate downstream. Consequently, this results in an attenuated peak with a lower peak discharge rate as it travels downstream. In this method, the parameter *K* has a greater influence on the shape of the hydrograph and its peak compared to *X*. However, a larger value of *X* in karst zones leads to an exponential increase in the magnitude of the wedge component. Therefore, while both *X* and *K* are significant factors shaping the hydrograph in such areas, their effects are distinct. Parameter *K* primarily impacts the timing and attenuation of the peak, influencing how quickly the flood peak propagates downstream. Conversely, *X* influences the distribution of flow between the prism and wedge components, determining the proportion of flow allocated to each segment of the storage volume. Dai et al. (2022) adjusted the HEC-HMS results for individual flood events in karst terrain, resulting in simulated outcomes that closely matched the actual flood data in the region. This modification allowed for a more accurate representation of flood events compared to the original model forecasts.

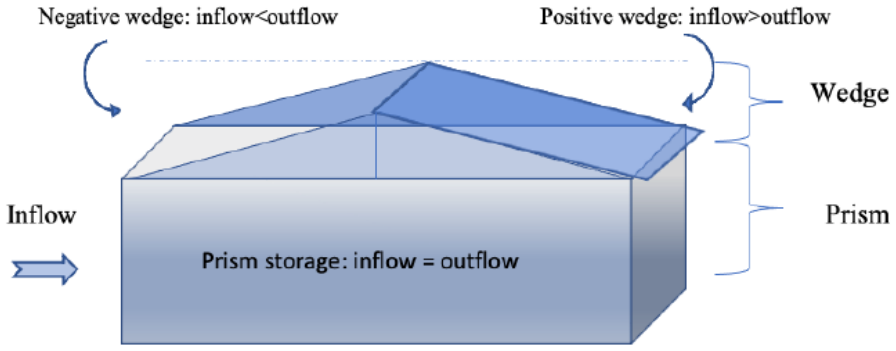

Figure B.36 Prism and wedge storage concepts in karst hydrology (Dai et al., 2022)

B.5.3.2 Delineation of Drainage Area in Karst Basins

In conventional hydrogeologic studies, the primary mapping unit, often defined as the groundwater basin, is utilized to characterize the aquifer's spatial and temporal properties and to construct a conceptual model. However, for a karst aquifer, the traditional concept of the term "*groundwater*

basin" is somewhat misleading as it downplays the highly interconnected nature of surface and subsurface waters, as well as the significant role of concentrated stormwater runoff as a recharge source. A more fitting term and conceptual model for most karst aquifers is the karst drainage basin (or karst basin), i.e., a mapping unit defined by the total area of surface and subsurface drainage that contributes water to a conduit network and its outlet spring or springs (Quinlan and Ewers, 1989; Ray, 2001). **Table B.18** presents the difference between the traditional groundwater basin and karst drainage basin delineation considerations.

Table B.18 Comparison between conventional groundwater and karst drainage basin delineation considerations

Characteristics	Karst Drainage Basin Delineation	Conventional Groundwater Basin Delineation
Mapping Unit Definition	Karst drainage basin is defined by total area of surface and subsurface drainage contributing to conduit network and outlet spring(s) (Quinlan and Ewers, 1989; Ray, 2001)	Groundwater basins typically are delineated based on hydrogeological properties such as hydraulic conductivity, recharge rates, and groundwater flow patterns (Toth, 1963)
Boundary Characteristics	Boundaries may not align with topographic drainage divides; recharge near boundaries may flow radially into adjacent basins (Quinlan and Ewers, 1989)	Boundaries generally coincide with topographic features such as ridges and drainage divides (Toth, 1963)
Recharge Sources	Direct injection of concentrated stormwater runoff and subsurface piracy of surface streamflows are significant recharge sources (Quinlan and Ewers, 1989)	Recharge predominantly from precipitation infiltration and lateral groundwater flow (Toth, 1963)
Flow Dynamics	Active flow concentrated in core of basin within conduit network, characterized by pipe-full or open-channel hydraulics; rapid changes in hydraulic gradients and flow directions (Quinlan and Ewers, 1989)	More uniform flow distribution across basin; hydraulic gradients and flow directions change gradually (Toth, 1963)
Temporal Variability	Contributing area and volume of discharged subsurface water change over time due to conduit development, hydraulic capacity changes, and sediment load fluctuations (Quinlan and Ewers, 1989)	Basin characteristics and flow dynamics exhibit relatively stable behavior over time, with minor variations due to seasonal changes and long-term geological processes (Toth, 1963)

Taylor and Greene (2008) provided a summary of Ray's (1999, 2001) findings, which established a framework for categorizing karst basins into three distinct hydrologic groups. These groups are delineated based on the hydraulic capacity of their conduit networks and the predominant source of recharge, whether allogenic or autogenic. These groups are as follows:

- *Overflow allogenic basins*: Characterized by trunk conduits primarily recharged through subsurface piracy of surface streams, yet with limited hydraulic capacity, allowing the surface channel to persist as a losing stream reach or an intermittent storm-overflow route.

- *Underflow allogenic basins*: These basins feature trunk conduits with increased hydraulic capacity, diverting all surface flow underground through streambed swallets, rendering the surface valley blind.
- *Local autogenic basins*: In these basins, all surface flow is captured by subsurface piracy, with the trunk conduit predominantly recharged by soil infiltration and internal sinkhole drainage. These categorizations are most applicable to shallow, unconfined karst aquifers in fluviokarst settings, although they also describe basins in doline karst and deeper partly confined karst aquifers.

Smart (1988) and Ray (2001) noted that many karst terrains undergo a progressive sequence of basin development from overflow allogenic to underflow allogenic to local autogenic over geologic time as karstification and subsurface piracy of surface streams intensify.

B.5.3.2.1 Methods of Identification of Karst Drainage Basin Area

Various techniques have been employed to estimate the contributing areas of karst basins (Ginsberg and Palmer, 2002), yet dye-tracer tests stand out as the most effective means of identifying point-to-point connections between flow inputs (such as sinkholes or sinking streams) and outputs (springs). This information is essential for defining the boundaries of karst drainage basins (White, 1993; Ray, 2001; Taylor and Greene, 2008). These tests can be conducted at multiple input sites by injecting different fluorescent dyes either simultaneously or sequentially. These tests aid in the determination of tracer-inferred groundwater flow directions and increase confidence in delineating the boundaries, approximate size, and shape of the basin under study as the number and distribution of tracer-determined flow paths expand.

Dye-tracer tests also play an important role in mapping the contributing areas of springs and surface streams, identifying and estimating water fluxes, and assessing water budgets for both surface and subsurface drainage basins, particularly in delineating areas indicative of *misbehaved drainage* where surface runoff is redirected via subsurface conduits (White and Schmidt, 1966; Ray, 2001). For instance, these tests conclusively revealed that the USGS Hydrologic Unit boundaries delineated for the Barren River basin in central Kentucky encompass surface drainage that contributes water to the adjacent Green River basin via subsurface conduits (Ray, 2001). **Figure B.37** illustrates the injection of dye tracers at strategic locations for different projects in karstic zones to assess the conduit network and enhance the accuracy of karst basin delineation.

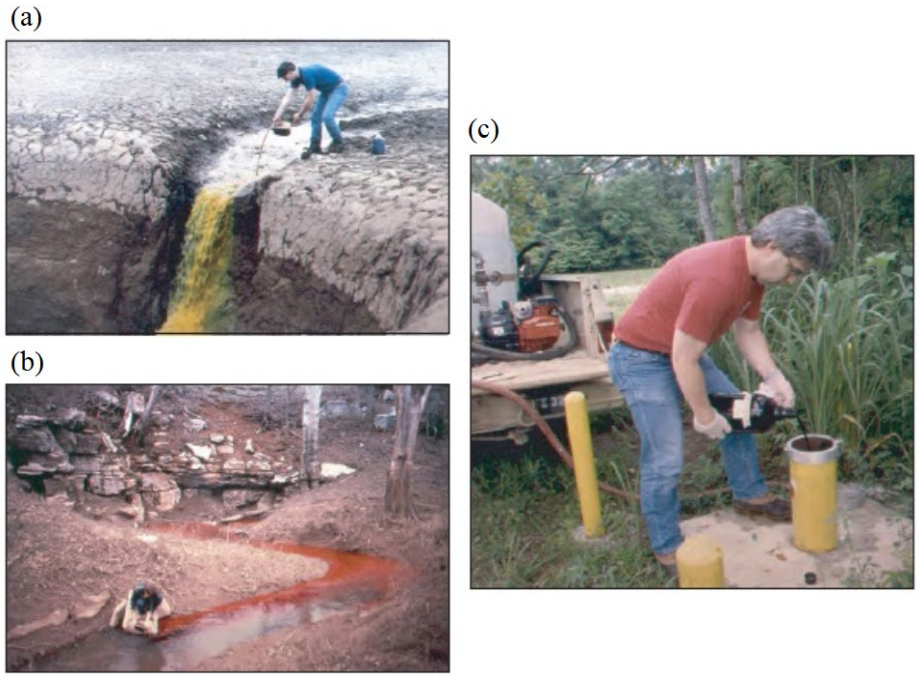

Figure B.37 Tracer injection in karst regions: (a) Sodium fluorescein injection into collapse sinkhole formed in a pond, (b) Rhodamine WT injection into a sinking stream, and (c) Injection of Rhodamine WT into a water level observation well (photographs by Charles J. Taylor, U.S. Geological Survey, Taylor and Greene, 2008).

B.5.3.2.2 Drainage System within Karst Zones

The karst drainage system comprises two primary elements: conduit networks (representing inflow boundaries) and springs (representing outflow boundaries). The following sections discuss each element and its respective physical characteristics.

Conduits Networks

Karst aquifers are characterized by their intricate dendritic or branching networks of conduits. The growth of these conduit networks follows a complex hydraulic-and-chemical feedback loop, wherein conduit enlargement leads to increased hydraulic capacity, discharge, and subsequent enhanced dissolution and physical corrosion, perpetuating further conduit enlargement and subsurface piracy of flows by larger conduits (Palmer, 1991& 1999; White, 1988 & 1999). **Figure B.38** shows the development stage of conduits in a karstic environment and their impact on the hydraulic gradient within the karst aquifer. In **Figure B.38a**, stage (a) represents the initiation of recharge, signifying the onset of conduit growth. Stage (b) demonstrates the modification in the hydraulic gradient due to the propagation of a faster-growing primary (P) conduit and a slower-growing secondary (S) conduit. Finally, stage (c) depicts the primary conduit breakthrough to the discharge boundary, subsequently hindering or decelerating the growth of the secondary conduit.

The integrated drainage network evolves through a sequence of stages that are shown in **Figure B.38b** which involves initial growth and breakthrough by primary conduits (1), followed by the capture of flow and connection of secondary conduits (2-4).

The largest conduits function as master drains, locally altering the hydraulic flow field to capture groundwater from the surrounding aquifer matrix, fractures, and smaller nearby conduits (Palmer, 1991, 1999; White, 1988 & 1999). Depending on their hydraulic capacity and interconnection, conduit networks can efficiently discharge substantial volumes of water and sediment through karst aquifers at rapid rates (White, 1993), with flow velocities often ranging from hundreds to thousands of feet per day in well-developed networks (White, 1988).

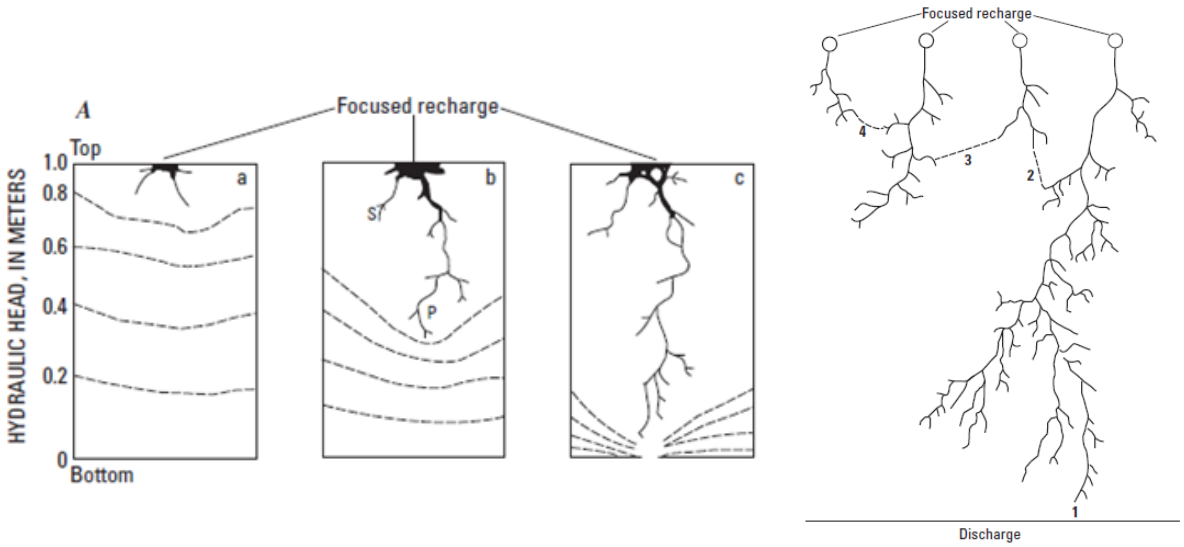

(a) (b)

Figure B.38 Development of an integrated drainage network in karstic terrain (Taylor and Greene, 2008)

Karst Springs Outlets

Karst springs serve as natural outlets for water discharged from conduit networks (**Figure B.39**), typically situated at local or regional groundwater discharge boundaries. These boundaries correspond to areas of minimum hydraulic head in the aquifer and are often near the elevation of adjacent base-level surface streams (White, 1988).

(a)

(b)

Figure B.39. Physical outlets for karst springs: (a) Orangeville Rise, southern Indiana, and (b) Rocky Spring, central Kentucky (Taylor and Greene, 2008)

In many karst aquifers, a tributary system of conduit drainage fosters convergent flow towards a trunk conduit, ultimately discharging through a single large spring (White, 1999). However, some karst aquifers exhibit a distributary flow pattern, where discharge occurs through multiple spring outlets. This distributary flow configuration arises from various geological phenomena, including the enlargement of fractures and smaller conduits near stream discharge boundaries, collapse or blockage of primary trunk conduits or springs leading to flow diversion and the development of alternative flow paths and outlets, or subsurface conduit piracy redirecting preexisting conduit flow (Quinlan and Ewers, 1989).

Traditionally, the classification of springs has been based on discharge, following Meinzer's scale (Meinzer, 1927), and considering additional factors such as physical attributes and whether discharge occurs through artesian or gravity flow mechanisms (USGS, 2005). However, a shift towards a flow-system perspective suggests that categorizing karst springs according to their hydrological function as conduits for conduit networks might offer greater practicality (Worthington, 1991, 1999). In many karst aquifers, a small number of perennial springs, known as underflow springs, function as the primary outlets for baseflow discharge from conduits (Worthington, 1991). The elevation of these underflow springs plays a crucial role in determining the water table elevation at the karst aquifer's output boundary, with variations in the water table's slope and fluctuations under different hydrological conditions primarily influenced by matrix hydraulic conductivity and conduit hydraulic capacity (Ford and Williams, 1989).

Furthermore, intermittent springs, also known as overflow springs, serve as spillway outlets during periods of elevated discharge, representing a transient form of distributary discharge. Over time, as conduits evolve and base levels along with water tables diminish, the upper sections of the karst aquifer may gradually drain, resulting in the abandonment of conduits at higher elevations (Hess and White, 1989). However, during high-flow periods, these higher-level conduits may reactivate and discharge through overflow springs, which now serve as outlets at the former underflow springs' locations.

B.5.3.3 Drainage Mechanism in Karst Aquifers

Karst terrains exhibit distinctive characteristics, particularly with regard to their diverse recharge sources characterized by significant variations in water residence time and contribution patterns to the conduit network (Taylor and Greene, 2008). These sources are classified as concentrated or diffuse, and as either autogenic or allogenic, depending on whether the recharge originates from precipitation falling directly on karstic terrain or nonkarstic areas (Gunn, 1983). These distinctions are important because the ratio of concentrated to diffuse recharge typically determines the distribution and interconnection of conduits, while the timing and relative proportions of water fluxes from allogenic and autogenic sources greatly influence the variability in spring discharge and water chemistry (Ford and Williams, 1989).

Figure B.40 presents a conceptual model, adapted from Gunn (1986), illustrating drainage mechanisms in a karst area. The model depicts several pathways through which water moves within the karst landscape, including overland flow, through flow, subcutaneous flow, shaft flow, vadose flow, and vadose seepage. These pathways exemplify the complex interplay of surface and subsurface processes that govern water movement in karst terrains, highlighting the intricate nature of karst hydrology.

Sinking or losing streams originating as gaining streams in nonkarstic regions are a significant source of concentrated allogenic recharge for many karst aquifers (Taylor and Greene, 2008). Conversely, surface runoff collected in sinkhole depressions represents a major source of concentrated autogenic recharge, which can immediately drain into the subsurface through throat-like openings known as swallets or percolate gradually through soil or alluvium layers (Gunn, 1983). Diffuse allogenic recharge may arise from interaquifer water transfer from non-karstic aquifers, but more commonly, it comes from water draining down unsaturated (vadose) zone shafts where karstic rocks are covered by non-soluble caprocks like sandstone.

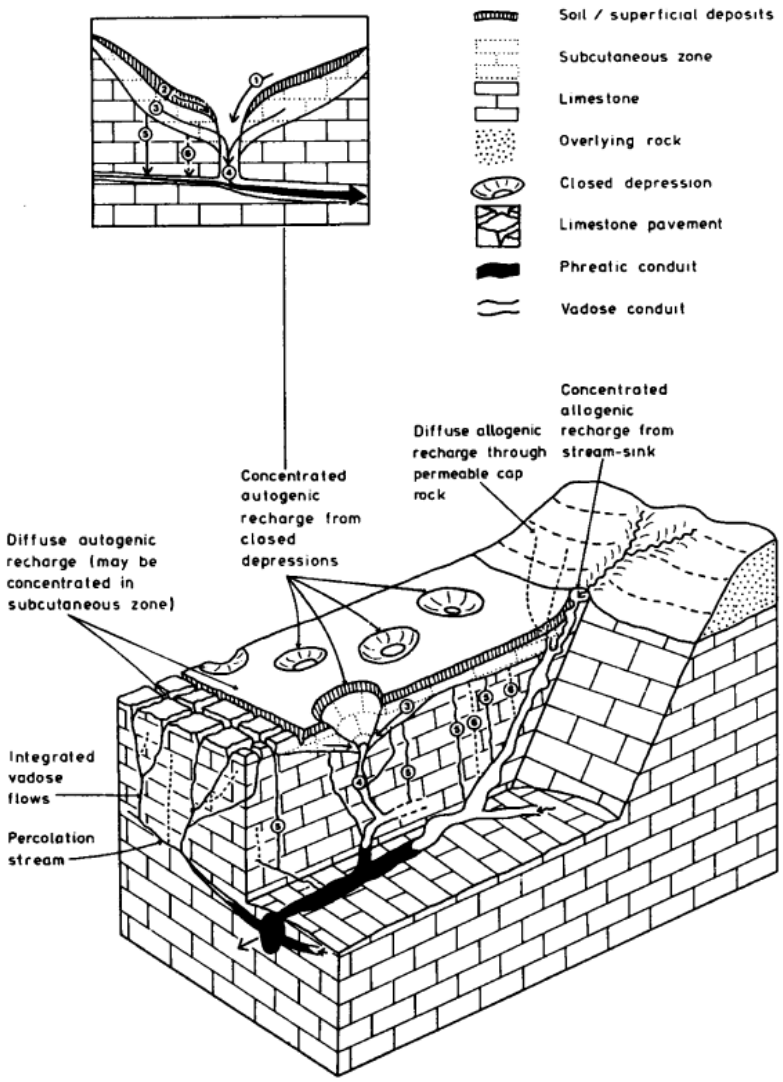

Figure B.40 Conceptual model of the drainage mechanism in karst areas (Gunn, 1986)

In typical studies of karst hydrology, while concentrated recharge detains considerable attention, the significant contribution of diffuse autogenic recharge, primarily through soil infiltration, is often overlooked, paralleling patterns observed in other hydrogeological settings. In a case study conducted in Missouri, U.S., Aley (1977) showed that diffuse areal recharge contributed approximately four times more water input to a karst aquifer compared to all concentrated recharge sources combined, and nearly twice as much as sinkholes and losing streams combined. Sinkhole swallets typically exhibit active inflow only during periods of intense surface runoff when soil and macropore infiltration capacity is surpassed, leading to intermittent or absent concentrated recharge inflows during many storm events.

An integral component of recharge and storage in most karst aquifers is the epikarst, a zone characterized by intense weathering, fracturing, and solution modification of bedrock near the soil-bedrock interface (Williams, 1983). The thickness and hydrogeological properties of the epikarst

vary widely within and among karst terrains due to factors such as stratigraphic variability, bedrock porosity, permeability, solubility, fracture density, and weathering intensity. Hydrologically, the epikarst typically functions as a leaky perched aquifer zone, contributing long-term, diffuse autogenic recharge to conduits (Klimchouk, 2004). Baseflow discharge from karst aquifers to springs and surface streams often stems from water stored in epikarst, with chemical hydrograph separation studies indicating that epikarst flushing may contribute up to 50 percent of spring discharge during storms (Trček and Krothe, 2002). Despite considerable research efforts directed toward understanding its development and hydrological functioning, the epikarst remains one of the least comprehended components of recharge in karst aquifers (Aley, 1997; Jones et al., 2004).

B.5.3.3.1 Hydrogeologic Properties and Dynamics of Karst Aquifers

Challenges in recharge assessment of karst aquifers often arise due to a limited understanding of water flux processes, inadequate characterization of hydrogeological frameworks, and uncertainties in measurement techniques, particularly in complex settings like karst formations (Taylor and Greene, 2008). A karst aquifer can be conceptualized as an open hydrologic system characterized by diverse surface and subsurface flows, with boundaries defined by catchment limits and conduit geometry (Ford and Williams, 1989). The hydrogeological attributes of karst aquifers are primarily influenced by the structure and organization of conduits, which often serve to bypass surface drainage by offering alternative subsurface pathways with reduced hydraulic gradients and resistance (White, 1999). Conduits represent a distinct form of permeability, separate from but interconnected with intergranular pores (bedrock matrix) and fractures, thus contributing to the heterogeneous nature of karst aquifers. This heterogeneity results in highly scale-dependent and temporally variable hydraulic properties, distinguishing karst aquifers from most granular and fractured-rock aquifers (Taylor and Greene, 2008). ASTM (2002) provided information on the differences in hydrogeologic properties among various types of aquifers, including granular, fractured rock, and karst aquifers. This information is presented in **Table B.19**.

The hydrogeology of karst regions is characterized by a complex network of interconnected fissures, fractures, and conduits embedded within a relatively low-permeability rock matrix. Predominantly, groundwater flow and transport occur through this network of openings, while groundwater storage primarily resides within the matrix. Consequently, karst aquifers exhibit high levels of heterogeneity and anisotropy, posing challenges to effective management and understanding.

Table B.19 Hydrogeologic properties of granular, fractured rock, and karst aquifers (ASTM, 2002)

Aquifer Characteristics	Aquifer Type		
	Granular	**Fractured Rock**	**Karst**
Effective porosity	Mostly primary, through intergranular pores	Mostly secondary, through joints, fractures, and bedding plane partings	Mostly tertiary (secondary porosity modified by dissolution); through pores, bedding planes, fractures, conduits, and caves
Isotropy	More isotropic	Probably anisotropic	Highly anisotropic
Homogeneity	More homogeneous	Less homogeneous	Non-homogeneous
Flow	Slow, laminar	Possibly rapid and possibly turbulent	Likely rapid and turbulent
Flow predictions	Darcy's law usually applies	Darcy's law may not apply	Darcy's law rarely applies
Storage	Within saturated zone	Within saturated zone	Within both saturated zone and epikarst
Recharge	Dispersed	Primarily dispersed, with some point recharge	Ranges from almost completely dispersed- to almost completely point-recharge
Temporal head variation	Minimal variation	Moderate variation	Moderate to extreme variation
Temporal water chemistry variation	Minimal variation	Minimal to moderate variation	Moderate to extreme variation

B.5.3.3.2 Flow Patterns in Karst Systems

Karst aquifers, characterized by their intricate network of conduits, fractures, and matrix porosity within soluble rock formations, present a complex system of groundwater flow. This section discusses the fundamental aspects of karst hydrogeology, exploring key factors such as allogenic recharge, conduit-carrying capacity, hydraulic conductivity of matrix and fracture systems, and the identification of flow regimes within karst basins.

Allogenic Recharge and Conduit-Carrying Capacity

As previously mentioned, underflow and overflow allogenic karst basins receive significant recharge from the subsurface piracy of surface streams, greatly influencing discharge and water chemistry variations in karst springs following precipitation events. Understanding the hydrology of these basins primarily involves quantifying the area where external water, known as allogenic recharge, enters the basin, and consolidating data from individual sinking or losing streams. Geographic Information System (GIS) facilitates the delineation of catchment areas of all contributing sinking or losing streams and the estimation of the relative proportion of allogenic recharge subbasin area to autogenic recharge (sinkhole-dominated) subbasin area (Taylor et al., 2005).

The evaluation of conduit-carrying capacity, as proposed by White (1999), involves comparing allogenic inputs from sinking or losing streams against discharge measurements from the basin's outlet springs (Taylor and Greene, 2008).

In underflow allogenic basins, where hydraulic capacities of conduits surpass maximum surface stream inputs, surface flows are entirely redirected underground upon reaching karstic bedrock, typifying a classic sinking stream scenario. Conversely, in overflow allogenic basins, conduit capacities may not accommodate the baseflow discharge of the allogenic stream, allowing perennial surface flow despite losses through streambed swallow holes, characteristic of a classic losing stream. Moreover, intermittent sinking streams, often termed *dry-bed streams* exhibit conduit capacities capable of handling baseflow discharge, yet stormflow discharge may exceed conduit capacity, leading to surface flow continuation down the channel (Brahana and Hollyday, 1988). White (1999) suggested characterizing conduit permeability by determining the critical flow threshold when allogenic stream discharge equals conduit capacity, although practical challenges, such as timing difficulties and potential clogging of swallow holes with sediment or debris, hinder obtaining such measurements (Currens and Graham, 1993).

Hydraulic Conductivity of Matrix and Fracture Systems

Due to the composite permeability contributed by matrix, fracture, and conduit-flow components, the response to hydraulic stresses within a karst aquifer varies significantly across different locations. Typically, investigation into the hydraulic conductivity of the matrix and fracture components is conducted using conventional hydrogeologic tools such as laboratory permeability tests on representative rock core samples for matrix permeability determination, while fracture hydraulic conductivity is assessed through straddle-packer hydraulic tests and borehole flow meters (Sauter, 1991). Aquifer tests, such as time-drawdown, distance-drawdown, or slug tests, offer insights into the integrated local transmissivity of the matrix and fracture system. Additionally, borehole geophysical methods, including cross-borehole tests, provide valuable data for permeability and flow characterization at local to subbasin scales (Paillet, 2001). However, the analysis of karst aquifer test data using conventional Darcian analytical methods may yield misleading results, requiring special consideration of the potential impacts of slow-flow and quick-flow karst components on the hydraulic responses represented by the well-hydraulic test data. Streltsova (1988) provided a review of aquifer-test methods suitable for investigating heterogeneous aquifers such as karst. It is crucial to evaluate separately the hydraulic conductivity (or transmissivity) and storage coefficients of large solutional openings or conduits if the test well penetrates such features, distinct from those of fractures (Greene et al., 1999).

Comparative studies examining hydraulic properties across various karst aquifers have consistently revealed that conduits, despite comprising less than 1 percent of the aquifer's porosity, contribute to over 95 percent of its permeability (Worthington et al., 2000). Similar to observations in studies of fractured rock aquifers, there is a general trend of increasing hydraulic conductivities with larger field scales (Sauter, 1991). Typically, the distribution of hydraulic conductivity and

other pertinent properties is correlated with lithostratigraphic facies changes or other physical alterations within the bedrock matrix (Rovey and Cherkauer, 1994).

Method of Identification of Flow Regime in Karst Basins

The interpretation and analysis of a spring hydrograph involve two fundamental assumptions: firstly, that the discharge of springs is influenced by external events like intense precipitation or recharge from a sinking stream, and secondly, that the hydrograph's shape is determined by the flow through various pathways with differing conductivities and velocities (Milanović, 1981a). By employing recession analysis, it becomes feasible to determine whether the overall flow characteristics of the basin are predominantly governed by rapid flow (conduit-dominated), slow flow (diffuse-dominated), or a combination of both, and to assess the timing and magnitude of changes in spring discharge corresponding to transitions between these flow regimes.

Analyzing a spring discharge hydrograph to delineate karst basin flow regimes typically involves utilizing methodologies outlined by Rorabaugh (1964) and Milanović (1981a,b). Despite being grounded in Darcian theory, these hydrograph analysis techniques have been effectively utilized in numerous investigations of karst basins (Baedke and Krothe, 2001; Shevenell, 1996; Padilla et al., 1994; Sauter, 1992; Milanović, 1981b). This approach for characterizing flow regimes relies on recession curves derived from spring hydrographs to compute the value of α, which denotes the recession slope. **Equation B.24** was presented by Taylor and Greene (2008) to identify flow regimes in karst zones.

$$Q_t = Q_o e^{-\alpha(t-t_o)} \quad \text{(B-24)}$$

where t is any time since the beginning of the recession for which discharge is calculated, t_o is the time at the beginning of the recession, usually set equal to zero, Q_t is spring discharge at time t, Q_o is spring discharge at the start of the recession (t_o), and α defines the slope, or recession constant, that expresses both the storage and transmissivity properties of the aquifer.

By analyzing a spring's recession curve, it becomes straightforward to identify a characteristic α value that delineates the slope of the recession curve. While certain hydrographs may yield a single α value that adequately represents the slope, it is not unusual for karst springs to display two to three significant changes in slope on a single limb of the hydrograph recession (**Figure B.41**). In such cases, it is beneficial to assess each slope change along with its associated α value. Typically, these changes are interpreted such that the initial and steepest slope reflects the transmission of the captured surface water into the karst aquifer, signifying rapid flow.

The primary stormwater runoff typically occurs through the largest conduits, marked by a steep recession slope on the hydrograph. Subsequently, there is a transition to a less steep, intermediate slope, indicating the depletion of the stormwater pulse or the emergence of a mixed discharge comprising both stormwater and stored groundwater from smaller conduits and larger fractures. Finally, the recession curve exhibits another change in slope, signifying the return to baseflow conditions, where the spring discharge is primarily sourced from groundwater storage flowing through smaller fractures and the bedrock matrix.

These distinct spring flow characteristics are commonly referred to as the quick-flow (or conduit-dominated) response, intermediate flow response, and slow-flow (or diffuse-dominated) response (**Figure B.41**). The calculated α value for a spring discharge recession curve, or each segment of a multi-sloped recession curve, typically reflects a characteristic value or range indicative of each flow regime type. For instance, the discharge hydrograph for San Marcos Springs from the Edwards aquifer in Texas demonstrates all three karst flow regimes i.e., quick-flow, mixed flow, and slow-flow (Taylor and Greene, 2008).

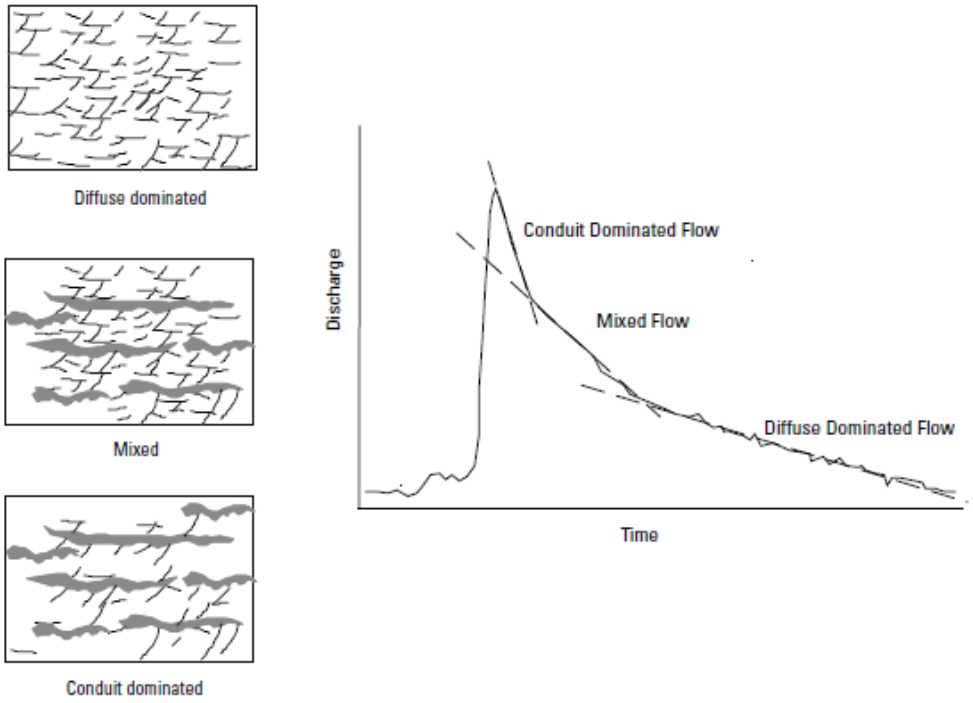

Figure B.41 Conceptual spring hydrograph showing changes in slope and dominant flow regime (conduit, mixed, diffuse) due to differing hydraulic responses (Taylor and Greene, 2008)

B.5.3.4 Methods of Recharge Estimation in Karstic Zones

A range of techniques exist for estimating recharge, primarily developed for detrital aquifers (De Vries and Simmers, 2002; Scanlon et al., 2002). It should be noted that the current understanding of these recharge processes remains incomplete (Hughes et al., 2008), prompting the development of new modeling techniques to better replicate them (Sanford, 2002; Andreo et al., 2008). Guardiola-Albert et al. (2015) examined six widespread methods for simulating the spatiotemporal distribution of recharge in karst aquifers. These methodologies are summarized below.

B.5.3.4.1 Soil Water Balance Method

The first method was proposed by Thornthwaite and Mather (1955). It is based on the basic principle of the Soil Water Balance method, which aims to equate the total inputs of water,

primarily precipitation, with the sum of the various outputs such as evapotranspiration, runoff, and groundwater recharge, and changes in soil moisture storage.

B.5.3.4.2 Visual Balan Method

Samper et al. (1999) introduced the Balan and Visual Balan hydrological model, widely adopted by hydrologists for balancing recharge equations across soil, unsaturated zone, and aquifer with minimal parameters. This model considers various inputs such as precipitation and irrigation, and outputs like surface runoff, evapotranspiration, interception, hypodermic flux, and groundwater flow. Infiltration estimation can be conducted using either the Horton equation (Horton, 1933) or the SCS Curve Number method (SCS, 1993). Additionally, it allows for the routing of water flow in the unsaturated zone to springs, with the option to deduct this from groundwater recharge. The parameters may be calibrated using piezometric level and flow data series (Samper, 1997; Blasco et al., 2004).

B.5.3.4.3 Chloride Mass Balance

The atmospheric chloride mass balance method depends on the conservative nature of the chloride ion (Eriksson and Khunakasem, 1969). Under steady-state conditions, usually spanning a significant period, e.g., one year, the chloride balance at a particular site can be expressed by **Equation B.25**.

$$RC_R = PC_p - E_s C_E \tag{B-25}$$

where P is the precipitation, R is the recharge, E_S is the mean surface runoff, C_P is the Cl^- concentration from rainfall plus dry from local dust and sea spray, C_R is the Cl^- concentration from recharge water, and C_E is the Cl^- concentration from surface runoff water.

B.5.3.4.4 APLIS

APLIS, developed by Andreo et al. (2008) and Marín (2009), is a tool for estimating autogenic recharge rates in carbonate aquifers. It combines geological, geographic, morphological, and edaphological factors to determine recharge levels. Recharge rates are directly linked to precipitation, with each aquifer requiring a specific constant of proportionality based on its unique variables. Variables are ranked from 1 to 10, indicating their impact on recharge, with successful applications observed in various Spanish karst aquifers (Andreo et al., 2008; Martos-Rosillo et al., 2008; Guardiola-Albert et al., 2015). The formula generating recharge rates is given by **Equation B.26**:

$$R = \frac{(A+P+3L+2I+S)}{0.9} \tag{B-26}$$

where A is the altitude, P is the slope, L is the lithology, I is the infiltration landforms, and S is the soil type. Each of these parameters is assigned a value based on field observations, maps, or regional data. The values are weighted and combined using a GIS-based approach to produce a vulnerability map. Areas are classified into different vulnerability zones (e.g., low, medium, high) based on the composite score.

B.5.3.4.5 Spatiotemporal Recharge Method

The method, developed by Pardo-Iguzquiza et al. (2012), utilizes a distributed recharge water-balanced approach, accounting for spatial variability with short time steps. Its main advance is the inclusion of concentrated infiltration in karst aquifers at the pixel level. Seasonal recharge rates, assumed to be steady-state, are estimated as the vertical hydraulic conductivity of saturated soil, derived from soil type maps. These parameters are considered equivalent, measured across a representative volume resembling a rectangular cuboid with horizontal dimensions matching the cell size and vertical dimension matching the soil-epikarst thickness. Additionally, the method proposes a remote sensing technique for estimating soil-epikarst effective thickness, based on soil characteristics like texture, particle size distribution, and organic matter content.

B.5.3.4.6 ZOODRM

ZOODRM is a distributed modeling code designed to compute spatial and temporal variations in groundwater recharge (Mansour and Hughes, 2004). Widely utilized in the UK (e.g., Hughes et al., 2008; Jackson et al., 2011) and also in Spain (e.g., Guardiola-Albert and Jackson, 2011), the model can simulate five types of recharge processes: direct recharge through soil (soil-based recharge), indirect recharge via runoff to surface water systems, routing in the unsaturated zone to springs, urban recharge (such as water mains leakage), and irrigation recharge (such as losses from fields). The specific type of recharge calculation is preselected for each node in the model. The model incorporates the FAO method (Allen et al., 1998) and a soil moisture balance approach suitable for semi-arid regions, known as the Wetting Threshold method (WT) (Lange et al., 2003). Recharge is simulated from the base of the soil zone using a Penman-Grindley soil moisture balance approach (Penman, 1948; Grindley, 1967), with the spatial distribution of vegetation assumed to be constant.

B.5.4 Flood-related Issues in Karst Regions

Flooding in karst terrains poses a significant geohazard, often resulting in damage to property, businesses, and roadways, as well as the formation of cover-collapse sinkholes and groundwater contamination. **Figure B.42** shows examples of infrastructure flooding in karst zones nationally (Tennessee, USA) and internationally (Kiltartan, Ireland).

Flooding in karst areas may result in the formation of cover-collapse sinkholes and groundwater contamination. Typically, three primary types of flooding are associated with karst terrain. In many instances, flooding incidents arise from a combination of these three fundamental types including recharge-related sinkhole flooding, flow-related flooding, and discharge-related flooding. **Table B.20** shows the characteristics of each type of flooding in karst areas (Zhou, 2007).

(a)

(b)

Figure B.42 (a) Flooding in a karst area in Tennessee, USA (Zhou, 2007), and (b) Overflow across the N18 National Road, Kiltartan, Ireland (Naughton et al., 2018)

Table B.20 Flooding types in karst zones (Zhou, 2007)

Type of Flooding	Description
Recharge-related Sinkhole Flooding	Occurs when a sinkhole's drainage capacity is inadequate to channel stormwater runoff into the subsurface. The sinkhole's intake or throat may become blocked by various obstructions such as trash disposal, soil, and debris eroded from the surrounding drainage basin. Human construction activities can exacerbate the situation by increasing runoff rates to a sinkhole, exceeding its capacity to accept water.
Flow-related Flooding	It is governed by the geological formations and structures in the area. Water within karst aquifers can swiftly move towards areas with smaller flow-through cross-sections or where water from other tributaries converges within the same drainage basin. Flooding arises when the volume of incoming water exceeds the capacity of conduits in the aquifer to handle it. Factors such as sedimentation, rock falls, or human activities can reduce the flow capacity of these conduits, further exacerbating the risk of flooding.
Discharge-related Flooding	Occurs when groundwater discharge decreases due to elevated water levels at discharge points. This situation can occasionally lead to a reversal in the direction of groundwater flow. Construction of dams in surface waterbodies that receive groundwater discharge can contribute to reducing discharge rates from the karst aquifer.

Understanding the specific type of flooding in karst areas is crucial for developing effective solutions to the flooding problem. Key measures to address karst flooding include (Zhou, 2007):

- Detection of areas prone to karst flooding and implementation of restrictions and laws on land use.
- Development of runoff and erosion control plans tailored to the unique characteristics of karst features.
- Implementation of solutions such as digging out clogged sinkholes, creating retention basins, or installing Class V Injection Wells to enhance stormwater drainage.
- Coordination of flood mitigation efforts with water quality control measures to prevent groundwater contamination.

B.5.4.1 Type of Flooding in Karst Zones

B.5.4.1.1 Recharge-related Floods

Compared to non-karst terrains, recharge conditions in karst areas are generally more favorable, with recharge categorized into autogenic and allogenic (Ford and Williams, 1989). Different sources for autogenic and allogenic recharge result in variations in water chemistry and recharge volume, impacting the development of secondary permeability (Palmer, 1991). The volume of recharge is ultimately regulated by the capacity of the input passage; excessive infiltration rates may lead to ponding and subsequent overflow or surface flooding in blind valleys and poljes (Lloyd et al., 1991).

Table B.21 provides a summary of the hydrogeological classification of sinkholes, associated recharge sources, and possible flooding types, with surface flooding affecting residential/commercial areas and infrastructures, while subsurface flooding impacts underground utilities and mining operations.

Table B.21 Hydrogeological classification of sinkholes, associated recharge sources, and possible flooding types (Zhou, 2007)

Recharge Passageways Through Sinkholes	Recharge Sources		Flooding Type	
	Autogenic	Allogenic	Autogenic	Allogenic
Swallets, drain shafts for sinking streams		×		×
Solution sinkholes, surface depressions, vertical shafts	×			×
Collapse sinkholes	×		×	×
Paleo-collapse columns	×	×		×

Determining the drainage capacity of sinkholes is a complex task, influenced by factors such as sinkhole type and its connection to the aquifer system. The capacity relies on various aspects,

including conduit size and the difference between sinkhole water levels and spring pressure (Bonacci, 1987). Sinkhole characteristics, like bowl size for mature solution sinkholes or throat openness for collapse sinkholes, further impact drain capacity. Evaluation of drain capacity requires detailed field descriptions and may involve in-situ monitoring or water-injection tests. Understanding drain capacity is crucial as sinkholes often serve as recharge points to aquifers. Zhou (2007) presented the relationship between flow data collected at a sinkhole site with associated spring. Dye tracer tests confirmed sinkhole-spring connectivity, with the spring draining a broader area, indicating significant stormwater runoff potential from the sinkhole (Stephenson et al., 1999; Ogden, 1994). **Figure B.43** depicts the relationship between recharges into karst sinkholes and spring discharge.

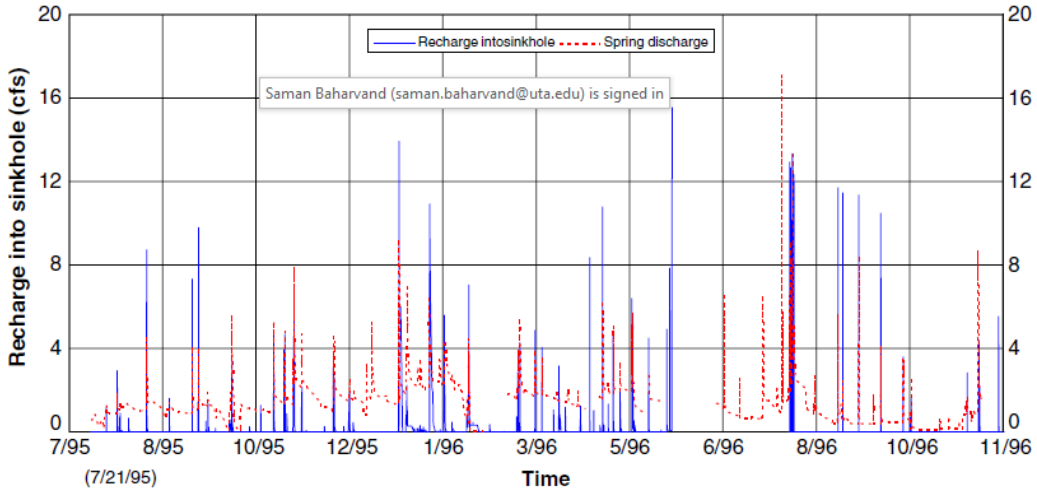

Figure B.43 Recharge into a sinkhole and discharge at a connected spring (Zhou, 2007)

B.5.4.1.2 Flow-related Flooding

As mentioned in previous sections, groundwater flow within karst aquifers comprises diffuse flow, conduit flow, and a transitional mix of both, with one type often dominating over the other. A defining characteristic of mature karst aquifers is the presence of master drains, typically active primary conduits that receive input from sinkhole drains (White, 1999). Flow predominantly occurs within fissures, enlarged fissures, and conduits. As water follows the path with the least resistance, it tends to migrate from small fissures or porous matrix towards enlarged fissures and conduits. Conduits, characterized by higher conductivity, attract groundwater from enlarged fissures, resulting in the collection and conveyance of groundwater through the main conduits, a phenomenon known as confluent flow (Zhou, 2000).

B.5.4.1.3 Discharge-related Flooding

The hydraulic interconnection between surface water and groundwater in karst aquifers is evident not only during recharge but also during discharge, with springs serving as natural outlets for karst water that may feed surface streams. However, inadequate surface channel capacity to accommodate the discharge from karst springs during storms can lead to flooding, similar to

surface water flooding. The most common flooding associated with discharge in karst areas arises from water impoundments at discharge points or surface rivers, such as the construction of reservoirs or dams. The implications of impounding a reservoir in a conduit-dominated karst area include an increase in the groundwater drainage base level, backflow into the aquifer along conduits, a decrease in the hydraulic gradient of the karst aquifer, and the transformation of dried or intermittent springs into perennial ones, among others. Consequently, karst valleys or depressions draining into the aquifer become more susceptible to flooding, as exemplified by disastrous events in the Nabapian karst valley of Guangxi Province, China, in 1993 and 1994 (Xiang et al., 1997).

B.5.4.2 Flood Mitigation Best Practices in Karst Areas

Sinkholes play dual roles in karst landscapes, acting as both sinks that channel surface water into the subsurface and sources from which groundwater discharges. Flooding in karst regions results from imbalances between water recharge and discharge. However, conducting a water balance analysis requires identifying the groundwater basin, which can be challenging in karst terrains due to the absence of well-defined divides. Delineating karst basins often demands specialized techniques such as tracer tests, geophysics or hydrogeophysics, and long-term groundwater monitoring.

Implementing best management practices (BMPs) remains the most effective strategy for flood control in karst areas. These practices should not only prevent flooding but also maintain site stability and improve water quantity. Effective flood prevention typically involves controlling runoff before it reaches sinkholes. Water quantity BMPs aim to increase sinkhole storage, reduce recharge rates, or enhance discharge capacity. Design criteria for flood control often prioritize reducing runoff peaks from rare rainfall events. Detention ponds, particularly dry ponds, can attenuate peak flows, intercept debris, and prevent flooding before water enters sinkholes. However, space limitations and potential sinkhole collapse risks may constrain detention pond construction. Other practices to reduce stormwater runoff volumes include increasing vegetation density, terracing slopes, using runoff spreaders, and employing porous pavement. Moreover, filtration systems tailored for sinkhole sites can serve dual purposes of flood control and water treatment (Zhou et al., 2005).

CHAPTER B6 : SUMMARY AND CONCLUSIONS

Playa lakes, arid regions, and karst terrains are integral components of Texas's landscape, each presenting distinctive geographical and hydrological attributes. These features are influenced by several factors including climate patterns, soil composition, and human activities, resulting in highly complex and varied hydrology. The behavior of water flowing in these areas is characterized by dynamic processes, presenting unique challenges for understanding and managing water resources effectively.

Currently, the absence of standardized guidelines for the hydrological and hydraulic design of transportation infrastructure in these landscapes poses significant challenges for engineers and designers. Without clear directives, professionals must rely heavily on individual judgment to navigate the complexities of hydrological parameters, leading to inconsistencies and potential inefficiencies in design practices. In response to this pressing need, there is a critical demand for a comprehensive review of existing knowledge and practices related to hydrological approaches in playa lakes, arid regions, and karst terrains. Such a review would serve to consolidate and synthesize the wealth of information scattered across various sources, including research studies, technical reports, and governmental publications. By systematically examining these sources, the review aims to explain the hydrological characteristics specific to each of these environments, shedding light on the underlying processes and challenges.

The primary objective of this review is to provide a holistic overview of the current state of knowledge and practices concerning hydrological approaches in playa lakes, arid regions, and karst terrains. By doing so, it seeks to fill existing gaps in understanding and pave the way for the development of comprehensive hydrological design guidance and standards tailored to the unique needs of Texas's diverse landscapes.

The methodology adopted to achieve the project's objective entails a systematic review, structured as follows: Initially, an examination of design guidance, standards, and recommendations pertinent to the hydrology and hydraulic design of transportation infrastructure, such as drainage and stormwater systems, was conducted. This encompassed a thorough review of various sources, including drainage design manuals from state departments of transportation, publications from the Federal Highway Administration (FHWA), stormwater design manuals from diverse states, cities, and communities, as well as international drainage design guidance and manuals.

We also reviewed more than 300 research studies and technical reports, which were presented at national and international conferences and published in scientific journals. This review aimed to uncover new approaches to hydrology and hydraulic studies in areas characterized by playa lakes, karst terrains, and arid conditions. The regions covered in these studies include not only the United States but also other parts of the world facing similar hydrology challenges. The results of this review show that despite numerous studies focusing on playa lakes, karst terrains, and arid areas,

there are not many studies addressing hydrologic challenges specific to these regions. The findings of this review are summarized below.

B.6.1 Hydrological Challenges Regarding Transportation Infrastructures in Playa Lakes, Arid Areas, and Karst Terrains

Playa Lakes

Hydrological studies in playa lakes are challenging due to several factors impacting the design of transportation infrastructure. Difficulties include estimating rainfall-runoff due to variable hydrological behavior, scarce data for model calibration, and complex topography. Estimating peak flows is also problematic due to rapid water level responses and potential flow alterations from sediment mobilization. The calculation of time of concentration encounters challenges due to complex drainage patterns and varying infiltration rates, especially with limited data availability. Additionally, characterizing depression storage is complicated by its variability and the temporal changes that affect storage capacity. Estimating infiltration rates is complicated by heterogeneous soil properties and vegetation impacts, with additional challenges in accurately quantifying evapotranspiration losses and groundwater interactions. Overall, modeling these processes requires careful parameterization due to the complex interplay between surface water, groundwater, and sediment transport, especially in data-scarce environments.

Arid Areas

Hydrological studies in arid areas encounter several unique challenges, significantly influenced by the region's distinctive climate and environmental conditions. One major difficulty is modeling rainfall-runoff relationships, as most hydrological methods and parameters are traditionally developed for humid climates where rainfall distribution is more consistent. This discrepancy becomes apparent in arid regions where rainfall events are typically intense and brief, making it hard to accurately predict flow intensity and direction due to factors like varying soil types, land cover, and rainfall intensity. The availability of data to assess peak rate factors is often sparse, complicating efforts to accurately predict flash floods. Additionally, arid areas are subject to extreme weather events, such as intense rainfall and droughts, with climate change likely to exacerbate these occurrences by altering precipitation patterns and increasing weather extremes. Vegetation cover in arid regions, which is much sparser than in humid areas, also affects water retention and hydrological processes, particularly as high evapotranspiration rates due to intense solar radiation and high temperatures quickly deplete soil moisture and surface water resources. Flash flooding is another significant risk in arid regions, where intense rainfall over short periods can quickly overwhelm drainage systems. Furthermore, many arid regions feature ephemeral or intermittent streams with limited channel storage, leading to a rapid runoff response to rainfall, which complicates the prediction of peak flows and timing. Hydrological models often fall short in these environments, as many are designed for conditions prevalent in more humid regions and lack the necessary adaptations for arid climates, leading to inaccuracies in simulations and predictions.

Karst Terrains

Karst hydrology introduces several challenges that complicate standard hydrological analysis and modeling due to the unique subterranean features of these landscapes. Rainfall-runoff processes are notably affected by the presence of sinkholes, caves, and underground rivers, which can rapidly channel water through the karst aquifer, leading to quick and sometimes severe flash flooding. This dynamic makes it hard to predict and respond to flood events as floodwater can appear and vanish abruptly. Moreover, the heterogeneity and anisotropy of karst terrains render the prediction of water movement highly unpredictable, complicating the determination of water sources, flow directions, and peak flows due to the aquifers' high connectivity. Additionally, variable losses occur as streams disappear and reappear, making uniform application of loss rates unreliable. The complex and varied nature of karst environments also makes data collection and the development of accurate hydrological models extremely challenging, further complicating efforts to predict floodwater behavior and create effective mitigation strategies.

B.6.2 Hydrologic Approaches to Playa Lakes, Arid Areas, and Karst Terrains

The Rational Method, NRCS (SCS) Method, and Regional Regression Equations (or similar methods developed outside of the U.S.) are widely adopted by national and international transportation agencies, states, cities, and communities. These methods are recommended for estimating peak flow and developing flow hydrographs in playa lakes, arid areas, and karst terrains with some modifications. Also, several research studies proposed approaches for modifying these methods and equations to address the hydrologic characteristics unique to these environments. These approaches are summarized here.

Playa Lakes

The national and international design manuals reviewed in this project offer limited guidance on the hydrology of playa lakes, with exceptions found in the Oklahoma Department of Transportation Roadway Drainage Manual (ODOT, 2014), the Abu Dhabi Storm Water and Sub-soil Drainage Systems Design Manual (Abu Dhabi Department of Municipalities and Transport, 2022), the City of Lubbock Drainage Criteria Manual (City of Lubbock, 2019), the City of Amarillo Stormwater Management Criterion Manual (City of Amarillo, 2008). These manuals provide specific recommendations as follows:

- Excluding non-contributing areas such as playas and dry lakebeds from the watershed area.
- Assigning different runoff coefficient (C) values in Rational Method for isolated and non-isolated playas.

While playa lakes can contribute significantly to flood mitigation, the primary focus of research studies on these features centers around various aspects such as their distribution, inundation characteristics, estimation of depth, storage volume, duration, and infiltration rates. Nonetheless, some research efforts have targeted flood forecasting and management in these vital components of arid and semi-arid regions. These efforts encompass developing models to simulate playa lake

behavior under different rainfall scenarios, analyzing hydrologic connectivity within watersheds, and examining the correlation between rainfall and playa lake response. For instance, in the Texas High Plains region, researchers have employed remote sensing data and hydrologic models to evaluate playa lake flood potential. Moreover, ongoing initiatives aim to enhance flood warning systems by integrating playa lake information. Despite these efforts, there is still much to learn about playa lake hydrology, as no study has been found that exclusively addresses the effect of these features on rainfall-runoff relationships, time of concentration, and peak flow estimate.

Arid Areas

Several national and international design manuals reviewed in this project provide some guidance on the hydrology of arid and semi-arid regions. These include Arizona Department of Transportation Highway Drainage Design Manual (ADOT, 2014), California Department of Transportation Highway Design Manual (Caltrans, 2020), New Mexico Department of Transportation Drainage Design Manual (NMDOT, 2018), TxDOT Hydraulic Design Manual (TxDOT, 2019), Federal Highway Administration- Highway Hydrology (FHWA, 2002). These documents provide specific recommendations as follows:

- Employing Rational Method runoff coefficient (C) values recommended for desert regions.
- Utilizing NRCS curve numbers (CN) recommended for arid and semi-arid areas.
- Applying regional regression equations and methods for flood frequency developed specifically for arid regions.
- Employing SCS Type II cumulative type curve for hydraulic modeling.

Hydrology of arid and semi-arid regions is characterized by low and highly variable precipitation, high evapotranspiration, and limited surface water resources. Therefore, research studies in this area have included developing hydrologic models to simulate the response of arid zone watersheds to rainfall events, analyzing the spatial and temporal variability of precipitation in arid regions, and studying the impacts of land use and climate change on flood risk in arid zones. This review showed that initial abstraction and time of concentration (T_c) play crucial roles in estimating peak flow and developing flood hydrographs in arid regions, yet accurately estimating these parameters presents significant challenges due to limited data availability.

Since conventional methodologies for estimating peak flow rate and flow hydrographs are developed for non-arid regions, several studies have attempted to modify these methods for arid regions. These attempts include modifying the curve number in the NRCS method by considering different initial loss values. Equations are proposed for calculating CN for dry and wet conditions based on antecedent moisture condition (AMC) and antecedent runoff condition (ARC). These methods have been utilized in several arid regions around the world and showed promising results; however, their applicability in other areas requires further investigation.

Time of concentration (T_c) can be calculated using various methods, including empirical, semi-empirical, and graphical methods. However, studies evaluating these methods in arid regions

reveal wide variability in their performance. Despite challenges, recent research has shown promise in refining empirical equations through graphical analyses, leading to more accurate estimations of Tc in arid environments. Overall, there have been several studies focusing on flood forecasting in arid regions with successful outcomes; however, research is needed to improve our understanding of the hydrologic processes and the impacts of climate change and land use on flood risk in these vulnerable regions.

Karst Terrains

The Florida, Kentucky, Pennsylvania, Virginia, and West Virginia Departments of Transportation offer some guidance on the hydrology of the karst region, each at different levels. Among these, the West Virginia Department of Transportation Drainage Manual (VWDOT, 2007) offers the most comprehensive approach to the hydrology of karst regions. It suggests a procedure for estimating infiltration loss in karst areas as part of the runoff estimate. Additionally, it recommends methods that can be utilized to account for karst loss. Some of these methods are adopted by the Federal Highway Administration (FHWA, 2023). These documents recommend the following approaches:

- Excluding non-contributing areas (due to karst topography features) such sinkholes and depressions from the watershed area.
- Applying empirical reduction factors to peak runoff.
- Adjusting the Rational Method runoff coefficient (*C*).
- Using an NRCS Type I rainfall distribution within a Type II area.
- Modifying curve number values or peak rate factors using the TR-20 method.
- Employing regression equations tailored for karst terrain.

The review of the literature showed that past and current research in karst regions primarily focuses on geotechnical and structural issues related to karstic features, groundwater movement and quality, water availability, and interactions between groundwater flow, erosion, and subsurface processes. There are few studies concentrating on hydrologic challenges for flood forecasting in karst landscapes at both national and international levels.

Unlike modeling drainage areas with soil pores, which have limited infiltration rates, karstic fissures and shafts allow for rapid and substantial flow discharge, contributing to shorter response times and higher peak flooding magnitudes. Additionally, water retention in voids and aquifers within karst formations can delay movement and reduce peak flood levels. Therefore, research on karst hydrology has focused on developing methods for estimating infiltration or loss through sinkholes and fissures within karst zones. One approach is modifying the NRCS curve number (CN) for karstic regions based on factors such as permeability, land use, and watershed drainage capacity. The modified NRCS-CN method has been extensively applied in Mediterranean karst regions for estimating surface runoff, peak discharge, and flash flooding, showing promising performance in assessing flood risks.

Researchers have also proposed modifications to soil moisture calculation to better account for the unique characteristics of karstic watersheds. In conventional methods, peak runoff estimation heavily relies on soil moisture conditions, determining infiltration rates and surface runoff generation. However, in karstic environments, where water rapidly infiltrates into subsurface conduits, soil moisture loss rates can differ significantly from non-karstic areas. To address these challenges, it is suggested to adapt soil moisture calculation methods to reflect the rapid drainage and subsurface flow processes characteristic of karstic watersheds. This may involve incorporating additional parameters or refining existing models to account for the complexities of flow pathways in these environments.

B.6.3 Conclusions

This review identified several hydrological challenges specific to transportation infrastructures in playa lakes, arid areas, and karst terrains, including difficulties in estimating rainfall-runoff relationships, predicting peak flows, and modeling flood behavior. Additionally, conventional hydrological methodologies often fall short in these environments, highlighting the need for tailored approaches.

While some existing design manuals offer limited guidance, further research is required to enhance our understanding of the hydrological processes in these landscapes and develop effective mitigation strategies. Future efforts should focus on refining existing methodologies, such as the Rational Method and NRCS methods, to better account for the unique characteristics of playa lakes, arid regions, and karst terrains.

Overall, by addressing the knowledge gaps and challenges identified in this review, we can better equip engineers and designers with the tools and insights needed to effectively manage water resources in Texas's diverse landscapes.

REFERENCES

Playa Lakes

Adams, K. D., and Sada, D. W. (2014). Surface water hydrology and geomorphic characterization of a playa lake system: Implications for monitoring the effects of climate change. Journal of Hydrology, 510, 92-102.

Abu Dhabi Department of Municipalities and Transport (2022). Storm water and Sub-soil Drainage Systems Design Manual - Drainage Manual. Volume 1: Design Manual. 3rd Edition. Government Abu Dhabi, United Arab Emirates

Austroads (2023) Guide to Road Design Part 5: Drainage – General and Hydrology Considerations, Austroads Ltd. Sydney NSW, Australia.

Ball J, Babister M, Nathan R, Weeks W, Weinmann E, Retallick M, Testoni I, (Editors) (2019) Australian Rainfall and Runoff: A Guide to Flood Estimation, © Commonwealth of Australia (Geoscience Australia).

Barnes, J.R., Ellis, W.C., Leggat, E.R., Scalapino, R.A., George, W.O., and Irelan, B., (1949). Geology and ground water in the irrigated region of the southern High Plains in Texas: Texas Board of Water Engineers Progress Report 7, 51 p.

Bauchert, J. A. (1996). Physical and chemical characteristics of playa soils in southwest Kansas (Doctoral dissertation, Texas Tech University).

Bexfield, L. M. (1995). Hydrologic and ecologic influence of playa basins in the southern High Plains, Texas and New Mexico. Southern High Plains NAWQA study, US Geological Survey.

Briere, P. R. (2000). Playa, playa lake, sabkha: Proposed definitions for old terms. Journal of Arid Environments, 45(1), 1-7.

Brown, R. F., Signor, D. C., and Wood, W. W. (1976). Artificial ground-water recharge as a water-management technique on the Southern High Plains of Texas and New Mexico (No. 76-730). US Geological Survey.

Bryant, R. G., and Rainey, M. P. (2002). Investigation of flood inundation on playas within the Zone of Chotts, using a time-series of AVHRR. Remote Sensing of Environment, 82(2-3), 360-375.

Busby, M. W. (1975). Flood-hazard Study: 100-year Flood Stage for Apple Valley Dry Lake, San Bernardino County, California (Vol. 11). US Department of the Interior.

Casula, K. (1995). Classification of playa lakes based on origin, morphology, and water quality parameters (Doctoral dissertation, Texas Tech University).

City of Amarillo (2008). Stormwater Management Criteria Manual. https://www.amarillo.gov/home/showpublisheddocument/10900/636473880556400000 (Accessed April 9, 2024).

City of Lubbock (2019). Drainage Criteria Manual. https://ci.lubbock.tx.us/storage/images/sRJoxWCNgXjrq2RsGkQFUpzYPpVrk6Xbc8FFBkGu.pdf (Accessed April 9, 2024).

City of Lubbock Drainage Manual 2019, The City of Lubbock, Texas, USA

Claborn, B.J., Urban, L.V., and Oppel, S.E., (1985). Frequency of significant recharge to the Ogallala aquifer from playa lakes: Water Resource Center Project G–935–03, 24 p.

Colorado Department of Transportation (CDOT) (2019). Drainage Design Manual, Chapter 7 - Hydrology. https://www.codot.gov/business/hydraulics/drainage-design-manual/chapter7_hydrology.pdf (Accessed April 9, 2024).

Curtis, D., and Beierman, H. (1980). Playa lakes characterization study. Planning aid report to Water and Power Resources Service, September.

De Deckker, P. (1988). Biological and sedimentary facies of Australian salt lakes. Palaeogeography, palaeoclimatology, palaeoecology, 62(1-4), 237-270.

Doña, C., Chang, N. B., Caselles, V., Sánchez, J. M., Pérez-Planells, L., Bisquert, M. D. M., ... and Camacho, A. (2016). Monitoring hydrological patterns of temporary lakes using remote sensing and machine learning models: Case study of la Mancha Húmeda Biosphere Reserve in central Spain. Remote Sensing, 8(8), 618.

Dugan, J.T., and Zelt, R.B., 2000, Simulation and analysis of soil-water conditions in the Great Plains and adjacent areas, central United States, 1951–80: U.S. Geological Survey Water Supply Paper 2427, 81 p.

Evans, P. W. (1990). Determining the bimodal infiltration patterns in three playa lakes (Doctoral dissertation, Texas Tech University).

Fish, E. B., Atkinson, E. L., Mollhagen, T. R., Shanks, C. H., and Brenton, C. M. (1998). Playa lakes digital database for the Texas portion of the Playa Lakes Joint Venture region. Technical Publication.

French, R. H., and Miller, J. J. (2012). Flood hazard identification and mitigation in semi-and arid environments. World Scientific.

French, R. H., Miller, J. J., and Dettling, C. (2003). Flood Assessment for Rogers Lake, Edwards Air Force Base, California. Division of Hydrologic Sciences, Desert Research Institute, Las Vegas and Reno, NV.

French, R. H., Miller, J. J., Dettling, C., and Carr, J. R. (2006). Use of remotely sensed data to estimate the flow of water to a playa lake. Journal of Hydrology, 325(1-4), 67-81.

Fryar, A. E., Mullican, W. F., and Macko, S. A. (2001). Groundwater recharge and chemical evolution in the southern High Plains of Texas, USA. Hydrogeology journal, 9, 522-542.

Ganesan, G., Rainwater, K., Gitz, D., Hall, N., Zartman, R., Hudnall, W., and Smith, L. (2016). Comparison of infiltration flux in playa lakes in grassland and cropland basins, Southern High Plains of Texas. Texas Water Journal. 7 (1): 25-39. Texas Water Journal, 25.

Gitz, D., and Brauer, D. (2016). Trends in Playa Inundation and water storage in the Ogallala Aquifer on the Texas High Plains. Hydrology, 3(3), 31.

Gouramanis, C., De Deckker, P., Wilkins, D., and Dodson, J. (2015). High-resolution, multiproxy palaeoenvironmental changes recorded from Two Mile Lake, southern Western Australia: implications for Ramsar-listed playa sites. Marine and Freshwater Research, 67(6), 748-770.

Grubb, H. W., and Parks, D. L. (1968). Multipurpose Benefits and Costs of Modifying Playa Lakes on the Texas High Plains. International Center for Arid and Semi-arid Land Studies, Texas Tech University, Lubbock, Texas.

Gurdak, J. J., and Roe, C. D. (2009). Recharge rates and chemistry beneath playas of the High Plains aquifer: a literature review and synthesis. Reston, VA, USA: US Geological Survey.

Gurdak, J. J., and Roe, C. D. (2010). Recharge rates and chemistry beneath playas of the High Plains aquifer, USA. Hydrogeology Journal, 18(8), 1747.

Gurdak, J. J., Hanson, R. T., McMahon, P. B., Bruce, B. W., McCray, J. E., Thyne, G. D., and Reedy, R. C. (2007). Climate variability controls on unsaturated water and chemical movement, High Plains aquifer, USA. Vadose Zone Journal, 6(3), 533-547.

Gustavson, T. C., Holliday, V. T., and Hovorka, S. D. (1995). Origin and development of playa basins, sources of recharge to the Ogallala aquifer, Southern High Plains, Texas and New Mexico (Vol. 229). Bureau of Economic Geology, The University of Texas at Austin.

Guthery, F. S., and Bryant, F. C. (1982). Status of playas in the Southern Great Plains. Wildlife Society Bulletin, 309-317.
Haukos, D. A., and Smith, L. M. (1992). 13.3. 7. Ecology of playa lakes. Waterfowl management handbook, 19.
Haukos, D. A., and Smith, L. M. (2003). Past and future impacts of wetland regulations on playa ecology in the Southern Great Plains. Wetlands, 23(3), 577-589.
Hauser, V. L. (1966). Hydrology, conservation, and management of runoff water in playas on the Southern High Plains (No. 8). Agricultural Research Service, US Department of Agriculture.
Hauser, V. L., and Lotspeich, F. B. (1968). Treatment of playa lake water for recharge through wells. Transactions of the ASAE, 11(1), 108-0111.
Hovorka, S. D. (1995). Quaternary evolution of playa lakes on the southern High Plains: a case study from the Amarillo area, Texas (Vol. 236). Bureau of Economic Geology, the University of Texas at Austin.
Hovorka, S. D. (1997). Quaternary evolution of ephemeral playa lakes on the Southern High Plains of Texas, USA: cyclic variation in lake level recorded in sediments. Journal of Paleolimnology, 17, 131-146.
Huda, A. N. (1996). Field verification of a dual-porosity flow model to estimate aquifer recharge rates through playa lakes (Doctoral dissertation, Texas Tech University).
James, T. S. (1998). Hydrologic budget of selected playa lakes in Lubbock, Texas (Doctoral dissertation, Texas Tech University).
Kansas Department of Transportation (KDOT) (2023). Drainage Design Manual, Section 3 - Hydrology. https://www.ksdot.gov/Assets/wwwksdotorg/bureaus/burRoadDesign/drainagemanualsections/Section_3.pdf (Accessed April 9, 2024).
Knowles, T. R., Nordstrom, P. L., and Klemt, W. B. (1984). Evaluating the ground-water resources of the High Plains of Texas (Vol. 3). Texas Department of Water Resources.
Lotspeich, F. B., Lehman, O. R., Hauser, V. L., and Stewart, B. A. (1971). Hydrogeology of a playa near Amarillo, Texas.
Luo, H. R., Smith, L. M., Allen, B. L., and Haukos, D. A. (1997). Effects of sedimentation on playa wetland volume. Ecological Applications, 7(1), 247-252.
McMahon, P. B., Dennehy, K. F., Bruce, B. W., Böhlke, J. K., Michel, R. L., Gurdak, J. J., and Hurlbut, D. B. (2006). Storage and transit time of chemicals in thick unsaturated zones under rangeland and irrigated cropland, High Plains, United States. Water Resources Research, 42(3).
Miller, J. J., and French, R. H. (2002). Flood Assessment for Mojave Creek, Edwards Air Force Base, California. Desert Research Institute. Las Vegas and Reno, NV.
Nativ, R. (1992). Recharge into Southern High Plains aquifer—possible mechanisms, unresolved questions. Environmental Geology and Water Sciences, 19(1), 21-32.
Nativ, R., and Smith, D. A. (1987). Hydrogeology and geochemistry of the Ogallala aquifer, Southern High Plains. Journal of Hydrology, 91(3-4), 217-253.
New Mexico Department of Transportation (NMDOT) (2018). Drainage Design Manual. https://www.dot.nm.gov/infrastructure/program-management/drainage-design/ (Accessed April 9, 2024).
Oklahoma Department of Transportation (ODOT) (2014). Drainage Manual, Chapter 7 - Hydrology. https://oklahoma.gov/content/dam/ok/en/odot/documents/chapter-7-hydrology.pdf (Accessed April 9, 2024).

Osterkamp, W. R., and Wood, W. W. (1987). Playa-lake basins on the Southern High Plains of Texas and New Mexico: Part I. Hydrologic, geomorphic, and geologic evidence for their development. Geological Society of America Bulletin, 99(2), 215-223.

Parker, D. B., Cahoon, J. E., Rogers, W. J., Rhoades, M. B., McCullough, M. C., and Robinson, C. (1998). Infiltration characteristics of cracked clay soils in bottoms of feedyard playa catchments. In 2001 ASAE Annual Meeting (p. 1). American Society of Agricultural and Biological Engineers.

Playa Lakes Joint Venture (PLJV). (2009). Probable playas in Floyd County, Texas. Available from: http://www.pljv.org/ PPv4_MapBook/PPv4_TX_Floyd_County.pdf.

Quillin, J. P., Zartman, R. E., and Fish, E. B. (2005). Spatial distribution of playa basins on the Texas High Plains. Texas Journal of Agriculture and Natural Resources, 18, 1-14.

Reeves Jr, C. C. (1966). Pluvial lake basins of west Texas. The Journal of Geology, 74(3), 269-291.

Reeves Jr, C. C. (1990). A proposed sequential development of lake basins, Southern High Plains, Texas and New Mexico. Geologic framework and regional hydrology: Upper Cenozoic Blackwater Draw and Ogallala formations, Great Plains, 209-232.

Sallenave, R., and Ganguli, A. (2021). PLAYA LAKES: Understanding Their Importance and How to Protect Them and Improve Their Function. College of Agricultural, Consumer and Environmental Sciences.

Scanlon, B. R., and Goldsmith, R. S. (1997). Field study of spatial variability in unsaturated flow beneath and adjacent to playas. Water Resources Research, 33(10), 2239-2252.

Scanlon, B. R., Dutton, A. R., and Sophocleous, M. A. (2002). Groundwater recharge in Texas. Austin, TX, USA: Bureau of Economic Geology, University of Texas at Austin.

Scanlon, B. R., Dutton, A., and Sophocleous, M. (2003). Groundwater recharge in Texas. Report, Texas Water Dev. Board, Austin, TX, 80 pp

Smith, L. M. (2003). Playas of the great plains. University of Texas Press.

Solvik, K., Bartuszevige, A. M., Bogaerts, M., and Joseph, M. B. (2021). Predicting Playa Inundation Using a Long Short-Term Memory Neural Network. Water Resources Research, 57(12), e2020WR029009.

Steiert, J., and Meinzer, W. (1994). Playas: jewels of the plains.

Stone, W. J. (1990). Natural recharge of the Ogallala aquifer through playas and other non-stream-channel settings, eastern New Mexico. Geologic Framework and Regional Hydrology: Upper Cenozoic Blackwater Draw and Ogallala Formations, Great Plains, 180-192.

Stone, W. J., and McGurk, B. E. (1985). Ground-water recharge on the southern high plains, east-central New Mexico. In New Mexico Geological Society Guidebook, 36th Field Conference (pp. 331-335). New Mexico Geological Society Santa Rosa.

Texas Department of Transportation (TxDOT) (2019). Hydraulic Design Manual. http://onlinemanuals.txdot.gov/TxDOTOnlineManuals/TxDOTManuals/hyd/hyd.pdf (Accessed April 9, 2024).

Texas Parks and Wildlife Department (TPWD) (n.d.). https://tpwd.texas.gov/landwater/land/habitats/high_plains/wetlands/playa.phtml (Accessed April 10, 2024).

Theis, C. V. (1937). Amount of ground-water recharge in the southern High Plains. Eos, Transactions American Geophysical Union, 18(2), 564-568.

Weinberg, A. P. G., Backhouse, S., and Gitz, D. (2015). A Water Resource Assessment of the Playa Lakes of the Texas High Plains.

Weinberg, A.P.G., Mark Olden, Dennis Gitz, and Cody Byars. (2021). "Playa Lakes in the Southern High Plains: Runoff, Infiltration, and Recharge". Texas Water Development Board. Report 386.

West, E. L. (1998). Hydrology of urban playa lakes in Lubbock, Texas (Doctoral dissertation, Texas Tech University).

Wood, W. W., and Sanford, W. E. (1994). Recharge to the Ogallala: 60 years after CV Theis' analysis. In Procedings of the Playa Basin Symposium (pp. 23-33).

Wood, W. W., and Sanford, W. E. (1995). Eolian transport, saline lake basins, and groundwater solutes. Water Resources Research, 31(12), 3121-3129.

Wood, W. W., Rainwater, K. A., and Thompson, D. B. (1997). Quantifying macropore recharge: Examples from a semi-arid area. Groundwater, 35(6), 1097-1106.

Wood, W., and Jones, B. F. (1990). Origin of solutes in saline lakes and springs on the southern High Plains of Texas and New Mexico.

Zartman, R. E., and Fish, E. B. (1989). Size, distribution, and orientation pattern of playa lakes in northwestern Castro County, Texas. Texas Journal of Agriculture and Natural Resources, 3, 31-33.

Zartman, R. E., Evans, P. W., and Ramsey, R. H. (1994). Playa lakes on the Southern High Plains in Texas: reevaluating infiltration. Journal of Soil and Water Conservation, 49(3), 299-301.

Zartman, R. E., Ramsey, R. H., Evans, P. W., Koenig, G., Truby, C., and Kamara, L. (1996). Outerbasin, annulus and playa basin infiltration studies. Texas Journal of Agriculture and Natural Resources, 9, 23-32.

Arid Arias

ABC News. (2023). State of emergency declared in western Texas due to flooding. Accessed through (https://abcnews.go.com/GMA/News/video/state-emergency-declared-western-texas-due-flooding-99784250)

Abdulla, F. A., and Al-Omari, A. S. (2008). Impact of climate change on the monthly runoff of a semi-arid catchment: Case study Zarqa River Basin (Jordan). Journal of Applied Biological Sciences, 2(1), 43-50.

Abushandi, E. (2011). Rainfall-runoff modeling in arid areas. Technical University of Freiberg (TUBAF) Freiberg. Doctoral Dissertation. Volltext (PDF).

Ahmadi, M., Moeini, A., Ahmadi, H., Motamedvaziri, B., and Zehtabiyan, G. R. (2019). Comparison of the performance of SWAT, IHACRES and artificial neural networks models in rainfall-runoff simulation (case study: Kan watershed, Iran). Physics and Chemistry of the Earth, Parts A/B/C, 111, 65-77.

Alamri, N., Afolabi, K., Ewea, H., and Elfeki, A. (2023). Evaluation of the time of concentration models for enhanced peak flood estimation in arid regions. Sustainability, 15(3), 1987.

Albishi, M. (2015). Unit hydrograph of watersheds in arid zones: case study in south western Saudi Arabia. Unpublished MSc. thesis, King Abdulaziz University, Jeddah.

Albishi, M., Bahrawi, J., and Elfeki, A. (2017). Empirical equations for flood analysis in arid zones: the Ari-Zo model. Arabian Journal of Geosciences, 10, 1-13.

Aldridge, B. N. (1970). Floods of November 1965 to January 1966 in the Gila River basin, Arizona and New Mexico, and adjacent basins in Arizona. US Government Printing Office.

Al-Ghobari, H., Dewidar, A., and Alataway, A. (2020). Estimation of surface water runoff for a semi-arid area using RS and GIS-based SCS-CN method. Water, 12(7), 1924.

Alsubeai, A. (2021). A hydrologic climate study for an arid region. South Dakota State University.
Arizona Department of Transportation (ADOT) (2014). Highway Drainage Design Manual, Volume 2, Hydrology, 2nd Edition. https://azdot.gov/sites/default/files/2019/07/2014_adot_hydrology_manual.pdf (Accessed April 9, 2024).
Arizona Department of Transportation, DOT, (1993). Highway Drainage Design Manual.
Babcock, H. M., and Cushing, E. M. (1942). Recharge to ground-water from floods in a typical desert wash, Pinal County, Arizona. Eos, Transactions American Geophysical Union, 23(1), 49-56.
Baldocchi, D., Xu, L., & Kiang, N. (2004). How plant functional-type, weather, seasonal drought, and soil physical properties alter water and energy fluxes of an oak-grass savanna and an annual grassland. Agricultural and Forest Meteorology, 123(1-2), 13-39.
Bailey, R. G. (1976). Ecoregions of the United States. unnumbered publication. Intermountain Region, USDA Forest Service, Ogden, Utah.
Bamufleh, S., Al-Wagdany, A., Elfeki, A., and Chaabani, A. (2020). Developing a geomorphological instantaneous unit hydrograph (GIUH) using equivalent Horton-Strahler ratios for flash flood predictions in arid regions. Geomatics, Natural Hazards and Risk, 11(1), 1697-1723.
Barakat, H. (2009). Arid lands: challenges and hopes. Earth System History and Natural Variability, 3, 209.
Basahi, J., Masoud, M., and Zaidi, S. (2016). Integration between morphometric parameters, hydrologic model, and geo-informatics techniques for estimating WADI runoff (case study WADI HALYAH—Saudi Arabia). Arabian Journal of Geosciences, 9, 1-18.
Basahi, J., Masoud, M., and Zaidi, S. (2016). Integration between morphometric parameters, hydrologic model, and geo-informatics techniques for estimating WADI runoff (case study WADI HALYAH—Saudi Arabia). Arabian Journal of Geosciences, 9, 1-18.
Bondelid, T. R., McCuen, R. H., and Jackson, T. J. (1982). Sensitivity of SCS models to curve number variation 1. JAWRA Journal of the American Water Resources Association, 18(1), 111-116.
Boulton, A. J., Findlay, S., Marmonier, P., Stanley, E. H., and Valett, H. M. (1998). The functional significance of the hyporheic zone in streams and rivers. Annual review of Ecology and systematics, 29(1), 59-81.
Bournas, A., and Baltas, E. (2021). Increasing the efficiency of the Sacramento model on event basis in a mountainous river basin. Environmental Processes, 8, 943-958.
California Department of Transportation (Caltrans) (2020). Highway Design Manual, U.S. Customary Units, 7th Edition. https://dot.ca.gov/-/media/dot-media/programs/design/documents/hdm-complete--092923-a11y3.pdf (Accessed April 9, 2024).
California Division of Highways, CDH, (1960). California Culvert Practice. Department of Public Works, Division of Highways: Sacramento, CA, USA.
Carter, R. W. (1961). Magnitude and frequency of floods in suburban areas. US Geological Survey Professional Paper, 424, 9-11.
Cataldo, J., Behr, C., Montalto, F., and Pierce, R. (2004). A summary of published reports of transmission losses in ephemeral streams in the US. National Center for Housing and the Environment, 42, 28-29.

Chow, V. T. (1962). Hydrologic determination of waterway areas for the design of drainage structures in small drainage basins. University of Illinois. Engineering Experiment Station. Bulletin; no. 462.

Chow, V. T., Maidment, D. R., and Mays, L. W. (1988). Applied hydrology.

City of El Paso (2022). Stormwater Design Manual. https://www.elpasotexas.gov/assets/Documents/CoEP/Planning-and-Inspections/Planning-Divisions/Combined-Storm-Water-Design-Manual.pdf (Accessed April 9, 2024).

City of Gainesville (2020). Drainage Criteria and Design Manual. https://www.gainesville.tx.us/DocumentCenter/View/1460/Drainage-Design-and-Criteria-Manual-Right-Side-Up (Accessed April 9, 2024).

City of South Salt Lake (2020). Stormwater Design Manual. https://sslc.gov/DocumentCenter/View/475/South-Salt-Lake-Stormwater-Design-Manual-PDF (Accessed April 9, 2024).

Comer, P., & Schulz, K. (2007). Standardized ecological classification for mesic upland sites in the United States: A synthesis of ecoregions and environmental data. NatureServe.

Commission for Environmental Cooperation, CEC, (1997). Ecological Regions of North America: Toward a Common Perspective. Montreal (Quebec), Canada. http://www.epa.gov/wed/pages/ecoregions/na_eco.htm#CEC1997.

Department of Public Works. (1995). California culvert practice, second edition. Sacramento, CA: DPW, Division of Highways.

Dick, G. S., Anderson, R. S., and Sampson, D. E. (1997). Controls on flash flood magnitude and hydrograph shape, Upper Blue Hills badlands, Utah. Geology, 25(1), 45-48.

Dooge, J. (1973). Linear theory of hydrologic systems (No. 1468). Agricultural Research Service, US Department of Agriculture.

Dunkerley, D. L. (1992). Channel geometry, bed material, and inferred flow conditions in ephemeral stream systems, Barrier Range, western NSW Australia. Hydrological Processes, 6(4), 417-433.

Egyptian Water Resources Research Institute (EWRRI) (n.d.) 2005-2006 Report prepared for the Development of Wadi Watir in Sinai, Egypt to the Egyptian Ministry of Water Resources and Irrigation

Elfeki, A., and Bahrawi, J. (2017). Application of the random walk theory for simulation of flood hazards: Jeddah flood 25 November 2009. International journal of emergency management, 13(2), 169-182.

Fang, X., Thompson, D. B., Cleveland, T. G., Pradhan, P., and Malla, R. (2008). Time of concentration estimated using watershed parameters determined by automated and manual methods. Journal of Irrigation and Drainage Engineering, 134(2), 202-211.

Farran, M. M., and Elfeki, A. M. (2020a). Statistical analysis of NRCS curve number (NRCS-CN) in arid basins based on historical data. Arabian Journal of Geosciences, 13, 1-15.

Farran, M. M., and Elfeki, A. M. (2020b). Variability of the asymptotic curve number in mountainous undeveloped arid basins based on historical data: case study in Saudi Arabia. Journal of African Earth Sciences, 162, 103697.

Farran, M. M., and Elfeki, A. M. (2020c). Evaluation and validity of the antecedent moisture condition (AMC) of Natural Resources Conservation Service-Curve Number (NRCS-CN) procedure in undeveloped arid basins. Arabian Journal of Geosciences, 13, 1-17.

Farran, M. M., Elfeki, A., Elhag, M., and Chaabani, A. (2021). A comparative study of the estimation methods for NRCS curve number of natural arid basins and the impact on flash flood predications. Arabian Journal of Geosciences, 14, 1-23.
Federal Aviation Administration (FAA). (1970). Advisory circular on airport drainage. U.S. Dept. of Transportation, Washington, DC.
Federal Emergency Management Agency (FEMA) (1990). FAN, An Alluvial Fan Flooding Computer Program User's Manual and Program Disk. September.
Federal Emergency Management Agency (FEMA) (1995). Flood Insurance Study Guideline and Specifications for Study Contractors, (FEMA37). January.
Federal Emergency Management Agency (FEMA) (2000). Guidelines for Determining Flood Hazards on Alluvial Fans. February 23
Federal Highway Administration (FHWA) (2001). Urban Drainage Design Manual. Hydraulic Engineering Circular No. 22, Second Edition. Publication No. FHWA-NHI-01-021.
Federal Highway Administration (FHWA) (2002). Highway Hydrology. Hydraulic Design Series No. 2, Second Edition. https://www.fhwa.dot.gov/engineering/hydraulics/pubs/hif02001.pdf (Accessed April 9, 2024).
Gaume, E., Bain, V., Bernardara, P., Newinger, O., Barbuc, M., Bateman, A., ... and Viglione, A. (2009). A compilation of data on European flash floods. Journal of Hydrology, 367(1-2), 70-78.
Georgakakos, K. P. (2006). Analytical results for operational flash flood guidance. Journal of Hydrology, 317(1-2), 81-103.
Giandotti, M. (1934). Previsione delle piene e delle magre dei corsi d'acqua. Istituto Poligrafico dello Stato, 8, 107–117.
Giandotti, M. (1940). Previsione empirica delle piene in base alle precipitazioni meteoriche, alle caratteristiche fisiche e morfologiche dei bacini; Applicazione del metodo ad alcuni bacini dell'appennino ligure. Memorie e studi idrografici, 10, 5-13.
Gochis, D. J., Brito-Castillo, L., and Shuttleworth, W. J. (2006). Hydroclimatology of the North American Monsoon region in northwest Mexico. Journal of Hydrology, 316(1-4), 53-70.
Goodrich, D. C., Lane, L. J., Shillito, R. M., Miller, S. N., Syed, K. H., and Woolhiser, D. A. (1997). Linearity of basin response as a function of scale in a semiarid watershed. Water resources research, 33(12), 2951-2965.
Goodrich, D.C. (2017) Arid zone hydrology. In: Vijay P. Singh, Eds. Handbook of Applied Hydrology. 2nd edition. New York, NY: McGraw-Hill Education. p. 88-1 to 88-7.
Graf, W. L. (1988). Fluvial processes in dryland rivers (Vol. 346). New York: Springer-Verlag.
Grimaldi, S., Petroselli, A., Tauro, F., and Porfiri, M. (2012). Time of concentration: a paradox in modern hydrology. Hydrological Sciences Journal, 57(2), 217-228.
Hafezparast, M., Araghinejad, S., Fatemi, S. E., and Bressers, J. T. (2013). A conceptual rainfall-runoff model using the auto calibrated NAM models in the Sarisoo River. Hydrology: current research, 4(1).
Haktanir, T., and Sezen, N. (1990). Suitability of two-parameter gamma and three-parameter beta distributions as synthetic unit hydrographs in Anatolia. Hydrological sciences journal, 35(2), 167-184.
Hawkins, R. H. (1993). Asymptotic determination of runoff curve numbers from data. Journal of irrigation and drainage engineering, 119(2), 334-345.

Hedman, E.R. and W.R. Osterkamp. (1982). Streamflow characteristics related to channel geometry of stream in western United States. U.S. Geological Survey Water Supply Paper 2193.
Herczeg, A. L., and Leaney, F. W. (2011). Environmental tracers in arid-zone hydrology. Hydrogeology Journal, 19(1), 17.
Hereford, R. (2002). Precipitation history of the Colorado Plateau region, 1900-2000 (Vol. 119, No. 2). US Department of the Interior, US Geological Survey.
Holmes, R. M., Fisher, S. G., and Grimm, N. B. (1994). Parafluvial nitrogen dynamics in a desert stream ecosystem. Journal of the North American Benthological Society, 13(4), 468-478.
Hughes, D. A., Andersson, L., Wilk, J., and Savenije, H. H. (2006). Regional calibration of the Pitman model for the Okavango River. Journal of Hydrology, 331(1-2), 30-42.
International Fund for Agriculture Development (IFAD), (2000). The Rangelands of Arid and Semiarid Areas. Available online: https://www.ifad.org/en/
Izzard, C. F., and Hicks, W. I. (1946). Hydraulics of runoff from developed surfaces. In Proc. Highway Research Board (Vol. 26, pp. 129-150).
Jacobson, P. J., Jacobson, K. M., Angermeier, P. L., and Cherry, D. S. (2000). Hydrologic influences on soil properties along ephemeral rivers in the Namib Desert. Journal of Arid Environments, 45(1), 21-34.
Jiang, Y., Yuan, Y., and Piza, H. (2015). A review of applicability and effectiveness of low impact development/green infrastructure practices in arid/semi-arid United States. Environments, 2(2), 221-249.
Johnstone, D., and Cross, W. P. (1949). Elements of applied hydrology.
JSCE. (1999). The collection of hydraulic formulae. Tokyo: Japan Society of Civil Engineers.
Jung, S. W. (2005). Development of empirical formulas for the parameter estimation of Clark's watershed flood routing model. Korea University, Seoul, Korea (in Korean with English abstract).
Kamel, A. H. (2008). Application of a hydrodynamic MIKE 11 model for the Euphrates River in Iraq. Slovak Journal of Civil Engineering, 2(1), 1-7.
Kamis, A. S., Bahrawi, J. A., and Elfeki, A. M. (2018). Reservoir routing in ephemeral streams in arid regions. Arabian Journal of Geosciences, 11, 1-13.
Keppel, R. V., and Renard, K. G. (1962). Transmission losses in ephemeral stream beds. Journal of the Hydraulics Division, 88(3), 59-68.
Keskin, F., Şensoy, A. A., Şorman, A., and Şorman, Ü. A. (2007). Application of Mike11 model for the simulation of snowmelt runoff in Yuvacik dam basin, Turkey. In International Congress on River Basin Management, The role of general directorate of state Hydraulic works (DSI) in development of water resources of Turkey.
Kibler, D. F., and Aron, G. (1982, May). Estimating basin lag and T c in small urban watersheds. In Spring Meeting, American Geophysical Union, Philadelphia, Pa.
Kirpich, Z. P. (1940). Time of concentration of small agricultural watersheds. Civil engineering, 10(6), 362.
Knighton, A. D., and Nanson, G. C. (1997). Distinctiveness, diversity and uniqueness in arid zone river systems. Arid Zone Geomorphology: Process, Form and Change in Drylands, Thomas DSG (ed). 2nd Edition, John Wiley and Sons, 185-203.
Kotb, G. and A. M. El Belasy. (2007). Protecting the economical area north west Suez gulf against flash flood hazards (south part). Fifth International Symposium on Environmental Hydrology. Cairo, Egypt.

Kuwait Ministry of Public Works (2012) .Design Manual for Roads and Bridges, Part 3: Kuwait Highway Drainage Design Manual. Edition 2, Roads Administration

Lane, L.J. (1983). Transmission Losses. In: National Engineering Handbook. IV. Hydrology. Washington, D.C., USDA, Soil Conservation Service, 21 p.

Levick, L. R., Goodrich, D. C., Hernandez, M., Fonseca, J., Semmens, D. J., Stromberg, J. C., ... and Kepner, W. G. (2008). The ecological and hydrological significance of ephemeral and intermittent streams in the arid and semi-arid American Southwest (p. 116). Washington, DC, USA: US Environmental Protection Agency, Office of Research and Development.

MacDermott, G. E. and Pilgrim, D. H. (1982). Design flood estimation for small catchments in New South Wales. Department of National Development and Energy. Australian Water Resources Council Technical Paper No. 73, pp. 233.

Marchi, L., Borga, M., Preciso, E., Sangati, M., Gaume, E., Bain, V., ... and Pogačnik, N. (2009). Comprehensive post-event survey of a flash flood in Western Slovenia: observation strategy and lessons learned. Hydrological Processes: An International Journal, 23(26), 3761-3770.

Maricopa County (2018). Drainage Policies and Standards. https://www.maricopa.gov/DocumentCenter/View/2369/Drainage-Policies-and-Standards-Manual-for-Maricopa-County---revised-82218-PDF (Accessed April 9, 2024).

Marko, K., Elfeki, A., Alamri, N., and Chaabani, A. (2019). Two dimensional flood inundation modelling in urban areas using WMS, HEC-RAS and GIS (Case Study in Jeddah City, Saudi Arabia). In Advances in Remote Sensing and Geo Informatics Applications: Proceedings of the 1st Springer Conference of the Arabian Journal of Geosciences (CAJG-1), Tunisia 2018 (pp. 265-267). Springer International Publishing.

Mata-Lima, H., Vargas, H., Carvalho, J., Gonçalves, M., Caetano, H., Marques, A., and Raminhos, C. (2007). Comportamento hidrológico de bacias hidrográficas: integração de métodos e aplicação a um estudo de caso. Rem: Revista Escola de Minas, 60, 525-536.

McCuen, R. H., Wong, S. L., and Rawls, W. J. (1984). Estimating urban time of concentration. Journal of hydraulic Engineering, 110(7), 887-904.

McMahon, T. A. (1979). Hydrological characteristics of arid zones. Proceedings... The Hydrology of areas of low precipitation, 1979.

Miller, D. A., and White, R. A. (1998). A conterminous United States multilayer soil characteristics dataset for regional climate and hydrology modeling. Earth interactions, 2(2), 1-26.

Morgali, J. R., and Linsley, R. K. (1965). Computer analysis of overland flow. Journal of the Hydraulics Division, 91(3), 81-100.

Mwelwa, E. M. (2004). The application of the monthly time step Pitman rainfall-runoff model to the Kafue River basin of Zambia (Doctoral dissertation, Rhodes University).

National Research Conservation Service, NRCS. (1997). Ponds Planning, design, construction. Washington DC: US Natural Resources Conservation Service, Agriculture Handbook no. 590.

National Research Conservation Service, NRCS. (2004). Estimation of Direct Runoff from Storm Rainfall. In National Engineering Handbook; United States Department of Agriculture, Natural Resources Conservation Science, US Government Printing office: Washington, DC, USA.

Nevada Department of Transportation (NDOT) (2006). Drainage Manual. https://www.dot.nv.gov/home/showpublisheddocument/1663/636183602579530000 (Accessed April 9, 2024).

New Mexico Department of Transportation (NMDOT) (2018). Drainage Design Manual. https://www.dot.nm.gov/infrastructure/program-management/drainage-design/ (Accessed April 9, 2024).

Niyazi, B., Khan, A. A., Masoud, M., Elfeki, A., Basahi, J., and Zaidi, S. (2022). Optimum parametrization of the soil conservation service (SCS) method for simulating the hydrological response in arid basins. Geomatics, Natural Hazards and Risk, 13(1), 1482-1509.

Olsen, H. (1987). Ancient ephemeral stream deposits: a local terminal fan model from the Bunter Sandstone Formation (L. Triassic) in the Tønder-3,-4 and-5 wells, Denmark. Geological Society, London, Special Publications, 35(1), 69-86.

Owolabi, A. A., and Kapangaziwri, E. (2012). The Role of Basin Physical Property Data in Assessing Water Stress in Water Resources Studies: The Application of the Pitman Rainfall-Runoff Model in Nigeria.

Pasini, F. (1914). Relazione sul progetto della bonifica renana. Bologna, Italy.

Qader, S. H., Dash, J., Alegana, V. A., Khwarahm, N. R., Tatem, A. J., and Atkinson, P. M. (2021). The role of earth observation in achieving sustainable agricultural production in arid and semi-arid regions of the world. Remote Sensing, 13(17), 3382.

Rammal, M., and Berthier, E. (2020). Runoff losses on urban surfaces during frequent rainfall events: a review of observations and modeling attempts. Water, 12(10), 2777.

Reed, S., Schaake, J., and Zhang, Z. (2007). A distributed hydrologic model and threshold frequency-based method for flash flood forecasting at ungauged locations. Journal of hydrology, 337(3-4), 402-420.

Reid, I. (1994). River landforms and sediment: evidence of climatic change. In: A.D. Abrahams and A.J. Parsons (Eds.), Geomorphology of Desert Environments. Chapman and Hall, London, p. 571 592.

Reid, I., and Frostick, L. E. (1989). Channel form, flows and sediments in deserts. Chapter 6 in "Arid Zone Geomorphology", DSG Thomas.

Reid, I., and Frostick, L. E. (2011). Channel form, flows and sediments of endogenous ephemeral rivers in deserts. Arid zone geomorphology: Process, form and change in drylands, 301-332.

Reid, I., Laronne, J. B., and Powell, D. M. (1998). Flash-flood and bedload dynamics of desert gravel-bed streams. Hydrological Processes, 12(4), 543-557.

Renard, K. G. (1970). The hydrology of semiarid rangeland watersheds (Vol. 41, No. 162). Agricultural Research Service, US Department of Agriculture.

Rodier, J. A. (1985). Aspects of arid zone hydrology. Facets of hydrology, 2, 205-247.

Rosenberg, N. J. (1987). Climate of the Great Plains region of the United States. Great Plains Agricultural Council Publication.

Saharia, M., Kirstetter, P. E., Vergara, H., Gourley, J. J., Hong, Y., and Giroud, M. (2017). Mapping flash flood severity in the United States. Journal of Hydrometeorology, 18(2), 397-411.

San Bernadino County (1986). Hydrology Manual. https://www.sbcounty.gov/uploads/DPW/docs/HydrologyManual.pdf (Accessed April 9, 2024).

San Bernadino County (2010). Hydrology Manual Addendum for Arid Regions. https://www.sbcounty.gov/uploads/DPW/docs/20100412_addendum.pdf (Accessed April 9, 2024).

Schulz, S., de Rooij, G. H., Michelsen, N., Rausch, R., Siebert, C., Schüth, C., ... and Merz, R. (2016). Estimating groundwater recharge for an arid karst system using a combined approach of time-lapse camera monitoring and water balance modelling. Hydrological Processes, 30(5), 771-782.

Seager, R., Ting, M., Held, I., Kushnir, Y., Lu, J., Vecchi, G., Huang, H.P., Harnik, N., Leetmaa, A., Lau, N.C. and Li, C. (2007). Model projections of an imminent transition to a more arid climate in southwestern North America. Science, 316(5828), 1181-1184.

Şen, Z. (2007). Hydrograph and unit hydrograph derivation in arid regions. Hydrological Processes: An International Journal, 21(8), 1006-1014.

Sharifi, S., and Hosseini, S. M. (2011). Methodology for identifying the best equations for estimating the time of concentration of watersheds in a particular region. Journal of irrigation and drainage engineering, 137(11), 712-719.

Sharp, A. L. and K.E. Saxton. (1962). Transmission losses in a mature stream valley. Journal of the Hydraulic Division, Proceedings of the American Society of Civil Engineers, 88, p. 121-142.

Shaw, J. R., and Cooper, D. J. (2008). Linkages among watersheds, stream reaches, and riparian vegetation in dryland ephemeral stream networks. Journal of Hydrology, 350(1-2), 68-82.

Sheridan, J. M. (1994). Hydrograph time parameters for flatland watersheds. Transactions of the ASAE, 37(1), 103-113.

Soliman, M. M. (2010). Engineering hydrology of arid and semi-arid regions. CRC Press.

Stanley, E. H., Fisher, S. G., and Grimm, N. B. (1997). Ecosystem expansion and contraction in streams. BioScience, 47(7), 427-435.

Stevanović, Z., and Milanović, P. (2015). Engineering challenges in karst. Acta Carsologica, 44(3).

Sultan of Oman (1994). Oman Highway Design Standard, Volume 1, Chapter 4: Design Standard and Specification. Oman Highway Design Standard. https://openjicareport.jica.go.jp/pdf/11349826_05.pdf (Accessed April 20, 2024).

Texas Department of Insurance (TDI), 2021. "Flash Flood Safety". Accessed online: https://www.tdi.texas.gov/pubs/videoresource/t5flood.pdf

Texas Department of Transportation (TxDOT) (2019). Hydraulic Design Manual. http://onlinemanuals.txdot.gov/TxDOTOnlineManuals/TxDOTManuals/hyd/hyd.pdf (Accessed April 9, 2024).

Thornes, J. B. (1994). Catchment and channel hydrology. In Geomorphology of desert environments (pp. 303-332). Dordrecht: Springer Netherlands.

Tooth, S. (2000). Process, form and change in dryland rivers: a review of recent research. Earth-Science Reviews, 51(1-4), 67-107.

U.S. Army Corps of Engineers (USACE) (1992). Guidelines for Risk and Uncertainty Analysis in Water Resources Planning. Report 92-R-1. Fort Belvoir, VA.

U.S. Army Corps of Engineers (USACE) (1993). Assessment of Structural Flood-Control Measures on Alluvial Fans. October.

U.S. Environmental Protection Agency, EPA, (2005). Letter from Benjamin H. Grumbles, Assistant Administrator, EPA, to Ms. Jeanne Christie, Executive Director, Association of State Wetland Managers, dated Jan. 9.

U.S. Geological Survey (USGS) Interagency Advisory Committee of Water Data (1982). Guidelines for Determining Flood Flow Frequency, Bulletin 17B, U.S. Geological Survey, https://utaedu.questionpro.com/07201-Survey Reston, VA.

USDA Natural Resources Conservation Service (NRCS) (2010). National Engineering Handbook: Part 630 –Hydrology. Published as NEH-4 Hydrology by the USDA Soil Conservation Service (SCS)

USDA-SCS (1972). National Engineering Handbook, Section 4: Hydrology. Washington, DC.

USDA-SCS report. (1985). National Engineering Handbook Section 4: hydrology, soil conservation service., Washington, DC.
USGS Geological Survey. (1997). Some perspectives on Comate and Floods in the Southwestern U.S. USGS Web Conference: Impacts of Climate Change and Land Use on the Southwestern United States, July 7 - 25, 1997. Accessed from Web site: https://www.usgs.gov/
USGS, (2006) The National Map, The Nation's Topographic Map for the 21st Century, United States Geological Survey. Online: http://nationalmap.gov/index.html
USGS. (2000). Equations for Estimating Clark Unit-Hydrograph Parameters for Small Rural Watersheds in Illinois. US Dept of the Interior and US Geological Survey, Branch of Information Services, Urbana, IL, USA.
Utah Department of Transportation (UDOT) (2018). Drainage Manual of Instruction. https://drive.google.com/file/d/1sxmhKziSdENiN03kQUhUlu8xyAHMdJol/view?usp=sharing. (Accessed April 9, 2024).
Viparelli, C. (1961). Ricostruzione dell'idrogramma di piena. Stab. Tip. G. Genovese.
Viparelli, C. (1963). Ricostruzione dell'idrogramma di piena. L'Energia Elettrica, 6, 421–428 (in Italian).
Wang, X., Liu, T., and Yang, W. (2012). Development of a robust runoff-prediction model by fusing the rational equation and a modified SCS-CN method. Hydrological Sciences Journal, 57(6), 1118-1140.
Webb, R. H., and Betancourt, J. L. (1992). Climatic variability and flood frequency of the Santa Cruz river, Pima County, Arizona (No. 2379). US Geological Surve,.
Wheater, H., Sorooshian, S., and Sharma, K. D. (Eds.). (2007). Hydrological modelling in arid and semi-arid areas. Cambridge University Press.
Whitford, W.G. (2002). Ecology of Desert Systems. Academic Press, San Diego, CA. 343 p.
Williams, G. B. (1922). Flood discharges and the dimensions of spillways in India. Engineering (London), 134(9), 321-322.
Wolman, M. G., and Gerson, R. (1978). Relative scales of time and effectiveness of climate in watershed geomorphology. Earth surface processes, 3(2), 189-208.
Wong, T. S. (2005). Assessment of time of concentration formulas for overland flow. Journal of Irrigation and Drainage Engineering, 131(4), 383-387.
Yang, S., Yang, D., Chen, J., Santisirisomboon, J., Lu, W., and Zhao, B. (2020). A physical process and machine learning combined hydrological model for daily streamflow simulations of large watersheds with limited observation data. Journal of Hydrology, 590, 125206.
Zahraei, A., Baghbani, R., and Linhoss, A. (2021). Applying a graphical method in evaluation of empirical methods for estimating time of concentration in an Arid Region. Water, 13(19), 2624.

Karst Regions

Alabama Department of Transportation (ALDOT) (2022). Hydraulic Manual. https://www.dot.state.al.us/publications/Design/pdf/HydraulicManual.pdf (Accessed April 9, 2024).
Aley, T. J. (1977). A model for relating land use and groundwater quality in southern Missouri. Hydrologic problems in Karst regions, 323-332.
Aley, T., (1997), Groundwater tracing in the epikarst, in Beck, B.F., and Stephenson, J.B., eds., The engineering geology and hydrogeology of karst terranes: Rotterdam, Netherlands, A.A. Balkema, p. 207–211.

Allen, R. G. (1998). Crop evapotranspiration. FAO irrigation and drainage paper, 56, 60-64.
Andreo, B., Vías, J., Durán, J. J., Jiménez, P., López-Geta, J. A., and Carrasco, F. (2008). Methodology for groundwater recharge assessment in carbonate aquifers: application to pilot sites in southern Spain. Hydrogeology Journal, 16, 911-925.
ASTM Subcommittee D–18–21, (2002), Standard guide for design of ground-water monitoring systems in karst and fractured-rock aquifers: West Conshohocken, Pa., American Society of Testing and Materials, Annual Book of ASTM Standards, v. 04.08, ASTM D5717–95, p. 1421–1438.
ASTM Subcommittee D–18-27 (2023), Standard Practice for Preliminary Karst Terrain Assessment for Site Development., American Society of Testing and Materials, Annual Book of ASTM Standards, v. 04.09, ASTM D8512-23.
Baedke, S. J., and Krothe, N. C. (2001). Derivation of effective hydraulic parameters of a karst aquifer from discharge hydrograph analysis. Water resources research, 37(1), 13-19.
Beck, H. E., Zimmermann, N. E., McVicar, T. R., Vergopolan, N., Berg, A., and Wood, E. F. (2018). Present and future Köppen-Geiger climate classification maps at 1-km resolution. Scientific data, 5(1), 1-12.
Blasco, O., San Román, J., and García Vera, M. A. (2004). Modelado numérico de flujo de la Unidad Hidrogeológica de Gallocanta (Cuenca del Ebro). In VIII Simposio de Hidrogeología. Zaragoza. Ed. Asociación Española de Hidrogeólogos (AEH) (pp. 513-523).
Bonacci, O. (1987). Karst hydrology. Springer Series in Physical Environment.
Brahana, J. V., and Hollyday, E. F. (1988). DRY STREAM REACHES IN CARBONATE TERRANES: SURFACE INDICATORS OF GROUND-WATER RESERVOIRS 1. JAWRA Journal of the American Water Resources Association, 24(3), 577-580.
Cao, Y., Zhang, J., Yang, M., Lei, X., Guo, B., Yang, L., ... and Qu, J. (2018). Application of SWAT model with CMADS data to estimate hydrological elements and parameter uncertainty based on SUFI-2 algorithm in the Lijiang River Basin, China. Water, 10(6), 742.
Carroll County (2011). Water Resource Management Manual Carroll County, Maryland. Department of Land and Resource Management Bureau of Resource Management. https://www.carrollcountymd.gov/media/16196/water-resource-manual-revised-april-2022.pdf (Accessed April 9, 2024).
Center for Ecology & Hydrology (CEH) (2008). Flood Estimation Handbook, Volume 4: Restatement and Application of the Flood Studies Report Rainfall-Runoff Method. Natural Environment Research Council (NERC), Wallingford, Oxfordshire, UK.
Chesapeake Stormwater Network (2009). Stormwater Design Guidelines for Karst Terrain in the Chesapeake Bay Watershed. Version 2. CSN Technical Bulletin No. 1. https://www.jeffersoncountyfoundation.org/wp-content/uploads/2020/06/CSN-TECHNICAL-BULLETIN-No.-1-STORMWATER-DESIGN-GUIDELINES-FOR-KARST-TERRAIN-IN-THE-CHESAPEAKE-BAY-WATERSHED-VERSION-2.0.pdf (Accessed April 9, 2024).
Chow, V. T. (Ed.). (1964). Handbook of applied hydrology: a compendium of water-resources technology (Vol. 1). McGraw-Hill Companies.
Currens, J. C., and Graham, C. D. R. (1993). Flooding of the Sinking Creek karst area in Jessamine and Woodford counties, Kentucky.
Dai, J., Rad, S., Xu, J., Wan, Z., Li, Z., Pan, L., and Shahab, A. (2022). Influence of karst reservoir capacity on flood in Lijiang Basin based on modified HEC-HMS through soil moisture accounting loss. Atmosphere, 13(10), 1544.

De Vries, J. J., and Simmers, I. (2002). Groundwater recharge: an overview of processes and challenges. Hydrogeology Journal, 10, 5-17.
De Waele, J., Martina, M. L., Sanna, L., Cabras, S., and Cossu, Q. A. (2010). Flash flood hydrology in karstic terrain: Flumineddu Canyon, central-east Sardinia. Geomorphology, 120(3-4), 162-173.
Dirks, H., Al Ajmi, H., Kienast, P., and Rausch, R. (2018). Hydrogeology of the umm er radhuma aquifer (Arabian Peninsula). Grundwasser, 23(1), 5-15.
Eriksson, E., and Khunakasem, V. (1969). Chloride concentration in groundwater, recharge rate and rate of deposition of chloride in the Israel Coastal Plain. Journal of Hydrology, 7(2), 178-197.
Federal Highway Administration (FHWA) (2023). Highway Hydrology: Evolving Methods, Tools, and Data. Hydraulic Engineering Circular No. 19. https://www.fhwa.dot.gov/engineering/hydraulics/pubs/hif23050.pdf (Accessed April 9, 2024).
Flippo, H.N., Jr. (1977). Floods in Pennsylvania: A Manual for Estimation of Their Magnitude and Frequency, Bulletin 13, Pennsylvania Department of Environmental Resources.
Florida Department of Transportation (FDOT) (2019). Drainage Design Guide. https://fdotwww.blob.core.windows.net/sitefinity/docs/default-source/roadway/drainage/files/drainagedesignguide/drainagedesignguide2024.pdf?sfvrsn=a5320a94_1 (Accessed April 9, 2024).
Ford, D. C., and Williams, P. W. (1989). Karst geomorphology and hydrology (Vol. 601). London: Unwin Hyman.
Ford, D., and Williams, P. D. (2007). Karst hydrogeology and geomorphology. John Wiley and Sons.
Ginsberg, M. H., and Palmer, A. N. (2002). Delineation of sourcewater protection areas in karst aquifers of the Ridge and Valley and Appalachian Plateaus physiographic provinces rules of thumb for estimating the capture zones of springs and wells. DIANE Publishing.
Goldscheider, N., Chen, Z., Auler, A. S., Bakalowicz, M., Broda, S., Drew, D., ... and Veni, G. (2020). Global distribution of carbonate rocks and karst water resources. Hydrogeology Journal, 28, 1661-1677.
Greene, E. A., Shapiro, A. M., and Carter, J. M. (1999). Hydrogeologic characterization of the Minnelusa and Madison aquifers near Spearfish, South Dakota (Vol. 98, No. 4156). US Department of the Interior, US Geological Survey.
Grindley, J. (1967). The estimation of soil moisture deficits. Water for Peace: Water Supply Technology, 3, 241.
Guardiola-Albert, C., and Jackson, C. R. (2011). Potential impacts of climate change on groundwater supplies to the Doñana wetland, Spain. Wetlands, 31(5), 907-920.
Guardiola-Albert, C., Martos-Rosillo, S., Pardo-Igúzquiza, E., Duran Valsero, J. J., Pedrera, A., Jiménez-Gavilán, P., and Linan Baena, C. (2015). Comparison of recharge estimation methods during a wet period in a karst aquifer. Groundwater, 53(6), 885-895.
Gunn, J. (1983). Point-recharge of limestone aquifers—a model from New Zealand karst. Journal of Hydrology, 61(1-3), 19-29.
Gunn, J. (1986). A conceptual model for conduit flow dominated karst aquifers. IAHS-AISH publication, (161), 587-596.
Hawkins, S. and D. Weichel (2015). Estimating Catchment Zones for Streams Located in Karst Systems in South-central Pennsylvania, Shippensburg University, PA

Hess, J.W., and White, W.B., 1989, Water budget and physical hydrology, in White, W.B., and White, E.L., eds., Karst hydrology concepts from the Mammoth Cave area: New York, Van Nostrand Reinhold, p. 105–126.

Highways England (2020). Design Manual for Roads and Bridges, CD 522 Drainage of runoff from natural catchments ((formerly HA 106/04).

Horton, R. E. (1933). The role of infiltration in the hydrologic cycle. Eos, Transactions American Geophysical Union, 14(1), 446-460.

Hughes, A. G., Mansour, M. M., and Robins, N. S. (2008). Evaluation of distributed recharge in an upland semi-arid karst system: the West Bank Mountain Aquifer, Middle East. Hydrogeology Journal, 16, 845-854.

Iacobellis, V., Castorani, A., Di Santo, A. R., and Gioia, A. (2015). Rationale for flood prediction in karst endorheic areas. Journal of Arid Environments, 112, 98-108.

Indiana Department of Transportation (INDOT) (2014). Design Manual, Chapter 202-Hydrology. https://www.in.gov/dot/div/contracts/design/Part%202/Chapter%20202%20-%20Hydrology.pdf (Accessed April 9, 2024).

Ireland National Roads Authority (NRA). (2015). Transport Infrastructure Ireland (TII) Road Drainage and Water Environment Standard, DN-DNG-03065, Volume 4, section 2, Part 1, NRA HD 45/15.

Jackson, C. R., Meister, R., and Prudhomme, C. (2011). Modelling the effects of climate change and its uncertainty on UK Chalk groundwater resources from an ensemble of global climate model projections. Journal of Hydrology, 399(1-2), 12-28.

Jiang, G., Guo, F., Wei, M. (2020). Hydrogeological characteristics of foot caves in a karst peak-forest plain in South China. Hydrogeol. J., 28, 535–548.

Jones, W. K., Culver, D. C., and Herman, J. S. (Eds.). (2004). Epikarst: Proceedings of the Sympoisum Held October 1 Through 4, 2003 Shepherdstown, West Virginia (Vol. 9). Karst Waters Institute.

Kastridis, A., and Stathis, D. (2020). Evaluation of hydrological and hydraulic models applied in typical Mediterranean Ungauged watersheds using post-flash-flood measurements. Hydrology, 7(1), 12.

Kentucky Transportation Cabinet (KYTC) (2010). Drainage Manual, DR 400 - Hydrology. https://transportation.ky.gov/Highway-Design/Drainage%20Manual/DR%20400%20Hydrology.pdf (Accessed April 9, 2024).

Klimchouk, A. B. (2004). Towards defining, delimiting and classifying epikarst: Its origin, processes and variants of geomorphic evolution. Epikarst. Special Publication, 9, 23-35.

Lange, J., Greenbaum, N., Husary, S., Ghanem, M., Leibundgut, C., and Schick, A. P. (2003). Runoff generation from successive simulated rainfalls on a rocky, semi-arid, Mediterranean hillslope. Hydrological Processes, 17(2), 279-296.

Laughland, J. (2007). Adjusting Hydrology Models and Using Karstic Features. Stormwater Management Design in Karst Terrain. Facility Design Group. County Engineer. Jefferson County, WV.

Laughland, J. C. (1996). Adjusting Hydrology Models for Karst Geology. Public Works. https://www.thefreelibrary.com/Adjusting+hydrology+models+for+karst+geology.-a018660215 (Accessed April 9, 2024).

Lloyd, J. W., Williams, G. M., Foster, S. S. D., Ashley, R. P., and Lawrence, A. R. (1991). Urban and industrial groundwater pollution. In Applied groundwater hydrology. A British perspective (pp. 134-148).

Mansour, M. M., and Hughes, A. G. (2004). User's manual for the distributed recharge model ZOODRM.

Marín, A. I. (2009). Los sistemas de información geográfica aplicados a la evaluación de recursos hídricos ya la vulnerabilidad a la contaminación de acuíferos carbonatados. Caso de la Alta Cadena (Provincia de Málaga). Bachelor Thesis, University of Malaga.

Martos-Rosillo, S., Pérez-Fernández, F., and Durán, J. J. (2008). Estimation of the average annual recharge in the carbonate aquifers of Sierra de Estepa (Seville) using the APLIS method. Geotemas, 10, 1567-5172.

Meinzer, O. E. (1927). Large springs in the United States (No. 557). US Government Printing Office.

Milanović, P. (2014). Hydraulic properties of karst groundwater and its impacts on large structures. H2Karst research in limestone hydrogeology, 19-48.

Milanović, P. T. (2000). Geological Engineering in Karst: dams, reservoirs, grouting, groundwater protection, water tapping, tunneling.

Milanovic´, P.T., (1981a). Karst hydrogeology: Littleton, Colo., Water Resources Publication, 434 p.

Milanovic´, P.T., (1981b). Water regime in deep karst—Case study of the Ombla Spring drainage area, in Yevjevich, V., ed., Karst hydrology and water resources, Proceedings of the U.S.-Yugoslavian Symposium, Dubrovnik, 1975: Littleton, Colo., Water Resources Publication, p. 165–191.

Minnesota Department of Transportation (MnDOT) (2000). Drainage Manual, Chapter 3 - Hydrology. https://edocs-public.dot.state.mn.us/edocs_public/DMResultSet/download?docId=26998192 (Accessed April 9, 2024).

Minnesota Pollution Control Agency (2008). The Minnesota Stormwater Manual. Version 2. https://stormwater.pca.state.mn.us/images/b/b8/Minnesota_Stormwater_Manual.pdf (Accessed April 9, 2024).

Missouri Department of Transportation (MoDOT, 2019). Engineering Policy Guide. Category:749 Hydrologic Analysis. https://epg.modot.org/index.php/Category:749_Hydrologic_Analysis (Accessed April 9, 2024).

Mo, C., Wang, Y., Ruan, Y., Qin, J., Zhang, M., Sun, G., and Jin, J. (2021). The effect of karst system occurrence on flood peaks in small watersheds, southwest China. Hydrology Research, 52(1), 305-322.

Naughton, O., McCormack, T., Gill, L., and Johnston, P. (2018). Groundwater flood hazards and mechanisms in lowland karst terrains. Geological Society, London, Special Publications, 466(1), 397-410.

New Mexico Department of Transportation (NMDOT) (2018). Drainage Design Manual. https://www.dot.nm.gov/infrastructure/program-management/drainage-design/ (Accessed April 9, 2024).

Office of Scientific and Technical Information. Technical Report.

Ogden, A. E. (1994). Investigation of sinkhole flooding problems in the Chilhowee Park area, Knoxville, Tennessee. Prepared for City of Knoxville Department of Engineering by Ground Water Consulting Services, Cookeville, 18.

Padilla, A., Pulido-Bosch, A., and Mangin, A. (1994). Relative importance of baseflow and quickflow from hydrographs of karst spring. Groundwater, 32(2), 267-277.

Paillet, F. L. (2001). Borehole geophysical applications in karst hydrogeology. US Geological Survey Karst Interest Group Proceedings.–Water Res. Invest. Rep, 1(4011), 116-123.
Palmer, A. N. (1991). Origin and morphology of limestone caves. Geological Society of America Bulletin, 103(1), 1-21.
Palmer, A. N. (1999). Patterns of dissolution porosity in carbonate rocks. Karst modeling. Karst Water Institute, Sp Publ, 5, 71-78.
Pardo-Igúzquiza, E., Durán-Valsero, J. J., Dowd, P. A., Guardiola-Albert, C., Liñan-Baena, C., and Robledo-Ardila, P. A. (2012). Estimation of spatio-temporal recharge of aquifers in mountainous karst terrains: application to Sierra de las Nieves (Spain). Journal of hydrology, 470, 124-137.
Parise, M. (2015). Karst Geo-hazard: Causal Factors and Management Issues. Acta Carsologica, 44(3).
Parise, M., and Gunn, J. (2007). Natural and anthropogenic hazards in karst areas: an introduction. Geological Society, London, Special Publications, 279(1), 1-3.
Parise, M., Gabrovsek, F., Kaufmann, G., and Ravbar, N. (2018). Recent advances in karst research: from theory to fieldwork and applications. Geological Society, London, Special Publications, 466(1), 1-24.
Parvez, M. B., and Inayathulla, M. (2019). Estimation of surface runoff by soil conservation service curve number model for upper Cauvery Karnataka. Int. J. Sci. Res. in Multidisciplinary Studies Vol, 5, 11.
Penman, H. L. (1948). Natural evaporation from open water, bare soil and grass. Proceedings of the Royal Society of London. Series A. Mathematical and Physical Sciences, 193(1032), 120-145.
Pennsylvania Department of Transportation (PennDOT) (2010). Drainage Manual. Chapter 7 - Hydrology. https://www.dot.state.pa.us/public/bureaus/design/PUB584/PDMChapter07.pdf (Accessed April 9, 2024).
Quinlan, J. F., and Ewers, R. O. (1989). Subsurface drainage in the Mammoth Cave area. In Karst hydrology: concepts from the Mammoth Cave area (pp. 65-103). Boston, MA: Springer US.
Rad, S., Junfeng, D., Jingxuan, X., Zitao, L., Linyan, P., Wan, Z., and Lin, L. (2022). Lijiang flood characteristics and implication of karst storage through Muskingum flood routing via HEC-HMS, S. China. Hydrology Research, 53(12), 1480-1493.
Ray, J. A. (1999). A model of karst drainage basin evolution, Interior Low Plateaus, USA: in. Karst modeling: Karst Waters Institute Special Publication, 5, 58.
Ray, J. A. (2001). Spatial interpretation of karst drainage basins. In Geotechnical and environmental applications of karst geology and hydrology (pp. 235-244).
Rovey, C. W., and Cherkauer, D. S. (1994). Relation between hydraulic conductivity and texture in a carbonate aquifer: Regional continuity. Groundwater, 32(2), 227-238.
Samper, J. (1997). Evaluación de la recarga a partir de modelos numéricos de flujo de acuíferos. In La evaluación de la recarga a los acuíferos en la Planificación Hidrológica (pp. 153-180). Instituto Tecnológico Geominero de España.
Samper, J., Huguer, L., Ares, J., and Garcia, M. A. (1999). User manual of Visual Balan V. 1.0 Interactive code for water balances and refueling estimation; Manual del usuario del programa Visual Balan V. 1.0. Codigo interactivo para la realizacion de balances hidrologicos y la estimacion de la recarga.
Sanford, W. (2002). Recharge and groundwater models: an overview. Hydrogeology journal, 10, 110-120.

Sauter, M. (1991, December). Assessment of hydraulic conductivity in a karst aquifer at local and regional scale. In Proceedings of the 3rd conference on hydrogeology, ecology, monitoring, and management of ground water in karst terranes, 4th–6th December (pp. 39-56).

Sauter, M. (1992). Assessment of hydraulic conductivity in a karst aquifer at local and regional scale. In Proceedings of the 3rd conference on hydrogeology, ecology, monitoring, and management of ground water in karst terranes, 4th–6th December (pp. 39-56).

Savvidou, E., Efstratiadis, A., Koussis, A. D., Koukouvinos, A., and Skarlatos, D. (2018). The curve number concept as a driver for delineating hydrological response units. Water, 10(2), 194.

Scanlon, B. R., Healy, R. W., and Cook, P. G. (2002). Choosing appropriate techniques for quantifying groundwater recharge. Hydrogeology journal, 10, 18-39.

Schulz, S., de Rooij, G. H., Michelsen, N., Rausch, R., Siebert, C., Schüth, C., and Merz, R. (2016). Estimating groundwater recharge for an arid karst system using a combined approach of time-lapse camera monitoring and water balance modelling. Hydrological Processes, 30(5), 771-782.

SCS. (1972). National Engineering Handbook. Supplement A, Section 4, Chapter 10.

Şen, Z. (2020). General modeling of karst spring hydrographs and development of a dimensionless karstic hydrograph concept. Hydrogeology journal, 28(2), 549-559.

Shevenell, L. (1996). Analysis of well hydrographs in a karst aquifer: estimates of specific yields and continuum transmissivities. Journal of hydrology, 174(3-4), 331-355.

Smart, C. C. (1988). A deductive model of karst evolution based on hydrological probability. Earth surface processes and landforms, 13(3), 271-288.

St. Johns River Water Management District (2018). Environmental Resource Permit Application's Handbook, Volume II: For Use Within the Geographic Limits of the St. Johns River Management District. https://www.flrules.org/gateway/readRefFile.asp?refId=9405&filename=010%204b3--AH%20II%20SJWMD.pdf (Accessed April 9, 2024).

Stephenson, J. B., Zhou, W. F., Beck, B. F., and Green, T. S. (2020). Highway stormwater runoff in karst areas-preliminary results of baseline monitoring and design of a treatment system for a sinkhole in Knoxville, Tennessee. In The Engineering Geology and Hydrology of Karst Terrains (pp. 173-181). CRC Press.

Stevanović, Z., and Milanović, P. (2015). Engineering challenges in karst. Acta Carsologica, 44(3).

Streltsova, T. D. (1987). *Well Testing in Heterogeneous Formations*. Exxon Monograph, John Wiley & Sons..

Taylor, C. J., and Greene, E. A. (2008). Hydrogeologic characterization and methods used in the investigation of karst hydrology. Field techniques for estimating water fluxes between surface water and ground water, 71-114.

Taylor, C. J., Nelson, H. L., Hileman, G., and Kaiser, W. P. (2005). Hydrogeologic-framework mapping of shallow, conduit-dominated karst—components of a regional GIS-based approach. US Geological Survey Karst Interest Group Proceedings. Rapid City, South Dakota, 103-113.

Tennessee Department of Environment and Conservation (2014) Tennessee Permanent Stormwater Management and Design Guidance Manual. Appendix B: Stormwater Design Guidelines for Karst Terrain. Division of Water Resources.

https://tnpermanentstormwater.org/manual/27%20Appendix%20B%20Stormwater%20Design%20Guidelines%20for%20Karst%20Terrain.pdf (Accessed April 9, 2024).
Tennessee Department of Transportation (TDOT) (2021). Drainage Manual, Chapter 4 - Hydrology. https://www.tn.gov/content/dam/tn/tdot/roadway-design/documents/drainage_manual/DM-Chapter-04.pdf (Accessed April 9, 2024).
Texas Department of Transportation (TxDOT) (2019). Hydraulic Design Manual. http://onlinemanuals.txdot.gov/TxDOTOnlineManuals/TxDOTManuals/hyd/hyd.pdf (Accessed April 9, 2024).
Texas Speleological Survey (2014). https://www.texasspeleologicalsurvey.org/karst_caving/karst_regions.php (Accessed April 18, 2024).
Tolmachev, V. (2005). Issues of environmental impacts of karst in standards on construction in Russia.- In: Stevanović Z and Milanović P (eds) Water resources and environmental problems in karst, Proceedings of international conference KARST 2005, University of Belgrade, Institute of Hydrogeology, Belgrade, pp. 713−718
Toth, J. (1963). A theoretical analysis of groundwater flow in small drainage basins. Journal of geophysical research, 68(16), 4795-4812.
Town of Cutler Bay (2018). Stormwater Manual. https://www.cutlerbay-fl.gov/sites/default/files/fileattachments/public_works/page/2871/tcb_stormwater_manual_complete_final_2019.pdf (Accessed April 9, 2024).
Transport Infrastructure Ireland (TII) (2013). Drainage Design For National Road Schemes - Sustainable, Drainage Options. Transport Infrastructure Ireland, Dublin. https://www.tiipublications.ie/ (Accessed downloads/SRM/1-Drainage-design-for-national-road-schemes-May-2014.pdf (Accessed April, 21)
Trček, B., and Krothe, N. C. (2002). The importance of three and four components storm hydrograph separation techniques for karst aquifers. In Proceedings of the Symposium "Evolution of Karst: Form Prekarst to Cessation"(Postojna, 2002).-Založba ZRC (pp. 395-401).
U.S. Geological Survey, (2005). User's Manual for the National Water Information System of the U.S. Geological Survey, Ground-Water Site-Inventory System: U.S. Geological Survey Open-File Report, ver. 4.5 (http://wwwnwis.er.usgs.gov/nwisdocs4_5/gw/gw_complete.pdf}
USACE (2002). Hydrologic Modeling System HEC-HMS Applications Guide. Hydrologic Engineering Center, Davis, CA.
Utah Department of Transportation (UDOT) (2018). Drainage Manual of Instruction. https://drive.google.com/file/d/1sxmhKziSdENiN03kQUhUlu8xyAHMdJol/view?usp=sharing. (Accessed April 9, 2024).
Vereecken, H., Schnepf, A., Hopmans, J. W., Javaux, M., Or, D., Roose, T., ... and Young, I. M. (2016). Modeling soil processes: Review, key challenges, and new perspectives. Vadose zone journal, 15(5), vzj2015-09.
Virginia Department of Conservation and Recreation (VA DCR) (1999). Virginia Stormwater Management Handbook. Technical Bulletin No. 2. Hydrological Modeling and Design in Karst. Division of Soil and Water Conservation. Richmond, VA.
Virginia Department of Environmental Quality (2013). Virginia Stormwater Management Handbook, Chapter 6, Appendix 6-B: Stormwater Design Guidelines for Karst Terrain in Virginia. https://swbmpvwrrc.wp.prod.es.cloud.vt.edu/wp-content/uploads/2018/07/24_Chap-6_App-6-B_Stormwater-Design-Guides-for-Karst-Terrain.pdf (Accessed April 9, 2024).

Virginia Department of Environmental Quality (VDEQ) (1999), Virginia Stormwater Management Handbook, Volumes I & II (First Edition) Richmond, VA: Virginia Department of Environmental Quality.

Virginia Department of Transportation (VDOT) (2023). Drainage Manual. https://swbmpvwrrc.wp.prod.es.cloud.vt.edu/wp-content/uploads/2018/07/24_Chap-6_App-6-B_Stormwater-Design-Guides-for-Karst-Terrain.pdf (Accessed Dec 19, 2024).

Wahyullah, W., Hendrayanto, H., and Suharnoto, Y. (2023). Simulation of the impact of land use change on surface run-off in Karst Leang Lonrong Sub-Watershed. Jurnal Pengelolaan Sumberdaya Alam dan Lingkungan (Journal of Natural Resources and Environmental Management), 13(2), 313-326.

Wang, D. (2018). A new probability density function for spatial distribution of soil water storage capacity leads to the SCS curve number method. Hydrology and Earth System Sciences, 22(12), 6567-6578.

Weary, D. J., and Doctor, D. H. (2014). Karst in the United States: a digital map compilation and database (No. 2014-1156). US Geological Survey.

West Virginia Department of Environmental Protection (2012). West Virginia Stormwater Management and Design Guidance Manual. Appendix C: Stormwater Management Design in Karst Areas. https://dep.wv.gov/WWE/Programs/stormwater/MS4/Documents/Appendix_C_Stormwater_Mgmt_Design_Karst_WV-SW-11-2012.pdf (Accessed April 9, 2024).

West Virginia Department of Transportation (WVDOT) (2007). Drainage Manual. https://transportation.wv.gov/highways/engineering/Pages/Manuals.aspx (Accessed April 9, 2024).

White, W. B. (1993) Analysis of Karst Aquifers. In: Alley, W.M., Ed., Regional Ground-Water Quality, Van Nostrand Reinhold, New York, 471-489.

White, W. B. (1988). Geomorphology and hydrology of karst terrains.

White, W. B. (1999). Conceptual models for karstic aquifers. Karst modeling, 5, 11-16.

White, W. B. (2002). Karst hydrology: recent developments and open questions. Engineering geology, 65(2-3), 85-105.

White, W. B., and Schmidt, V. A. (1966). Hydrology of a karst area in east-central West Virginia. Water Resources Research, 2(3), 549-560.

Williams, P. W. (1983). The role of the subcutaneous zone in karst hydrology. Journal of hydrology, 61(1-3), 45-67.

Worthington, S. H., Ford, D. C., and Davies, G. J. (2000). Matrix, fracture and channel components of storage and flow in a Paleozoic limestone aquifer. In Groundwater flow and contaminant transport in carbonate aquifers (pp. 113-128).

Worthington, S. R. (1999). A comprehensive strategy for understanding flow in carbonate aquifers. Karst modeling, 35, 30-37.

Worthington, S. R. H. (1991). Karst Hydrogeology of the Canadian Rocky mountains. Hamilton, 227 p (Doctoral dissertation, Ph. D. thesis, Department of Geography/Mc Master University).

Xiang, S.J., Zhang, M. L., Gong, W.X., (1997). Submergence of the Banwen underground river by the Yantan Reservoir and subsequent flooding disasters. In: Beck BF, Stephenson JB (eds) The engineering geology and hydrogeology of Karst Terranes. Rotterdam, Balkema, pp 273–278

Zhang, H. L., Wang, Y. J., Wang, Y. Q., Li, D. X., and Wang, X. K. (2013). The effect of watershed scale on HEC-HMS calibrated parameters: a case study in the Clear Creek watershed in Iowa, US. Hydrology and Earth System Sciences, 17(7), 2735-2745.

Zhou, W. (2000). Studies of confluent flow in mature karst aquifers using analog models and numerical mixing cell models. In Groundwater flow and contaminant transport in carbonate aquifers (pp. 157-168).
Zhou, W. (2007). Drainage and flooding in karst terranes. Environmental Geology, 51(6), 963-973.

Appendix B Supplemental Materials

Table ABSM.1 SHPs Playa Lakes area in different counties of Texas

No.	County Name	Area (acres)	No.	County Name	Area (acres)
1	Andrews	1694	25	Hemphill	97
2	Armstrong	15035	26	Hockley	9862
3	Bailey	5252	27	Howard	3247
4	Borden	2817	28	Hutchinson	3078
5	Briscoe	20286	29	Lamb	13293
6	Carson	16314	30	Lipscomb	245
7	Castro	19381	31	Lubbock	15236
8	Cochran	2395	32	Lynn	10934
9	Crosby	19408	33	Martin	5893
10	Dallam	4272	34	Midland	3918
11	Dawson	10585	35	Moore	4849
12	Deaf Smith	11296	36	Motley	738
13	Deaf Smith	6	37	Ochiltree	16130
14	Dickens	3983	38	Oldham	4281
15	Donley	1579	39	Parmer	9793
16	Ector	1999	40	Potter	3393
17	Floyd	35314	41	Randall	13879
18	Gaines	333	42	Reagan	49
19	Garza	4158	43	Roberts	1421
20	Glasscock	7412	44	Sherman	4226
21	Gray	13435	45	Swisher	25814.
22	Hale	26773	46	Terry	2784
23	Hansford	7302	47	Wheeler	0.5
24	Hartley	4014	48	Yoakum	210

Table ABSM.2 Infiltration estimates beneath playas of the southern High Plains (from Gurdak and Roe, 2010)

Study	No. of Playas	Infiltration Rate	Approach	Setting	Notes
Lehman and Clark (1975)	1	1 mm/h (day 0) 0.05 mm/h (day 1) 0.02 mm/h (day 10)	Constant head permeameter	Playa floor	Randall clay; feedyard runoff
		40 mm/h (day 0) 1 mm/h (day 8) 0.05 mm/h (day45)	Constant head permeameter	Interplaya	Permeable buried soil; feedyard runoff
Evans (1990)	3	10 mm/min (Min) 46 mm/min (Ave) 660 mm/min (Max)	Double-ring infiltrometer	Playa floor	Stage I infiltration
		22 mm/min (Min) 79 mm/min (Ave) 1,041 mm/min (Max)	Double-ring infiltrometer	Playa floor	Stage I infiltration
		12 mm/min (Min) 163 mm/min (Ave) 2,490 mm/min (Max)	Double-ring infiltrometer	Playa floor	Stage I infiltration
		0 mm/min (Min) 33 mm/min (Ave) 38 mm/min (Max)	Double-ring infiltrometer	Playa floor	Stage III infiltration
		0.0 mm/min (Min) 12.0 mm/min (Ave) 63.5 mm/min (Max)	Double-ring infiltrometer	Playa floor	Stage III infiltration
		0.0 mm/min (Min) 15.0 mm/min (Ave) 38.0 mm/min (Max)	Double-ring infiltrometer	Playa floor	Stage III infiltration
Zartman et al. (1994, 1996)	1	2,946 mm/h (min. 1) 610 mm/h (min. 5)	127–mm diameter cylinder infiltrometers	Playa floor (center)	(10 s fill time)
		1,524 mm/h (min. 1) 508 mm/h (min. 5)	127–mm diameter cylinder infiltrometers	Playa floor (outerbasin)	(10 s fill time)
		2,235 mm/h (min. 1) 559 mm/h (min. 5)	127–mm diameter cylinder infiltrometers	annulus	(10 s fill time)
		269 mm/h (min. 1) 51.0 mm/h (min. 130)	2,032–mm diameter basin infiltrometer	Playa floor (center)	(~1 hr fill time)
		140 mm/h (min. 1) 25.0 mm/h (min. 130)	2,032–mm diameter basin infiltrometer	Playa floor (outerbasin)	(~1 hr fill time)
		81.0 mm/h (min. 1) 25.0 mm/h (min. 130)	2,032–mm diameter basin infiltrometer	Annulus	(~1 hr fill time)
		53.0 mm/h (min. 1) 9.40 mm/h (day1)	8,890–mm diameter basin infiltrometer	Playa floor (center)	(~1 hr fill time)

Table ABSM.2 *Continued.*

Study	No. of Playas	Infiltration Rate	Approach	Setting	Notes
Wood et al. (1997)	2	1,140 mm/yr (Min) 1,930 mm/yr (Ave) 2,720 mm/yr (Max)	Water budget	Playa floor	-
		750 mm/yr (Min) 1,185 mm/yr (Ave) 1,620 mm/yr (Max)	Water budget	Playa floor	-
Parker et al. (2001)	2	112 mm/h (min. 1) 0.10 mm/h (min. 5) 0.10 mm/h (min. 60)	Flexible-wall permeameter	Playa floor #1* (Min)	15 Samples
		276 mm/h (min. 1) 7.9 mm/h (min. 5) 1.30 mm/h (min. 60)	Flexible-wall permeameter	Playa floor #1 (Ave)	15 Samples
		506 mm/h (min. 1) 25 mm/h (min. 5) 3.30 mm/h (min. 60)	Flexible-wall permeameter	Playa floor #1 (maximum)	15 Samples
		193 mm/h (min. 1) 0.1 mm/h (min. 5) 0.1 mm/h (min. 60)	Flexible-wall permeameter	Playa floor #2* (Min)	11 Samples
		346 mm/h (min. 1) 30.5 mm/h (min. 5) 2.30 mm/h (min. 60)	Flexible-wall permeameter	Playa floor #2 (Ave)	11 Samples
		502 mm/h (min. 1) 114 mm/h (min. 5) 6.1 mm/h (min. 60)	Flexible-wall permeameter	Playa floor #2 (Max)	11 Samples

*shows two different playas that were studied by Parker et al. (2001)

Table ABSM.3 Recharge Estimates for the Southern High Plains (from Gurdak and Roe, 2009)

Study	Recharge (mm/yr)	Approach	Setting
Water budget approaches			
Johnson (1901)	76–102	Observation	Regional
Gould (1906)	152	Observation	Regional
Theis (1937)	3.2–17.0	Darcy′slaw	Regional
White et al.(1946)	1.5	Water budget	Regional
Barnes et al. (1949)	2.5	Water budget	Interplaya: nonspecific
Cronin (1961)	13	Darcy′s law	Regional
Havens (1966)	20.6	Water budget	Regional
Rayner et al. (1973)	4.4	Water budget	Regional
Lansford et al. (1974)	0.40	GW modeling	Regional
Brutsaert et al. (1975)	10	Water budget	Regional
Morton (1980)	5.1–55.9	GW modeling	Regional
Texas Department of Water Resources (1981)	12.7–25.4	GW modeling	Regional
Bureau of Reclamation (1982)	23	Water budget	Regional
Bureau of Reclamation (1982)	25	Water budget	Playa floor
Wood and Osterkamp (1984a)	2.5	Literature	Regional
Wood and Osterkamp (1984b)	40.0	Literature	Playa annulus
Wood and Osterkamp (1984b)	60.0	Luckey et al.(1986)	Playa annulus
Luckey et al. (1986)	2.5–25.4	GW modeling	Regional
Wood and Osterkamp (1987)	50.0	Luckey et al. (1986)	Regional
Wood and Osterkamp (1987)	40.0	Luckey et al. (1986)	Playa annulus
Nativ and Riggio (1989)	0.25–41	Water budget	Playa floor
Dugan et al. (1994)	13.0–38.0	Water budget	Regional
Mullican et al. (1997)	10.2	GW modeling	Interplaya: nonspecific
Luckey and Becker (1999)	1.6–2.1	GW modeling	Interplaya: nonspecific
Luckey and Becker (1999)	16.0–24.0	GW modeling	Interplaya: rangeland
Dugan and Zelt (2000)	2.5–38.1	Percentage of irrigation	Interplaya: irrigated cropland
Dutton et al. (2000)	3.6–42.7	GW modeling	Regional
Stovall et al. (2000)	15.2–139.7	GW modeling	Regional

Table ABSM.3 *Continued*

Study	Recharge (mm/yr)	Approach	Setting
Stovall et al. (2000)	25–50	GW modeling	Interplaya: non-irrigated cropland
Unsaturated zone approaches			
Klemt (1981)	4.8	Neutron probe	Regional
Klemt (1981)	2.8–5.1	Neutron probe	Interplaya: non-irrigated cropland
Knowles et al. (1984)	1.5–14.5	Neutron probe	Interplaya: nonspecific
Knowles et al. (1984)	20.0	Neutron probe	Interplaya: rangeland
Stone (1984)	0.2	CMB	Interplaya: irrigated cropland
Stone (1984)	0.2–1.3	CMB	Interplaya: rangeland
Stone (1984)	2.8	CMB	Playa floor
Stone and McGurk (1985)	0.75	CMB	Interplaya: rangeland
Stone and McGurk (1985)	12.2	CMB	Playa floor
Wood and Sanford (1995a)	77(±8)	UZ tritium	Playa annulus
Wood et al. (1997)	77(±8)	UZ tritium	Playa floor
Scanlon and Goldsmith (1997)	0.1–4.0	CMB	Interplaya: nonspecific
Scanlon and Goldsmith (1997)	6.0–10	CMB	Playa floor (neglects runoff to playas)
Scanlon and Goldsmith (1997)	60.0–100	CMB	Playa floor (includes runoff to playas)
Scanlon and Goldsmith (1997)	120	UZ tritium	Playa floor
Wood et al. (1997)	27–31	UZ tritium	Playa floor
McMahon et al. (2006)	17–32	UZ tritium	Interplaya: irrigated cropland
McMahon et al. (2006)	0.2	CMB	Interplaya: rangeland
Scanlon et al. (2007)	4.8–92	CMB	Interplaya: non-irrigated cropland

Table ABSM. 3 *Continued*

Study	Recharge (mm/yr)	Approach	Setting
Groundwater approaches			
Brown and Signor (1973)	0.6–2.0	GW budget	Regional
Nativ and Smith(1987) , Nativ(1988)	13.0–82.0	Tritium	Playa floor
Mullican et al. (1994)	6	GW modeling	Interplaya: nonspecific
Mullican et al. (1994)	99–219	GW modeling	Playa floor
Wood and Sanford (1994)	9	CMB	Playa annulus
Wood and Sanford (1995a)	11(±2)	CMB	Regional
Scanlon and Goldsmith (1997)	200–600	GW chemistry	Playa floor
Wood et al. (1997)	22–44	CMB	Playa floor
Wood et al. (1997)	145–257	CMB	Playa floor
Gurdak et al. (2007a)	198–200	Spectral analysis	Regional

NRSC (SCS) Curve Number Method

The Natural Resources Conservation Service (NRCS) method, formerly known as the Soil Conservation Service (SCS), is used to estimate stormwater runoff, peak discharge and volume, calculate the time of concentration, and (4) develop stormwater hydrographs. This approach is more sophisticated than the rational method. It considers temporal rainfall distribution, the initial rainfall losses due to interception and depression storage, and a decreasing time-averaged infiltration rate during a storm. This method can be used in the design of stormwater control and management facilities such as storm drain systems, outlet structures, culvers, and others. The NRCS method uses the runoff curve number (*CN*) to estimate storm runoff. The stormwater runoff estimation using the NRCS method is discussed in several hydrology textbooks and stormwater management technical manuals. In this method, the stormwater runoff can be calculated using **Equations B.9** and **B.10** (**Section B.4.3.1.1**), **Figure ABSM.1**, or **Table ABSM.4.**

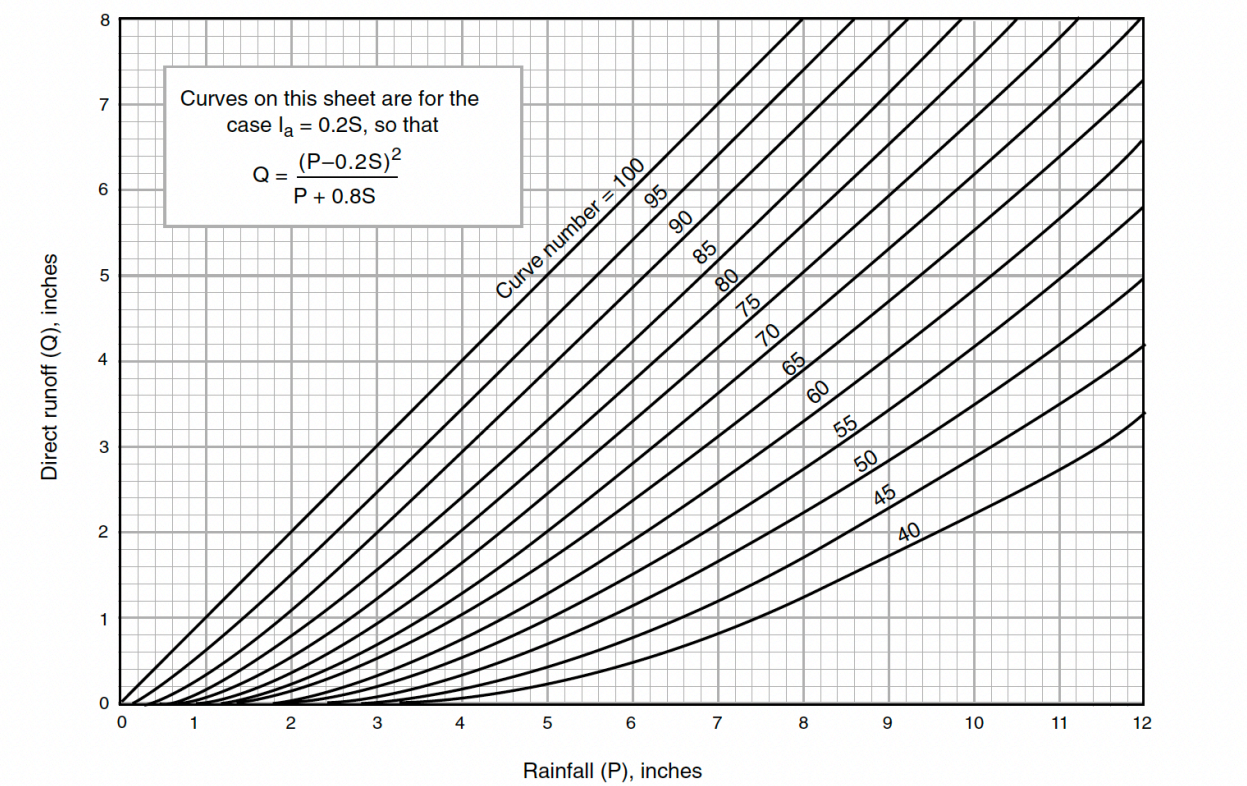

Figure ABSM.1 Graphical Solution of NRSC Runoff Equations A.9 and A.10 (USDA, 1986)

Table ABSM.4 Runoff Depth for Selected *CN*'s and Rainfall Amounts[1] (USDA, 1986)

Rainfall	Runoff depth for curve number of—												
	40	45	50	55	60	65	70	75	80	85	90	95	98
	inches												
1.0	0.00	0.00	0.00	0.00	0.00	0.00	0.00	0.03	0.08	0.17	0.32	0.56	0.79
1.2	.00	.00	.00	.00	.00	.00	.03	.07	.15	.27	.46	.74	.99
1.4	.00	.00	.00	.00	.00	.02	.06	.13	.24	.39	.61	.92	1.18
1.6	.00	.00	.00	.00	.01	.05	.11	.20	.34	.52	.76	1.11	1.38
1.8	.00	.00	.00	.00	.03	.09	.17	.29	.44	.65	.93	1.29	1.58
2.0	.00	.00	.00	.02	.06	.14	.24	.38	.56	.80	1.09	1.48	1.77
2.5	.00	.00	.02	.08	.17	.30	.46	.65	.89	1.18	1.53	1.96	2.27
3.0	.00	.02	.09	.19	.33	.51	.71	.96	1.25	1.59	1.98	2.45	2.77
3.5	.02	.08	.20	.35	.53	.75	1.01	1.30	1.64	2.02	2.45	2.94	3.27
4.0	.06	.18	.33	.53	.76	1.03	1.33	1.67	2.04	2.46	2.92	3.43	3.77
4.5	.14	.30	.50	.74	1.02	1.33	1.67	2.05	2.46	2.91	3.40	3.92	4.26
5.0	.24	.44	.69	.98	1.30	1.65	2.04	2.45	2.89	3.37	3.88	4.42	4.76
6.0	.50	.80	1.14	1.52	1.92	2.35	2.81	3.28	3.78	4.30	4.85	5.41	5.76
7.0	.84	1.24	1.68	2.12	2.60	3.10	3.62	4.15	4.69	5.25	5.82	6.41	6.76
8.0	1.25	1.74	2.25	2.78	3.33	3.89	4.46	5.04	5.63	6.21	6.81	7.40	7.76
9.0	1.71	2.29	2.88	3.49	4.10	4.72	5.33	5.95	6.57	7.18	7.79	8.40	8.76
10.0	2.23	2.89	3.56	4.23	4.90	5.56	6.22	6.88	7.52	8.16	8.78	9.40	9.76
11.0	2.78	3.52	4.26	5.00	5.72	6.43	7.13	7.81	8.48	9.13	9.77	10.39	10.76
12.0	3.38	4.19	5.00	5.79	6.56	7.32	8.05	8.76	9.45	10.11	10.76	11.39	11.76
13.0	4.00	4.89	5.76	6.61	7.42	8.21	8.98	9.71	10.42	11.10	11.76	12.39	12.76
14.0	4.65	5.62	6.55	7.44	8.30	9.12	9.91	10.67	11.39	12.08	12.75	13.39	13.76
15.0	5.33	6.36	7.35	8.29	9.19	10.04	10.85	11.63	12.37	13.07	13.74	14.39	14.76

1/ Interpolate the values shown to obtain runoff depths for CN's or rainfall amounts not shown.

The curve number (*CN*) resembles the runoff coefficient (*C*) used in the rational method and incorporates the hydrological effect of land use, soil type, and antecedent moisture in stormwater runoff calculations. The *CN* is a dimensionless number between 0 and 100. For natural soil *CN* is smaller than 100, and for impervious material *CN* =100.

In NRSC method, the soil type and texture are classified as group A, B, C, and D. The soil group type, texture and minimum infiltration rate of each soil type are listed in **Table ABSM.5**. The antecedent moisture condition of soil may vary greatly. Based on moisture condition these soils are grouped into three categories: (I) dry conditions (low moisture), (II) average conditions, and (III) wetter conditions (high moisture, heavy rainfall over the preceding few days).

Table ABSM.5 Hydrologic Soil Groups (USDA, 1986)

Group	Soil Textures	Minimum Infiltration Rate (in/h)
A	Sand, loamy sand, or sandy loam	> 0.3
B	Silt loam or loam	0.15 - 0.3
C	Sandy clay loam	0.05 - 0.15
D	Clay loam, silty clay loam, sandy clay, silty clay, or clay	0.0 - 0.05

The NRCS has developed a system of curve numbers (*CNs*) that are based on land use, soil type, and antecedent moisture (38). Four generalized tables have been developed for average antecedent moisture condition (Condition II). These tables provide *CN*s for (1) urban areas, (2) cultivated agricultural lands, (3) other agricultural lands, and (4) arid and semiarid rangelands. These tables are provided in **Tables ABSM.6a** to **ABSM.6d**. The adjustment of curve numbers for dry condition (I) and wet condition (III) are also tabulated in **Table ABSM.7**. A composite *CN* is determined and used in stormwater runoff estimation from a watershed with several different land uses. Composite curve numbers can be calculated by using the weighted-average method. The runoff estimation using the NRCS method is discussed in detail in publications of U.S. Department of Agriculture (USDA, 1986), and several textbooks and stormwater technical manuals.

Table ABSM.6(a) Curve Numbers for Urban Areas for Average Antecedent Moisture Condition (Condition II) (USDA, 1986)

Cover Description		Curve Numbers for Hydrologic Soil Group			
Cover Type and Hydrologic Condition	Average Percent Impervious Area[1]	A	B	C	D
Fully developed urban areas (vegetation established)					
Open space (lawn, parks, golf courses, cemeteries, etc.):[2]					
Poor condition (grass cover < 50%)		68	79	86	89
Fair condition (grass cover 50-75%)		49	69	79	84
Good condition (grass cover > 75%)		39	61	74	80
Impervious area:					
Paved parking lots, roofs, driveways, etc. (excluding right- of-way)		98	98	98	98
Streets and roads:					
Paved; curbs and storm sewers (excluding right-of-way)		98	98	98	98
Paved; open ditched (including right-of-way)		83	89	92	93
Gravel (including right-of-way)		76	85	89	91
Dirt (including right-of way)		72	82	87	89
Western desert urban areas:					
Natural desert landscaping (pervious areas only) [3]		63	77	85	88
Artificial desert landscaping (impervious weed barrier, desert shrub with 1- to 2-inch sand or gravel mulch and basin borders)		96	96	96	96
Urban districts:					
Commercial and business	85	89	92	94	95
Industrial	72	81	88	91	93
Residential districts by average lot size:					
1/8 acre or less (town houses)	65	77	85	90	92
1/4 acre	38	61	75	83	87
1/3 acre	30	57	72	81	86
1/2 acre	25	54	70	80	85
1 acre	20	51	68	79	84
2 acres	12	46	65	77	82
Developing urban areas					
Newly graded areas (pervious areas only, no vegetation) [4]		77	86	91	94
Idle lands (CN's are determined using cover types similar to those in Table 2.2c of Ref. 12).					

[1] The average percent impervious area shown was used to develop the composite *CN's*. Other assumptions are as follows: impervious areas are directly connected to the drainage system, impervious areas have a *CN* of 98, and pervious areas are considered equivalent to open space in good hydrologic condition. *CN's* for other combinations of conditions may be computed using Figure 2.3 or Figure 2.4 in USDA (1986).

[2] *CNs* shown are equivalent to those of pasture. Composite *CN's* may be computed for other combinations of open space cover type.

[3] Composite *CN's* for natural desert landscaping should be computed using Figure 2.3 or Figure 2.4 in USDA (1986) based on the impervious area percentage (*CN* = 98) and the pervious area *CN*. The pervious area *CN's* are assumed equivalent to desert shrub in poor hydrologic condition.

[4] Composite *CN's* to be used for the design of temporary measures during grading and construction should be computed using Figure 2.3 or Figure 2.4 in USDA (1986) based on the degree of development (impervious area percentage) and the *CN's* for the newly graded pervious areas.

Table ABSM.6(b*)* Curve Numbers for Cultivated Agricultural Lands for Average Antecedent Moisture Condition (Condition II) (USDA, 1986)

Cover Description			Curve Numbers for Hydraulic Soil Group			
Cover Type	Treatment[1]	Hydrologic condition[2]	A	B	C	D
Fallow	Bare soil	–	77	86	91	94
	Crop residue cover (CR)	Poor*	76	85	90	93
		Good**	74	83	88	90
Row crops	Straight row (SR)	Poor	72	81	88	91
		Good	67	78	85	89
	SR + CR	Poor	71	80	87	90
		Good	64	75	82	85
	Contoured (C)	Poor	70	79	84	88
		Good	65	75	82	86
	C + CR	Poor	69	78	83	87
		Good	64	74	81	85
	Contoured & terraced (C&T)	Poor	66	74	80	82
		Good	62	71	78	81
	C&T + CR	Poor	65	73	79	81
		Good	61	70	77	80
Small grain	SR	Poor	65	76	84	88
		Good	63	75	83	87
	SR + CR	Poor	64	75	83	86
		Good	60	72	80	84
	C	Poor	63	74	82	85
		Good	61	73	81	84
	C + CR	Poor	62	73	81	84
		Good	60	72	80	83
	C&T	Poor	61	72	79	82
		Good	69	70	78	81
	C&T + CR	Poor	60	71	78	81
		Good	58	69	77	80
Close-seeded or broadcast legumes or rotation meadow	SR	Poor	66	77	85	89
		Good	58	72	81	85
	C	Poor	64	75	83	85
		Good	55	69	78	83
	C&T	Poor	63	73	80	83
		Good	51	67	76	80

[1] Crop residue cover applied only if residue is on at least 5% of the surface throughout the year.

[2] Hydraulic condition is based on combination factors that affect infiltration and runoff, including (a) density and canopy of vegitative areas, (b) amount of year-round cover, (c) amount of grass or close-seeded legumes, (d) percent of residue cover on the land surface (good ≥ 20%), and (e) degree of surface roughness.

*Poor: Factors impair infiltration and tend to increase runoff.

**Good: Factors encourage average and better than average infiltration and tend to decrease runoff.

Table ABSM.6(c) Curve Numbers for Other Agricultural Lands for Average Antecedent Moisture Condition (Condition II) (USDA, 1986)

Cover Description		Curve Numbers for Hydraulic Soil Group			
Cover Type	Hydrologic Condition	A	B	C	D
Pasture, grassland, or range—continuous forage for grazing[1]	Poor	68	79	86	89
	Fair	49	69	79	84
	Good	39	61	74	80
Meadow–continuous grass, protected from grazing and generally mowed for hay	–	30	58	71	78
Brush–brush-weed-grass mixture with brush the major element[2]	Poor	48	67	77	83
	Fair	35	56	70	77
	Good	30[3]	48	65	73
Woods–grass combination (orchard or tree farm)[4]	Poor	57	73	82	86
	Fair	43	65	76	82
	Good	32	58	72	79
Woods[5]	Poor	45	66	77	83
	Fair	36	60	73	79
	Good	30[3]	55	70	77
Farmsteads–buildings, lanes, driveways, and surroundings lots	–	59	74	82	86

[1] Poor: < 50%) ground cover or heavily grazed with no mulch
Fair: 50 - 75% ground cover and not heavily grazed
Good: > 75% ground cover and lightly or only occasionally grazed

[2] Poor: <5 0% ground cover
Fair: 50 - 75% ground cover
Good: >75% ground cover

[3] Actual curve number is less than 30; use $CN = 30$ for runoff computations

[4] *NC's* shown were computed for areas with 50% woods and 50% grass (pasture) cover. Other combinations of conditions may be computed from the *CN's* for woods and pasture

[5] Poor: Forest litter, small trees, and brush are destroyed b heavy grazing or regular burning
Fair: Woods are grazed but not burned, and some forest litter covers the soil
Good: Woods are protected from grazing, and litter and brush adequately cover the soil

Table ABSM.6(d) Curve Numbers for Arid and Semiarid Rangelands for Average Antecedent Moisture Condition (Condition II)

Cover Description		Curve Numbers for Hydrologic Soil Group			
Cover Type	Hydrologic Condition[1]	A[2]	B	C	D
Herbaceous–mixture of grass, weeds, and low-growing brush, with brush the minor element	Poor		80	87	93
	Fair		71	81	89
	Good		62	74	85
Oak-aspen–mountain brush mixture of oak brush, aspen, mountain mahogany, bitter brush, maple, and other brush	Poor		66	74	79
	Fair		48	57	63
	Good		30	41	48
Pinyon-juniper–pinyon, juniper, or both; grass understory	Poor		75	85	89
	Fair		58	73	80
	Good		41	61	71
Sagebrush with grass understory	Poor		67	80	85
	Fair		51	63	70
	Good		35	47	55
Desert shrub–major plants include saltbrush, greasewood, creosotebush, blackbrush, bursage, palo verde, mesquite, and cactus	Poor	63	77	85	88
	Fair	55	72	81	86
	Good	49	68	79	84

[1] Poor: < 30% ground cover (litter, grass, and brush overstory)
Fair: 30 - 70% ground cover
Good: > 70% ground cover

[2] Curve numbers for group A have been developed only for desert shrub

Table ABSM.7 Adjustment of Curve Numbers for Dry (I) and Wet Antecedent Moisture Conditions (USDA, 1986)

Curve Number for Condition	Corresponding Curve Number for Condition	
II	I	III
100	100	100
95	87	99
90	78	98
85	70	97
80	63	94
75	57	91
65	45	83
60	40	79
55	35	75
50	31	70
45	27	65
40	23	60
35	19	55
30	15	50
25	12	45
20	9	39
15	7	33
10	4	26
5	2	17
0	0	0